ONE-DIMENSIONAL MATHEMATICAL MODEL OF TIME-DEPENDENT SALINITY MEASUREMENT AND CONTROLLING IN CHAO PHRAYA RIVER FOR WATER SUPPLY PROCESS

A THESIS SUBMITTED IN PARTIAL FULFILLMENT OF THE REQUIREMENT FOR THE DEGREE OF DOCTOR OF PHILOSOPHY IN APPLIED MATHEMATICS

DEPARTMENT OF APPLIED MATHEMATICS
FACULTY OF SCIENCE
KING MONGKUT'S INSTITUTE OF TECHNOLOGY LADKRABANG

2020
KMITL-2020-SC-D-001-016

ONE-DIMENSIONAL MATHEMATICAL MODEL OF TIME-DEPENDENT SALINITY MEASUREMENT AND CONTROLLING IN CHAO PHRAYA RIVER FOR WATER SUPPLY PROCESS

KHEMISARA KULMART

A THESIS SUBMITTED IN PARTIAL FULFILLMENT OF THE REQUIREMENT FOR THE DEGREE OF DOCTOR OF PHILOSOPHY IN APPLIED MATHEMATICS

DEPARTMENT OF APPLIED MATHEMATICS
FACULTY OF SCIENCE
KING MONGKUT'S INSTITUTE OF TECHNOLOGY LADKRABANG

2020

KMITL-2020-SC-D-001-016

หัวข้อวิทยานิพนธ์	ตัวแบบเชิงคณิตศาสตร์หนึ่งมิติของการวัดและการควบคุมความเค็มที่ขึ้นกับเวลาในแม่น้ำเจ้าพระยาสำหรับกระบวนการผลิตน้ำประปา
ชื่อนักศึกษา	นางสาวเขมิสรา กุลมาตย์
รหัสประจำตัว	58605001
ปริญญา	ปรัชญาดุษฎีบัณฑิต (คณิตศาสตร์ประยุกต์)
ภาควิชา	คณิตศาสตร์
พ.ศ.	2563
อาจารย์ที่ปรึกษาวิทยานิพนธ์	ผศ.ดร. นพรัตน์ โพธิ์ชัย

บทคัดย่อ

วัตถุประสงค์หลักของการวิจัยครั้งนี้เพื่อพัฒนาแบบจำลองคณิตศาสตร์โดยใช้เทคนิคเชิงตัวเลขวิธีไฟไนต์ดิฟเฟอเรนซ์ สำหรับการประมาณค่าความเค็มและควบคุมการรุกล้ำความเค็มแบบหนึ่งมิติในแม่น้ำเจ้าพระยาบริเวณใกล้สถานีสูบน้ำดิบสำแล โดยการประยุกต์ใช้แบบจำลองคณิตศาสตร์เพื่อพยากรณ์การรุกล้ำความเค็มตามแนวลำน้ำในแม่น้ำเจ้าพระยา ผลการศึกษาจากแบบจำลองการพัดพาและการแพร่กระจายระหว่างค่าความเค็มและสมบัติอัตราการไหลของกระแสน้ำพบว่าสมการคณิตศาสตร์มีความเหมาะสมสำหรับการประมาณค่าความเค็มในแม่น้ำเจ้าพระยาบริเวณสถานีสูบน้ำดิบสำแล รวมทั้งการปรับเทียบแบบจำลองเพื่อหาค่าตัวแปรที่เหมาะสม แบบจำลองคณิตศาสตร์ที่พัฒนาขึ้นมานี้สามารถใช้ตรวจวัดค่าความเค็มและสารต่างๆ ในลำน้ำได้ถ้ามีข้อมูลเกี่ยวกับอัตราการระบายของสารดังกล่าวและลักษณะของลำน้ำ ได้แก่ พื้นที่หน้าตัดของลำน้ำ ตำแหน่งของ node ต่างๆ ปริมาณการไหล ค่าสัมประสิทธิ์การแพร่กระจายและการพัดพา อัตราการสลายตัวของสาร และปริมาณสารที่ระบายลงในแต่ละส่วนของลำน้ำ โดยค่าที่ได้จากแบบจำลองกับค่าที่ตรวจวัดได้จริงอยู่ในเกณฑ์ที่ยอมรับได้ ผลการศึกษาครั้งนี้สามารถนำไปเป็นแนวทางกำหนดมาตรการบริหารจัดการน้ำเพื่อควบคุมการรุกล้ำของความเค็มในแม่น้ำเจ้าพระยาและเพื่อลดผลกระทบสำหรับการผลิตน้ำประปาในกรุงเทพมหานครในอนาคตต่อไป

คำสำคัญ : การรุกล้ำความเค็ม ตัวแบบเชิงคณิตศาสตร์หนึ่งมิติ แม่น้ำเจ้าพระยา วิธีไฟไนต์ดิฟเฟอ-เรนซ์ สถานีสูบน้ำดิบสำแล

Thesis Title	One-dimensional Mathematical Model of Time-dependent salinity Measurement and Control in Chao Phraya River for Water Supply Process
Student Name	Khemisara Kulmart
Student ID	58605001
Degree	Doctor of Philosophy (Applied Mathematics)
Department	Mathematics
Year	2020
Thesis Advisor	Asst. Prof. Dr. Nopparat Pochai

Abstract

The main objectives of this research were to develop a mathematical model and use finite-difference numerical techniques to estimate one-dimensional salinity of water along Chao Phraya River and to control salinity intrusion at Samlae Pump Station, located near the estuary of Chao Phraya River. The mathematical model was used to simulate the diffusion and advection of salinity along the river and the salinity intrusion into Chao Phraya River. The results from the salinity transportation and distribution model show that the mathematical equation was acceptably suitable for estimation of salinity values in the Chao Phraya River near Samlae Pump Station. The model was calibrated to find the proper parameters values for this use. This mathematical model was developed to calculate advection and diffusion of salt in water. It was able to do so when there were enough data on the diffusion rate of salt as well as the characteristics of the water passages: cross sectional area, positions of nodes, volume of water flow, salinity dilution rate, dissolution rate and the amount of salt dissolved in each part of a water passage. The estimates from the model were in acceptably good agreement with the actual measured values from the field. The findings from this study can be used as suggestions for setting up some water-management measures to control salinity intrusion along Chao Phraya River and lessen its impact on tap water production for Bangkok Metropolitan in the future.

Keywords: Chao Phraya River; Finite difference method; One-dimensional advection and diffusion equation; Salinity Intrusion; Samlae Pump Station

Acknowledgements

I would like to express my sincere gratitude to my advisor, Assistant Professor Dr. Nopparat Pochai, for giving me an opportunity to create this thesis, for providing me invaluable support and guidance as, and for understanding and encouraging me until the completion of the thesis.

I am fully indebted to the thesis committee members: Associate Professor Suwon Tangmanee, Assistant Professor Dr. Kanchana Kamnungkit, Assistant Professor Jaipong Kasemsuwan and Dr. Wannaporn Sanprasert for their useful comments.

I gratefully acknowledge the financial support from the Centre of Excellence in Mathematics Program of the Commission on Higher Education, the essential salinity measurement data provided by the Water Resources and Environment Department and the Metropolitan Waterworks Authority, and the knowledge and skills instilled in me by various instructors at King Mongkut's Institute of Technology Ladkrabang.

I would also like to thank Mr. Pratana Kangsadal for proofreading the English in this thesis as well as Mr. Witsarut Klaychang and Mr. Nattawut Pongnu for their help with computer programming.

Finally, I would like to express my gratitude to my father and mother who have always given me tremendous support and encouragement throughout my entire life.

Table of contents

Table of contents (continued)

Table of contents (continued)

List of tables

List of tables (continued)

List of tables (continued)

Table **Page**

List of figures

List of figures (continued)

List of figures (continued)

List of figures (continued)

Figure **Page**

Chapter 1
Introduction

1.1 Research Motivation

Water is an essential natural resource for the livelihood of humans, animals, and plants. It is the most abundant matter compared to other matters in our planet. Water is the most miraculous thing on earth, supporting the lives of every living thing. Human communities, ancient and modern, have always depended on good water sources. Human beings have become the species that use and exploit water for their own benefits the most. This statement also applies with the use of water in Thailand.

Chao Phraya River is a major river in Thailand. It is a confluence of Ping, Wang, Yom and Nan rivers at Pak Nam Pho, Mueang District, Nakhon Sawan Province, flowing pass Chai nat, Sing Buri, Ang Thong, Ayutthaya, Pathum Thani, Bangkok, and Samut Prakan provinces for a total distance of 300 kilometers (See Figure 1.1).

Figure 1.1 Chao Phraya River from a high view [44].

(From: https://www.bangkokpost.com/business/news/1158472/golden-location-with-curved-view-of-chao-phraya-river)

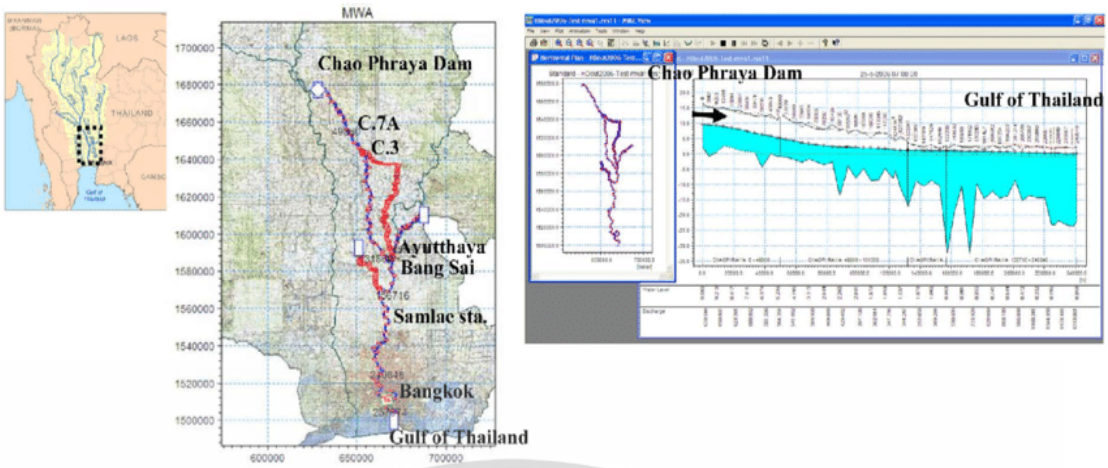

Figure 1.2 Location of the Lower Chao Phraya River ($13.58^{\circ}-15.67^{\circ}N, 100.10^{\circ}-101.00^{\circ}E$) and our model of released freshwater from dams to alleviate seawater intrusion [8].

Economic, industrial, agricultural and energy sectors of nation states and of the world during the last couple of decades have clearly expanded, causing an exponential demand of water, hence water becomes more valuable. It has been estimated that two-thirds of human population will face a huge pressure in terms of freshwater shortage as well as water quality by the year 2025. Moreover, global warming is another factor that causes severe freshwater shortage. Furthermore, natural sea level changes cause intrusion of seawater into lower rivers, exacerbating freshwater shortage [1] (See Figure 1.2). Water in an estuary are different from those in the areas above the estuary in terms of saltwater content. Since high salinity water has a higher density than freshwater and when higher level of seawater than the upstream freshwater level in summer, the volume and direction of freshwater flow in upper estuary vary strongly with tidal changes compared to lower estuary. Also, since the flow of freshwater into the sea is inversely proportional to the sea level and the present sea level is higher than before due to global warming, seawater intrudes into upstream rivers for a longer time and distance [2, 3].

Ocean Tide affects the flow of seawater to the inner part of the estuary, which causes deposition of salty sediment layers on the riverbed. It does this by producing varying friction between water mass and riverbed, blocking the natural flow of freshwater out and away from the estuary and hence deposition of sediment

layers on the riverbed. When there is an ebb tide, the freshwater layer in the current near the surface of a river flows downstream and wash away the salty sediment into the sea, but where there is a high tide, the undesirable reverse process happens.

Chao Phraya River is the main river of the central region. essential for ecological conservation, agriculture, industry and daily consumption of inhabitants along both sides of the river. Water in Chao Phraya River is influenced by tidal bore that takes place at an estuary at the end of it. During a dry season, the bore can extend its influence on the river flow to as distant as Phra Nakhon Si Ayutthaya province, 130 km North of the estuary. The salinity level at a seawater intrusion monitoring station that we investigated at Samlae Canal, Pathum Thani province, 96 km north of the estuary, is even much higher than that. A bird-eye-view image of the station is shown in Figure 1.3. The station is a small monitoring unit of a larger pumping facility that pumps water in the river into the canal connected as a source of freshwater to the Metropolitan Waterworks facility that provides potable tap water for inhabitants in Bangkok, the capital city of Thailand. Therefore, a high salinity level at this station may cause shortage of tap water in Bangkok, negatively affecting the lives of millions of people, as well as the productivity of the agriculture in the areas along the river upstream from the estuary [4].

In 1992, the Royal Irrigation Department began to measure the salinity level of water in Chao Phraya River, Tha Chin River and Mae Klong River and found that during a dry season from January to June, the salinity level was considerably high. Three monitoring stations were erected to measure salinity index at the following locations: 1) Chao Phraya River under the Buddha Yotfa Bridge of in Bangkok, 2) Tha Chin River in front of Sam Pran District Office in Nakhon Pathom Province, 3) Mae Klong River at the estuary of Damnoen Saduak Canal in Damnoen Saduak District, Ratchaburi Province. The alarm level of high salinity at these monitoring points was set at 2.00 g / L (the standard level of salinity for agricultural purposes). Later in 2004, the monitoring station under the Buddha Yotfa bridge was decommissioned, and a new station at Thanam Non in Nonthaburi province was commissioned to monitor the salinity level in Chao Phraya River near Bangkok, which actually benefited the productive agricultural areas in Nonthaburi province, as the station can provide accurate readings of the salinity level in the areas.

Later, in 2007, abiding to Her Majesty Queen Regent Sirikit's speech on August 11th, 2007 regarding solutions to improve water quality in the severely deteriorated Chao Phraya River, governmental agencies jointly came up with ways to preserve the river and solve its water quality problems. The Royal Irrigation Department set up more salinity monitoring stations along the river, from a location below Chao Phraya Dam in Sapphaya District, Chai Nat Province, 194 km upstream from the estuary, to a location in front of Samut Prakarn provincial town hall, less than 10 km upstream from the estuary. A total of 32 monitoring stations were commissioned along Chao Phraya River, providing detailed readings of salinity level, along the river from the estuary to the dam, at any time. Based on the results from daily salinity measurements from January to April 2014 at Samlae monitoring Station, at the station of the Royal Irrigation Department (Samsen) in Bangkok and at Thanam Non station, the salinity index had begun to exceed the standard level for raw water for consumption (0.25 g/l according to World Health Organization) being pumped into the Metropolitan Water work facility to produce tap water in Bangkok (See Figure 1.4). During the period of January 27th to February 13th, 2014, the salinity level was sometimes even higher than 1 g/l continually for up to 20 hours per day. The highest hourly salinity level recorded was 1.92 g/l on February 15th, 2014 at 22.00 hr. It was the highest salinity level ever recorded since the Royal Irrigation Department has started to measure it from 1992 up until the present day, a total of 23 years.

Based on previous statistical data from the Royal Irrigation Department, the salinity level in the past was very high from mid-April to the middle of May of every year. However, in 2016 onwards, it has been very high much earlier, starting from the end of January. It reached the highest level in the middle of February. According to measurements of salinity levels at the locations of Thanam Non District in Nonthaburi Province to Bangsai District in Phra Nakhon Si Ayutthaya Province, the salinity levels of water in those areas were too high to for agricultural purposes, higher than 2.0 g/l. The distance from those areas to the estuary was 79–93 kilometers. The distance of which the salinity levels were within the standard level for production of tap water, at 0.25 g/l, was about 95–112 kilometers North of the estuary. Measured at the water monitoring station designated as "C.29" in Bangsai District, Phra Nakhon Si Ayutthaya Province, the average flow of freshwater down the river during January to early February, 2014 was only 70 m^2/s, significantly lower than

the average flow in the recent past, at about 100 m^2/s even though freshwater had continuously been released from the nearest Dam at a rate of 55-70 m^2/s during that particular period. At the same period, in 2013, the flow speed was about 10 m^2/s higher than that, but the salinity level was still obstinately high. There was a panic among the staff of the Royal Irrigation Department when the salinity level at Samlae Pump Station in Pathum Thani reached 0.5 g/l on March 31st, 2016. "The Drought Crisis" had caused a higher than standard salinity level. By the close seawater intrusion monitoring at Samlae Pump Station (See Figure 1.3), Krachaeng Subdistrict, Mueang District, Pathum Thani, the major source of tap water production for inhabitants of Bangkok, Nonthaburi and Samut Prakan provinces, it was found that the salinity level kept increasing more frequently and extensively. For this reason, the staff of the station intermittently stopped pumping the raw water in the river in up into the canal for tap water processing for short few hours. When the salinity level in the water plummeted, they would start pumping it up again. If the salinity level had kept rising for a longer period of time, the Metropolitan Waterwork Authority would have had to find move the pump station further North where the salinity was acceptable or the Royal Irrigation Department would have to devise a better strategy for keeping in check the salinity level of water in Chao Phraya River (See Figure 1.5-1.8) [2, 4].

Recent in-depth studies of processes in natural phenomena as well as advances in computer hardware and software have made mathematical models for calculating parameters of natural phenomena more popular. Those studies expressed important parameters of certain natural phenomena as mathematical equation or model based on some assumptions. The solutions to those equations were calculated by numerical methods. Several recent studies have been on developing of mathematical models for calculating levels of some substances in the water of a river including salinity [3, 8]. Hence, mathematical models have been demonstrated to be useful augments to real measurement data.

Figure 1.3 Chao Phraya River and Samlae Canal Pump Station [45].

(From: http://englishnews.thaipbs.or.th/six-provinces-warned-rising-water-level-chao-phraya/)

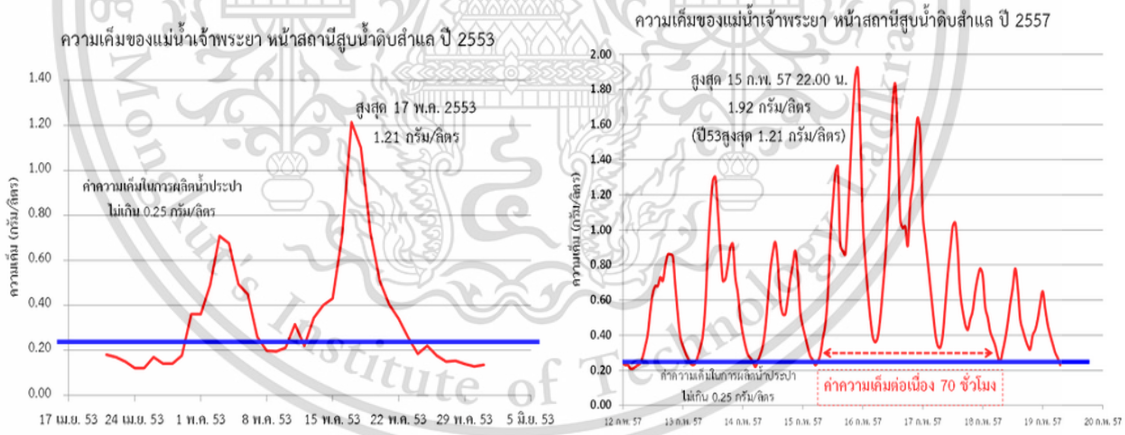

Figure 1.4 Salinity Level in Chao Phraya River in 2010 and 2014 measured at Samlae Pump Station [46].

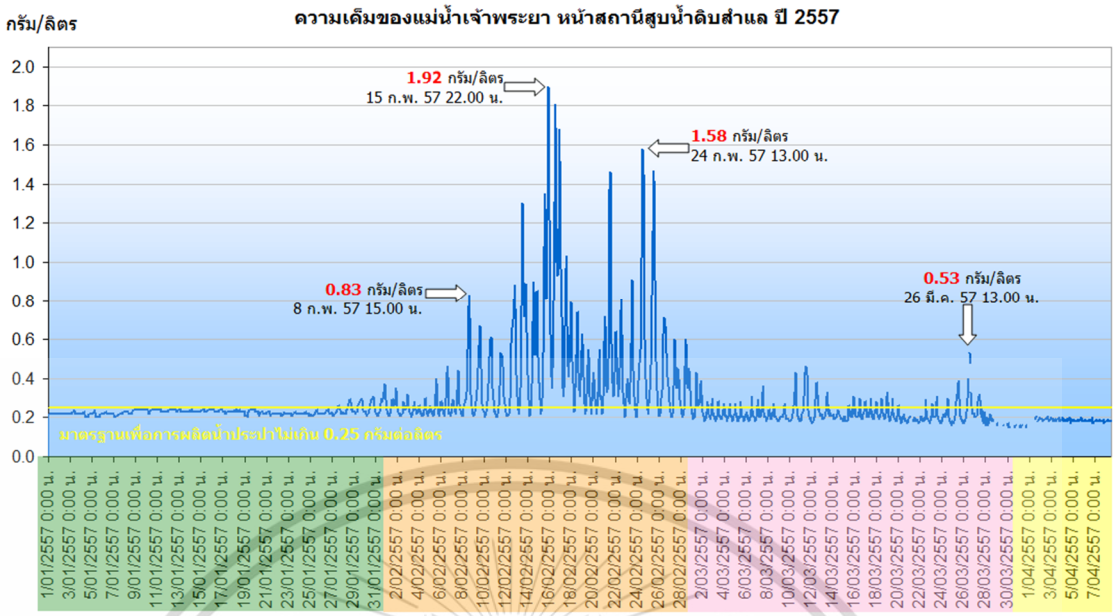

Figure 1.5 Salinity Level in the Chao Phraya River at the Samlae Pump Station in 2014 [46].

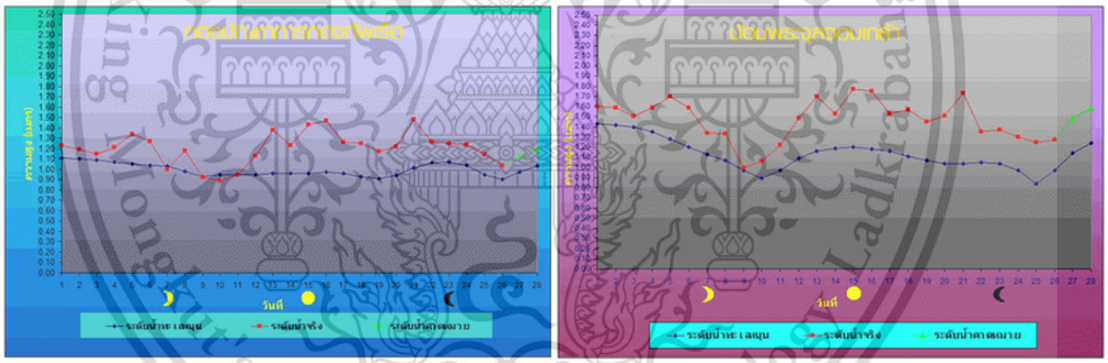

Figure 1.6 Graphs of sea levels in the Gulf of Thailand around the areas of the Royal Thai Navy Headquaters Pump Station and the Chulachomklao Fort Pump Station; red lines are actual sea level; blue lines are estimated sea level by the Royal Irrigation Department [46].

Figure 1.7 Bhumibol Dam, Tak Province, Thailand.

Figure 1.8 Bhumibol Dam at Tak Province (Left) and at Chao Phraya Dam at Chai Nat Province (Right), Thailand, releasing Budget water down Chao Phraya River.

Therefore, this thesis developed a one-dimensional finite difference model of time-dependent salinity measurement and Control of water in Chao Phraya River. The proposed model was developed based on real salinity levels measured at eight different water monitoring stations along the lower segment of Chao Phraya River and MacCormack scheme. The model can benefit water resource management process in the future.

1.2 Objectives of the study

The main objectives of this thesis were as follows:

1) To develop a finite different model for salinity measurement of water supply in Chao Phraya River near Samlae Pump Station, Thailand;

2) To estimate the salinity level of water at eight different water monitoring stations along a lower segment of Chao Phraya River with the developed model; To apply the developed mathematical model in real-life situations, providing precise estimates of salinity level at different locations along the lower segment of Chao Phraya in Chao Phraya River as needed data for the staff of the Royal Irrigation Department to be able to optimize the amount of freshwater to be released from the nearest upriver dam.

1.3 Scope of the study

The scope of the thesis is restricted to application of finite difference method to measure salinity intrusion in Chao Phraya River in the form of one-dimensional model. The focused areas in this study cover eight salinity intrusion monitoring stations: Phra Nakhon Tai, Khlong Lat Pho, Wat Sai Ma Nuea, Wat Makham, Samlae Pump Station, Wat Phai Lom, Wat Pho Taeng Nuea and Wat Ban Paeng Temple from the upstream Chao Phraya River to the estuary, a total distance of 160 kilometers (See Figure 1.9). Hourly salinity intrusion measurement was done at every station started on March 2nd, 2017. Samlae Pump Station was the station that the actual hourly salinity levels were taken from.

Figure 1.9 Map of the monitoring stations [3].

1.4 Benefits of the study

The mathematical model constructed in this research has been used to support the planning and preparation of water management and water supply process by the Royal Irrigation Department (See Figure 1.10-1.11). Its estimates were used to predict levels of salinity intrusion in Chao Phraya River during the summer of 2014. The department planned to use it regularly for the future right after. The model can be used by various governmental organizations associated with water management to lower their tool and labor costs for salinity intrusion measurement at every monitoring station. In addition to the benefit of cost reduction, this model can estimate data at hard-to-access areas. Hopefully, this model will be used and published by governmental organizations for the benefits of the general public in the future.

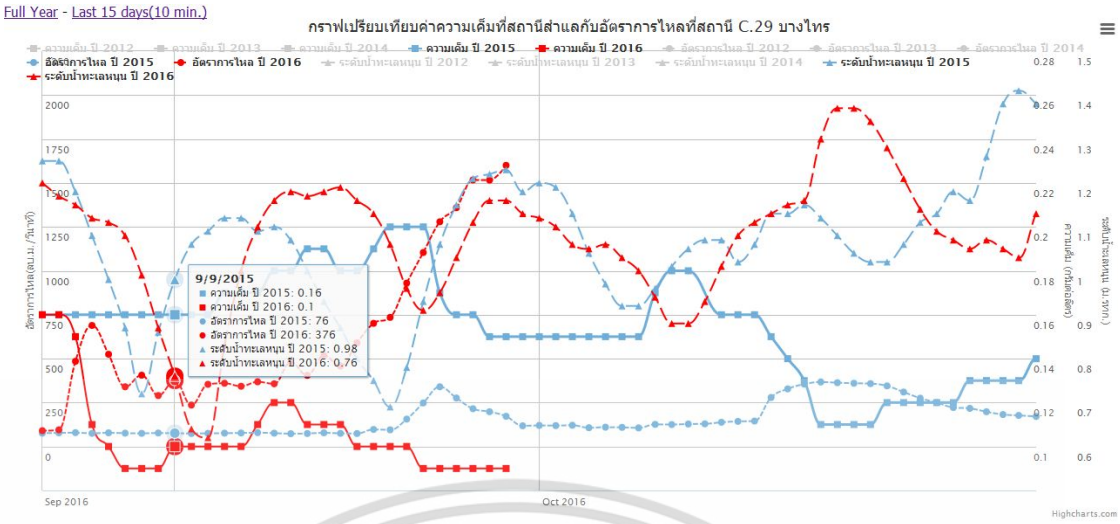

Figure 1.10 Graph of salinity level and seawater inflow rate at Sam Lae station and C.29 Bang Sai station on 09/09/2015 [47].

(From: http://water.rid.go.th/hwm/wmg/water/chart/chart_s.php)

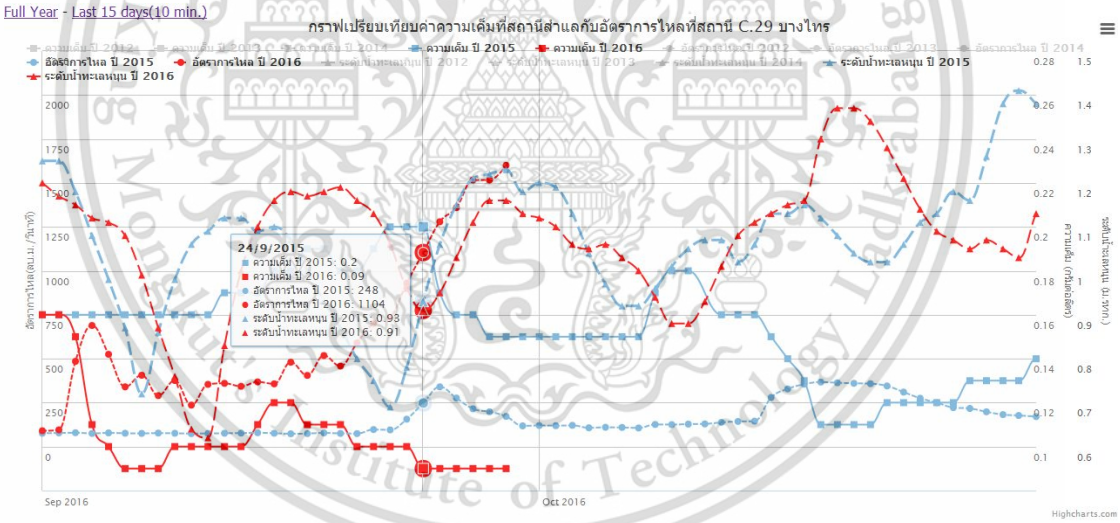

Figure 1.11 Graph of salinity level and seawater inflow rate at Sam Lae station and C.29 Bang Sai station on 24/09/2015 [47].

(From: http://water.rid.go.th/hwm/wmg/water/chart/chart_s.php)

Chapter 2

Theory and Literature Reviews

2.1 Chao Phraya River Estuary

2.1.1 Study area description

Chao Phraya Basin covers an area of about 162,600 km^2, on the Lower Central Plain of Thailand ($14^\circ - 20^\circ N, 98^\circ - 101^\circ E$). The basin is 980 km long in the north-to-south direction (See Figure 2.1) [40]. The elevation of the plain ranges from 25 m above the mean sea level at Nakorn Sawan province in the north to less than 4 meters at Ayutthaya province and to about 2 meters in the vicinity of Bangkok. Soils in the flood plain deposits are mostly sandy clay and are formed throughout the northern half of the plain. The basin has been used for paddy fields and is a major rice production region for the country. The annual rainfall varies from 1,200 to 1,600 mm in the upper basin and is about 1,200 mm in the north and west bank areas of the lower basin. Temperatures are usually high in March or April and low between November and January. The temperature difference between the highest and the lowest within a year is about $4^\circ - 7^\circ C$.

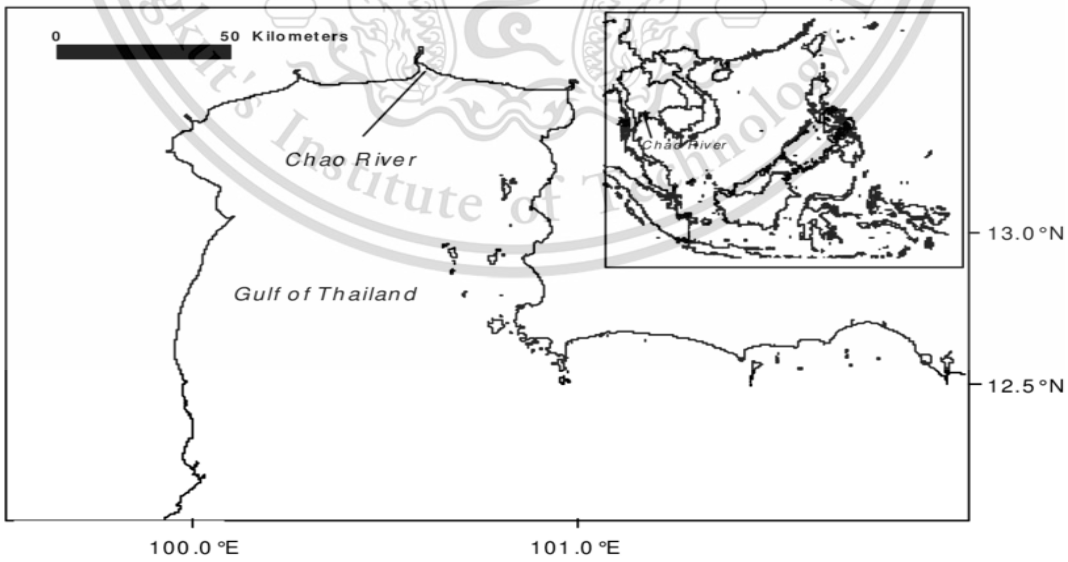

Figure 2.1 Location of Chao Phraya River estuary, Thailand.

Chao Phraya River ($13.58^{\circ}-15.67^{\circ}N, 100.10^{\circ}-101.00^{\circ}E$) is 375 km long and flows down from Nakon sawan Province to the Gulf of Thailand at Samut Prakarn Province. The river basin area is about 19,390 km^2. The size of the population living in the basin is approximately 8 million. The depth of the river ranges from 5 to 20 m and the width ranges from 200 to 1,200 m. The river traverses several large cities and major agricultural regions of the country. Chao Phraya River basin collects domestic and industrial waste discharges from sources along the river. Only two urban centers, Bangkok and Uthai Thani have operating sewage treatment systems. Although some industrial sites have some form of wastewater treatment system, most tend to dispose of raw effluent to the nearest waterways, usually a street drain or smaller stream.

The river has several dams for storing water to irrigate agricultural areas. Water is released from a major dam, Chao Phraya Dam, to the lower basin for the purposes of salinity control, irrigation, navigation, industry and domestic consumption. However, the discharge hydrographic of the Chao Phraya River still exhibits a periodic annual variation. A hydrological cycle starts in April when the released freshwater is typically at its minimum. From May to August the released water gradually increases, and from August to October, the increase is more rapid, peaking in October. The discharge then decreases fairly rapidly during November and December, with the rate of decease slowing until the minimum flow condition is again experienced in April. During the low flow period from January to April, the discharge typically ranges from 50 to 200 $m^3\ sec^{-1}$. Tidal intrusion extends far upstream (175 km) during a low river flow condition and contracts down to about 75 km upstream during a high stream flow condition. At a freshwater discharge rate of 4,000 $m^3\ sec^{-1}$, common during a wet season, tidal fluctuations are not observed upstream of Pak Kret ($14.076475^{\circ}N, 100.5257139^{\circ}E$). However, increased salinity level from the sea are noticeable downstream of Nontaburi ($13.862707^{\circ}N, 100.475875^{\circ}E$), about 60 km from the river mouth.

The estuarine section of Chao Phraya River (approximately 70 km south of the river mouth) can be divided into two portions, the upper estuary and the lower estuary. The physical dimensions of the estuary are shown in Table 2.1. For the purpose of water budgetary analysis, the estuary is assumed to be a well-mixed system.

Table 2.1 Physical dimensions of the estuary of Chao Phraya River.

Compartment	Mean length (km)	Mean width (m)	Surface area ($10^6 m^2$)	Mean depth (m)	Volume ($10^6 m^3$)
Upper estuary	52	450	23.4	10	234
Lower estuary	18	800	14.4	10	144

2.2 One-dimensional advection-diffusion-equation

In this research, we consider the following one-dimensional advection-diffusion equation [17],

$$\frac{\partial u}{\partial t} + \beta \frac{\partial u}{\partial x} = \alpha \frac{\partial^2 u}{\partial x^2}, \quad \text{for all } 0<x<1 \text{ and } 0 < t \le T, \tag{2.1}$$

with an initial condition,

$$u(x,0) = f(x), \quad \text{for all } 0 \le x \le 1, \tag{2.2}$$

and boundary conditions,

$$u(0,t) = g_0(t), \quad \text{for all } 0 < t \le T, \tag{2.3}$$

$$u(1,t) = g_1(t), \quad \text{for all } 0 < t \le T, \tag{2.4}$$

Saline Water is water that contains a significant concentration of dissolved salts.

Advection is the transport of a substance. Most generally, the adverted substance is a fluid. An example of advection is the transport of pollutants or silt in a river by bulk water flow downstream.

Diffusion is the net movement of molecules or atoms from a region of high concentration to a region of low concentration (See Figure 2.2 - 2.4).

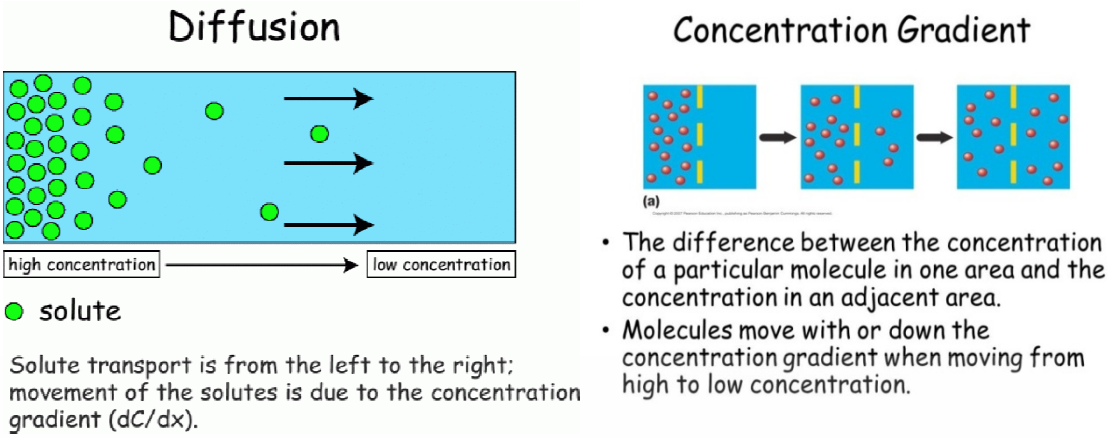

Figure 2.2 Showing diffusion of the substance [41].

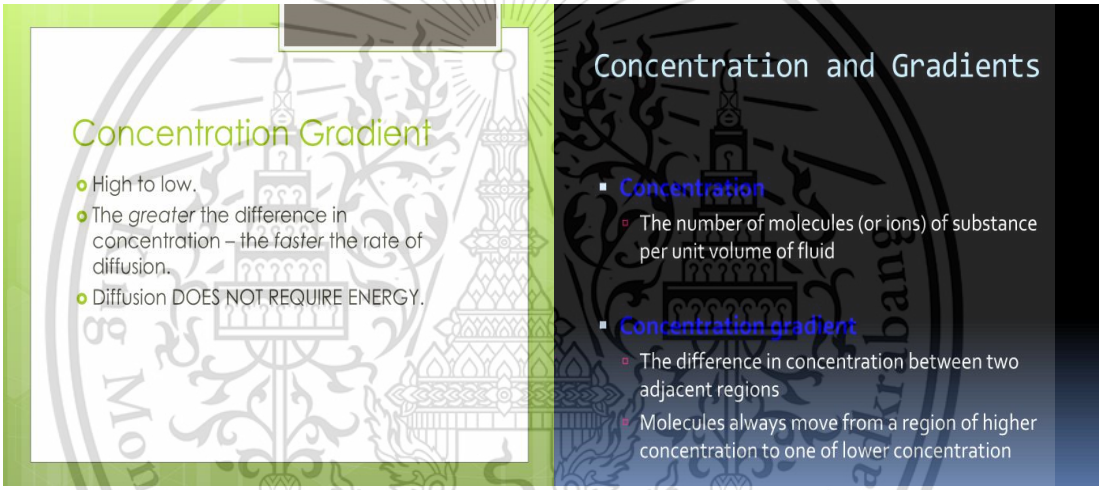

Figure 2.3 Showing diffusion of the substance [41].

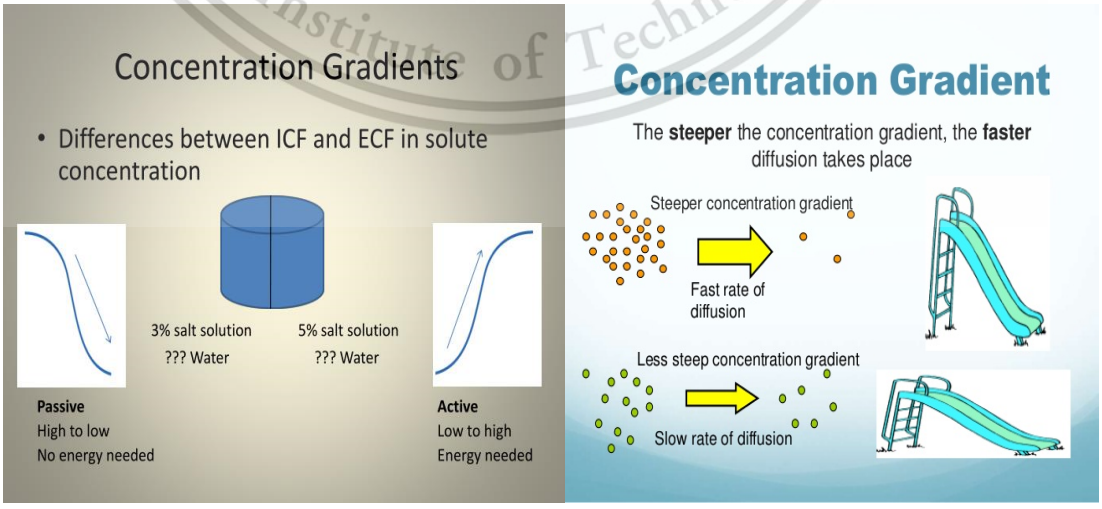

Figure 2.4 Diffusion of a substance [41].

Transient term is used to describe the rate of change of $c(x,t)$ the solute concentration per unit of time.

Radiation is the emission or transmission of energy in the form of waves or particles through space or through a material medium.

2.3 Exact solution of the problem

The known exact solution of the advection-diffusion equation with simple initial and boundary conditions is used to test the two numerical methods. These methods are applied to solve (2.1) - (2.4) [17].

Consider (2.1) - (2.4) with

$$f(x) = \exp(-\frac{(x+0.5^2)}{0.00125}), \tag{2.5}$$

$$g_0(0,t) = \frac{0.025}{\sqrt{0.000625+0.02t}} \exp\left(-\frac{(0.5-t)^2}{(0.00125+0.04t)}\right), \tag{2.6}$$

$$g_1(1,t) = \frac{0.025}{\sqrt{0.000625+0.02t}} \exp\left(-\frac{(1.5-t)^2}{(0.00125+0.04t)}\right), \tag{2.7}$$

$$\alpha = 0.01 \ , \beta = 1.0,$$

for which the exact solution is

$$u(x,t) = \frac{0.025}{\sqrt{0.000625+0.02t}} \exp\left(-\frac{(x+0.5-t)^2}{(0.00125+0.04t)}\right), \tag{2.8}$$

and the theoretical solution to the problem is [11,15]

$$C(x,t) = \frac{1}{2}\, erfc\, (\frac{x-Ut}{\sqrt{4Dt}}) + \frac{1}{2} \exp\,(\frac{Ux}{D})\, erfc\left(\frac{x+Ut}{\sqrt{4Dt}}\right). \tag{2.9}$$

2.4 Two Explicit Schemes for numerically solving the Advection-Diffusion-Equation

Consider the following approximation of the derivatives in the advection – diffusion equation (2.1) that incorporates a weight ϕ as follows [17];

$$\left.\frac{\partial u}{\partial t}\right|_i^n + \beta \left.\frac{\partial u}{\partial x}\right|_i^n = \alpha \left.\frac{\partial^2 u}{\partial x^2}\right|_i^n, \tag{2.10}$$

$$\left.\frac{\partial u}{\partial t}\right|_i^n = \frac{\left(u_i^{n+1} - u_i^n\right)}{\Delta t}, \tag{2.11}$$

$$\left.\frac{\partial u}{\partial x}\right|_i^n = \phi \frac{\left(u_i^{n+1} - u_{i-1}^n\right)}{\Delta x} + (1-\phi)\frac{\left(u_{i+1}^n - u_{i-1}^n\right)}{2\Delta x}, \tag{2.12}$$

$$\left.\frac{\partial^2 u}{\partial x^2}\right|_i^n = \frac{\left(u_{i+1}^n - 2u_i^n - u_{i-1}^n\right)}{(\Delta x)^2}. \tag{2.13}$$

This gives the weighted explicit finite-difference formula below,

$$u_i^{n+1} = \frac{1}{2}\left(2s + c(1+\phi)\right)u_{i-1}^n + \left(1 - 2s - c\phi\right)u_i^n + \frac{1}{2}\left(2s - c(1-\phi)\right)u_{i+1}^n, \tag{2.14}$$

for $1 \le i \le M-1$ and $0 \le n \le N-1$,

where

$$c = \beta \frac{\Delta t}{\Delta x} \tag{2.15}$$

and

$$s = \alpha \frac{\Delta t}{(\Delta x)^2}. \tag{2.16}$$

A Von Neumann stability of (2.14) yielded [39] the stability condition

$$\frac{\left(c^2 - c\phi\right)}{2} \le s \le \frac{\left(1 - c\phi\right)}{2}. \tag{2.17}$$

The modified equivalent partial differential equation of this method is in the following form [17];

$$\frac{\partial u}{\partial t} + \beta \frac{\partial u}{\partial x} - \left(\alpha + \frac{\beta \Delta x}{2}\left(\phi - c\right)\right)\frac{\partial^2 u}{\partial x^2} + \frac{\beta \left(\Delta x\right)^2}{6}\left(1 - 6s - 3c\phi + 2c^2\right)\frac{\partial^3 u}{\partial x^3} + o\left(\left(\Delta x\right)^3\right) = 0. \tag{2.18}$$

It is notable that the amounts of numerical diffusion are independent of the values of s , although the usable range of c changes with s .

2.4.1 Forward-Time Central-Space (FTCS) Explicit Finite Difference Scheme

Putting $\phi = 0$ in (2.14) gives the following FTCS scheme finite difference formula for solving the advection-diffusion equation.

$$u_i^{n+1} = \frac{1}{2}(2s + c)u_{i-1}^n + \left(1 - 2s\right)u_i^n + \frac{1}{2}\left(2s - c\right)u_{i-1}^n. \tag{2.19}$$

This scheme is stable [17] in the following region,

$$\frac{c^2}{2} \le s \le \frac{1}{2}. \tag{2.20}$$

2.4.2 MacCormack Explicit Finite Difference Scheme

In a stream water quality model, the governing equations are the dynamic one-dimensional advection-dispersion-reaction equations (ADREs). A simplified representation, by averaging the equation over the depth, is reported in [26-28,29,31] as follows:

$$\begin{aligned}\frac{\partial u}{\partial t}+\frac{\partial d}{\partial x}&=-u,\\ \frac{\partial d}{\partial t}+\frac{\partial u}{\partial x}&=0,\end{aligned} \tag{2.21}$$

with the initial conditions $u=0 and\, d=0$ at $t=0$ and boundary conditions $d(0,t)=f(t)$ and $\partial d/\partial x=0$ at $x=1$.

$$\frac{\partial C}{\partial t}+u\frac{\partial C}{\partial x}=D\frac{\partial^2 C}{\partial x^2}-KC, \tag{2.22}$$

First of all, we consider the traditional MacCormack scheme. The scheme is an explicit finite difference scheme with a two-step predictor-corrector method. The first step is a modification of forward time central space (FTCS) by changing the central space evaluation at time n to a forward space evaluation. This step is a forward time forward space (FTFS) scheme. The FTFS scheme approximates the temporal and special derivatives and the decay in (2.21) in the following description.

We can approximate $C(x_i,t_n)$ with C_i^n, the value of the difference approximation of $C(x,t)$ at point $x=i\Delta x$ and $t=n\Delta t$, where $0\le i\le M$ and $0\le n\le N$. The grid point (x_n,t_n) is defined by $x_i=i\Delta x$ for all $i=0,1,2,...,M$ and $t_n=n\Delta t$ for all $n=0,1,2,...,N$ in which M and N are positive integers. Using the forward time forward space technique [27,33] with (2.21), we get the following discretization: [14]

$$\begin{aligned}C&\cong C_i^n,\\ \frac{\partial C}{\partial t}&\cong\frac{C_i^{n+1}-C_i^n}{\Delta t},\\ \frac{\partial C}{\partial x}&\cong\frac{C_{i+1}^n-C_i^n}{\Delta t},\\ \frac{\partial^2 C}{\partial x^2}&\cong\frac{C_{i+1}^n-2C_i^n+C_{i-1}^n}{\Delta t},\\ u&\cong\widehat{U_i^n}.\end{aligned} \tag{2.23}$$

Note that $\widehat{U_i^n}$ can be determined by applying Crank-Nicolson method to the hydrodynamic model of (2.21) [30, 31, and 32].

Substituting (2.23) into (2.22), we get

$$\frac{C_i^{n+1}-C_i^n}{\Delta t}+\widehat{U}_i^n\left(\frac{C_{i+1}^n-C_i^n}{\Delta x}\right) = D\left(\frac{C_{i+1}^n-2C_i^n+C_{i-1}^n}{(\Delta x)^2}\right)-KC_i^n, \tag{2.24}$$

for $1\le i\le M$ and $0\le n\le N-1$. Substitute the difference equation into (2.24), and then define slope S_{i_1} as

$$S_{i_1}=-\widehat{U_i^n}\left(\frac{C_{i+1}^n-C_i^n}{\Delta x}\right)+D\left(\frac{C_{i+1}^n-2C_i^n+C_{i-1}^n}{(\Delta x)^2}\right)-KC_i^n. \tag{2.25}$$

Let $\lambda=D\Delta t/(\Delta x)^2$ and $\gamma_i^{n+1}=(\Delta t/\Delta x)\widehat{U_i^{n+1}}$, and then define $\gamma_i^{'n}=\gamma_i^n/\Delta t=\widehat{U_i^n}/\Delta x$ and $\gamma^{'}=D/(\Delta x)^2=\lambda/\Delta t$. Equation (2.25) takes a simplified form:

$$S_{i_1}=-\gamma_i^{'n}(C_{i+1}^n-C_i^n)+\lambda'(C_{i+1}^n-2C_i^n+C_{i-1}^n)-KC_i^n, \tag{2.26}$$

or

$$S_{i_1}=(\lambda'-\gamma_i^{'n})C_{i+1}^n-(2\lambda'-\gamma_i^{'n}+K)C_i^n+\lambda' C_{i-1}^n. \tag{2.27}$$

For the upper boundary, where $i=1$, plug the known value of the left boundary $C_0^n=C_0$ to (2.27) in the right hand side; we obtain

$$S_{1_i}=(\lambda'-\gamma_1^{'n})C_2^n-(2\lambda'-\gamma_1^{'n}+K)C_1^n+\lambda' C_0^n. \tag{2.28}$$

For the lower boundary, where $i=M$, substitute the approximate unknown value of the right boundary with the forward difference approximation to $\partial C/\partial x=0$. Let $C_M=C_{M-1}$ and rearrange; we obtain

$$S_{M_1}=-\left(\lambda'+K\right)C_{M-1}^n+\lambda' C_{M-2}^n.$$

From the Euler formula, we obtain the MacCormack predictor step formulation:

$$C_i^{n+1} = C_i^n + S_{i_1}\Delta t. \tag{2.29}$$

The second step is a modified backward time central space (BTCS) scheme. The central space evaluation time n is replaced with a backward space evaluation time. It is essentially a backward time space (BTBS) scheme. The BTBS scheme approximates the temporal and spatial derivatives and the decay in (2.22) with the following discretization:

$$\begin{aligned} C &\cong \frac{1}{2}(C_i^n + C_i^{n+1}), \\ \frac{\partial C}{\partial t} &\cong \frac{C_i^{n+1} - C_i^n}{\Delta t}, \\ \frac{\partial C}{\partial x} &= \frac{C_i^{n+1} - C_i^n}{\Delta t}, \\ \frac{\partial^2 C}{\partial x^2} &\cong \frac{1}{2}\left(\frac{C_{i+1}^n - 2C_i^n + C_{i-1}^n}{(\Delta x)^2} + \frac{C_{i+1}^{n+1} - 2C_i^{n+1} + C_{i-i}^{n+1}}{(\Delta x)^2} \right). \end{aligned} \tag{2.30}$$

Because the value at time $n+1$ have been calculated in the predictor step, this second step is also explicit. It follows that the slope based on their predictor points can be calculated as follows:

$$S_{i_2} = \lambda' C_{i+1}^{n+1} - (2\lambda' + \gamma_i'^{n+1} + K)C_i^{n+1} + \left(\lambda' + \gamma_i'^{n+1} \right) C_{i-1}^{n+1}. \tag{2.31}$$

For the upper boundary, where $i = 1,$ plugging in the known value of the left boundary $C_0^{n+1} = C_0$ to the right hand side of (2.31), we obtain

$$S_{1_2} = \lambda' C_2^{n+1} - (2\lambda' + \gamma_1'^{n+1} + K)C_1^{n+1} + \left(\lambda' + \gamma_1'^{n+1} \right) C_0. \tag{2.32}$$

For the lower boundary, where $i = M,$ substituting the unknown value of the right boundary by the backward difference approximation to $\frac{\partial C}{\partial x} = 0$ and letting $C_{M+1} = C_M$ and rearranging the equation; we obtain

$$S_{M_2} = \lambda' C_M^{n+1} - \left(2\lambda' + \gamma_M'^{n+1} + K \right) C_M^{n+1} + (\lambda' + \gamma_M'^{n+1}) C_{M-1}^{n+1}. \quad (2.33)$$

From both steps, the MacCormack scheme takes the following from:

$$C_i^{n+1} = C_i^n + \frac{\Delta t}{2}(S_{i_1} + S_{i_2}).$$

The MacCormack scheme is conditionally stable subjected to the constraints in (2.24). The stability requirements for the scheme are [34]

$$\lambda = \frac{D\Delta t}{(\Delta x)^2} < \frac{1}{2}, \qquad \gamma_i^n = \frac{\widehat{U_i^n}}{\Delta x} < 0.9. \quad (2.34)$$

where λ, the diffusion coefficient, is a number (dimensionless) and γ_i^n is the advection number or Courant number (dimensionless).

2.5 Interpolation techniques

2.5.1 Lagrange interpolating polynomials

Since Taylor polynomials are not appropriate for interpolation, alternative methods are needed. In this section, we describe approximating polynomials that can be determined simply by specifying certain points on the plane through which they must pass.

The problem of determining a polynomial of degree 1 that passes through two distinct points (x_0, y_0) and (x_1, y_1) is the same as the problem of approximating a function f for which $f(x_0) = y_0$ and $f(x_1) = y_1$ by means of a first-degree polynomial interpolation that agrees with the values of f at some given points [22, 23].

Consider a linear polynomial

$$P(x) = \frac{(x - x_1)}{(x_0 - x_1)} y_0 + \frac{(x - x_0)}{(x_1 - x_0)} y_1.$$

When $x = x_0$,

$$P(x_0) = 1.y_0 + 0.y_1 + y_0 = f(x_0),$$

and when $x = x_1$,

$$P(x_1) = 0.y_0 + 1.y_1 = y_1 = f(x_1),$$

so P has the required properties (See Figure 2.2). The technique used for constructing P is a method of "interpolation" often applied when one wants to find an exact value from a finite number of entries in trigonometric or logarithmic tables.

To generalize the concept of linear interpolation, consider the construction of a polynomial of degree at most n that passes through the $n+1$ points $(x_0, f(x_0)), (x_1, f(x_1)), ..., (x_n, f(x_n))$. (See Figure 2.5-2.6) The linear polynomial passing through $(x_0, f(x_0))$ and $(x_1, f(x_1))$ is constructed by using the quotients

$$L_0(x) = \frac{(x - x_1)}{(x_0 - x_1)} \quad \text{and} \quad L_1(x) = \frac{(x - x_0)}{(x_1 - x_0)},$$

when $x = x_0, L_0(x_0) = 1$ and $L_1(x_0) = 0$ and when $x = x_1, L_0(x_1) = 0$ and $L_1(x_1) = 1$.

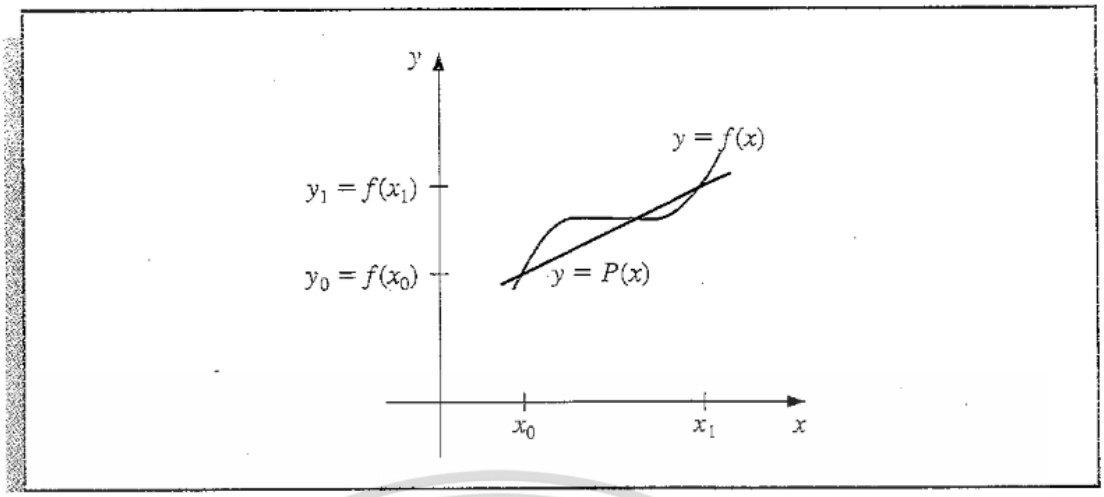

Figure 2.5 A linear polynomial passing through $(x_0, f(x_0))$ and $(x_1, f(x_1))$.

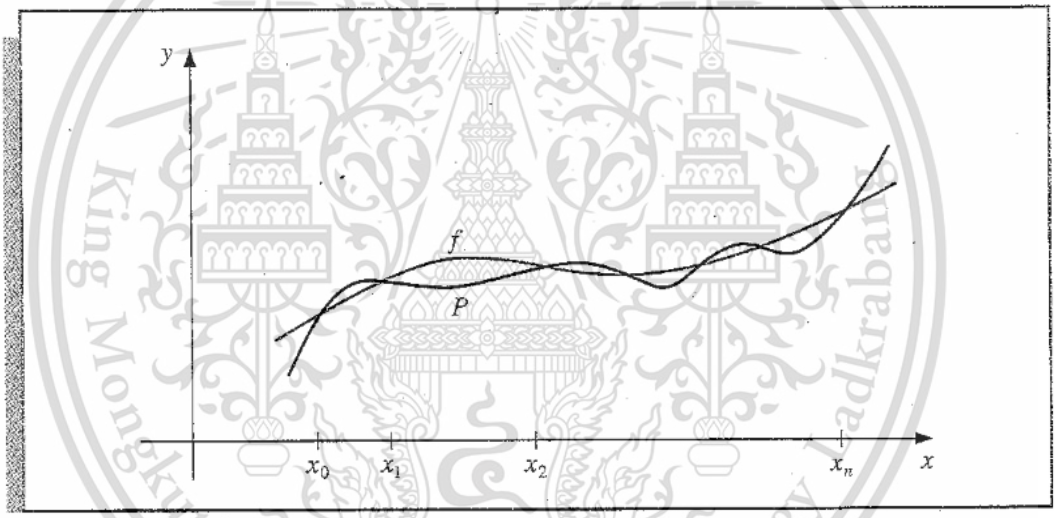

Figure 2.6 A polynomial of degree at least 2 passing through $(x_0, f(x_0)), (x_1, f(x_1)), ..., (x_n, f(x_n))$ points.

For the general case, we need to construct, for each $k = 0,1,...,n$, a quotient $L_{n,k}(x)$ with properties that $L_{n,k}(x_i) = 0$ when $i \neq k$ and $L_{n,k}(x_k) = 1$. To satisfy $L_{n,k}(x_i) = 0$, for each $i \neq k$, it requires that the numerator of $L_{n,k}$ contains the term

$$(x - x_0)(x - x_1)...(x - x_{k-1})(x - x_{k+1})...(x - x_n). \tag{2.35}$$

To satisfy $L_{n,k}(x_k) = 1$, the denominator of L_k must be equal to (2.35) evaluated at $x = x_k$.

Thus,

$$L_{n,k}(x) = \frac{(x-x_0)...(x-x_{k-1})(x-x_{k+1})...(x-x_n)}{(x_k-x_0)...(x_k-x_{k-1})(x_k-x_{k+1})...(x_k-x_n)}$$
$$= \prod_{\substack{i=0 \\ i\neq k}}^{n} \frac{(x-x_i)}{(x_k-x_i)}.$$

A sketch of the graph of a typical $L_{n,k}$ (in the case where n is even and k is odd) is shown in Figure 2.7.

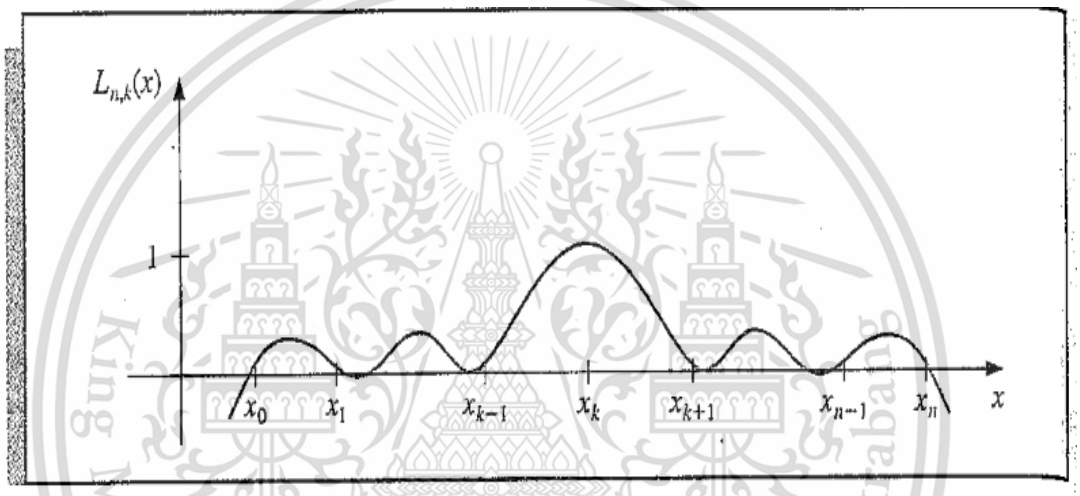

Figure 2.7 Showing a sketch of the graph of a typical $L_{n,k}$.

The interpolating polynomial is easily expressed when the form of $L_{n,k}$ is known. This polynomial, called the **Lagrange interpolating polynomial,** is defined in the following theorem.

Theorem 2.1 If $x_0, x_1, \ldots, x_n$ are $(n+1)$ distinct numbers and f is a function whose values are given at these number points, then there exists a unique polynomial P of degree at most n with a property that

$$f(x_k) = P(x_k) \quad \text{for each} \quad k = 0,1,...,n.$$

This polynomial is given by

$$P(x) = f(x_0)L_{n,0}(x) + \ldots + f(x_n)L_{n,n}(x) = y_1 = \sum_{k=0}^{n} f(x_k)L_{n,k}(x), \tag{2.36}$$

where

$$L_{n,k}(x) = \frac{(x-x_0)(x-x_1)\ldots(x-x_{k-1})(x-x_{k+1})\ldots(x-x_n)}{(x_k-x_0)(x_k-x_1)\ldots(x_k-x_{k-1})(x_k-x_{k+1})\ldots(x_k-x_n)} = \prod_{\substack{i=0 \\ i\neq k}}^{n} \frac{(x-x_i)}{(x_k-x_i)}, \tag{2.37}$$

for each $k = 0,1,\ldots,n.$

We write $L_{n,k}(x)$ simply as $L_k(x)$ when there is no confusion as to its degree.

2.5.2 Cubic spline interpolation

Previous sections of this chapter concern approximation of arbitrary functions on closed intervals by polynomials. The oscillatory nature of high–degree polynominal and its property that a fluctuation over a small portion of an interval can induce large fluctuations over the entire range restricts their use in many situations. As an example, consider the graph in Figure 2.8, which shows the Lagrange polynomial for the data given at the beginning of this chapter. Although the polynomial fits the data well, its behavior is abrupt beyond the endpoints [22, 23].

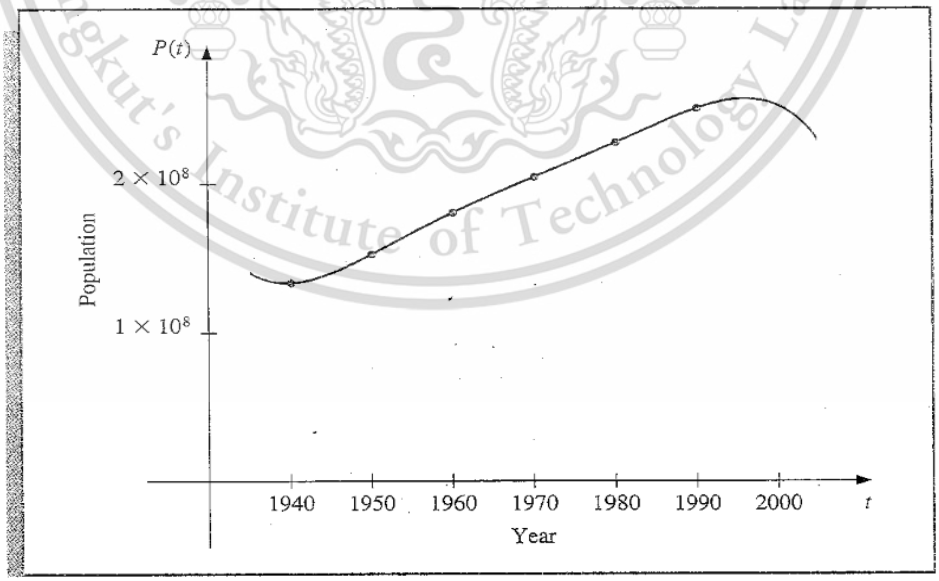

Figure 2.8 Lagrange polynomial for the collected measurement data.

An alternative approach is to divide the interval into a collection of subintervals and construct a (generally) different approximating polynomial for each subinterval. Approximation by functions of this type is called **piecewise polynomial approximation.**

The simplest piecewise polynomial approximation is piecewise linear interpolation, which consists of joining a set of data points

$$\{(x_0, f(x_0)), (x_1, f(x_1)), \ldots (x_n, f(x_n))\}$$

by a series of straight lines such as those shown in Figure 2.9. This is the method of interpolation used in elementary courses involving the study of trigonometric or logarithmic functions when intermediate values are required from a collection of tabulated values.

A disadvantage of linear function approximation is that at each of the endpoints of the subintervals, there is no assurance of differentiability, which, in a geometrical context, means that the interpolating function is not "smooth" at these points. Often, it is clear from the physical conditions that such a smoothness condition is required and that the approximating function must be continuously differentiable.

An alternative procedure is to use a piecewise polynomial of Hermit type. For example, if the values of the function f and f' are known at each of the points $x_0 < x_1 < \ldots < x_n$, a Hermit polynomial of degree three can be used on each of the

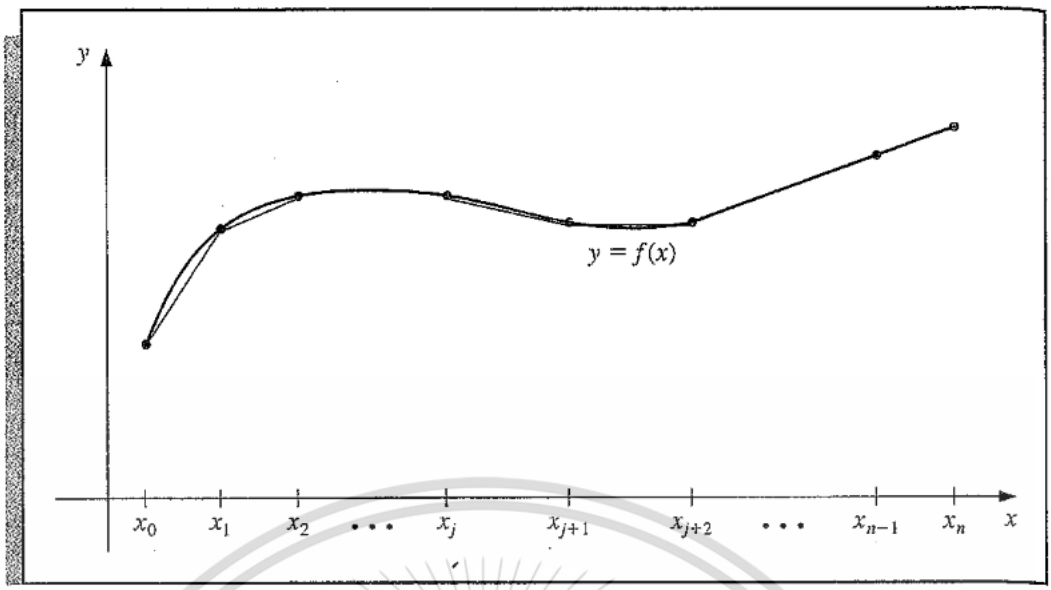

Figure 2.9 Simplest piecewise polynomial approximation, i.e., piecewise linear interpolation.

Subintervals $[x_0, x_1], [x_1, x_2], \ldots, [x_{n-1}, x_n]$ to obtain a function that is continuously differentiable on the interval $[x_0, x_n]$. To determine the appropriate Hermite cubic polynomial on a given interval is simply a matter of computing the function $H_3(x)$ for that interval. Since in the construction of the Lagrange interpolating polynomials, H_3 of the first degree needs to be determined, this can be accomplished without great difficulty. The problem with using Hermite piecewise polynomials for general interpolation concerns the need to know the derivative of the function being approximated. Often, the function is known but not its derivative.

The remainder of this section considers approximation using piecewise polynomials that requires no derivative information, except perhaps at the endpoints of the interval in which the function is being approximated.

The simplest type of differentiable piecewise polynomial function on an entire interval $[x_0, x_n]$ is the function obtained by fitting a quadratic polynomial between each successive pair of nodes. This is done by constructing a quadratic on $[x_0, x_1]$ that agrees with the function at x_0 and x_1. Then, constructing another quadratic on $[x_1, x_2]$ that agrees with the function at x_1 and x_2, and so on. Since a general quadratic polynomial has three arbitrary constants: a constant term, the coefficient of x, and the coefficient of x^2, and only two conditions are required to

fit the data at the endpoints of each subinterval, flexibility exists that allows the quadratic to be chosen so that the interpolating function has a continuous derivative on $[x_0, x_n]$. The difficulty with this procedure arises when there is a need to specify conditions about the derivative of the interpolating function at the endpoints x_0 and x_n when the number of constants are not sufficient to ensure that the conditions will be satisfied.

The most common piecewise polynomials approximation using cubic polynomials between each successive pair of nodes is called cubic spline interpolation. A general cubic polynomial involves four constants; so there is sufficient flexibility in the cubic spline procedure to ensure not only that the interpolating function is continuously differentiable on the interval, but also that it has a continuous second derivative on that interval. The construction of cubic spline does not, however, assume that the derivatives of the interpolating function agree with those of the function, even at the nodes (See Figure 2.10).

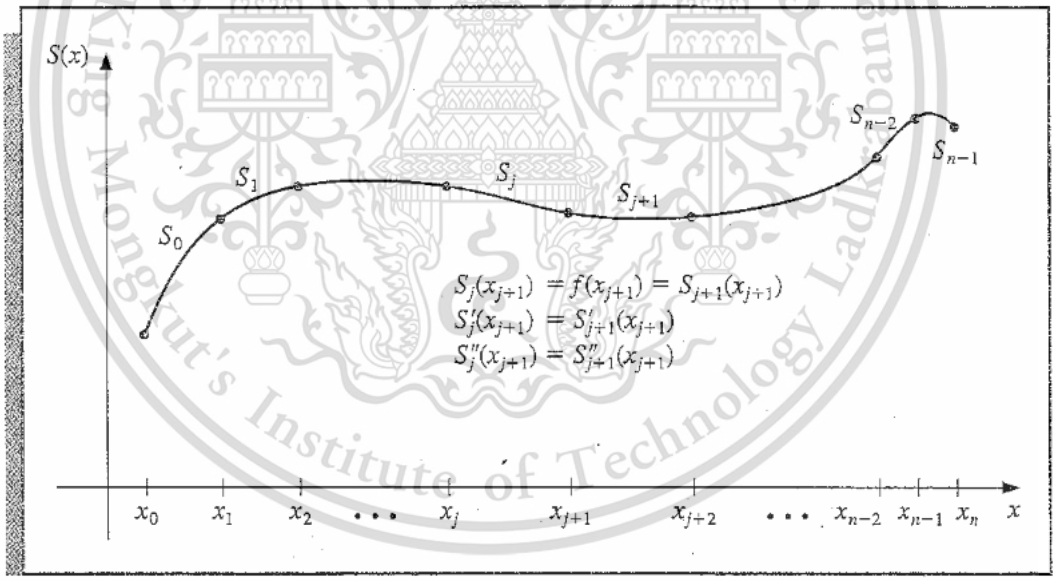

Figure 2.10 A general cubic polynomial.

Definition 2.1 Given a function f defined on $[a, b]$ and a set of numbers, called **nodes,** $a = x_0 < x_1 < \ldots < x_n = b$, **a cubic alpine interpolate,** S, for f is a function that satisfies the following conditions:

a. S is a cubic polynomial, denoted S_j, on subinterval $[x_j, x_{j+1}]$ for each $j = 0,1,\ldots,n-1$;

b. $S(x_j) = f(x_j)$ for each $j = 0,1,\ldots,n$;

c. $S_{j+1}(x_{j+1}) = S_j(x_{j+1})$ for each $j = 0,1,\ldots,n-2$;

d. $S'_{j+1}(x_{j+1}) = S'_j(x_{j+1})$ for each $j = 0,1,\ldots,n-2$;

e. $S''_{j+1}(x_{j+1}) = S''_j(x_{j+1})$ for each $j = 0,1,\ldots,n-2$;

f. One of the following sets of boundary conditions is satisfied:

(i) $S''(x_0) = S''(x_n) = 0$ **(free boundary)**

(ii) $S'(x_0) = f'(x_0)$ and $S'(x_n) = f'(x_n)$. **(clamped boundary)**

Although cubic splines can be defined with other boundary conditions, the given conditions are sufficient for our purpose. When the free boundary condition happens, the spline is called **a natural spline,** and its graph approximates the shape that a long flexible string would assume when it is forced to go through each of the data points $\{(x_0, f(x_0)), (x_1, f(x_1)), \ldots, (x_n, f(x_n))\}$.

In general, a clamped boundary condition leads to a more accurate approximation since it includes more information about the function. However, for this type of boundary condition to hold, it is necessary to have either the values of the derivative at the endpoints or an accurate approximation to those values.

To construct a cubic spline interpolate for a given function f , the conditions in the definition are applied to a cubic polynomial,

$$S_j(x) = a_j + b_j(x - x_j) + c_j(x - x_j)^2 + d_j(x - x_j)^3.$$

For each $j = 0,1,\ldots,n-1$.

Clearly,

$$S_j(x_j) = a_j = f(x_j),$$

and if condition (c) is applied,

$$a_{j+1} = S_{j+1}(x_{j+1}) = S_j(x_{j+1}) = a_j + b_j(x_{j+1} - x_j) + c_j(x_{j+1} - x_j)^2 + d_j(x_{j+1} - x_j)^3$$

for each $j = 0,1,\ldots,n-2$.

Since the term $(x_{j+1} - x_j)$ will be used repeatedly in this development, it is convenient to introduce a simpler notation,

$$h_j = x_{j+1} - x_j$$

for each $j = 0,1,...,n-1$. If we also define $a_n = f(x_n)$, then the equation

$$a_{j+1} = a_j + b_j h_j + c_j h_j^2 + d_j h_j^3 \tag{2.38}$$

holds for each $j = 0,1,...,n-1$.

In a similar manner, define $b_n = S'(x_n)$ and observe that

$$S'_j(x) = b_j + 2c_j(x - x_j) + 3d_j(x - x_j)^2$$

implies $S'_j(x_j) = b_j$ for each $j = 0,1,...,n-1$. Applying the condition (d), we have

$$b_{j+1} = b_j + 2c_j h_j + 3d_j h_j^2 \tag{2.39}$$

for each $j = 0,1,...,n-1$.

Another relation between the coefficients of S_j is obtained by defining $c_n = S''(x_n)/2$ and applying condition (e). In this case,

$$c_{j+1} = c_j + 3d_j h_j \tag{2.40}$$

for each $j = 0,1,...,n-1$.

Solving for d_j in Equation (2.40) and substituting this value into Equation (2.38) and (2.39) gives new equations,

$$a_{j+1} = a_j + b_j h_j + \frac{h_j^2}{3}(2c_j + c_{j+1}) \tag{2.41}$$

and

$$b_{j+1} = b_j + h_j(c_j + c_{j+1}), \tag{2.42}$$

for each $j = 0,1,...,n-1$.

The final relationship involving the coefficients is obtained by solving an appropriate equation in the form of equation (2.41), first for b_j,

$$b_j = \frac{1}{h_j}(a_{j+1} - a_j) - \frac{h_j}{3}(2c_j + c_{j+1}), \tag{2.43}$$

and then, with a reduction of the index, for b_{j-1},

$$b_{j-1} = \frac{1}{h_{j-1}}(a_j - a_{j-1}) - \frac{h_{j-1}}{3}(2c_{j-1} + c_j).$$

Substituting these values into the equation derived from Eq. (2.42), when the index is reduced by 1, gives the following linear system of equations

$$h_{j-1}c_{j+1} + 2(h_{j-1} - h_j)c_j + h_j c_{j+1} = \frac{1}{h_j}(a_{j+1} - a_j) - \frac{3}{h_{j-1}}(a_j + a_{j-1}) \tag{2.44}$$

for each $j = 1,2,...,n-1$. This system involves, as unknowns, only $\{c_j\}_j^n = 0$, The values of $\{h_j\}_{j=0}^{n-1}$ and $\{a_j\}_{j=0}^{n}$ are given by the spacing of the nodes $\{x_j\}_{j=0}^{n}$ and the values of f at the nodes.

Note that once the values of $\{c_j\}_{j=0}^{n}$ are known, it is a simple matter to find the remainder of the constants $\{b_j\}_{j=0}^{n-1}$ from Eg. (2.43) and $\{d_j\}_{j=0}^{n-1}$ from Eq. (2.40) as well as to construct the cubic polynomial $\{S_j\}_{j=0}^{n-1}$.

The major question that arises in connection with this constructions is whether the values of $\{c_j\}_j^n = 0$ can be found by using the system of equations given in (2.44), and if so, whether these values are unique. The following theorems indicate that, when either of the boundary conditions given in part (f) of the definition are imposed, the answer to both questions is affirmative. The proofs of these theorems require some material from linear algebra, which is discussed in Chapter 6.

Theorem 2.2 If f is defined at $a = x_0 < x_1 < ... < x_n = b$, then f has a unique natural spline interpolate on the nodes $x_0, x_1, ..., x_n$, that is, a spline interpolate that satisfies the boundary conditions $S''(a) = 0$ and $S''(b) = 0$.

Proof The boundary conditions in this case imply that $C_n = S''(x_n)/2 = 0$ and that

$$0 = S''(x_0) = 2c_0 + 6d_0(x_0 - x_0);$$

so

$$c_0 = 0.$$

The two equations $c_0 = 0$ and $c_n = 0$ together with the equations in (2.44) produce a linear system described by a vector equation ***Ax=b***, where ***A*** is the $(n+1)$ by $(n+1)$ matrix,

$$A = \begin{bmatrix} 1 & 0 & 0 & & & 0 \\ h_0 & 2(h_0+h_1) & h_1 & & & \\ 0 & h_1 & 2(h_1+h_2) & h_2 & & 0 \\ & & \ddots & \ddots & \ddots & \\ & & h_{n-2} & 2(h_{n-2}+h_{n-1}) & h_{n-1} & \\ 0 & & 0 & 0 & 1 & \end{bmatrix},$$

and **b** and **x** are vectors.

$$b = \begin{bmatrix} 0 \\ \frac{3}{h_1}(a_2 - a_1) - \frac{3}{h_0}(a_1 - a_0) \\ \vdots \\ \frac{3}{h_{n-1}}(a_n - a_{n-1}) - \frac{3}{h_{n-2}}(a_{n-1} - a_{n-2}) \\ 0 \end{bmatrix} \text{ and } x = \begin{bmatrix} c_0 \\ c_1 \\ \vdots \\ c_n \end{bmatrix}.$$

The matrix ***A*** is strictly diagonally dominant, so it satisfies the hypotheses of Theorem 6.19 in Section 6.6. Therefore, the linear system has a unique solution for $c_0, c_1, \ldots, c_n$.

The solution to a cubic spline problem with boundary conditions $S''(x_0) = S''(x_n) = 0$ can be obtained by applying Algorithm 3.4.

2.6 Literature review

There have been many researchers who investigated about water-quality models for streams and rivers as follows.

In [3], focused on salinity intrusion in the area of Tha Chin estuarine, Thailand. He developed a mathematical model called "MIKE-HD/AD" and showed that the model can be applied to forecasting of natural phenomena related to salinity intrusion. The model predicted that the maximum distance of salinity intrusion would reach 55 km. or about 3 km. further up the river in 2025. Therefore, a measure for controlling the salinity intrusion needs to be formulate. One way is to increase the freshwater flow rate in the Tha Chin River, which would help pushing against the salinity intrusion. His simulation showed that the most suitable flow rate for the case of this Tha Chin River was about 20-40 m^3/s. A higher flow rate would not help pushing against the salinity intrusion any better.

In [5], investigated longitudinal salinity intrusion as well as dispersion in Tha Chin River caused by the rise of sea level. In his investigation, he applied a mathematical simulation called "MIKE11-HD/AD" developed by DHI Water Environment and Health. Actually, two competitive models were used in this study: MIKE11-AD, and a hydrodynamic Module to forecast dispersion and salinity intrusion along the mentioned river. It was found that the coefficient of salinity dispersion was 400 m^2/s according to the data of 2010.

In [6], also used MIKE11-HD and a Hydrodynamic Module developed by DHI Water Environment and Health to simulate salinity intrusion in Tha Chin River. The simulations included the hydrography of the river, the dispersion of salinity intrusion along the river, and a way to solve the salinity intrusion problem in agricultural areas. They suggested that freshwater released from the upriver dam at a rate of 40 m^3/s can push against the intrusion and maintain the salinity level at less than or equal to 0.75 g/l in those areas.

In [7], investigated the salinity intrusion in the lower Tha Chin River affected by the addition of shortcut canals. The additional canals were dug in order to drain water quickly away from Bangkok during the rainy season. The MIKE11-AD and Advection-Dispersion Model estimated that the coefficients of salinity dispersion in

the Tha Chin River were 400 $m^2/2$ and showed that the addition of shortcut canals caused more salinity intrusion.

In [8], investigated the effects of climate change on sea level rise and how the sea level rise affected hydraulic conditions, water supply, salinity level, and agricultural areas in the lower area of Chao Phraya River by using MIKE 11 model. The model itself was divided into two parts: a hydrodynamic model and an advection-dispersion model. Calibrations of both models were done by adjusting their own key coefficients. Scenarios from the IPCC SRES (RCP8.5) report were simulated, showing that sea level rise would reach 1.16 meters in 2100. In addition to this, the salinity level at Samlae Pumping Station would also rise to around 0.37 - 0.75 g/l, exceeding the standard salinity level for freshwater supply. It would also exceed the standard for agricultural areas. The findings from this particular study provide a good guideline for water-work authorities in terms of raw water resource management for production of water supply and water used for agricultural purposes in the Chao Phraya River Basin.

In [9], came up with a numerical modeling of salinity's advective transport in the coastal areas, associated with artificial diffusion and using upstream differences. This model could be used with small grids of two to four kilometers in the case of tidal problems, while larger grids can be used for non-tidal problems.

In [10], used a tidally and cross-sectionally averaged model with Hansen and Rattray equation to simulate salinity distribution as well as vertical exchange flow along the estuary of Hudson River. They simulated the distribution and exchange flow in the northern San Francisco Bay and Hudson River. Despite a huge difference in terms of bathymetry, this approach could be used with other estuaries. However, an alternative approach should be used when there are inconsistencies between observations and simulated results.

In [11], aimed to create "numerical solutions of one-dimensional advection-diffusion equation using a sixth-order compact difference scheme in space and a four-order Runge-Kutta scheme in time". The solution scheme was quite flexible at solving the equation of contaminant transport, and the particular solutions were very accurate.

In [12], simulated pollution caused by sewage effluent in the nonuniform water flow in a stream with inconsistency in current velocity with two mathematical

models: Crank-Nicolson hydrodynamic model and backward time central space scheme dispersion model. He clearly showed that this particular model could actually be applied to real cases related to sewage effluent in canals connected to other reservoirs or streams.

In [13], focuses on a better version of the finite difference scheme for solving the advection-dispersion-reaction equation (ADRE) by considering the effect of the stream's nonuniform water flow. Two models, a hydrodynamic model and an advection-dispersion-reaction model, were used to simulate pollution from sewage effluent. Crank-Nicolson hydrodynamic model as well as an explicit scheme of the dispersion model were used as numerical techniques. The author revised and modified the explicit scheme of the dispersion model with forward time central space (FTCS) and Saulyev schemes. Both schemes were compared in terms of stability in order to show how they could be applied to real-world problems.

In [14], developed two mathematical models formulated as one-dimensional equations: a hydrodynamic model related to elevation of water and flow velocity field and a dispersion model related to pollutant concentration field. The models simulated the quality of water in a nonuniform flow stream. The traditional Crank-Nicolson method was used as the numerical technique in the first model. The second model used velocity fields of water calculated from the hydrodynamic model. The numerical technique in the model was a modified MacCormack method. The author proposed a modified MacCormack scheme for better prediction accuracy with no major loss of computational efficiency.

In [15], simulated the quality of water in a nonuniform flow stream similar to [12-15]. The first model was the same hydrodynamic model he used in those works, while the second was an advection-diffusion-reaction model that provided pollutant concentration field. Both models were in the form of one-dimensional equations. Similar to those prior works, the traditional Crank-Nicolson technique was used in the first model. The advection-diffusion-reaction model used velocity fields of the flow calculated from the first model as input. This second model used a new fourth-order scheme and a Saulyev scheme as numerical techniques. These simple alterations to these two schemes helped improve the prediction accuracy compared to that provided by traditional schemes.

In [16], used a finite difference method to solve “the one-dimensional steady convection-diffusion equation with variable coefficients”, and the results were used to optimize the costs of water treatment.

In [17], developed several numerical methods based on the two-level finite difference approximation to solve one-dimensional advection-diffusion equation with constant coefficient. The development was based on a modified version of equivalent partial differential equation approach, developed by Warming and Hyett in 1974. The modified approach allowed for acceptable errors. As a result, these new methods were more precise and efficient than conventional techniques. The new schemes were also without numerical diffusion.

In [18], used a finite volume method to estimate solutions to pollutant concentration equation. Their model was a one-dimensional model of water quality measurement in a stream. The solutions provided rational results that could be applied to water quality measurement.

In [19], used a finite element technique to solve one-dimensional steady convection-diffusion equation with constant coefficients to optimize costs of water treatment. The results led to a way to lower water pollution level down to the standard level with a minimum cost.

In [20], used an Optimal Homotopy Asymptotic Method (OHAM) to simulate the dispersion of pollutants in water. The numerical technique used was Runge-Kutta-Fehlberg fourth-fifth order method. The end results showed that the OHAM solution and the numerical solution agreed well.

In [34], a connection was reported between cubic spline and a popular compact finite difference formula. The author claimed that nonuniform meshes provide some advantages, while uniform meshes provide an additional way to help treat edge effects.

In [35], data were interpolated with two types of cubic spline function- cubic spline interpolation C^2 continuity and Piecewise Cubic Hermite Spline (PCHIP) with C^1 continuity. Both cubic splines were numerically compared with each other as well as with linear splines. They were all in good agreement.

In [36], made some simple modifications to Saulyev and MacCormack schemes and used them in stream water quality modeling. The modified schemes were used to solve a dynamic one-dimensional advection-dispersion-reaction

equation (ADRE). The schemes provided a better prediction accuracy with no major loss in efficiency.

In [37], compared teeth method to cubic spline method in terms of modeling error in modeling children's teeth: an example shows the efficiency, accuracy, and simplicity of the cubic spline method.

Chapter 3
Research methodology

3.1 One-dimensional salinity intrusion model with a diversion dam

3.1.1 The governing equation

The mathematical model simulating transportation and diffusion processes is a one-dimensional advection-diffusion-reaction equation (ADRE). The advection-diffusion equation is [9, 11, 15, and 17]

$$\frac{\partial S}{\partial t}+U\frac{\partial S}{\partial x}=D\frac{\partial^2 S}{\partial x^2},\ \text{for all}\ \ 0\le x\le L\ \ \text{and}\ \ \ 0\le t\le T \tag{3.1}$$

where $S(x,t)$ is salinity level (g/l); U is water flow velocity in the x-direction (m/s); D is salinity diffusion coefficient (m^2/s); L is the length of a condimental stream; and T is the stationary time of simulation.

Let

$$U=(u_s-ku_w). \tag{3.2}$$

Substitute equation (3.2) into equation (3.1), we get

$$\frac{\partial S}{\partial t}+(u_s-ku_w)\frac{\partial S}{\partial x}=D\frac{\partial^2 S}{\partial x^2}, \tag{3.3}$$

where u_s is salinity flow velocity; u_w is freshwater flow velocity released by the diversion dam; and k is salinity dilution rate by freshwater, for all $0<x\le L, 0\le t\le T$.

3.1.2 Initial and boundary conditions

The effects of salinity intrusion into an estuarine, which are likely to become more severe in the future, are caused by ocean tides. The initial salinity values are different depending on the measurement time and the location or distance along the river.

3.1.2.1 Initial condition

The initial condition was assumed to be

$$S(x,0) = f(x), \text{ for all } 0 \le x \le L \tag{3.4}$$

where $f(x)$ is a given salinity level function along a considered river.

3.1.2.2 Boundary conditions

The left boundary condition was assumed to be

$$S(0,t) = g(t), \text{ for all } 0 < t \le T, \tag{3.5}$$

where $g(t)$ is a given salinity level function at the first monitoring station. The right boundary condition was assumed to be

$$\frac{\partial S}{\partial x}(L,t) = k_0, \quad \text{for all } 0 < t \le T, \tag{3.6}$$

where k_0 is the rate of change of salinity level at the last monitoring station.

3.2 Numerical techniques

Salinity level was approximated by using two explicit finite difference methods. We could approximate $S(x_i, t_n)$ by S_i^n, the value of the difference approximate of $S(x,t)$ at point $x = i\Delta x$ and $t = n\Delta t$, where $0 \le i \le n$ and $0 \le n \le N$. Grid point (x_i, t_n) is defined as $x_i = i\Delta x$, for all $i = 0,1,2,...,M$ and $t_n = n\Delta t$ for all $n = 0,1,2,...,N$, in which M and N are positive integers.

3.2.1 Forward-time central-space (FTCS)

We define the terms of Equation (3.3) according to [13]

$$S \cong S_i^n, \tag{3.7}$$

$$\frac{\partial S}{\partial x} \cong \frac{S_i^{n+1} - S_1^n}{\Delta t}, \tag{3.8}$$

$$\frac{\partial S}{\partial x} \cong \frac{S_{i+1}^n - S_{i-1}^n}{2\Delta x}, \tag{3.9}$$

$$\frac{\partial^2 S}{\partial x^2} \cong \frac{S_{i+1}^{n+1} - 2S_1^n + S_{i-1}^n}{(\Delta x)^2}, \tag{3.10}$$

$$u_s = u_{s_i}^n, \tag{3.11}$$

$$u_w = u_{w_i}^n. \tag{3.12}$$

Substituting the forward-time central-space terms in Equations (3.7) - (3.12) into Equation (3.3), we get the following discretization:

$$\frac{S_i^{n+1} - S_i^n}{\Delta t} + (u_{s_i}^n - k u_{w_i}^n)\left(\frac{S_{i+1}^n - S_{i-1}^n}{2\Delta x}\right) = D\left(\frac{S_{i+1}^n - 2S_i^n + S_{i-1}^n}{(\Delta x)^2}\right). \tag{3.13}$$

It follows that

$$\begin{aligned} S_i^{n+1} &= \frac{\Delta t D}{(\Delta x)^2}\left(S_{i+1}^n - 2S_i^n + S_{i-1}^n\right) - \frac{(u_{s_i}^n - k u_{w_i}^n)\Delta t}{2\Delta x}\left(S_{i+1}^n - S_{i-1}^n\right) + S_i^n, \\ &= \frac{\Delta t D}{(\Delta x)^2} S_{i+1}^n - \frac{2\Delta t D}{(\Delta x)^2} S_i^n + \frac{\Delta t D}{(\Delta x)^2} S_{i-1}^n - \frac{(u_{s_i}^n - k u_{w_i}^n)\Delta t}{2\Delta x} S_{i+1}^n + \frac{(u_{s_i}^n - k u_{w_i}^n)\Delta t}{2\Delta x} S_{i-1}^n + S_i^n, \\ &= \left(\frac{\Delta t D}{(\Delta x)^2} + \frac{(u_{s_i}^n - k u_{w_i}^n)\Delta t}{2\Delta x}\right) S_{i+1}^n + \left(-\frac{2\Delta t D}{(\Delta x)^2} + 1\right) S_i^n + \left(\frac{\Delta t D}{(\Delta x)^2} - \frac{(u_{s_i}^n - k u_{w_i}^n)\Delta t}{2\Delta x}\right) S_{i+1}^n, \end{aligned} \tag{3.14}$$

where $$\lambda = \frac{D\Delta t}{(\Delta t)^2}, \tag{3.15}$$

and $$\gamma_i^n = \frac{\Delta t}{\Delta x}(u_{s_i}^n - k u_{w_i}^n), \tag{3.16}$$

$$= \left(\lambda + \frac{1}{2}\gamma_i^n\right) S_{i+1}^n + (-2\lambda + 1) S_i^n + \left(\lambda - \frac{1}{2}\gamma_i^n\right) S_{i+1}^n. \tag{3.17}$$

3.2.2 MacCormack Scheme for the advection equation

We assume that the length of the river is $L=1$. We also assume that the salinity level at the initial condition in the first step of the MacCormack scheme was approximated by Equation (3.3) by forward time and forward space scheme (FTFS) as follows [14],

$$S \cong S_i^n, \tag{3.18}$$

$$\frac{\partial S}{\partial t} \cong \frac{S_i^{n+1} - S_i^n}{\Delta t}, \tag{3.19}$$

$$\frac{\partial S}{\partial x} \cong \frac{S_{i+1}^n - S_i^n}{\Delta x}, \tag{3.20}$$

$$\frac{\partial^2 S}{\partial x^2} \cong \frac{S_{i+1}^n - 2S_i^n + S_{i-1}^n}{(\Delta x)^2} \tag{3.21}$$

$$u_s = u_{s_i}^n, \tag{3.22}$$

$$u_w = u_{w_i}^n. \tag{3.23}$$

Substituting Equations (3.18) - (3.23) into Equation (3.3), we get

$$\left(\frac{S_i^{n+1} - S_i^n}{\Delta t}\right) + (u_{s_i s}^n - k u_{w_i}^n)\left(\frac{S_{i+1}^n - S_i^n}{\Delta x}\right) = D\left(\frac{S_{i+1}^n - 2S_i^n + S_{i-1}^n}{(\Delta x)^2}\right), \tag{3.24}$$

for all $1 \le i \le M$ and $0 \le n \le N-1$. We obtain

$$\left(\frac{S_i^{n+1} - S_i^n}{\Delta t}\right) = -\frac{(u_{s_i}^n - k u_{w_i}^n)}{\Delta x}\left(S_{i+1}^n - S_i^n\right) + \frac{D}{(\Delta x)^2}\left(S_{i+1}^n - 2S_i^n + S_{i-1}^n\right). \tag{3.25}$$

Letting $(C_i)_1 = \left(\frac{S_i^{n+1} - S_i^n}{\Delta t}\right)$. Then, Equation (3.25) becomes

$$(C_i)_1 = -\frac{(u_{s_i}^n - k u_{w_i}^n)}{\Delta x}\left(S_{i+1}^n - S_i^n\right) + \frac{D}{\Delta x^2}\left(S_{i+1}^n - 2S_i^n + S_{i-1}^n\right), \tag{3.26}$$

$$= -\frac{(u_{s_i}^n - ku_{k_i}^n)}{\Delta x} S_{i+1}^n - \frac{(u_{s_i}^n - ku_{k_i}^n)}{\Delta x} S_i^n + \frac{D}{\Delta x^2} S_{i+1}^n - \frac{2D}{\Delta x^2} S_i^n + \frac{D}{\Delta x^2} S_{i-1}^n. \quad (3.27)$$

$$= A_1 S_{i+1}^n + A_2 S_i^n + A_3 S_{i-1}^n, \quad (3.28)$$

where $A_1 = -\frac{(u_{s_i}^n - ku_{w_i}^n)}{\Delta x} + \frac{D}{(\Delta x)^2}, A_2 = \frac{(u_{s_i}^n - ku_{w_i}^n)}{\Delta x} - \frac{2D}{(\Delta x)^2}$ and $A_3 = \frac{D}{(\Delta x)^2}$.

On the left boundary condition, where $i = 1$, we obtain

$$\left(C_{_1}\right)_1 = A_1 S_2^n + A_2 S_1^n + A_3 S_0^n = A_1 S_2^n + A_2 S_1^n + A_3 S_0. \quad (3.29)$$

For the right boundary condition, where $i = M$, we substitute the approximated unknown value on the right boundary condition with the forward difference approximation, so we have

$$S_M = S_{M-1}. \quad (3.30)$$

$$\left(C_M\right)_1 = A_1 S_M^n + A_2 S_{M-1}^n + A_3 S_{M-2}^n, = \left(A_1 + A_2\right) S_{M-1}^n + A_3 S_{M-2}^n. \quad (3.31)$$

We obtain the MacCormack predictor step formulation

$$S_i^{n+1} = S_i^n + \left(C_i\right)_1 \Delta t. \quad (3.32)$$

The second step of the MacCormack scheme is approximation of Equation (3.3) by using a backward time and backward space scheme (BTBS).

$$\frac{\partial S}{\partial t} \cong \frac{S_i^{n+1} - S_i^n}{\Delta t}, \quad (3.33)$$

$$\frac{\partial S}{\partial x} \cong \frac{S_i^{n+1} - S_{i-1}^{n+1}}{\Delta x}, \quad (3.34)$$

$$\frac{\partial^2 S}{\partial x^2} \cong \frac{S_{i+1}^{n+1} - 2S_i^{n+1} + S_{i-1}^{n+1}}{(\Delta x)^2}. \tag{3.35}$$

Substituting Equations (3.33) - (3.35) into Eq. (3.3), we get

$$\frac{S_i^{n+1} - S_i^n}{\Delta t} + (u_{s_i}^n - ku_{w_i}^n)\left(\frac{S_i^{n+1} - S_{i-1}^{n+1}}{\Delta x}\right) = D\left(\frac{S_{i+1}^{n+1} - 2S_i^{n+1} + S_{i-1}^{n+1}}{(\Delta x)^2}\right). \tag{3.36}$$

Then

$$\frac{S_i^{n+1} - S_i^n}{\Delta t} = -(u_{s_i}^n - ku_{w_i}^n)\left(\frac{S_i^{n+1} - S_{i-1}^{n+1}}{\Delta x}\right) + D\left(\frac{S_{i+1}^{n+1} - 2S_i^{n+1} + S_{i-1}^{n+1}}{(\Delta x)^2}\right). \tag{3.37}$$

Letting $(C_i)_2 = \frac{S_i^{n+1} - S_i^n}{\Delta t}$. Then, Equation (3.37) becomes

$$(C_i)_2 = -\frac{(u_{s_i}^n - ku_{w_i}^n)}{\Delta x}\left(S_i^{n+1} - S_{i-1}^{n+1}\right) + \frac{D}{(\Delta x)^2}\left(S_{i+1}^{n+1} - 2S_i^{n+1} + S_{i-1}^{n+1}\right), \tag{3.38}$$

$$= \frac{D}{(\Delta x)^2} S_{i+1}^{n+1} + \left(-\frac{(u_{s_i}^n - ku_{w_i}^n)}{\Delta x} - \frac{2D}{(\Delta x)^2}\right) S_i^{n+1} + \left(\frac{(u_{s_i}^n - ku_{w_i}^n)}{\Delta x} + \frac{D}{(\Delta x)^2}\right) S_{i-1}^{n+1},$$

$$(C_i)_2 = B_1 S_2^{n+1} + B_2 S_1^{n+1} + B_3 S_0^{n+1}, \tag{3.39}$$

where $B_1 = \frac{D}{(\Delta x)^2}, B_2 = -\frac{(u_{s_i}^n - ku_{w_i}^n)}{\Delta x} - \frac{2D}{(\Delta x)^2}$ and $B_3 = \frac{(u_{s_i}^n - ku_{w_i}^n)}{\Delta x} + \frac{D}{(\Delta x)^2}$.

On the left boundary condition, where $i = 1,$ we obtain

$$(C_1)_2 = B_1 S_2^{n+1} + B_2 S_1^{n+1} + B_3 S_0^{n+1} = B_1 S_2^{n+1} + B_2 S_1^{n+1} + B_3 S_0. \tag{3.40}$$

For the right boundary condition, where $i = M$, we substitute the approximated unknown value on the right boundary condition with the backward difference approximation, we have

$$S_{M+1} = S_M . \tag{3.41}$$

$$(C_M)_2 = (B_1 + B_2) S_M^{n+1} + B_3 S_{M-1}^{n+1}. \tag{3.42}$$

From the stability condition, the MacCormack scheme takes following form,

$$S_i^{M+1} = S_i^n + \frac{\Delta t}{2}\left((C_i)_1 + (C_i)_2\right), \tag{3.43}$$

which makes the scheme conditionally stable when

$$\frac{D\Delta t}{(\Delta x)^2} < 0.5, \tag{3.44}$$

and

$$(u_s - k u_w)\frac{\Delta t}{(\Delta x)} < 0.9. \tag{3.45}$$

3.3 Iterative method for interpolation of the initial and boundary conditions

3.3.1 Lagrange interpolating polynomials

The problem of determining a polynomial of degree one that passes through distinct points (x_0, y_0) and (x_1, y_1) is the same as approximating a function f for which $f(x_0) = y_0$ and $f(x_1) = y_1$. The first-degree polynomial interpolation agrees with the values of f at the given points [21].

Define the functions

$$L_0 = \frac{x - x_0}{x_0}, \tag{3.46}$$

and

$$L_1(x) = \frac{x - x_0}{x_1 - x_0}. \tag{3.47}$$

The linear Lagrange interpolating polynomials through (x_0, y_0) and (x_1, y_1) is

$$P(x) = L_0(x) f(x_0) + L_1(x) f(x_1), \tag{3.48}$$

and

$$\frac{x-x_1}{x_1-x_2}\ f(x_0)\ +\ \frac{x-x_0}{x_1-x_0}\ f(x_1). \tag{3.49}$$

Note that

$$L_0(\mathrm{x}_0)=1\ ,\quad L_0(\mathrm{x}_1)=0,\quad L_1(\mathrm{x}_0)=0\quad \text{and}\quad L_1(\mathrm{x}_1)=1.$$

These imply that

$$P(x_0)=1\cdot f(x_0)+0\cdot f(x_1)=f(x_0)=y_0$$

and

$$P(x_1)=0\cdot f(x_0)+1\cdot f(x_1)=f(x_1)=y_1.$$

Hence, P is the unique polynomial of degree at most one that passes through (x_0,y_0) and (x_1,y_1).

Theorem 3.1 If $x_0,x_1,\ldots,x_n$ are $n+1$ distinct numbers and f is a function whose values are given at these number points, then a unique polynomial $P(x)$ of degree at most n exists with

$$f(x_k)=P(x_k),\ \text{ for each }\ k=0,1,\ldots,n.$$

The polynomial is given by

$$P(x)=f(x_0)L_{n,0}(x)+\ldots+f(x_n)L_{n,n}(x)=\sum_{k=0}^{n}f(x_k)L_{n,k}(x), \tag{3.50}$$

where,

$$L_{n,k} = \frac{(x-x_0)(x-x_1)...(x-x_{k-1})(x-x_{k+1})...(x-x_n)}{(x_k-x_0)(x_k-x_1)...(x_k-x_{k-1})(x_k-x_{k+1})...(x_k-x_n)}, \tag{3.51}$$

$$= \prod_{\substack{i=0 \\ i\neq k}}^{n} \frac{(x-x_i)}{(x_k-x_i)}, \tag{3.52}$$

for each $k = 0,1,...,n.$

3.3.2 Cubic spline interpolation

Cubic spline interpolation method is piecewise polynomial approximation with a unique cubic equation for each subinterval. The method obeys the necessary conditions that the first and second derivatives of the cubic spline are continuous in the interested interval [24,25].

Suppose $(x_0, y_0), (x_1, y_1), (x_2, y_2), \ldots, (x_n, y_n)$ are a collection of $n+1$ node pairs, where $a = x_0 < x_1 < ... < x_n = b.$ Function $S(x)$ approximates each pair of nodes and is called a cubic spline if there exist n cubic polynomials that satisfies these conditions,

(1) $S(x)$ is a cubic polynomial on each subinterval $[x_i, x_{i+1}]$ where $i = 0,1,...,n-1$

$$S_i(x) = a_i + b_i(x-x_i) + c_i(x-x_i)^2 + d_i(x-x_i)^3, \tag{3.53}$$

$a_i, b_i, c_i,$ and d_i are unknown constant coefficients of each cubic polynomial,

(2) $S_{i+1}(x_{i+1}) = S_i(x_{i+1})$ where $i = 0,1,...,n-2$, (3.54)

(3) $S'_{i+1}(x_{i+1}) = S'_i(x_{i+1})$ where $i = 0,1,...,n-2$, (3.55)

(4) $S''_{i+1}(x_{i+1}) = S''_i(x_{i+1})$ where $i = 0,1,...,n-2$, (3.56)

(5) One of sets of boundary conditions is satisfied according to this condition as

(i) $S''(x_0) = S''(x_n) = 0$ (natural boundary), (3.57)

(ii) $S'(x_0) = y_0'$ and $S'(x_n) = y_n'$ (clamped boundary). (3.58)

For the natural boundary conditions, there are n linear equations for coefficients $c_0, c_1, c_2, ..., c_n$, so we can solve the solution of c_i from a tridiagonal linear system $\boldsymbol{T}\mathbf{x}=\mathbf{b}$, where $\boldsymbol{T}$ is a tridiagonal matrix of $n \times n$ as follows,

$$\boldsymbol{T} = \begin{bmatrix} 1 & 0 & 0 & 0 & 0 & 0 \\ h_0 & 2(h_0+h_1) & h_1 & \ddots & \ddots & 0 \\ 0 & h_1 & 2(h_1+h_2)_2 & h_2 & \ddots & 0 \\ 0 & \ddots & \ddots & \ddots & \ddots & 0 \\ 0 & \ddots & \ddots & h_{n-2} & 2(h_{n-2}+h_{n-1}) & h_{n-1} \\ 0 & 0 & 0 & 0 & 0 & 1 \end{bmatrix}, \quad (3.59)$$

$$\mathbf{b} = \begin{bmatrix} \alpha_0 \\ \alpha_1 \\ \vdots \\ \alpha_{n-1} \\ \alpha_n \end{bmatrix} = \begin{bmatrix} 0 \\ \frac{3}{h_1}(a_2-a_1) - \frac{3}{h_0}(a_1-a_0) \\ \vdots \\ \frac{3}{h_{n-1}}(a_n-a_{n-1}) - \frac{3}{h_{n-2}}(a_{n-1}-a_{n-2}) \\ 0 \end{bmatrix}, \quad (3.60)$$

$$\text{and } \mathbf{x} = \begin{bmatrix} c_0 \\ c_1 \\ \ddots \\ c_n \end{bmatrix} \quad (3.61)$$

Then, $\mathbf{b}$ and $\mathbf{x}$ are vectors of n dimensions.

$$h_i = x_{i+1} - x, \quad (3.62)$$

$$\alpha_i = \frac{3}{h_i}(a_{i+1}-a_i) - \frac{3}{h_{i-1}}(a_i - a_{i-1}) \text{ for } i = 1, 2, ..., n-1. \quad (3.63)$$

a_i, b_i and d_i can be calculated by the following equations,

$$a_i = y_i \text{ where } i = 0, 1, ..., n, \quad (3.64)$$

$$b_i = \frac{(a_{i+1} - a_i)}{h_i} - \frac{h_i(c_{i+1} - 2c_i)}{3} \text{ where } i = 0,1,...,n-1, \quad (3.65)$$

and $$d_i = \frac{(c_{i+1} - c_i)}{3h_i} \text{ where } i = 0,1,...,n-1. \quad (3.66)$$

The resulting coefficients can always be written in the form of cubic function on $[x_i, x_{i+1}]$ where $i = 0,1,...,n-1$ as

$$S_i(x) = a_i + b_i(x - x_i) + c_i(x - x_i)^2 + d_i(x - x_i)^3. \quad (3.67)$$

3.4 Examples

3.4.1 Advection – Diffusion Equation

$$\frac{\partial c}{\partial t} + U\frac{\partial c}{\partial x} = D\frac{\partial^2 c}{\partial x^2} + Q \quad (3.68)$$

where $c(x,t)$ is salinity level;

U is flow velocity in the x-direction;

D is diffusion coefficient in the x-direction;

Q is sink or source function.

3.4.2 Numerical Method

3.4.2.1 Implicit method

$$-(p + \frac{1}{2}r)c_{m-1}^{n+1} + (1+2p)c_m^{n+1} - (p - \frac{1}{2}r)c_{m+1}^{n+1} = c_m^n + \Delta tQ, \quad (3.69)$$

where $$r = \frac{Ul}{h}, p = \frac{Dl}{h^2}.$$

3.4.2.2 Numerical test of the implicit method

Examples 3.1 We consider a one-dimensional advection-diffusion equation with a wind velocity of $U = 0.1$ m/s. The grid spacing is $\Delta x = 0.25$ m. In this example, we consider 3 cases:

1) diffusion coefficient: $D=1$ m^2/s;

2) diffusion coefficient: $D=0.1$ m^2/s;

3) diffusion coefficient: $D=0.01$ m^2/s;

when the time interval is $\Delta t=0.1$ and $\Delta t=0.01$ second.

Table 3.1 Salinity $c(x,t)$ when $D=1, \Delta x=0.25$ m. and $\Delta t=0.1$ sec.

t \ x	0	0.25	0.50	0.75	1
0	0.0000	0.0000	0.0000	0.0000	0.0000
0.2	0.1000	0.0646	0.0395	0.0246	0.0179
0.4	0.1000	0.0788	0.0605	0.0474	0.0407
0.6	0.1000	0.0857	0.0731	0.0636	0.0585
0.8	0.1000	0.0902	0.0814	0.0748	0.0712
1.0	0.1000	0.0932	0.0871	0.0825	0.0801

Table 3.2 Salinity $c(x,t)$ when $D=0.1, \Delta x=0.25$ m. and $\Delta t=0.1$ sec.

t \ x	0	0.25	0.50	0.75	1
0	0.0000	0.0000	0.0000	0.0000	0.0000
0.2	0.1000	0.0246	0.0049	0.0009	0.0002
0.4	0.1000	0.0401	0.0122	0.0032	0.0008
0.6	0.1000	0.0503	0.0197	0.0065	0.0022
0.8	0.1000	0.0575	0.0265	0.0104	0.0043
1.0	0.1000	0.0628	0.0326	0.0147	0.0069

Table 3.3 Salinity $c(x,t)$ when $D=0.01, \Delta x=0.25$ m. and $\Delta t=0.1$ sec.

t \ x	0	0.25	0.50	0.75	1
0	0.0000	0.0000	0.0000	0.0000	0.0000
0.2	0.1000	0.0069	0.0004	0.0000	0.0000

Table 3.3 (Continued).

x / t	0	0.25	0.50	0.75	1
0.4	0.1000	0.0133	0.0011	0.0001	0.0000
0.6	0.1000	0.0193	0.0023	0.0002	0.0000
0.8	0.1000	0.0250	0.0038	0.0004	0.0000
1.0	0.1000	0.0303	0.0055	0.0008	0.0001

Table 3.4 Salinity $c(x,t)$ when $D=1, \Delta x=0.25$ m. and $\Delta t=0.01$ sec.

x / t	0	0.25	0.50	0.75	1
0	0.0000	0.0000	0.0000	0.0000	0.0000
0.2	0.1000	0.0697	0.0441	0.0265	0.0177
0.4	0.1000	0.0808	0.0636	0.0507	0.0437
0.6	0.1000	0.0871	0.0756	0.0669	0.0622
0.8	0.1000	0.0914	0.0836	0.0778	0.0746
1.0	0.1000	0.0942	0.0890	0.0851	0.0830

Table 3.5 Salinity $c(x,t)$ when $D=0.1, \Delta x=0.25$ m. and $\Delta t=0.01$ sec.

x / t	0	0.25	0.50	0.75	1
0	0.0000	0.0000	0.0000	0.0000	0.0000
0.2	0.1000	0.0267	0.0044	0.0005	0.0001
0.4	0.1000	0.0423	0.0122	0.0027	0.0005
0.6	0.1000	0.0523	0.0202	0.0061	0.0017
0.8	0.1000	0.0591	0.0273	0.0102	0.0037
1.0	0.1000	0.0641	0.0335	0.0146	0.0064

Table 3.6 Salinity $c(x,t)$ when $D=0.01, \Delta x=0.25$ m. and $\Delta t=0.01$ sec.

t \ x	0	0.25	0.50	0.75	1
0	0.0000	0.0000	0.0000	0.0000	0.0000
0.2	0.1000	0.0070	0.0003	0.0000	0.0000
0.4	0.1000	0.0135	0.0010	0.0000	0.0000
0.6	0.1000	0.0196	0.0021	0.0002	0.0000
0.8	0.1000	0.0253	0.0035	0.0003	0.0000
1.0	0.1000	0.0307	0.0053	0.0006	0.0001

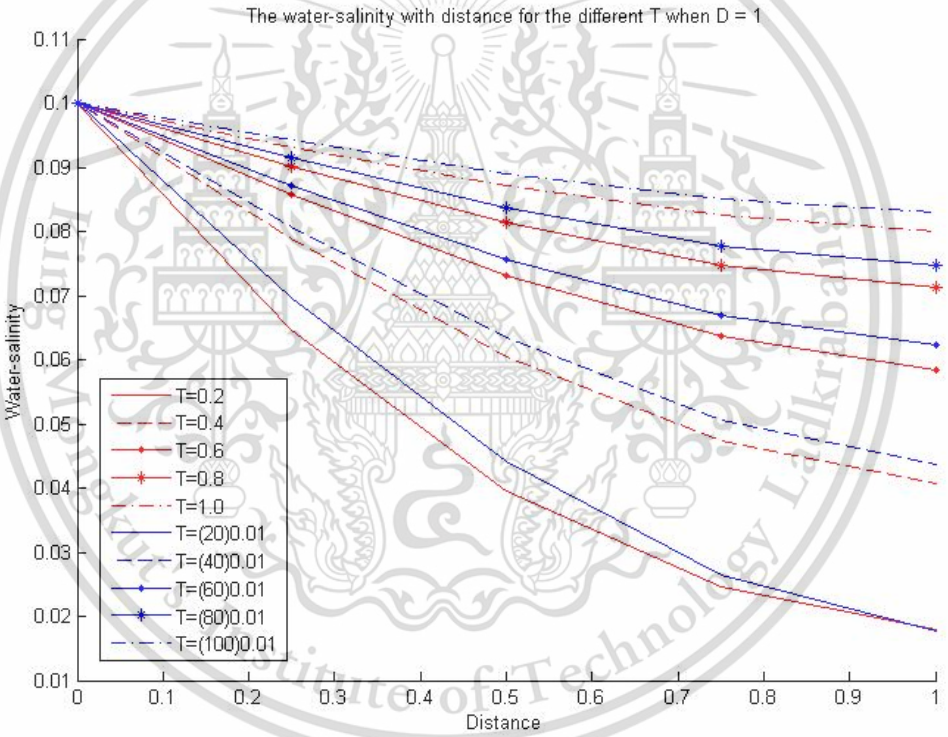

Figure 3.1 Salinity versus distance for each T when $D=1$.

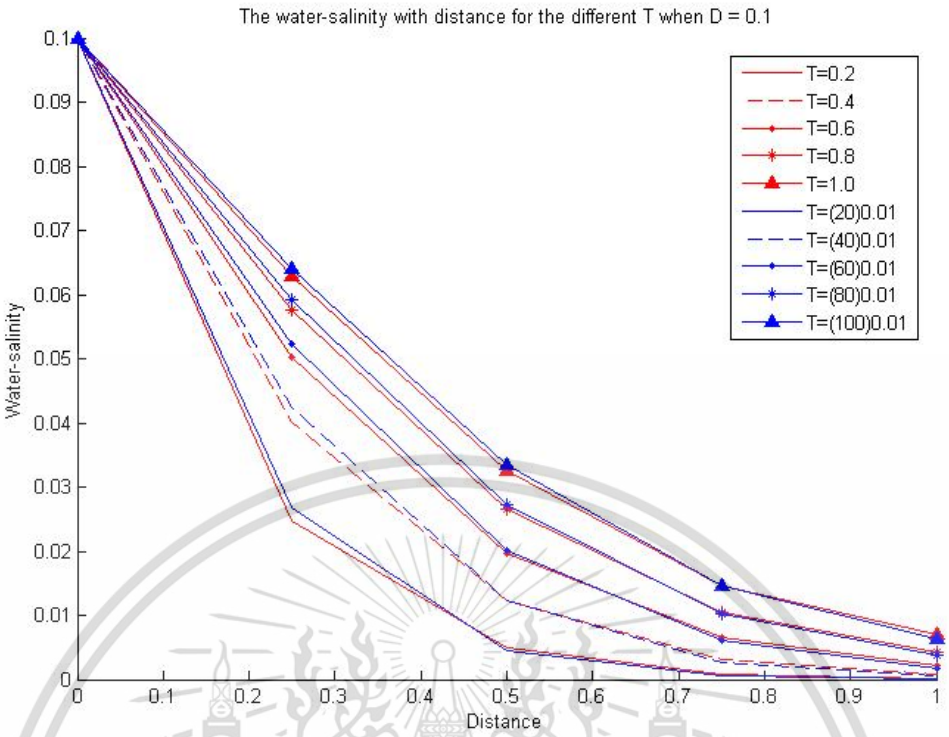

Figure 3.2 Salinity versus distance for each T when $D=0.1$.

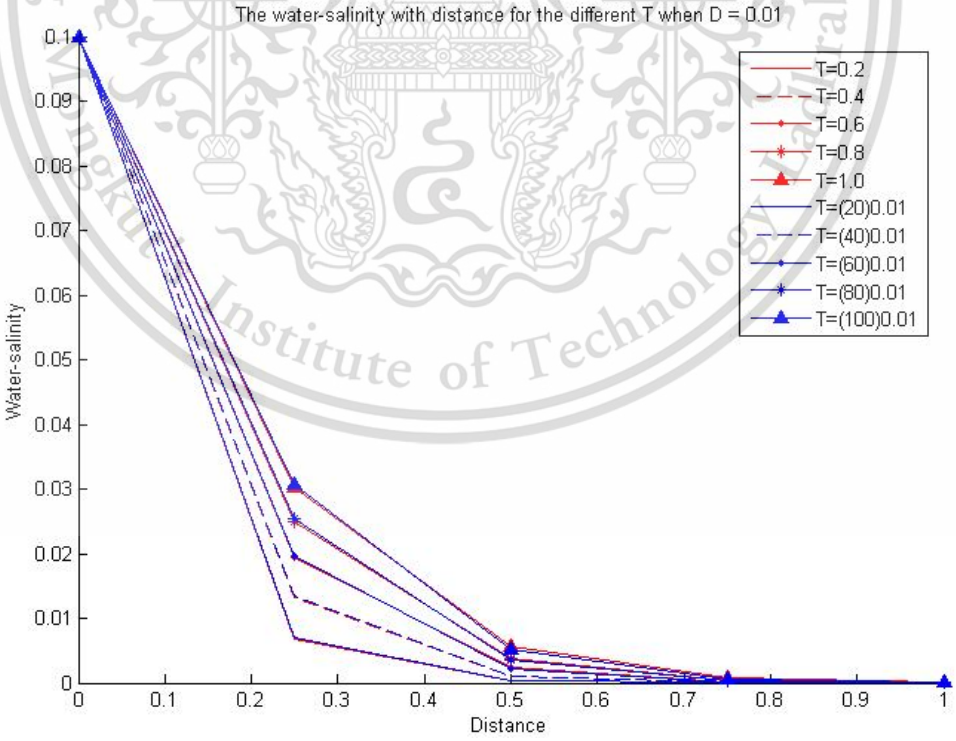

Figure 3.3 Salinity versus distance for each T when $D=0.01$.

Example 3.2 We consider a one-dimensional advection-diffusion equation with a wind velocity of $U = 0.1$ m/s and $Q = -0.001$. The grid spacing was $\Delta x = 0.25$ m. We consider 3 cases:

1) diffusion coefficient: $D = 1$ m^2/s;

2) diffusion coefficient: $D = 0.1$ m^2/s;

3) diffusion coefficient: $D = 0.01$ m^2/s;

when the time interval is $\Delta t = 0.1$ and $\Delta t = 0.01$ second.

Table 3.7 Salinity $c(x,t)$ when $D = 1, \Delta x = 0.25$ m and $\Delta t = 0.1$ s.

x / t	0	0.25	0.50	0.75	1
0	0.0000	0.0000	0.0000	0.0000	0.0000
0.2	0.1000	0.0645	0.0394	0.0245	0.0177
0.4	0.1000	0.0787	0.0603	0.0472	0.0403
0.6	0.1000	0.0856	0.0728	0.0632	0.0581
0.8	0.1000	0.0900	0.0811	0.0744	0.0707
1.0	0.1000	0.0930	0.0868	0.0821	0.0796

Table 3.8 Salinity $c(x,t)$ when $D = 0.1, \Delta x = 0.25$ m and $\Delta t = 0.1$ s.

x / t	0	0.25	0.50	0.75	1
0	0.0000	0.0000	0.0000	0.0000	0.0000
0.2	0.1000	0.0245	0.0047	0.0007	0.0000
0.4	0.1000	0.0398	0.0118	0.0028	0.0004
0.6	0.1000	0.0499	0.0191	0.0059	0.0016
0.8	0.1000	0.0571	0.0258	0.0097	0.0035
1.0	0.1000	0.0623	0.0318	0.0137	0.0060

Table 3.9 Salinity $c(x,t)$ when $D=0.01, \Delta x=0.25$ m and $\Delta t=0.1$ s.

t \ x	0	0.25	0.50	0.75	1
0	0.0000	0.0000	0.0000	0.0000	0.0000
0.2	0.1000	0.0067	0.0002	-0.0002	-0.0002
0.4	0.1000	0.0129	0.0007	-0.0003	-0.0004
0.6	0.1000	0.0188	0.0017	-0.0004	-0.0006
0.8	0.1000	0.0243	0.0030	-0.0004	-0.0008
1.0	0.1000	0.0295	0.0046	-0.0002	-0.0009

Table 3.10 Salinity $c(x,t)$ when $D=1, \Delta x=0.25$ m and $\Delta t=0.01$ s.

t \ x	0	0.25	0.50	0.75	1
0	0.0000	0.0000	0.0000	0.0000	0.0000
0.2	0.1000	0.0696	0.0439	0.0263	0.0175
0.4	0.1000	0.0806	0.0633	0.0504	0.0434
0.6	0.1000	0.0870	0.0753	0.0665	0.0618
0.8	0.1000	0.0912	0.0833	0.0774	0.0742
1.0	0.1000	0.0940	0.0887	0.0846	0.0825

Table 3.11 Salinity $c(x,t)$ when $D=0.1, \Delta x=0.25$ m and $\Delta t=0.01$ s.

t \ x	0	0.25	0.50	0.75	1
0	0.0000	0.0000	0.0000	0.0000	0.0000
0.2	0.1000	0.0265	0.0042	0.0003	-0.0001
0.4	0.1000	0.0420	0.0119	0.0023	0.0001
0.6	0.1000	0.0519	0.0196	0.0055	0.0011
0.8	0.1000	0.0586	0.0266	0.0094	0.0029
1.0	0.1000	0.0635	0.0326	0.0137	0.0054

Table 3.12 Salinity $c(x,t)$ when $D=0.01, \Delta x=0.25$ m and $\Delta t=0.01$ s.

t \ x	0	0.25	0.50	0.75	1
0	0.0000	0.0000	0.0000	0.0000	0.0000
0.2	0.1000	0.0068	0.0001	-0.0002	-0.0002
0.4	0.1000	0.0131	0.0006	-0.0004	-0.0004
0.6	0.1000	0.0191	0.0015	-0.0004	-0.0006
0.8	0.1000	0.0246	0.0027	-0.0005	-0.0008
1.0	0.1000	0.0299	0.0043	-0.0004	-0.0009

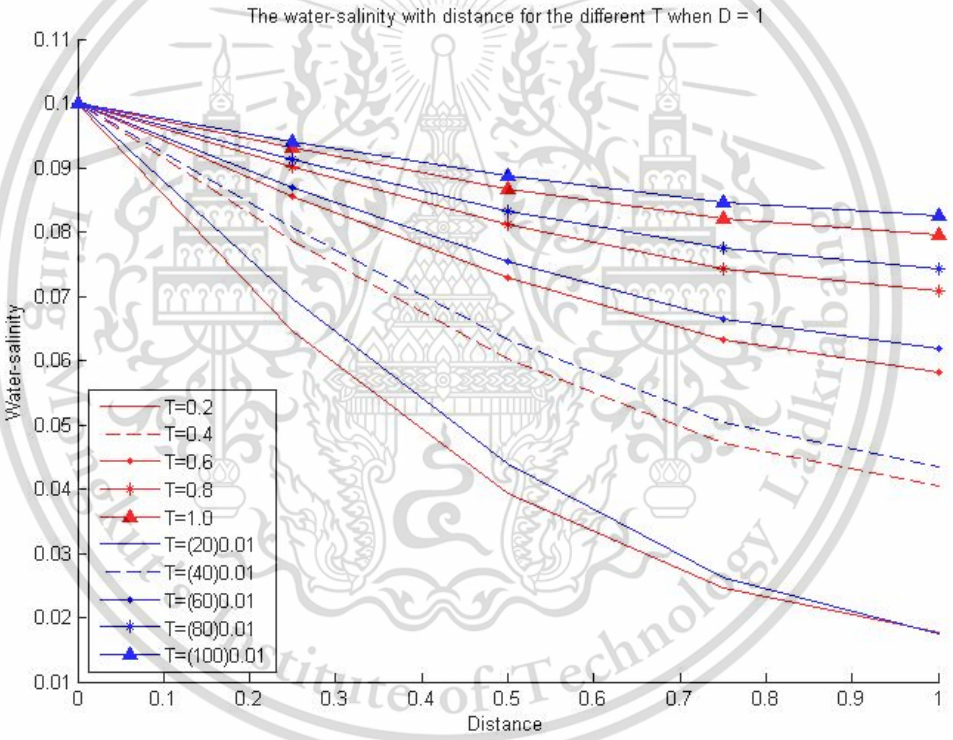

Figure 3.4 Salinity versus distance for each T when $D=0.1$.

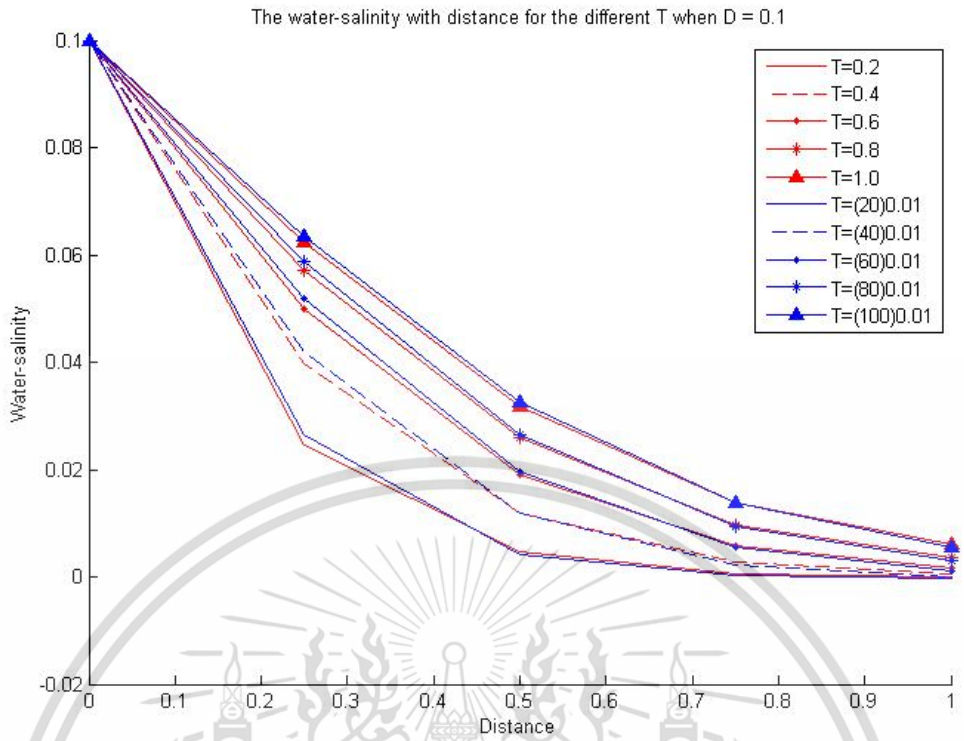

Figure 3.5 Salinity versus distance for each T when $D=0.1$.

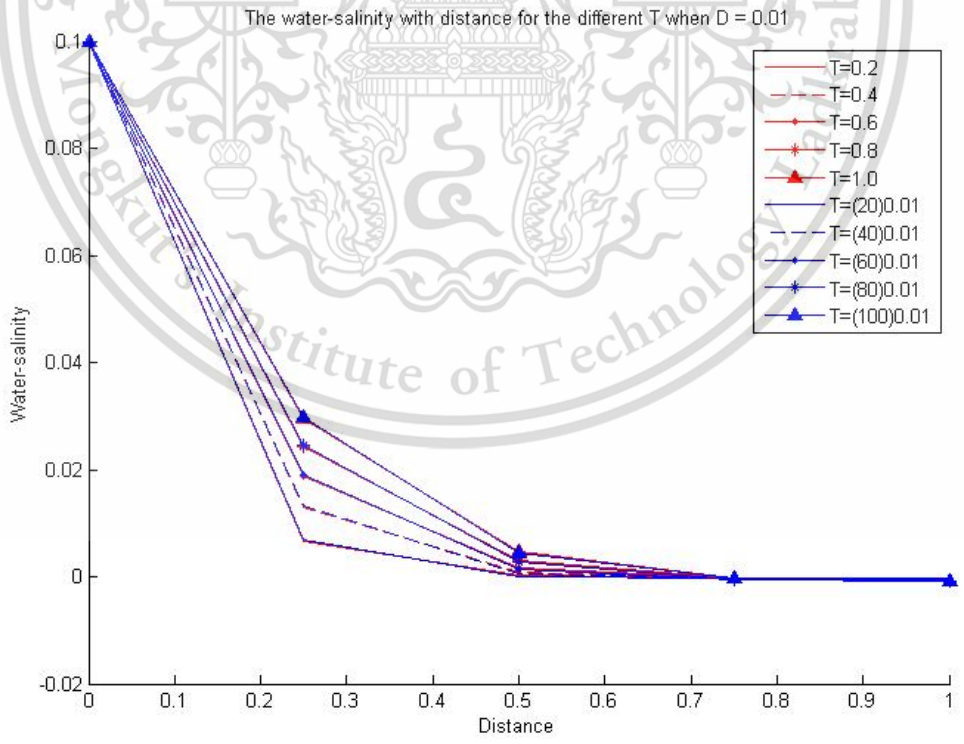

Figure 3.6 Salinity versus distance for each T when $D=0.01$.

Example 3.3 We consider a one-dimensional advection-diffusion equation with a wind velocity of $U = 0.1$ m/s and $Q = -0.001|\sin(xt)|$. The grid spacing is $\Delta x = 0.25$ m. The diffusion coefficient is $D = 0.01|\sin(x+t)|, \Delta x = 0.25$ m^2/s, when the time interval is $\Delta t = 0.1$ and $\Delta t = 0.01$ second.

Table 3.13 Salinity $c(x,t)$ when $D = 0.01|\sin(x+t)|, \Delta x = 0.25$ m and $\Delta t = 0.1$ sec.

t \ x	0	0.25	0.50	0.75	1
0	0.0000	0.0000	0.0000	0.0000	0.0000
0.2	1.0000	0.0137	0.0002	0.0000	0.0000
0.4	1.0000	0.0342	0.0010	0.0000	-0.0001
0.6	1.0000	0.0601	0.0029	0.0000	-0.0002
0.8	1.0000	0.0901	0.0062	0.0002	-0.0003
1.0	1.0000	0.1226	0.0113	0.0006	-0.0004

Table 3.14 Salinity $c(x,t)$ when $D = 0.01|\sin(x+t)|, \Delta x = 0.25$ m and $\Delta t = 0.01$ sec.

t \ x	0	0.25	0.50	0.75	1
0	0.0000	0.0000	0.0000	0.0000	0.0000
0.2	1.0000	0.0120	0.0001	0.0000	0.0000
0.4	1.0000	0.0311	0.0007	0.0000	-0.0001
0.6	1.0000	0.0561	0.0022	-0.0001	-0.0002
0.8	1.0000	0.0855	0.0051	0.0000	-0.0003
1.0	1.0000	0.1178	0.0095	0.0003	-0.0004

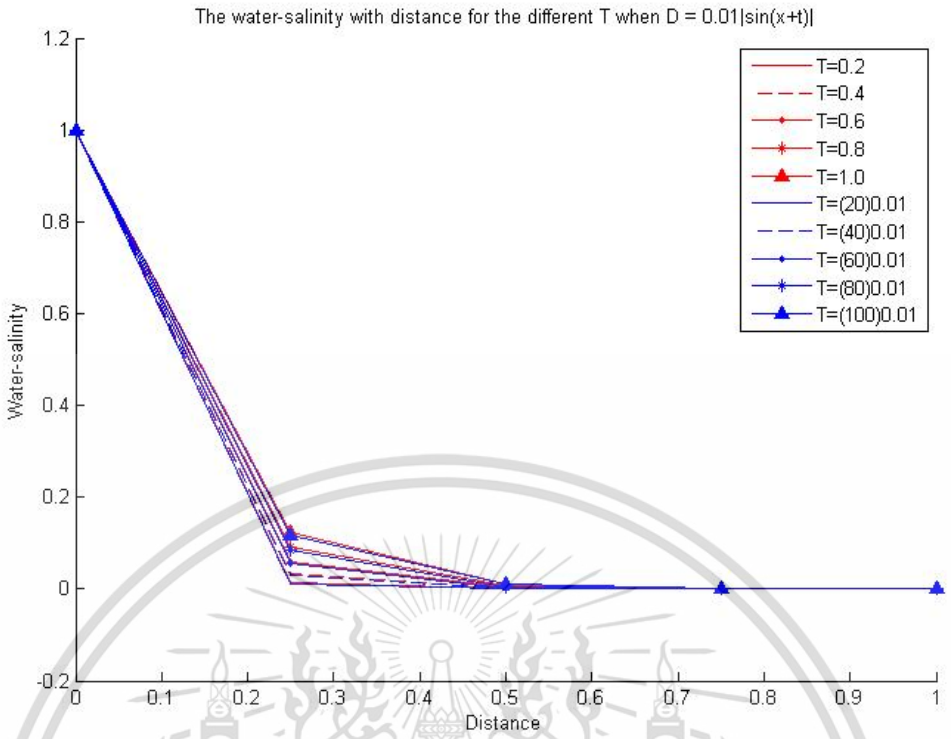

Figure 3.7 Salinity versus distance for each T when $D = 0.01|\sin(x+t)|$.

3.4.2.2 Lagrange interpolating polynomial test

A polynomial interpolation constructs a polynomial that passes through $n+1$ data points $(x_0, y_0), (x_1, y_1), ..., (x_n, y_n)$.

A Lagrange interpolating polynomial is given by

$$P(x) = f(x_0)L_{n,0}(x) + ... + f(x_n)L_{n,\mathrm{n}}(x_n) = \sum_{k=0}^{n} f(x_k)L_{n,\mathrm{k}}(x), \tag{3.70}$$

Where, for each $k = 0, 1, ..., n$

$$L_{n,k}(x) = \prod_{\substack{t=0 \\ t=k}}^{n} \frac{(x - x_i)}{(x_k - x_i)}. \tag{3.71}$$

Example 3.4 It is suspected that a high amount of tannin in mature oak leaves inhibits winter moth *(Operophtera bromata L., Geometridae)* larvae that extensively damages these trees in certain years.

Table 3.15 Average weight (mg).

Day	0	6	10	13	17	20	28
Sample 1 average weight(mg)	6.67	17.33	42.67	37.33	30.10	29.31	28.74
Sample 2 average weight(mg)	6.67	16.11	18.89	15.00	10.56	9.44	8.89

We use Lagrange interpolation to approximate the average weight curve for each sample.

The polynomial of sample 1:

$$n=2: \qquad P_1=\frac{547}{1200}x^2-\frac{23}{24}x+\frac{667}{100};\ x=\{0,1,...,10\}$$

The polynomial of sample 2:

$$n=2: \qquad P_2=\frac{-527}{6000}x^2-\frac{6301}{3000}x+\frac{667}{100};\ x=\{0,1,...,10\} \tag{3.72}$$

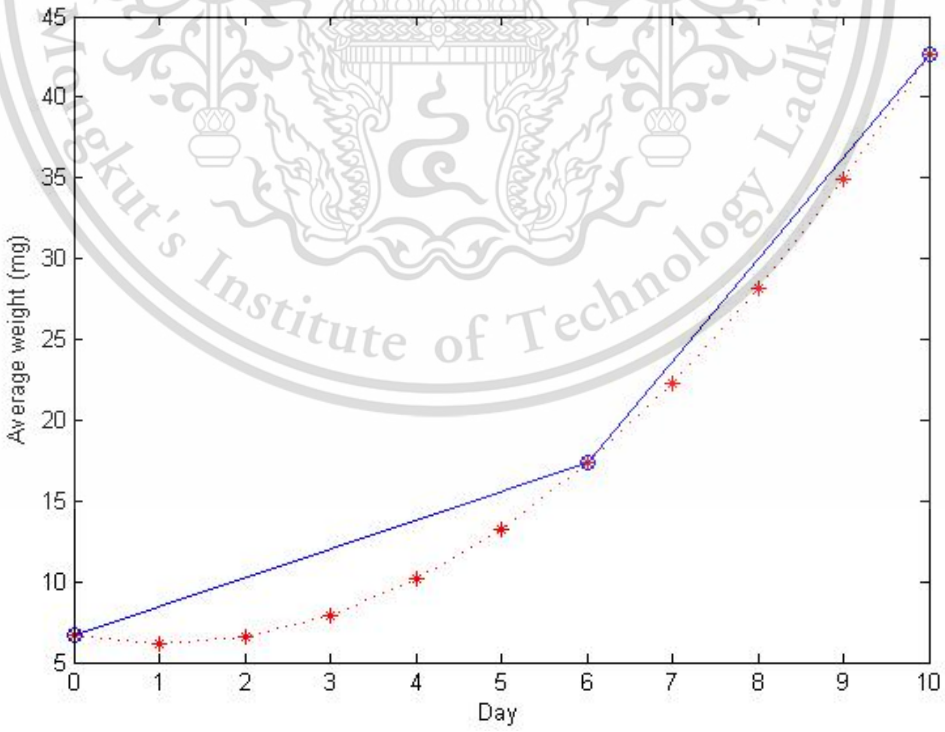

Figure 3.8 Lagrange interpolation to approximate the average weight when $n=2$ (Sample 1).

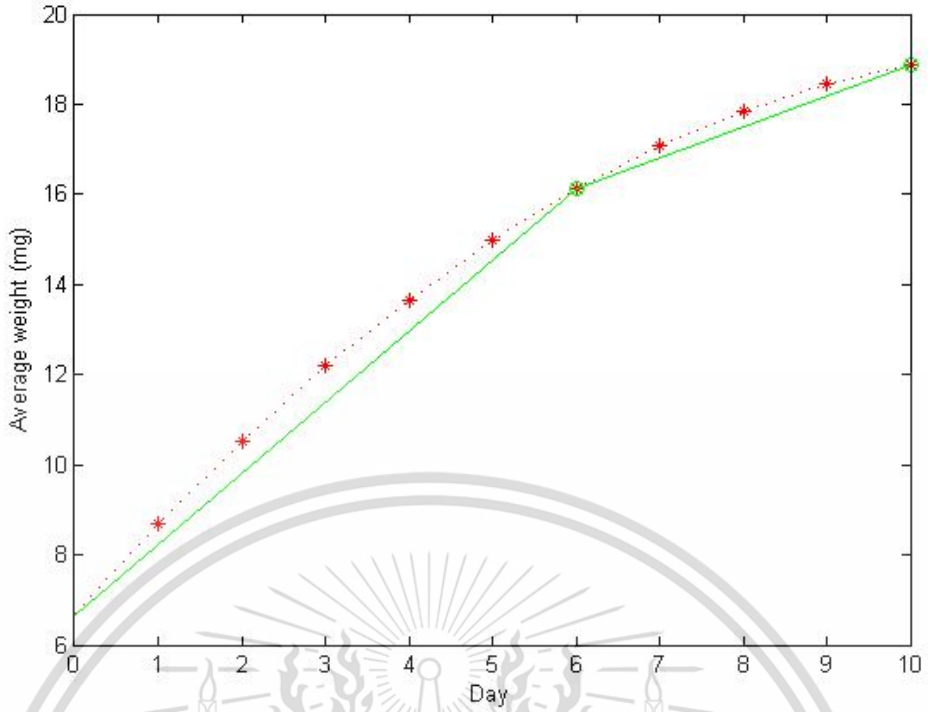

Figure 3.9 Lagrange interpolation to approximate the average weight when $n = 2$ (Sample 2).

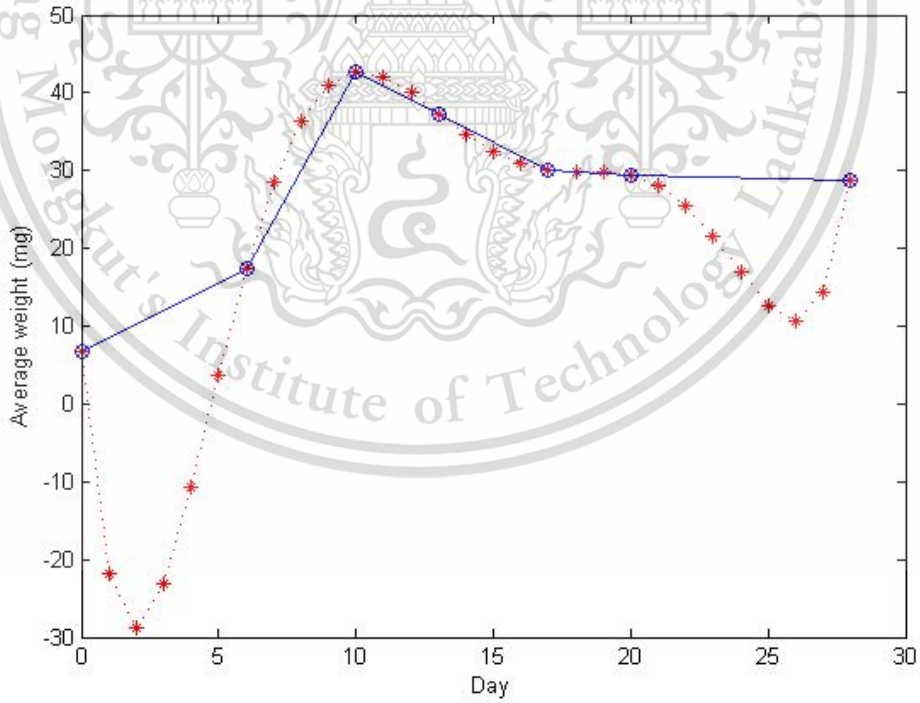

Figure 3.10 Lagrange interpolation to approximate the average weight when $n = 6$ (Sample 1).

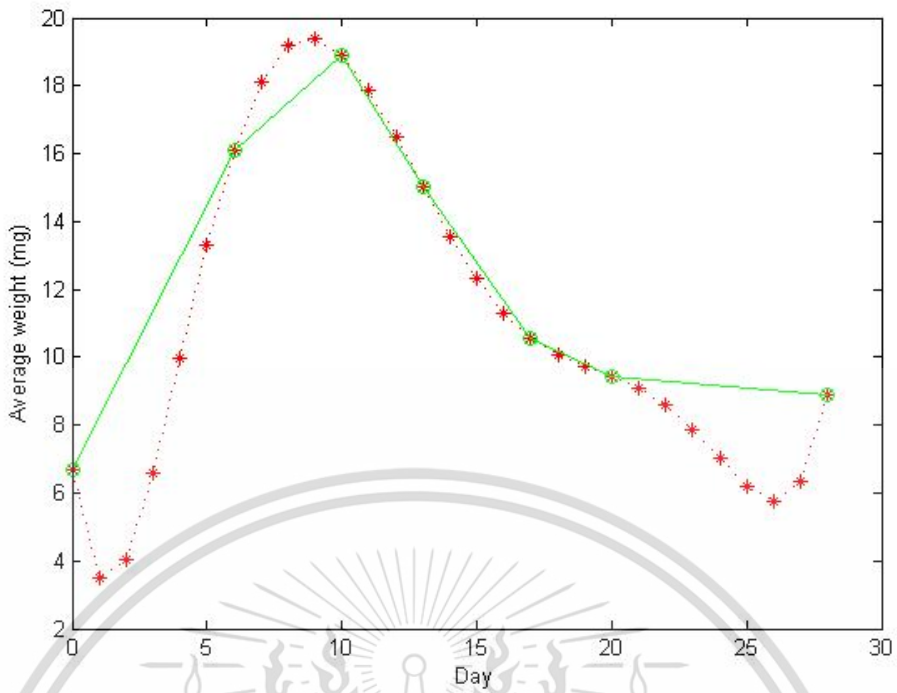

Figure 3.11 Lagrange interpolation to approximate the average weight when $n=6$ (Sample 2).

Example 3.5

Table 3.16 Report of water-quality measurements at Sam Lae station.

รายงานข้อมูลการตรวจวัดคุณภาพน้ำ สถานีสำแล

ณ วันที่ 22 มิถุนายน พ.ศ. 2559

-	วันที่	เวลา	กรด-ด่าง pH	ความเค็ม Salinity (g/l)	ความขุ่น Turbidity (NTU)	ความนำไฟฟ้า Conductivity (µS/cm)	สารละลาย TDS (mg/l)	คลอโรฟิลล์ Chlorophyll (µg/l)	ออกซิเจนในน้ำ DO (mg/l)	อุณหภูมิ Temp (°C)	ความลึกน้ำวัด Depth (Meters)	ความนำไฟฟ้า 25 °C Conductivity 25 °C (µS/cm)	ระดับน้ำ Water Level (ม.รทก)
1	22/06/2559	00:00	7.05	0.27	44.40	631	370	5.40	1.67	31.27	2.19	561.00	-
2	22/06/2559	01:00	7.02	0.34	29.70	786	460	5.10	1.12	31.24	2.08	699.00	-
3	22/06/2559	02:00	7.02	0.32	6.80	756	440	3.00	1.12	31.22	1.93	672.00	-
4	22/06/2559	03:00											
5	22/06/2559	04:00	7.09	0.23	12.60	552	320	3.30	2.17	31.24	1.69	491.00	-
6	22/06/2559	05:00	7.08	0.23	11.20	539	310	3.10	2.19	31.22	1.61	479.00	-
7	22/06/2559	06:00	7.10	0.21	10.00	498	290	3.10	2.46	31.25	1.63	443.00	-
8	22/06/2559	07:00	7.13	0.20	12.10	480	280	3.50	2.67	31.27	1.75	427.00	-
9	22/06/2559	08:00	7.10	0.21	14.10	499	290	3.10	2.43	31.25	1.77	444.00	-
10	22/06/2559	09:00	7.09	0.22	13.80	517	300	3.60	2.28	31.24	1.74	460.00	-
11	22/06/2559	10:00	7.10	0.21	14.30	497	290	3.10	2.49	31.28	1.60	442.00	-
12	22/06/2559	11:00	7.19	0.19	11.70	445	260	2.40	3.44	31.61	1.47	393.00	-

Source: [http://rwc.mwa.co.th/page/stats/?id=S1]

We use Lagrange interpolation to approximate the salinity level, $n=10$:

$$P_{sal} = \frac{173}{1330560000}x^{10} - \frac{4517}{570240000}x^{9} + \frac{138493}{665280000}x^{8} - \frac{292583}{95040000}x^{7} + \frac{138493}{665280000}x^{6} - \frac{30512231}{190080000}x^{5} + \frac{18964111}{332640000}x^{4} - \frac{167421823}{142560000}x^{3} + \frac{1243937}{10395000}x^{2} - \frac{163}{1548}x + \frac{27}{100} \quad (3.73)$$

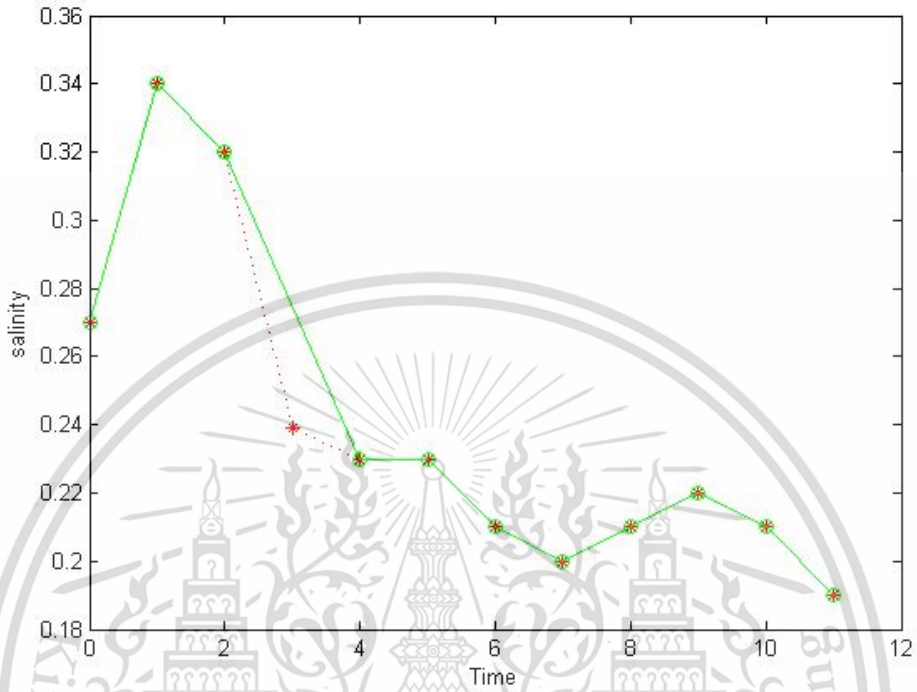

Figure 3.12 Lagrange interpolation to approximate the salinity level when $n = 10$.

We calculated the salinity level by using an implicit method for solving a finite difference equation. In the future, finite difference solutions would give reasonable results for salinity level as expected.

Chapter 4
Main Results and discussion

This section reports all main results and discusses them. Briefly, the reported results are (1) results of comparison of estimates from numerical FTCS and MacCormack Scheme and from solving for exact solution, (2) results of parameter adjustment to match measurement data and (3) results of comparison between estimates from MacCormack scheme and those from actual measurement.

4.1 Comparison between FTCS, MacCormack Scheme and exact solution

4.1.1 Exact solution used as baseline

Exact solution gives the absolutely accurate values of a solution to a mathematical equation or model. However, a problem with solving for exact solution is that, for a complex problem with complicated boundary conditions, the system of equations itself may not be easy or even possible to be solved exactly. Our use of advection-diffusion equation falls under this category. Although it can be solved exactly for simple boundary conditions, it cannot be solved exactly for complex, real-world boundary conditions. Nonetheless, for testing the accuracy of our numerical methods, we obtained values of the exact solution for simple boundary conditions and used them as baseline for comparing the two numerical methods under the same simple boundary conditions. The exact solution that we used was Eq. (4.1) [11, 15].

$$S(x,t) = \frac{1}{2} erfc\left(\frac{x-(u_s - ku_w)t}{\sqrt{4Dt}}\right) + \frac{1}{2} e^{\frac{(u_s - ku_w)x}{D}} erfc\left(\frac{x+(u_s - ku_w)t}{\sqrt{4Dt}}\right). \quad (4.1)$$

Assuming that the length of the stream is [$L = 1$, and the physical parameters are $u_s = 0.10$, $u_w = 0.50, k = 0.10$ and $D = 0.001$.], we generated the baseline values from the equation in the form of a curve. For comparison, this baseline curve is plotted in the same graph with the curves of numerical solutions from FTCS technique and

MacCormack finite difference technique under the same simple boundary conditions (Figure 4.1-4.2). The maximum errors of both techniques are compared in Table 1.

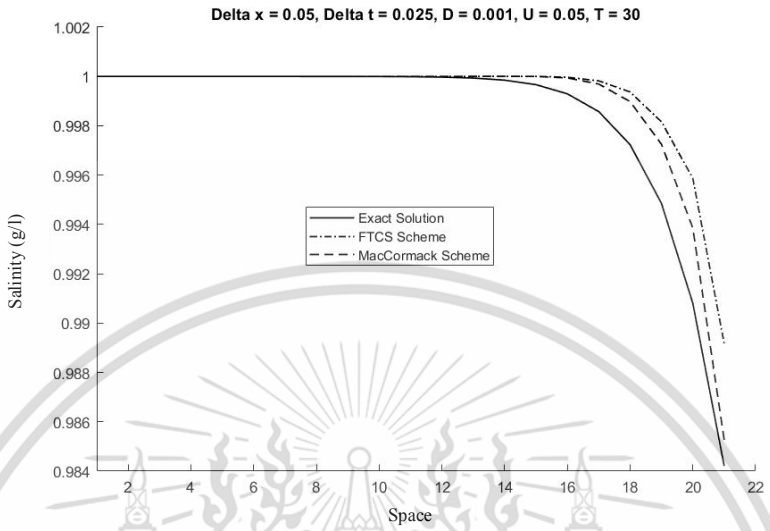

Figure 4.1 Graph of values from numerical FTCS and MacCormack Scheme $(T = 30)$ that varied with distance, with values from the exact solution as baseline.

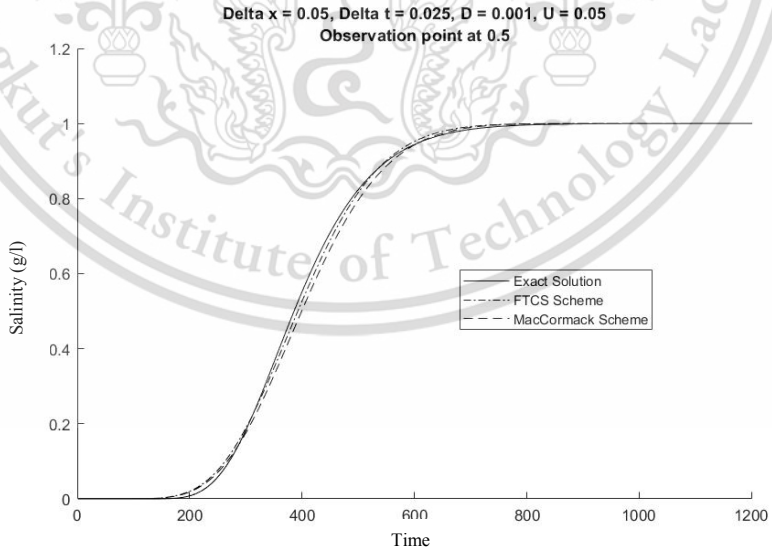

Figure 4.2 Graph of values from numerical FTCS and MacCormack Scheme $(x = 0.5)$ that varied with time, with values from the exact solution as baseline.

Table 4.1 Maximum errors from FTCS and MacCormack Scheme $(T = 30)$.

			Maximum Error $(T = 30)$	
U	Δx	Δt	FTCS $(\times 10^{-3})$	MacCormac $(\times 10^{-3})$
		0.025	4.9603	1.0560
0.05	0.05	0.0125	4.3918	2.5147
		0.0025	3.9305	3.5663
	Δx	Δy	FTCS $(\times 10^{-4})$	MacCormac $(\times 10^{-4})$
		0.025	4.2020	4.4842
0.06	0.05	0.0125	4.2101	4.3272
		0.0025	4.2039	4.2236
	Δx	Δy	FTCS $(\times 10^{-6})$	MacCormac $(\times 10^{-6})$
		0.025	3.3521	2.5421
0.07	0.05	0.0125	3.1199	2.7862
		0.0025	2.8867	2.8267
	Δx	Δy	FTCS $(\times 10^{-8})$	MacCormac $(\times 10^{-8})$
		0.025	11.992	8.9140
0.08	0.05	0.0125	7.7429	0.23177
		0.0025	4.2872	3.0090
	Δx	Δy	FTCS $(\times 10^{-3})$	MacCormac $(\times 10^{-3})$
	0.05		3.9305	3.5662
0.05	0.025	0.0025	3.0798	2.2728
	0.0125		3.3893	1.0846

4.1.2 Comparison between values of the exact solution and those of MacCormack Scheme augmented by an interpolation function for left boundary condition, simulating real-word conditions

4.1.2.1 Assuming that flow velocity and diffusion coefficients are $u_s = 0.10$,$u_w = 0.90$, $k = 0.10$ and $D = 1$, and the length of the stream is $L = 1$. The exact solution to the current problem as stated in [17] is

$$S(x,t) = \frac{0.025}{\sqrt{0.000625 + 0.02t}} \exp\left[-\frac{(x + 0.5 - t)^2}{(0.00125 + 0.04t)} \right]. \tag{4.2}$$

The approximated solution from MacCormack Scheme and the exact solution are shown in Figure 4.3.

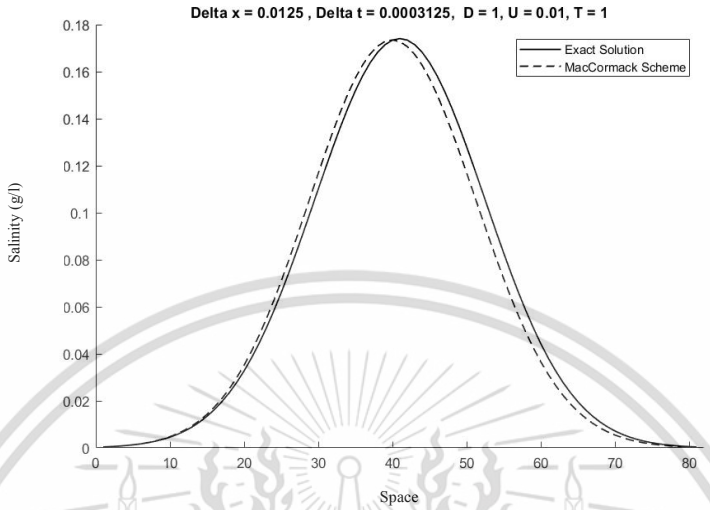

Figure 4.3 Graph of the exact solution curve and the MacCormack Scheme $(T = 30)$ approximated curve augmented by an interpolation function for left boundary condition.

4.1.2.2 Assuming that the flow velocity and diffusion coefficients are taken to be $u_s = 1.1, u_w = 1.0,\ k = 0.10$ and $D = 0.01$. Let the length of the stream be $L = 1$. The MacCormack finite difference technique Eq. (3.43) and Lagrange interpolation technique Eq. (3.50) provided approximated solutions. The numerical solution obtained with Lagrange interpolation was compared to the exact solution (Eq. 4.2), as shown in Figure 4.4. The absolute errors of the technique are shown in Table 2.

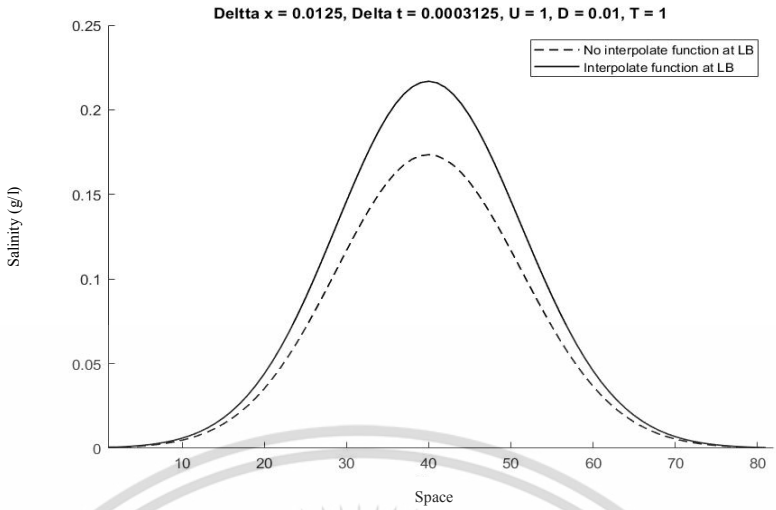

Figure 4.4 Comparison of solutions with interpolation function at LB and no interpolation at LB.

Table 4.2 Absolute errors at $\Delta x = 0.0125,\ \Delta t = 0.0003125,\ U = 1,\ D = 0.01,\ T = 1$**, with interpolation function.**

Interval	Interpolation function to the LB	Given	Absolute Error
0.1	0.00373196	0.004657925	0.000925965
0.2	0.020993865	0.026210873	0.005217008
0.3	0.070919809	0.088575277	0.017655468
0.4	0.143042256	0.178725066	0.03568281
0.5	0.172768923	0.215963928	0.043195005
0.6	0.126011625	0.157593105	0.03158148
0.7	0.056151619	0.070261077	0.014109459
0.8	0.015495382	0.019399664	0.003904282
0.9	0.002686808	0.003365737	0.000678929

4.1.3 Numerical simulation

4.1.3.1 Simulation with MacCormack Scheme and various parameter values

Simulation 1: We considered a segment of a river 160 km. long. The salinity intrusion was set to have flow velocities of $u_s = 0.5, 0.7, 0.9$ m/s. The salinity diffusion coefficient (D) was set at 0.1m^2/s. The fresh water was released by a diversion dam at a flow velocity (u_w) of 0.5 m/s. The percentage dilution capacity of freshwater (*k*) to reduce salinity was set at 30%. Other physical parameters assumed are listed in Table 3.

Table 4.3 Physical parameters in simulation runs.

$L(km)$	u_s	u_w	D	k	$Time$(hrs)
160	0.5	0.5	0.1	0.30	222.23
160	0.7	0.5	0.1	0.30	158.73
160	0.9	0.5	0.1	0.30	123.46

The values of approximated salinity intrusion or $S(x,0)$ (g/l) are shown in Figure 4.5 and Table 4.

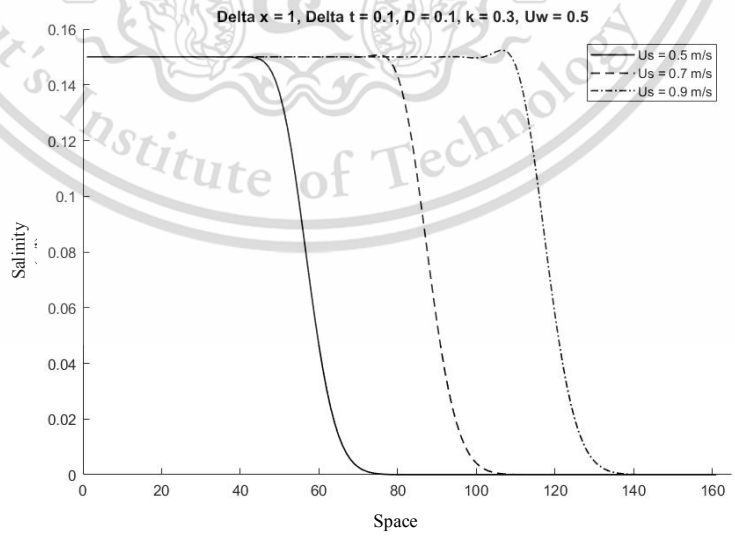

Figure 4.5 Comparison of seawater flow velocities set at three different u_s, with the initial condition $S(x,0) = 0$ and boundary conditions $S(0,t) = 0.15, S(160,t) = 0.$

Table 4.4 Comparison of analytical and approximated salinity intrusion at different values of u_s $(0.5, 0.7 \text{ and } 0.9)$.

Distance from the estuary (km.)	Salinity (g/l)		
	u_s = 0.5 m/s	u_s = 0.7 m/s	u_s = 0.9 m/s
20	0.1500	0.1500	0.1500
40	0.1500	0.1500	0.1500
60	0.0379	0.1500	0.1500
80	1.6753×10^{-5}	0.1385	0.1500
100	1.9767×10^{-11}	0.0029	0.1497
120	2.2452×10^{-19}	1.6686×10^{-7}	0.0480
140	5.6023×10^{-29}	9.7113×10^{-14}	6.4519×10^{-5}
160	5.1481×10^{-40}	1.2894×10^{-21}	6.8165×10^{-10}

Simulation 2: We later changed the initial and boundary conditions to be $S(x,0) = f(x)$ and $S(160,t) = 0$, the peak salinity values were compared as u_s was set to be 0.5,0.7,0.9 m/s. $S(x,t)$ or the salinity concentrations (g/l) at different times and places are shown in Figure 4.6.

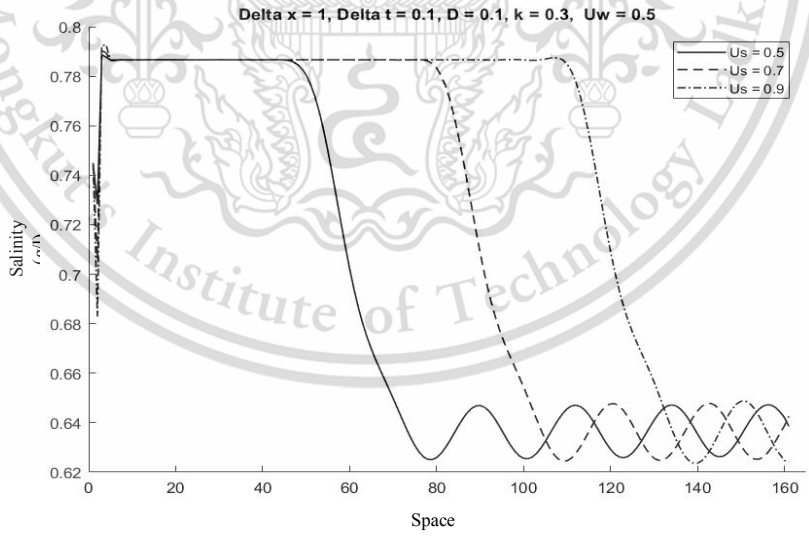

Figure 4.6 Simulated salinity concentrations as u_s was set to be 0.5, 0.7 and 0.9 m/s. with an initial condition of $S(x,0) = f(x)$ and boundary conditions of $S(0,\text{t}) = g(\text{t})$, $S(160,t) = 0$.

Simulation 3: The initial and boundary conditions were interpolated to $S(160,t)=0$. the peak salinity concentrations when u_s was set to be 0.5, 0.7 and 0.9 m/s are shown in Figure 4.7.

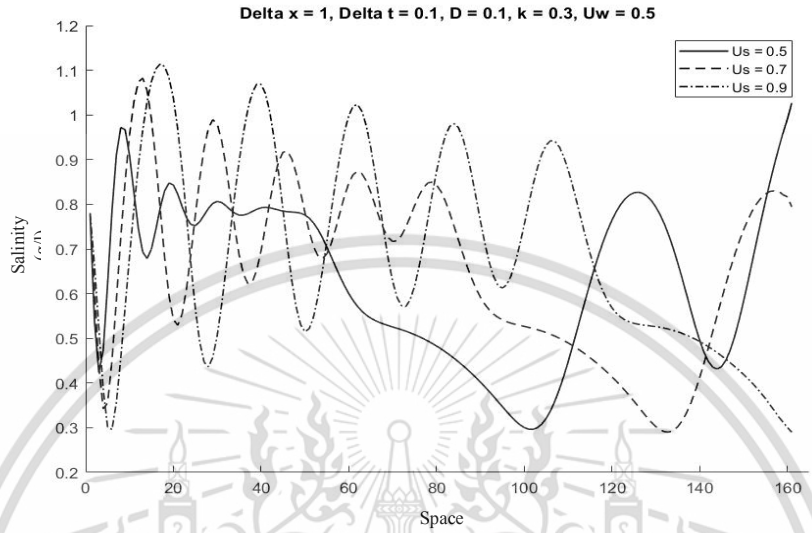

Figure 4.7 Peak salinity concentrations as u_s was set to be 0.5, 0.7 and 0.9 m/s with interpolated initial condition and boundary condition to $S(160,t)=0$.

Simulation 4: We considered a segment of the river 160 km. long. The flow velocity of salinity intrusion was set to $u_s = 0.9$ m/s. The salinity diffusion coefficient was set as $D=0.1,0.3$ and $0.5\,\mathrm{m}^2/\mathrm{s}$. The flow velocity of freshwater released by the diversion dam was 0.5 m/s. The percentage dilution capacity (D) of freshwater to reduce the salinity concentration was 30%. Other physical parameters are listed in Table 5.

Table 4.5 Set physical parameters in simulation runs.

$L(km)$	u_s	u_w	D	k	$Time(hrs)$
160	0.9	0.5	0.1	0.30	123.46

The initial values of approximated salinity intrusion or $S(x,0)$ (g/l) are shown in Figure 4.8.

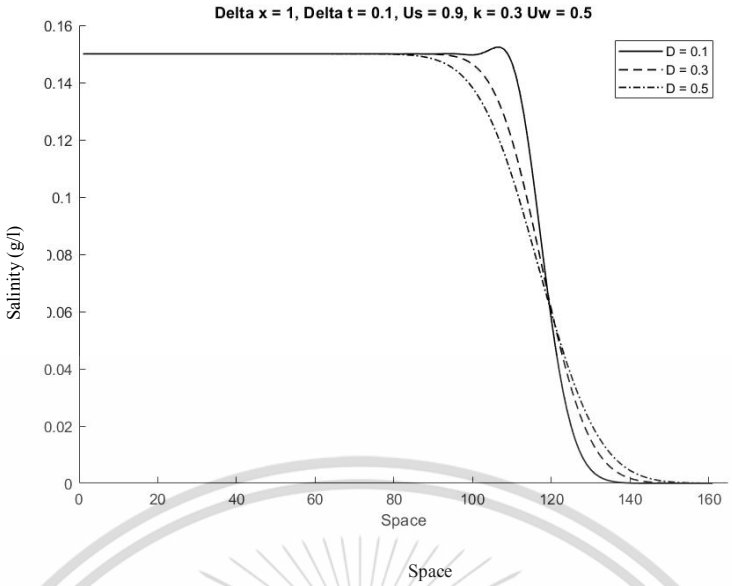

Figure 4.8 Comparison of analytical and approximated salinity intrusion level $S(x,0)$ (g/l) at three different set values of D (0.1, 0.3 and 0.5 m/s).

Simulation 5: The flow velocity of salinity intrusion was set to $u_s = 0.9$ m/s. The salinity diffusion coefficient was set to $D = 0.1\,\mathrm{m}^2/\mathrm{s}$. The flow velocity of freshwater released by the diversion dam was 0.5 m/s. The percentage dilution capacity of freshwater to reduce salinity was set at 30, 50 and 70%. Other physical parameters were listed in Table 6.

Table 4.6 Physical parameters in simulation runs.

$L(km)$	u_s	u_w	D	k	$Time(hrs)$
160	0.9	0.5	0.1	0.30	123.46

The values of approximated salinity intrusion or $S(x,0)$ (g/l) are shown in Figure 4.9.

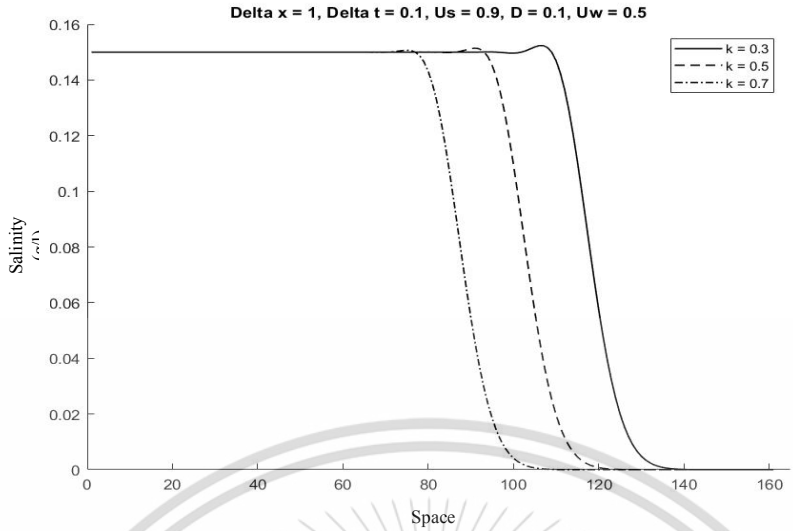

Figure 4.9 Comparison of analytical and approximated salinity intrusion concentrations or $S(x,0)$ (g/l) as k was set to 0.3, 0.5 and 0.7.

Simulation 6: The flow velocity of salinity intrusion was set to $u_s = 0.9$ m/s. The salinity diffusion coefficient was set to $D = 0.1\,\text{m}^2/\text{s}$. The flow velocity of freshwater released by the diversion dam was set at 0.5, 0.7 and 0.9 m/s. The percentage dilution capacity of freshwater to reduce the salinity was set at 30%. Other physical parameters are listed in Table 7.

Table 4.7 Physical parameters in simulation runs.

$L(km)$	u_s	u_w	D	k	$Time(hrs)$
160	0.9	0.5	0.1	0.30	123.46

The values of approximated salinity intrusion or $S(x,0)$(g/l) are shown in Figure 4.10.

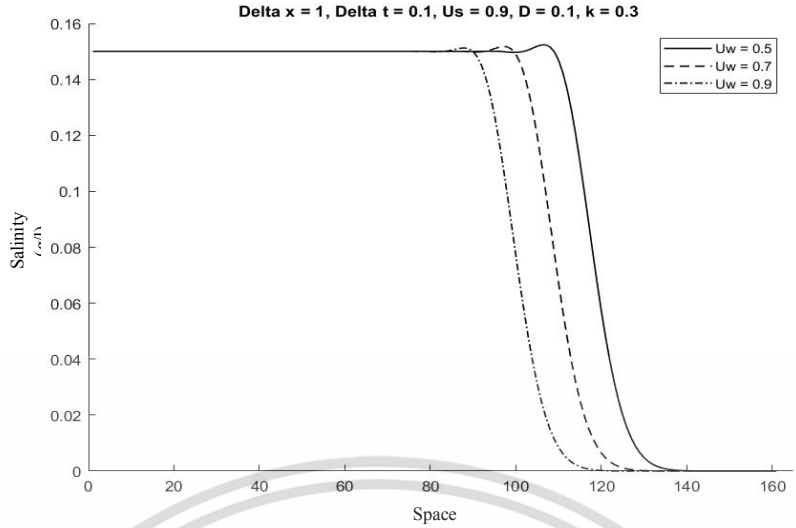

Figure 4.10 Comparison of analytical and approximated salinity intrusion or $S(x,0)$ (g/l) as u_s was set at 0.9 and u_w was set at 0.5, 0.7 and 0.9 m/s).

Simulation 7: The flow velocity of salinity intrusion was set to $u_s = 0.9$ m/s. The salinity diffusion coefficient was set to $D = 0.1\,\text{m}^2/\text{s}$. The flow velocity of freshwater released by the diversion dam was set at 0.5, 0.7 and 0.9 m/s. The percentage dilution capacity of freshwater to reduce the salinity was set at 30%. Other physical parameters are listed in Table 8.

Table 4.8 Physical parameters in simulation runs.

$L(km)$	u_s	u_w	D	k	$Time(hrs)$
160	0.5	0.5	0.1	0.30	222.23

The values of approximated salinity intrusion or $S(x,0)$ (g/l) are shown in Figure 4.11.

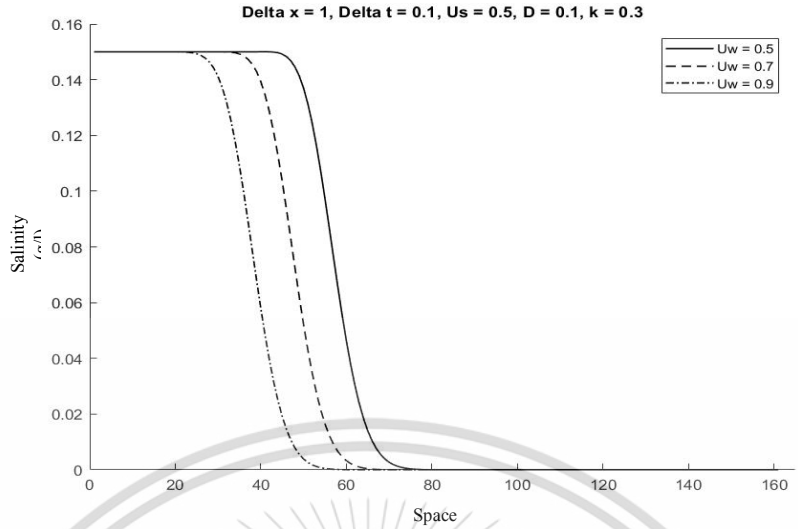

Figure 4.11 Comparison of analytical and approximated salinity concentrations or $S(x,0)$ (g/l) as u_s was set at 0.5 and u_w was set to 0.5, 0.7 and 0.9 m/s.

The salinity intrusion levels $S(x,0)$ (g/l) were derived from the advection-diffusion equation (3.20) and MacCormack technique (3.43) depended on the set parameters (u_s, u_w, k, D). When u_s was high, salinity intruded further from the mouth of the estuary. This situation is likely to happen more frequently [3].Changes in u_w influence changes in u_s which, in turn, dramatically influences salinity intrusion. Based on these findings, deeper future studies may shed more light on this phenomenon.

4.1.4 Approximated salinity concentrations obtained by numerical simulation with MacCormack Scheme

The approximated salinity concentrations obtained by numerical simulation with MacCormack Scheme and various parameter settings are shown in Figure (a)-(d).

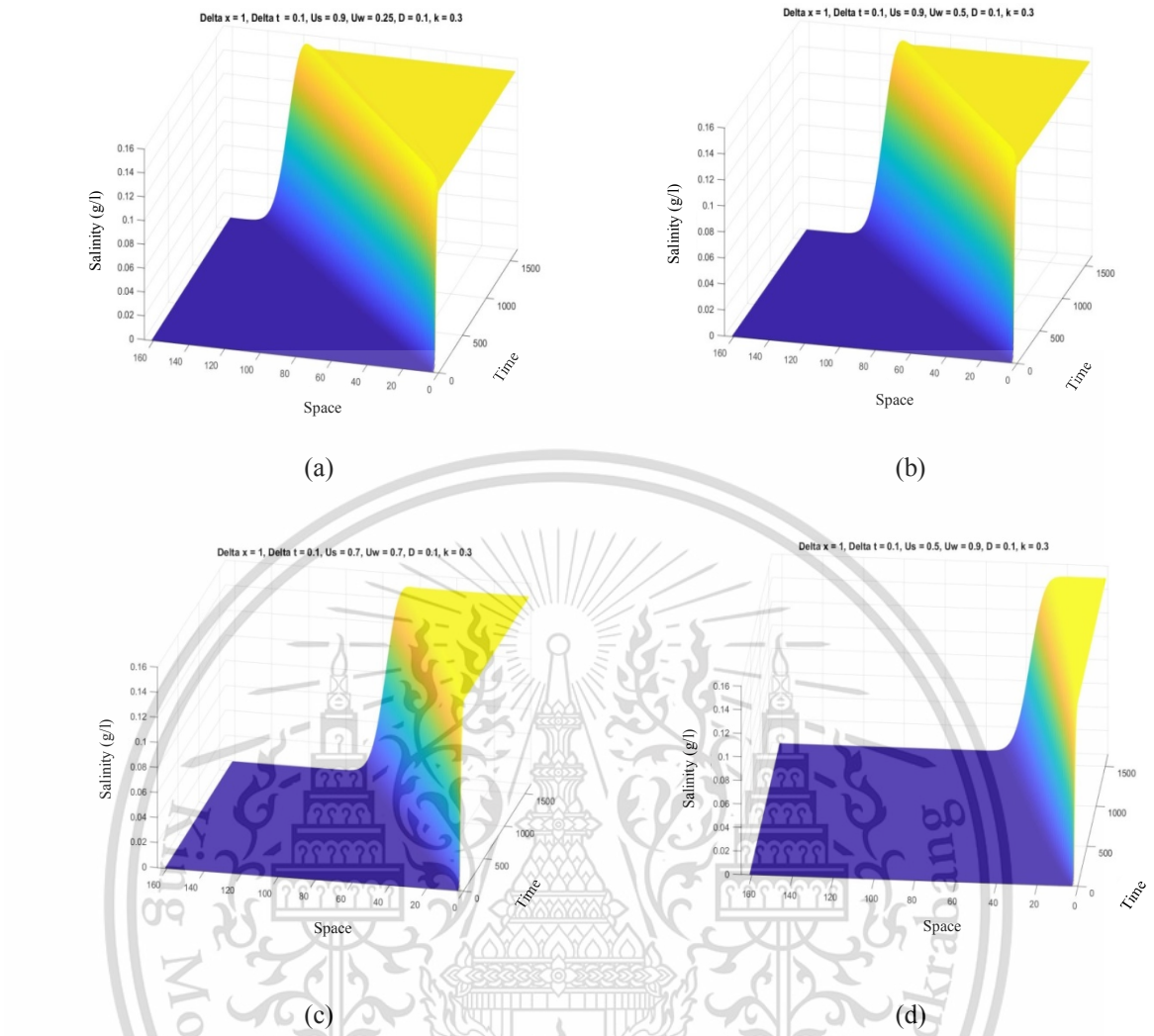

Figure 4.12 (a)-(d): Comparison of analytical and approximated salinity concentrations or $S(x,0)$ (g/l) as u_s was set to 0.9 m/s; u_w was set to 0.25, 0.5, 0.75 and 0.9 m/s; and delta $x = 1$, delta $t = 0.1, D = 0.1, k = 0.3$.

4.1.5 Discussion

The results from numerical simulation of salinity intrusion with one-dimensional advection-diffusion equation show that the interpolation function and MacCormack scheme were acceptably accurate. In recent years, the salinity intrusion u_s during the dry season of every year was high because the amount of freshwater in the river was low. In addition, the fluctuation of salinity level was caused by changes in the level of ocean tide at the estuary. The level and distance of salinity intrusion into the river will continue to increase in the future. The value of the parameters that we used in the model came from actual salinity intrusion data and

data of release of water from the upriver dam. From the efficiency test, the simulation model and parameters showed a reliable trend for real use. When the velocity of freshwater u_w released from the dam was properly increased, the salinity level in the river would decrease to a suitable level. Eq. (2.3) can be used to measure and estimate the value of salinity intrusion in the river with high enough precision to be used for water management planning in the future.

4.2 Parameter adjustment to match measurement data

4.2.1 Cubic spline interpolation of field data

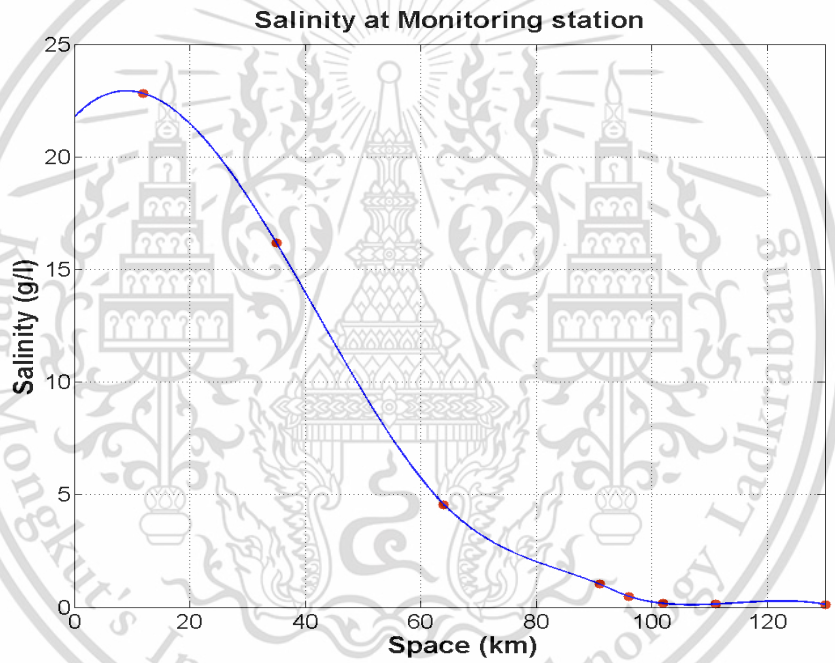

Figure 4.13 Cubic spline interpolated initial condition $S(x,0)$ (g/l)
(Salinity level at the monitoring station; Distance).

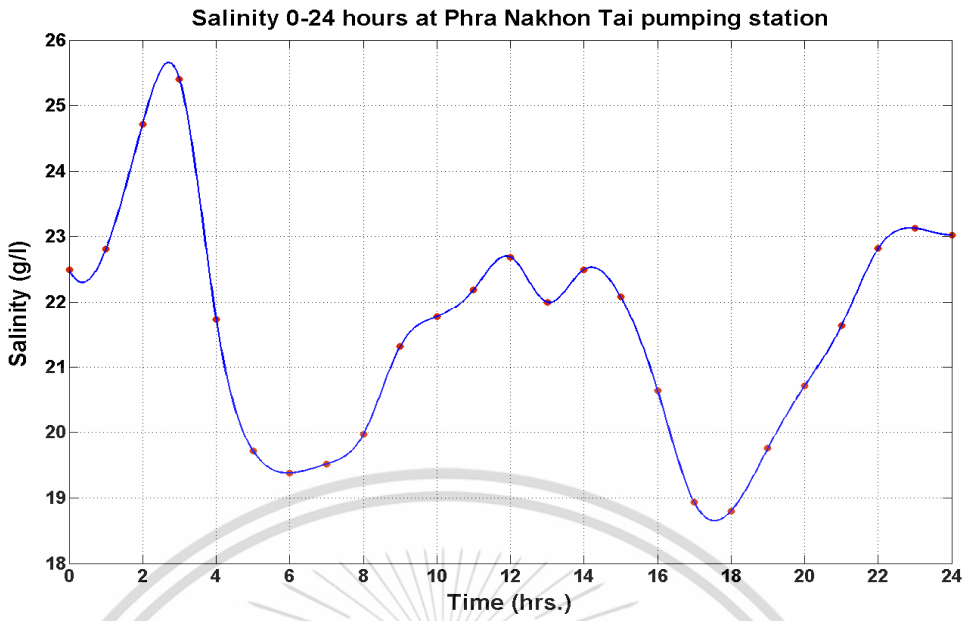

Figure 4.14 Cubic spline interpolated left boundary condition, $S(0,t)$ (g/l). (Salinity level at the 0th –24th hour on 03/05/2014 at Phra Nakorn Tai pumping station)

4.2.2 Approximated salinity intrusion from MacCormack Scheme

4.2.2.1 Approximated salinity intrusion at various values of main parameters

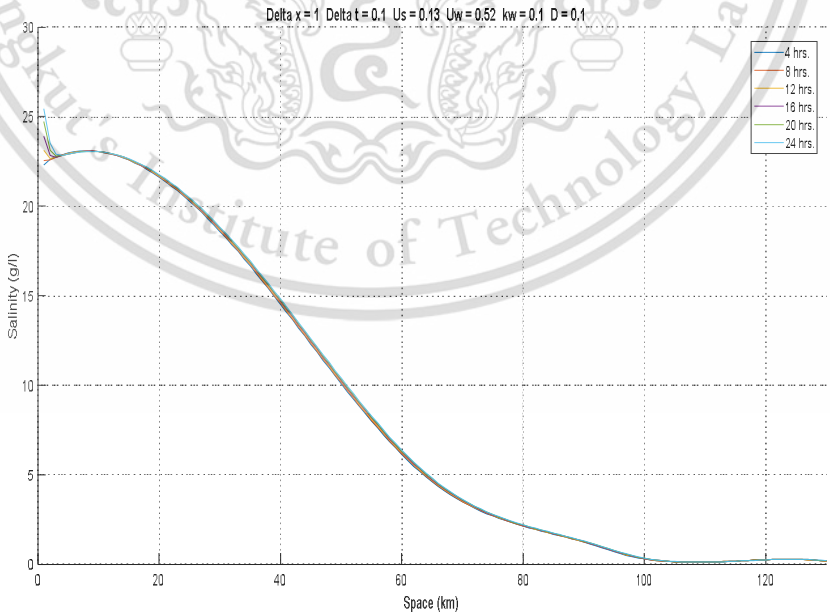

Figure 4.15 Approximated salinity concentrations (g/l) as $u_s = 0.13$ at the 4th, 8th, 12th, 16th, 20th and 24th hr.

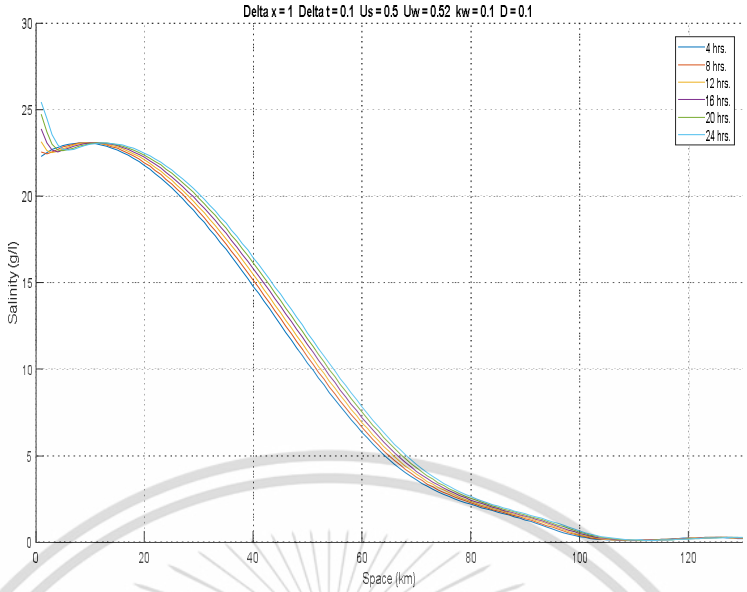

Figure 4.16 Approximated salinity concentrations (g/l) as $u_s = 0.25$ at the 4th, 8th, 12th, 16th, 20th and 24th hr.

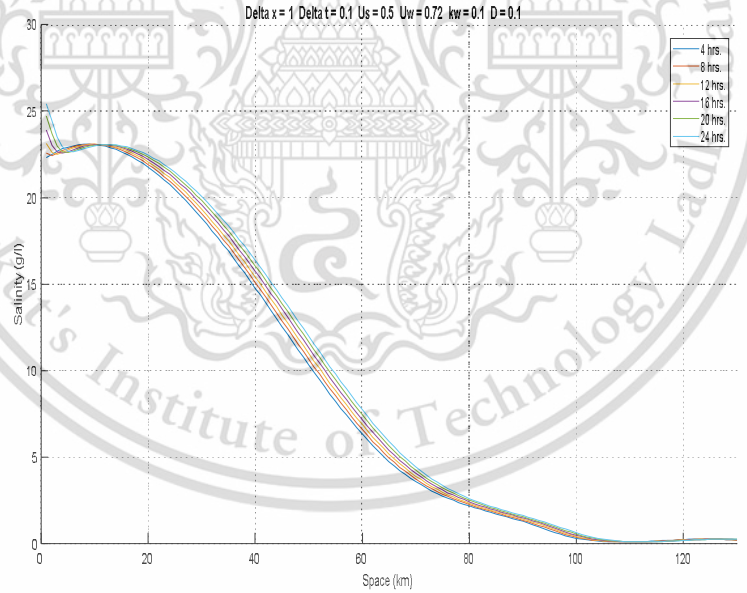

Figure 4.17 Approximated salinity concentrations (g/l) as at the 4th, 8th, 12th, 16th, 20th and 24th hr.

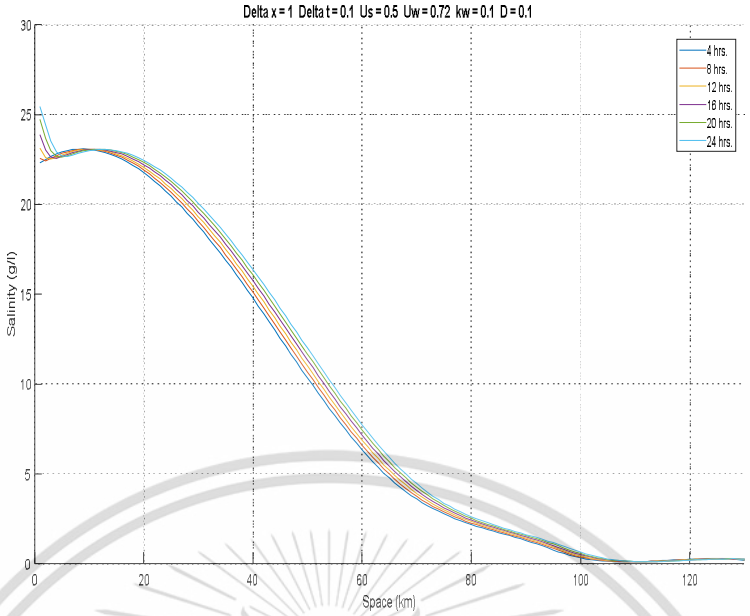

Figure 4.18 Approximated salinity concentrations (g/l) as at the 4th, 8th, 12th, 16th, 20th and 24th hr.

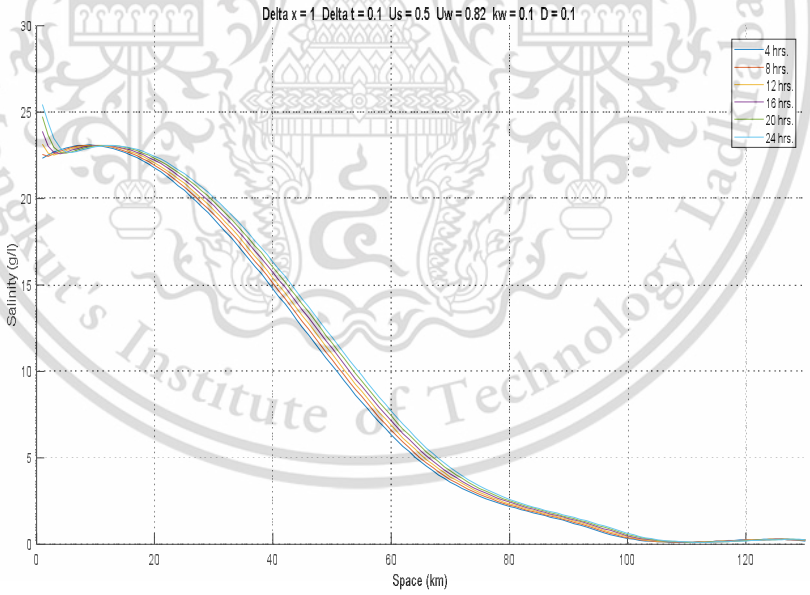

Figure 4.19 Approximated salinity concentrations (g/l) as $u_s = 0.5$ at the 4th, 8th, 12th, 16th, 20th and 24th hr.

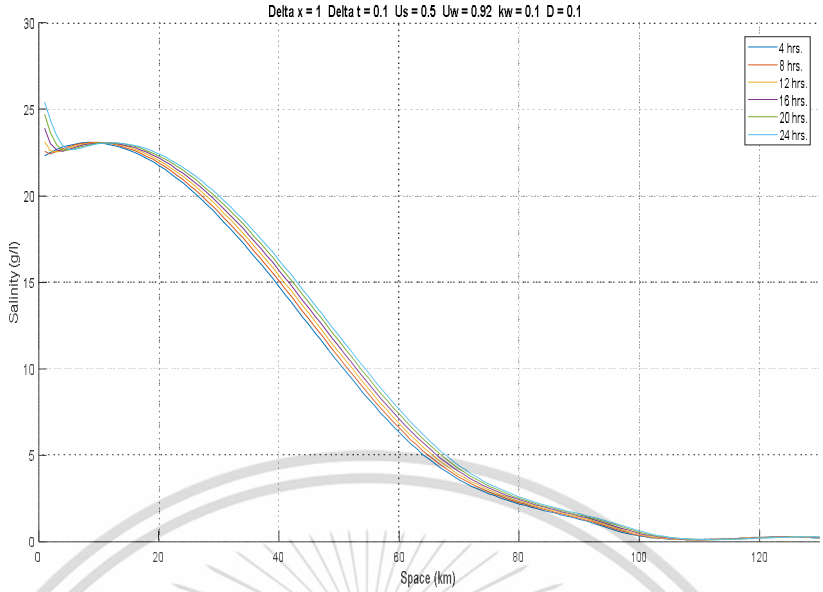

Figure 4.20 Approximated salinity concentrations (g/l) as $u_s = 0.5$ at the 4th, 8th, 12th, 16th, 20th and 24th hr.

Table 4.9 Approximated salinity concentrations (g/l) as D = 0.1, k_w = 0.1, u_w = 0.52, u_s = 0.13 at 12, 35, 64, 91, 96, 102, 111 and 130 km. from the estuary and at the 4^{th}, 8^{th},12^{th},16^{th},20^{th} and 24^{th} hr of 03/05/2014.

Number	Monitoring Station	Space (km)	Salinity Concentration $S(x,t)$ (g/l)					
			4^{th} hr	8^{th} hr	12^{th} hr	16^{th} hr	20^{th} hr	24^{th} hr
1	Phra Nakhon Tai	12	22.8212	22.8320	22.8424	22.8524	22.8620	22.8711
2	Khlong Lat Pho	35	16.2369	16.2937	16.3503	16.4067	16.4630	16.5191
3	Wat Sai Ma Nuea	64	4.5998	4.6400	4.6804	4.7211	4.7622	4.8035
4	Wat Makham	91	1.0339	1.0477	1.0615	1.0751	1.0888	1.1023
5	Samlae Pump Station	96	0.5046	0.5192	0.5338	0.5486	0.5633	0.5781
6	Wat Phai Lom	102	0.1749	0.1801	0.1854	0.1910	0.1967	0.2026
7	Wat Pho Taeng Nuea	111	0.1387	0.1374	0.1362	0.1350	0.1340	0.1330
8	Wat Ban Paeng Temple	130	0.1395	0.1479	0.1553	0.1621	0.1682	0.1739

Table 4.10 Approximated salinity concentrations (g/l) as D = 0.1, k_w = 0.1, u_w = 0.52, u_s = 0.25 at 12, 35, 64, 91, 96, 102, 111 and 130 km. from the estuary and at the 4th, 8th, 12th, 16th, 20th and 24th hr of 03/05/2014.

Number	Monitoring Station	Space (km)	salinity concentration $S(x,t)$ (g/l)					
			4th hr	8th hr	12th hr	16th hr	20th hr	24th hr
1	Phra Nakhon Tai	12	22.8431	22.8736	22.9015	22.9268	22.9495	22.9695
2	Khlong Lat Pho	35	16.3253	16.4696	16.6130	16.7553	16.8966	17.0369
3	Wat Sai Ma Nuea	64	4.6564	4.7548	4.8553	4.9577	5.0621	5.1683
4	Wat Makham	91	1.0563	1.0920	1.1271	1.1616	1.1957	1.2292
5	Samlae Pump Station	96	0.5237	0.5584	0.5940	0.6303	0.6671	0.7043
6	Wat Phai Lom	102	0.1809	0.1928	0.2058	0.2199	0.2352	0.2517
7	Wat Pho Taeng Nuea	111	0.1362	0.1327	0.1295	0.1267	0.1243	0.1223
8	Wat Ban Paeng Temple	130	0.1442	0.1573	0.1696	0.1809	0.1914	0.2010

Table 4.11 Approximated salinity concentrations (g/l) as D = 0.1, k_w = 0.1, u_w = 0.52, u_s = 0.5 at 12, 35, 64, 91, 96, 102, 111 and 130 km. from the estuary and at the 4th, 8th, 12th, 16th, 20th and 24th hr of 03/05/2014.

Number	Monitoring Station	Space (km)	salinity intrusion concentration $S(x,t)$ (g/l)					
			4th hr	8th hr	12th hr	16th hr	20th hr	24th hr
1	Phra Nakhon Tai	12	22.8850	22.9472	22.9964	23.0323	23.0547	23.0632
2	Khlong Lat Pho	35	16.5049	16.8251	17.1403	17.4502	17.7546	18.0532
3	Wat Sai Ma Nuea	64	4.7743	4.9989	5.2334	5.4773	5.7303	5.9919
4	Wat Makham	91	1.1014	1.1798	1.2554	1.3286	1.4000	1.4699
5	Samlae Pump Station	96	0.5642	0.6440	0.7274	0.8127	0.8983	0.9829
6	Wat Phai Lom	102	0.1940	0.2230	0.2576	0.2983	0.3456	0.3996
7	Wat Pho Taeng Nuea	111	0.1314	0.1243	0.1190	0.1159	0.1151	0.1168
8	Wat Ban Paeng Temple	130	0.1546	0.1791	0.2018	0.2217	0.2382	0.2511

Table 4.12 Approximated salinity concentrations (g/l) as D = 0.1, k_w = 0.1, u_w = 0.72, u_s = 0.5 at 12, 35, 64, 91, 96, 102, 111 and 130 km. from the estuary and at the 4th, 8th, 12th, 16th, 20th and 24th hr of 03/05/2014.

Number	Monitoring Station	Space (km)	salinity intrusion concentrations $S(x,t)$ (g/l)					
			4th hr	8th hr	12th hr	16th hr	20th hr	24th hr
1	Phra Nakhon Tai	12	22.8818	22.9419	22.9902	23.0263	23.0501	23.0613
2	Khlong Lat Pho	35	16.4908	16.7972	17.0991	17.3962	17.6883	17.9751
3	Wat Sai Ma Nuea	64	4.7649	4.9792	5.2025	5.4345	5.6749	5.9233
4	Wat Makham	91	1.0979	1.1730	1.2455	1.3159	1.3844	1.4516
5	Samlae Pump Station	96	0.5610	0.6370	0.7165	0.7978	0.8797	0.9608
6	Wat Phai Lom	102	0.1929	0.2204	0.2530	0.2911	0.3351	0.3854
7	Wat Pho Taeng Nuea	111	0.1317	0.1249	0.1197	0.1164	0.1152	0.1163
8	Wat Ban Paeng Temple	130	0.1537	0.1773	0.1993	0.2186	0.2349	0.2480

Table 4.13 Approximated salinity concentrations (g/l) as D = 0.1, k_w = 0.1, u_w = 0.82, u_s = 0.5 at 12, 35, 64, 91, 96, 102, 111 and 130 km. from the estuary and at the 4th, 8th, 12th, 16th, 20th and 24th hr of 03/05/2014.

Number	Monitoring Station	Space (km)	salinity intrusion concentration $S(x,t)$ (g/l)					
			4th hr	8th hr	12th hr	16th hr	20th hr	24th hr
1	Phra Nakhon Tai	12	22.8802	22.9393	22.9870	23.0232	23.0475	23.0599
2	Khlong Lat Pho	35	16.4837	16.7833	17.0785	17.3691	17.6550	17.9358
3	Wat Sai Ma Nuea	64	4.7602	4.9693	5.1871	5.4132	5.6473	5.8891
4	Wat Makham	91	1.0961	1.1696	1.2406	1.3095	1.3766	1.4424
5	Samlae Pump Station	96	0.5593	0.6335	0.7110	0.7904	0.8703	0.9497
6	Wat Phai Lom	102	0.1924	0.2191	0.2507	0.2875	0.3300	0.3784
7	Wat Pho Taeng Nuea	111	0.1319	0.1252	0.1200	0.1167	0.1153	0.1161
8	Wat Ban Paeng Temple	130	0.1533	0.1764	0.1980	0.2171	0.2332	0.2464

Table 4.14 Approximated salinity concentrations (g/l) as D = 0.1, k_w = 0.1, u_w = 0.92, u_s = 0.5 at 12, 35, 64, 91, 96, 102, 111 and 130 km. from the estuary and at the 4th, 8th, 12th, 16th, 20th and 24th hr of 03/05/2014.

Number	Monitoring Station	Space (km)	salinity intrusion concentration $S(x,t)$ (g/l)					
			4th hr	8th hr	12th hr	16th hr	20th hr	24th hr
1	Phra Nakhon Tai	12	22.8786	22.9366	22.9837	23.0199	23.0448	23.0583
2	Khlong Lat Pho	35	16.4766	16.7693	17.0578	17.3419	17.6216	17.8964
3	Wat Sai Ma Nuea	64	4.7555	4.9594	5.1717	5.3919	5.6198	5.8550
4	Wat Makham	91	1.0944	1.1661	1.2356	1.3030	1.3687	1.4331
5	Samlae Pump Station	96	0.5577	0.6300	0.7055	0.7830	0.8610	0.9386
6	Wat Phai Lom	102	0.1918	0.2178	0.2484	0.2840	0.3249	0.3715
7	Wat Pho Taeng Nuea	111	0.1321	0.1255	0.1204	0.1170	0.1154	0.1160
8	Wat Ban Paeng Temple	130	0.1528	0.1755	0.1966	0.2155	0.2315	0.2447

Table 4.15 Approximation of salinity intrusion concentrations (g/l) by MacCormack Scheme when u_s was varied from 0.13, 0.25 and 0.5 m/s and u_w was varied from 0.52, 0.72, 0.82 and 0.92 m/s, at D = 0.1, k_w = 0.1, at the distance of 12, 35, 64, 91, 96, 102, 111 and 130 (km) from the estuary and the time of 4 hrs after the initial time point.

Monitoring Station/ Distance (km)	Salinity Intrusion Concentration at 4 hrs. and $D = 0.1$, $k_w = 0.1$						Real data Salinity (g/l) 05-04-2014
	$u_w = 0.52$, $u_s = 0.13$	$u_w = 0.52$, $u_s = 0.25$	$u_w = 0.52$, $u_s = 0.5$	$u_w = 0.72$, $u_s = 0.5$	$u_w = 0.82$, $u_s = 0.5$	$u_w = 0.92$, $u_s = 0.5$	
Phra Nakhon Tai/12	22.8212	22.8431	22.8850	22.8818	22.8802	22.8786	21.84
Khlong Lat Pho/35	16.2369	16.3253	16.5049	16.4908	16.4837	16.4766	12.60
Wat Sai Ma Nuea/64	4.5998	4.6564	4.7743	4.7649	4.7602	4.7555	5.53
Wat Makham/91	1.0339	1.0563	1.1014	1.0979	1.0961	1.0944	0.49
Samlae Pump Station/96	0.5046	0.5237	0.5642	0.5610	0.5593	0.5577	0.25
Wat Phai Lom/102	0.1749	0.1809	0.1940	0.1929	0.1924	0.1918	0.16
Wat Pho Taeng Nuea/111	0.1387	0.1362	0.1314	0.1317	0.1319	0.1321	0.15
Wat Ban Paeng Temple/130	0.1395	0.1442	0.1546	0.1537	0.1533	0.1528	0.13

Table 4.16 Approximation of salinity intrusion concentrations (g/l) by MacCormack Scheme when $D = 0.1, k_w = 0.1$, at a distance of 12, 35, 64, 91, 96, 102, 111 and 130 (km) from the estuary and the time of 24 hrs after the initial time point.

Monitoring Station/ Distance (km)	Salinity Intrusion Concentration at 24 hrs. and $D = 0.1$, $k_w = 0.1$						Real data Salinity (g/l) 05-04-2014
	$u_w = 0.52$, $u_s = 0.13$	$u_w = 0.52$, $u_s = 0.25$	$u_w = 0.52$, $u_s = 0.5$	$u_w = 0.72$, $u_s = 0.5$	$u_w = 0.82$, $u_s = 0.5$	$u_w = 0.92$, $u_s = 0.5$	
Phra Nakhon Tai/12	22.8711	22.9695	23.0632	23.0613	23.0599	23.0583	22.77
Khlong Lat Pho/35	16.5191	17.0368	18.0532	17.9751	17.9358	17.8964	13.55
Wat Sai Ma Nuea/64	4.8035	5.1683	5.9919	5.9233	5.8891	5.8550	4.37
Wat Makham/91	1.1023	1.2292	1.4699	1.4516	1.4424	1.4331	1.27
Samlae Pump Station/96	0.5781	0.7043	0.9829	0.9608	0.9497	0.9386	0.58
Wat Phai Lom/102	0.2026	0.2517	0.3996	0.3854	0.3784	0.3715	0.16
Wat Pho Taeng Nuea/111	0.1330	0.1223	0.1168	0.1163	0.1161	0.1160	0.15
Wat Ban Paeng Temple/130	0.1739	0.2010	0.2511	0.2480	0.2464	0.2447	0.13

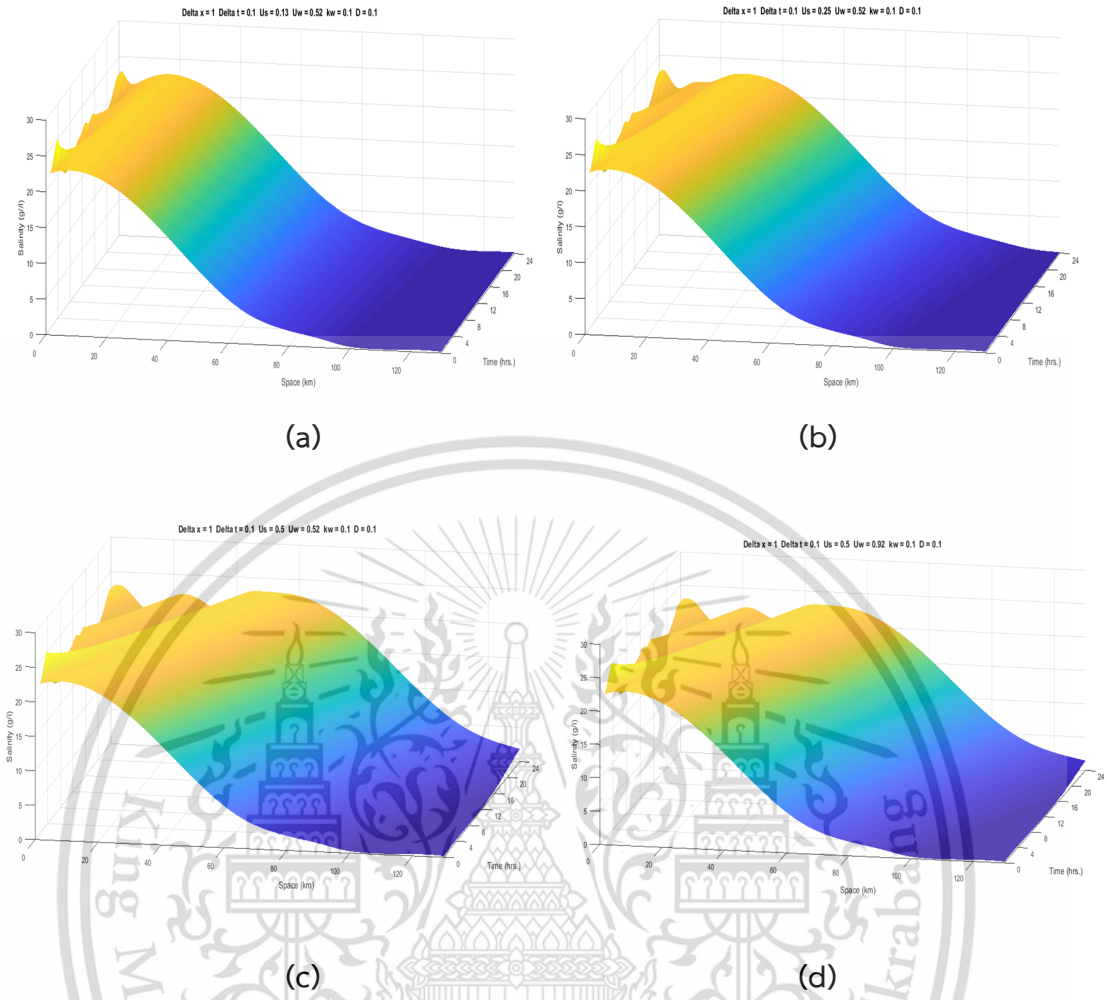

Figure 4.21 (a)-(d): Approximated salinity concentrations (g/l) with MacCormack Scheme and cubic spline interpolation of initial and boundary conditions shown as surfaces (a), (b), (c), and (d) of different combinations of parameter values.

4.2.3 Discussion

In our setting up of the model, it was necessary for u_s and u_w to assume values that would give accurate salinity estimates as compared to the actual measured values. Initially, by trial and error, a suitable tentative range for u_s was found to be 0.13-0.50, and that for u_w was found to be 0.52-0.92. After these ranges were discovered, the model was run repeatedly with several discrete values in these ranges, and the estimates were compared to the measured values. A good fit was found for u_w at 0.52 and u_s at 0.13. It was taken that these values were optimal for our purpose. The estimates and actual values are tabulated in Table 15 and 16 for

these optimal u_w and u_s values, at 4 and 24 hrs after the initial time point. It can be seen that the average difference between those values across all monitoring stations did not exceed 0.42% across the whole range of estimates.

The approximated salinity concentrations from a one-advection-diffusion equation numerically simulated with MacCormack Scheme are shown in Figures 21. (a)-(d). The effect on the approximation from changes in the values of parameters (u_w , u_s), can be seen in the salinity surfaces in the figure (all the surfaces were plotted with time points in the range of 0-24 hrs and space points in the range of 0-130 km). In a similar manner, for every different graph in Figures 15-20, the curve was plotted using the same points in time: the 4th, 8th, 12th, 16th, 20th and 24th hr. In the first case (Figure 15), the parameters were $D=0.1$, $k_w = 0.1$, $u_w = 0.52$ and $u_s = 0.13$ and the salinity concentrations are as listed in Table 9. In the second case (Figure 16), the parameters were $D=0.1$, $k_w = 0.1$, $u_w = 0.52$ and $u_s = 0.25$ and the salinity concentrations are listed in Table 10. In the third case (Figure 17), the parameters are when $D=0.1$, $k_w = 0.1$, $u_w = 0.52$ and $u_s = 0.5$. and the salinity concentrations are as listed in Table 11. In the fourth case (Figure 18), the parameters are when $D=0.1$, $k_w = 0.1$, $u_w = 0.72$ and, $u_s = 0.5$ and the salinity concentrations are listed in Table 12. In the fifth case (Figure 19), the parameters are when $D=0.1$, $k_w = 0.1$, $u_w = 0.82$ and $u_s = 0.5$. and the salinity concentrations are listed in Table 13. In final case (Figure 20), the parameters are when $D=0.1$, $k_w = 0.1$, $u_w = 0.92$ and $u_s = 0.5$. and the salinity concentrations are listed in Table 14.

We modified the U term in original one-dimensional advection-diffusion equation [9, 11, 15 and 17] from being only salinity flow velocity, u_s, to include freshwater velocity, u_w, and salinity dilution rate, k_w, in the form of $U = (u_s - ku_w)$ to account for released freshwater flow from the upriver dam that pushes against most seawater intrusion, and the modification seemed to simulate the real situation at Chao Phraya River well.

4.3 Comparison between estimates from MacCormack scheme and actual measured values.

This study is divided into two main steps. In the first step, hourly-based data collected at 8 monitoring stations along the Chao Phraya River during 05/3-10/2014

were interpolated with cubic spline to the initial condition $S(x,0)$ (g/l) and left boundary condition $S(0,t)$ (g/l), adequately approximating the actual values of these conditions (see Figure 22 and 23). In the second step, salinity concentrations along Chao Phraya River at all monitoring stations were numerically simulated and approximated by a simple advection-diffusion equation and MacCormack Scheme. Figure 24 and 25 show the approximated salinity concentrations in a red line together with scattered points of real data from two monitoring stations, one closest to the estuary and another one more distant to the estuary.

The optimum values of u_s and u_w in our model were found by assigning 6 u_s values and 6 u_w values (see Figure 26 to 29) to the model and determining the simulated salinity concentration for each combination of these u_s and u_k values. Then, the simulated concentration was compared to real salinity concentration to find the best match. It turned out that at $D=0.1$, $k=0.15$, $u_w=0.6$, $u_s=0.1$, the simulated concentrations best matched the real concentrations at two monitoring stations. We also used these optimum parameters to run our model at different times and compared the resulting simulated salinity concentrations to the real concentrations at 4th, 8th, 12th, 16th, 20th and 24th hr. points at one monitoring station and found good matches between those values (See Table 17).

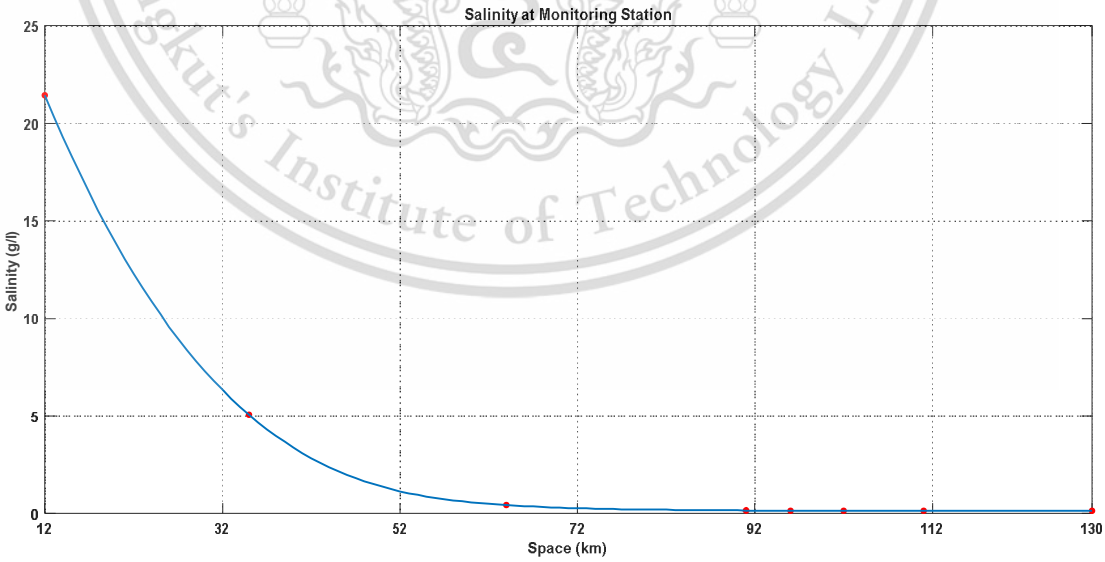

Figure 4.22 Cubic spline interpolated initial condition, $S(x,0)$ (g/l).

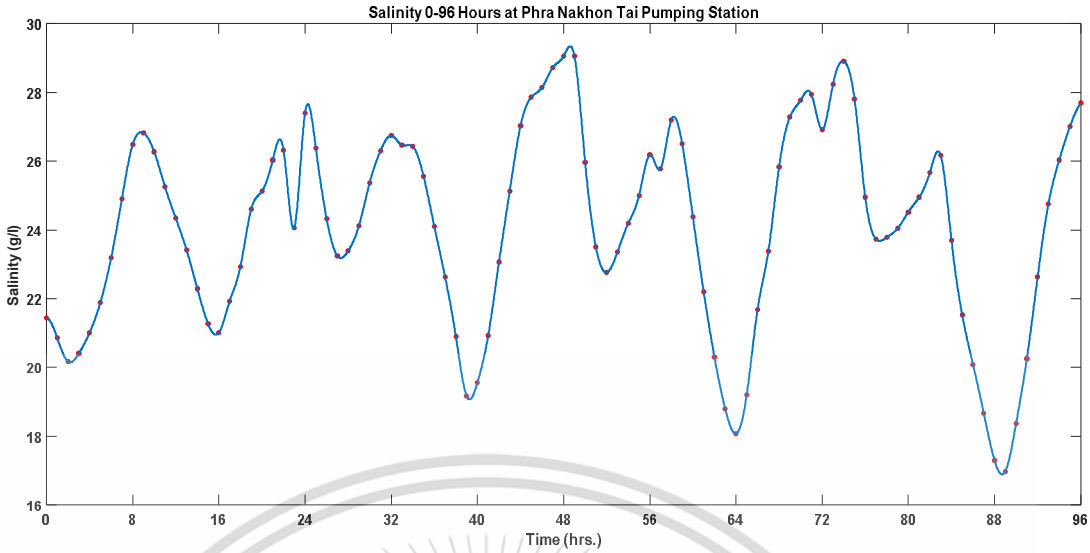

Figure 4.23 Cubic spline interpolated left boundary condition, $S(0,t)$ (g/l).

4.3.1 Comparison between actual and approximated data

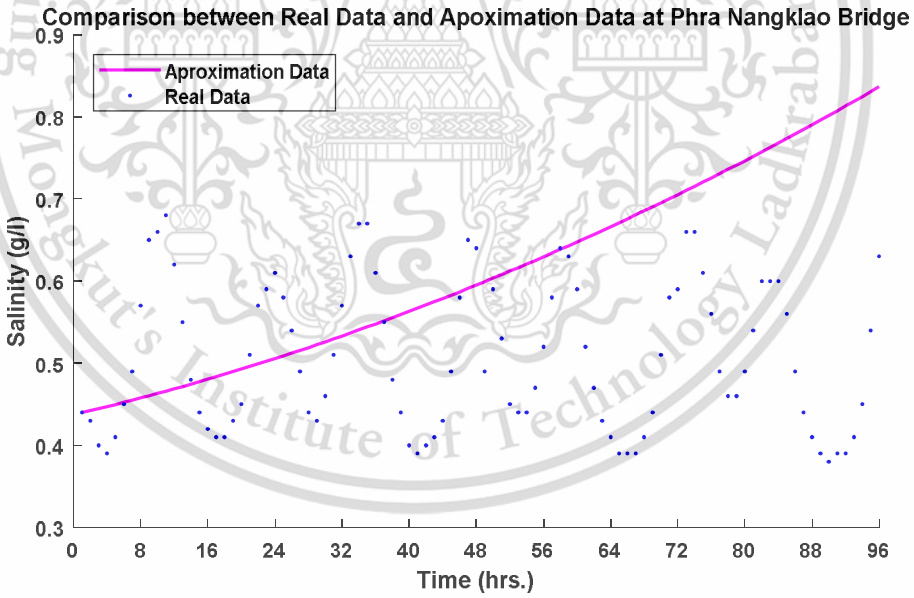

Figure 4.24 Comparison of salinity concentrations (g/l) in 05/3-10/2014 between real (blue dots) and approximated (red-line) at a monitoring station, closest to the estuary.

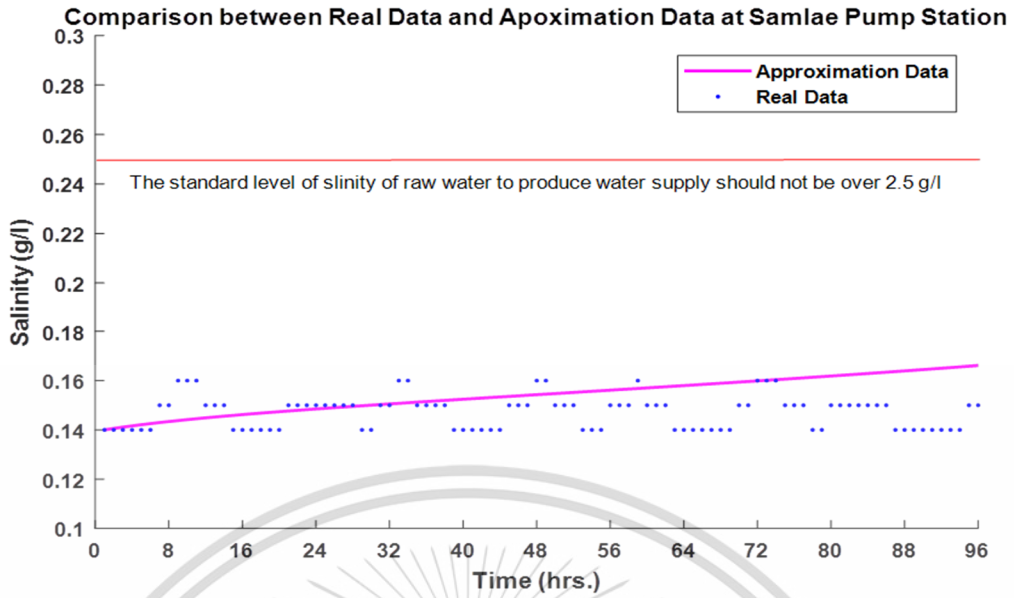

Figure 4.25 Comparison of salinity intrusion concentrations (g/l) in 05/3-10/2014 between real (blue dots) and approximated (red-line) at another monitoring station, 96-km distant from the estuary.

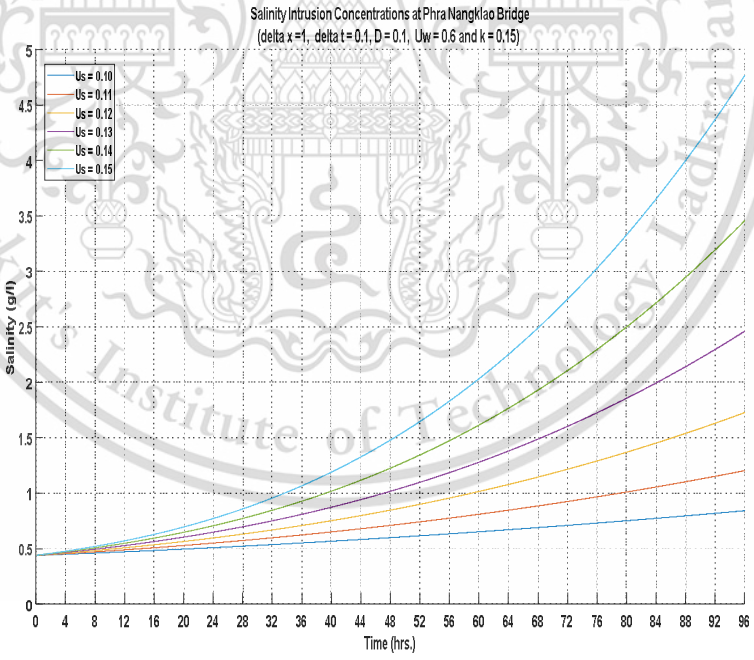

Figure 4.26 Comparison of salinity concentration curves for different u_s at a monitoring station, closest to the estuary.

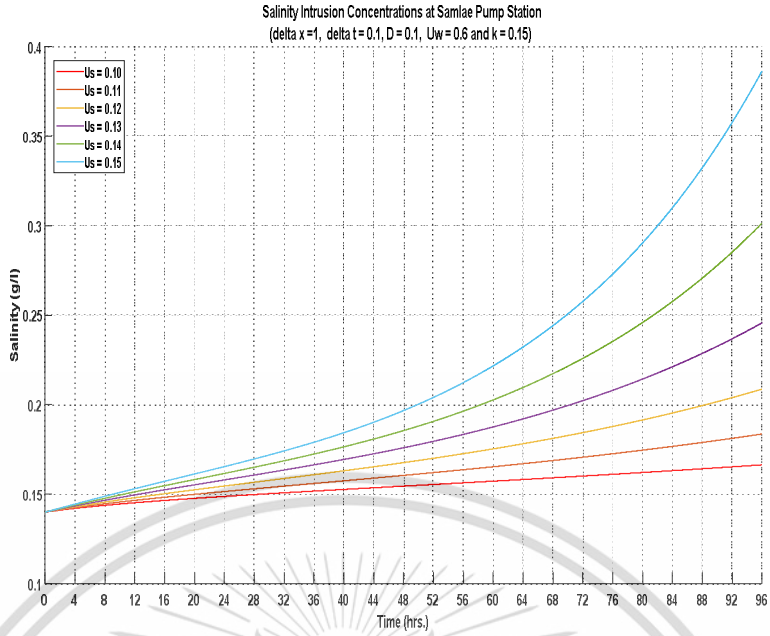

Figure 4.27 Comparison of salinity concentration curves for different u_s at a monitoring station, 96-km distant from the estuary.

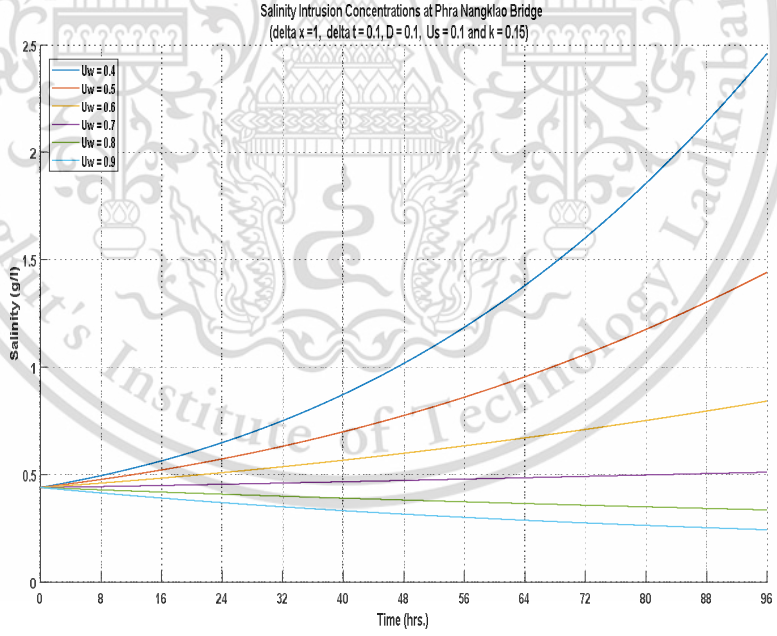

Figure 4.28 Comparison of the salinity concentration curves for different u_w at a monitoring station, closest to the estuary.

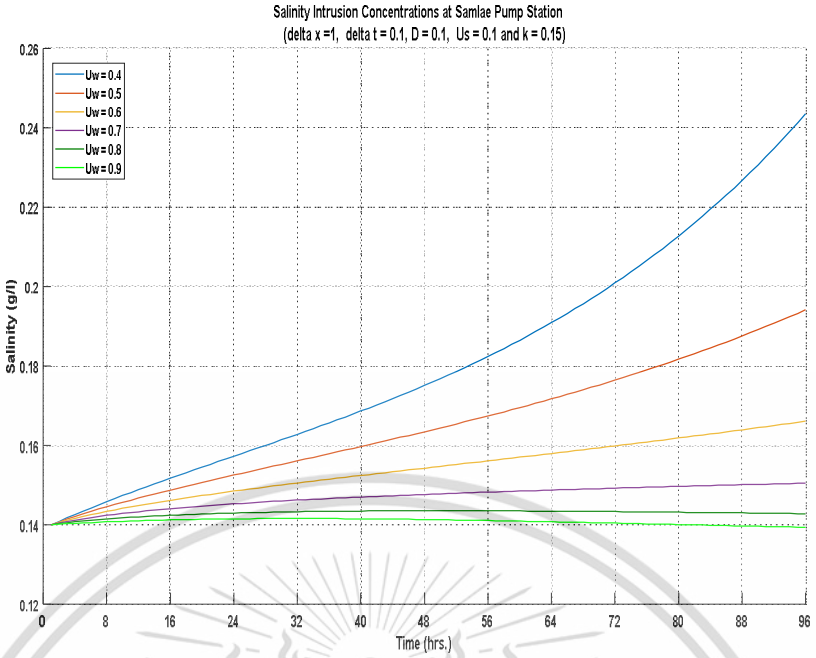

Figure 4.29 Comparison of salinity concentration curves for different u_w at a monitoring station, 96-km distant to the estuary.

Table 4.17 Comparison between real salinity concentrations (g/l) and approximated concentrations with $D = 0.1$, $k = 0.15$, $u_w = 0.6$, $u_s = 0.1$ at a monitoring station and at 4th, 8th, 12th, 16th, 20th and 24th hr. points.

Date 3-May-14	Salinity Concentration $S(x,t)$ (g/l)					
	4th hr	8th hr	12th hr	16th hr	20th hr	24th hr
Real data	0.14	0.16	0.15	0.14	0.15	0.15
Approximated data	0.1421	0.1438	0.1452	0.1465	0.1477	0.1488
Error (%)	1.5019	10.1335	3.1820	4.6474	1.5509	0.8261
Date 4-May-14	Salinity Concentration $S(x,t)$ (g/l)					
	4th hr	8th hr	12th hr	16th hr	20th hr	24th hr
Real data	0.14	0.16	0.15	0.14	0.15	0.16
Approximated data	0.1498	0.1508	0.1517	0.1527	0.1536	0.1545
Error (%)	6.9928	5.7643	1.1563	9.0511	2.3971	3.4291

Table 4.17 (Continued).

Date 5-May-14	Salinity Concentration $S(x,t)$ (g/l)					
	4th hr	8th hr	12th hr	16th hr	20th hr	24th hr
Real data	0.14	0.15	0.15	0.14	0.14	0.16
Approximated data	0.1554	0.1563	0.1573	0.1582	0.1592	0.1601
Error (%)	11.0213	4.2329	4.8506	13.0091	13.6879	0.0810
Date 6-May-14	Salinity Concentration $S(x,t)$ (g/l)					
	4th hr	8th hr	12th hr	16th hr	20th hr	24th hr
Real data	0.15	0.15	0.15	0.14	0.14	0.16
Approximated data	0.1611	0.1621	0.1631	0.1642	0.1653	0.1664
Error (%)	7.4098	8.0805	8.7666	17.2888	18.0613	3.9978

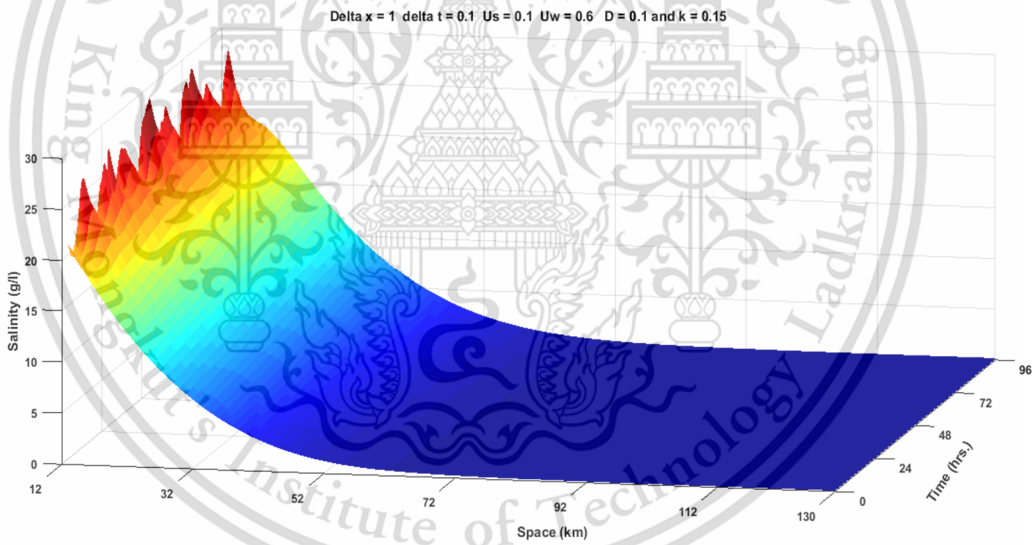

Figure 4.30 Approximated salinity concentrations (g/l) in 05/3-10/2014 calculated with MacCormack Scheme and cubic spline interpolated initial and boundary conditions.

4.3.2 Discussion

In this study, salinity intrusion concentrations along the Chao Phraya River were approximated with a one-dimensional advection-diffusion equation and compared with real concentrations automatically monitored in real-time at several

monitoring stations (from which data were affected by tides at the estuary). The values of the parameters (u_s , u_w) in the equation were optimized to match the actual data. The resulting match between the approximated and real values was satisfactory. These optimum parameter values will also be used in a future experiment for testing a new, improved model.

Chapter 5
Conclusion and suggestions

5.1 Conclusion

5.1.1 We have developed a one-dimensional advection-diffusion equation model and applied numerical techniques to simulate concentrations of salinity intruded from the estuary into lower Chao Phraya River. Two numerical techniques were tested to see which one gave the best simulation results: finite difference MacCormack Scheme and forward time central space (FTCS) scheme. Using the exact solution of the advection-diffusion equation that assumed simple-to-solve initial and boundary conditions as the reference solution, it was found that the MacCormack Scheme provided better simulation results than the FTCS scheme under such assumed conditions. Therefore, MacCormack Scheme was selected as the numerical technique for our purpose. For interpolating the initial condition $S(x,0)$ (g/l) and left boundary condition $S(0,t)$ (g/l) from the discrete measurement data points, another technique, Lagrange interpolation technique was used, but it was found that using either this interpolation technique or using the actual discrete values of the conditions did not provide very much different simulation results.

5.1.2 By trial and error, the optimal values of u_s and u_w for the MacCormack Scheme were found by comparing the simulation results under certain assumed values of u_s and u_w to the actual measured values to be 0.13 and 0.52, respectively. The average difference between those simulated and actual salinity values did not exceed 0.42% across the whole range of estimates and all monitoring stations, verifying that the model was valid for our purpose.

5.1.3 The MacCormack Scheme and cubic spline interpolation technique were used as the final techniques for the proposed model. We chose cubic spline over Lagrange interpolation technique because both of them did not give very much different simulation results but cubic spline provided a smoother curve of interpolation. The estimates from the final model was tested against the actual measured salinity values on 3 May 2014 and found to have an average deviation of not more than 3.64 % across the distance of 96 km and the range of time of 4 days

after the initial time point. To conclude, our proposed model was well able to approximate the salinity values of salinity intrusion along the Chao Phraya River near Samlae Pump Station (from which data were affected by tides downstream). Moreover, since our proposed model and numerical techniques are simple, requiring only a few parameters, it can be facilely applied with only a few minor and simple modifications, to other salinity intrusion cases or the cases of other harmful substances in a river or canal.

5.2 Suggestions

Water management authority and related agents can use our model and techniques on a regular basis to lower operational cost as well as in a crisis when actual measurements cannot be readily obtained in a timely manner.

Furthermore, researchers of salinity intrusion into Chao Phraya River or other similar kind of rivers can use our data as baseline information for investigation in their study in the future.

References

[1] Chinnarasri, C. Phothiwijit, K. and Apipattanavis, S. 2017. "A Study of Flow Characteristics in the Lower Chao Phraya River using Acoustic Doppler Velocity Technology." *KMUTT Research and Development Journal*. 40(2) : 217-235.

[2] National Research Council of Thailand. 2012-2016. National research policy and strategy. Bangkok: National Research Council of Thailand.

[3] Intaboot, N. and Taesombat, W. 2014. "Longitudinal Salinity Intrusion and Dispersion along the Thachin River Due to Sea Level Rise." *Journal of Science and Technology*. 3 : 71-86.

[4] Department, Royal lrrigation. 2014. Summary of situation of salinity and Measures to reduce the impact. Bangkok : Bureau of Water Management and Hydrology.

[5] Intaboot, N. and Taesombat. W. 2014. "A study on salinity intrusion and control measuer in the Thachin River." *Research and Development Journal*. 25 : 45-57.

[6] Atiharuthaisook, K. and Kanasut, J. 2017. "Salinity intrusion Analysis in Thachin River." *Thaicid National Symposium*. 2017 : 137-154.

[7] Intaboot, N. 2016. "The salinity intrusion effected form addition shortcut canal in the lower Thachin River." *Kasem Bundit Engineering Journal*. 6 : 76-90.

[8] Wongsa, S. 2015. "Impact of Climate Change on Water Resources Management in the Lower Chao Phraty Basin,Thailand." *Journal of Geoscience and Environment Protection*. 3 : 53-58.

[9] Owen, A. 1984. "Artificial diffusion in the numerical modelling of the advective transport of salinity." *Applied Mathematical Modelling*. 8 : 116-120.

[10] David, K. Rockwell Geyer, W. and Lerczak, J.A. 2008. "Subtidal Salinity and Velocity in the Hudson River Estuary: Observations and Modeling." *American Meteorological Society*. 2008 : 753-770.

[11] Gurarslan, G. Karahan ,H. Alkaya, D. and Sari, M. 2013. "Numerical Solution of Advection-Diffusion Equation Using a Sixth-Order Compact Finite Difference Method." *Mathematical Problems in Engineering*. 2013 : 1-7.

[12] Pochai, N. 2009. "A numerical computation of a non-dimensional form of stream water quality model with hydrodynamic advection-dispersion-reaction equations." *Nonlinear Analysis: Hybrid System*. 3 : 666-673.

[13] Pochai, N. 2011. "A numerical Treatment of Nondimensional Form of Water Quality Model in a Nonuniform Flow Stream Using Saulyev Scheme." *Mathematical Problems in Engineering*. 2011 : 1-15.

[14] Pochai, N. 2014. "Numerical Treatment of a Modified MacCormack Scheme in a Nondimensional Form of the Water Quality Models in a Nonuniform Flow Stream." *Journal of Applied Mathematics*. 2014 : 1-8.

[15] Pochain, N. 2017. "Unconditional stable numericl techniques for a water-quality model in a non-uniform flow stream." *Advances in Difference Equations*. 2017 : 1-13.

[16] Pochai, N. and Deepana, R. 2011. "An Optimal Control of Water Pollution in a Stream Using a Finite Difference Method." *World Academy of Science*. 80 : 1186-1188.

[17] Dehghan, M. 2004. "Weighted finite difference techniques for the one-dimensional advection-diffusion equation." *Applied Mathematics and Computation*. 147 : 307-319.

[18] Seesod, N. and Pochai, N. 2013. "A numerical Computation to a Water-Quality Measurement in a Stream Using the Finite Volume Method." *International Conference on Engineering, Applied Sciences, and Technology*. 2013 : 98-100.

[19] Pochai, N. Tangmanee, S. Crane, L.J. and Miller, J.J.H. 2006. "A Mathematical Model of Water Pollution Control Using the Finite Element Method." *PAMM.Proc.Appl.Math.Mech*. 6 : 755-756.

[20] Mabood, F. and Pochai, N. 2013. "Asymptotic Solution for a water Quality Model in a Uniform Stream." *International Journal of Engineering Mathematics*. 2013 : 1-4.

[21] Burden, R.L. and Faires, J.D. 2011. *Numerical Analysis.* Boston, Mass, USA : Brook and Cole.

[22] Burden R.L. 1993. *Numerical Analysis*. BOSTON : PWS Publishing Company.

[23] Amparo, G. Segura, J. and Temme N.M. 2007. *Numerical Method for Special Functions.* USA : Society for Industrial and Applied Mathematics.

[24] Gao, S. Zhang, Z. and Cao, Cungen. 2011. "Differentiation and numerical integral of the cubic spline interpolation." *Journal of computers*. 6(10) : 2037-2044.

[25] Richard, L.B. and Douglas Faires, J. 2010. *Numerical Analysis*. 9th ed. Boston : Brooks/Cole.

[26] Chen, J.Y. Ko, C. Bhattacharjee, S. and Elimelech, M. 2001. "Role of spatial distributiion of porous medium surface charge heterogeneity in colloid transport." *Colloids and Surfaces A*. 191 : 3-15.

[27] Li, G. and Jackson, C. R. 2007. "Simple, accurate, and efficient revisions to MacCormack and Saulyev schemes: high Peclet numbers." *Applied Mathematics and Computation*. 186 : 610-622.

[28] O'Loughlin E. M. and Bowmer, K. H. 1975. "Dilution and decay of aquatic herbicdes in flowing channels." *Journal of Hydrology*. 26 : 217-235.

[29] Stamou, A. I. 1992. "Improving the numerical modeling of river water quality by using high order difference schemes." *Water Research*. 26 : 1563-1570.

[30] Pochai, N. Tangmanee,S. Crane, L.J. and Miller, J. J. H. 2008. "A water quality computation in the uniform channel." *Journal of Interdisciplinary Mathrmatics*. 11(6) : 803-814.

[31] Pochai, N. 2009. "A numerical computation of a non-dimensional form of stream water quality model with hydrodynamic advertion-dispersion-reeaction equations." *Journal of Nonlinear Analysis : Hybrid Systems*. 3(4) : 666-673

[32] Pochai, N. 2011. "A numerical treatment of nondimensional form of water quality model in a nonuniform flow stream using Saulyev scheme." *Mathematical Problems in Engineering.* 2011 : Article ID 491317, 15 pages.

[33] Mitchell, A.R. 1969. *Computational Methods in Partial Differential Equations.* John Wiley & Sons.

[34] Bradie, B. 2005. *A Friendly Introduction to Numerical Analysis.* Prentice Hall.

[35] Corless, R.M. Compact finite differences and cubic splines, May 19, 2018. https://www.researchgate.net/publication/325282964_Compact_Finite_Differences_and_Cubic_Splines.

[36] Li, G. and Jackson C.R. Simple, accurate, and efficient revisions to MacCormack and Saulyev schemes : High peclet numbers, Applied mathematics and computation ,2007,186:610622.https://www.researchgate.net/publication/220557939_Simple_accurate_and_efficient_revisions_to_MacCormack_and_Saulyev_schemes_High_Peclet_numbers.

[37] Ariffin, S. Karim, A. Cubic Spline Interpolation for Petroleum Engineering Data, Applied mathematical sciences, 2014, 8(102):5083 - 5098. http://www.m-hikari.com/ams/ams-2014/ams-101-104-2014/karimAMS101-104-2014.pdf.

[38] Ahmad, R.R. Ghazali, N. Rambely, A.S. Din, U.K.S. and Hassan, N. 2012. "Application of Cubic Spline in the implementation of braces for the case of a child." Journal of mathematics and statistics. 8(1) : 144-149.

[39] Hindmarsh, A.C. Gresho, P.M. and Griffitha, D.F. 1984. "The stability of explicit Euler time-integration for certain finite difference approximations of the advection-diffusion equation." *Int. J. Numer. Methods Fluids*. 4(9) : 853 - 897.

[40] Advection. [Online] Avaulable: http://en.wikipedia.org/wiki/Advection.

[41] Diffusion. [Online] Avaulable: http://en.wikipedia.org/wiki/Diffusion.

[42] Radiation. [Online] Avaulable: http://en.wikipedia.org/wiki/Radiation.

[43] Saline water. [Online] Avaulable: http://en.wikipedia.org/wiki/Saline_water.

[44] Chao Phraya River from a high view. [Online] Avaulable: https://www.bangkokpost.com/business/news/1158472/golden-location-with-curved-view-of-chao-phraya-rive.

[45] Chao Phraya River and Samlae Canal Pump Station . [Online] Avaulable: http://englishnews.thaipbs.or.th/six-provinces-warned-rising-water-level-chao-phraya/.

[46] Salinity Level. [Online] Avaulable: http://hydrology.rid.go.th/sediment-wq/index.php/th/water-quality

[47] Graph of salinity level and seawater inflow rate at Sam Lae station. [Online] Avaulable: http://water.rid.go.th/hwm/wmg/water/chart/chart_s.php.

Appendix

Appendix A

Universal Journal of Mechanical Engineering 7(6): 386-397, 2019

"Simulation of Salinity Intrusion in Chao Phraya River by a Developed Mathematical Model and MacCormack scheme with Cubic Spline Interpolation"

Receive October 9, 2019; Revised November 6, 2019; Accepted November 20, 2019

Universal Journal of Mechanical Engineering 7(6): 386-397, 2019 http://www.hrpub.org
DOI: 10.13189/ujme.2019.070610

Simulation of Salinity Intrusion in Chao Phraya River by a Developed Mathematical Model and MacCormack Scheme with Cubic Spline Interpolation

Khemisara Kulmart[1], Nopparat Pochai[1,2,*]

[1]Department of Mathematics, King Mongkut's Institute of Technology Ladkrabang, Thailand
[2]Centre of Excellence in Mathematics, Thailand

Received October 9, 2019; Revised November 6, 2019; Accepted November 20, 2019

Abstract The purpose of this research was to develop a mathematical model for controlling salinity intrusion in Chao Phraya River, Thailand, using one-dimensional advection-diffusion equation. There have been many research studies that applied a mathematical model called dispersion model to estimating salinity concentration. Our proposed dispersion model is simple, using very few parameters, but can simulate salinity intrusion adequately. We used MacCormack scheme to approximate salinity intrusion and cubic spline interpolation technique to approximate field data including initial salinity concentrations and the concentrations at the left boundary. The MacCormack scheme and Cubic Spline interpolation technique were quite suitable for approximating real data, and the proposed mathematical model was able to predict salinity intrusion adequately.

Keywords Salinity Intrusion, MacCormack Scheme, Cubic Spline Interpolation, Chao Phraya River

1. Introduction

Rivers and canals are vital to the existence and livelihood of people. Chao Phraya River originated from the confluence of the Nan and Ping rivers in Nakhon Sawan Province, Thailand. The river flows southwards for about 370 kilometers through the central plains of the country to Bangkok and then down to the sea at the Gulf of Thailand.

Chao Phraya River is maintained by the Water Transmission and Maintenance Project. A main objective of the project is to fix problems related to drought and salinity intrusion. Chao Phraya Dam releases fresh water down into the river to counter salinity intrusion from the sea [1].

In addition to the lack of fresh water during the dry season, the rise and fall of tides around an estuary is another factor that causes salinity intrusion in the Chao Phraya River. The higher level the tides are, the more salt water is pushed upwards a river. Therefore, the Thai government set a measure to constantly monitor the quality of water sources. The real-time water quality monitoring system is generally updated on an hourly basis (see Figure 1)[2] .

Ten stations along Chao Phraya river monitor the salinity concentration in real-time. If the salinity concentration exceeds the standard, the station will issue a warning to related agencies so that counter measures can be made and implemented (See Figure 2)[3] .

A mathematical model is an inexpensive tool that can help approximate, predict, and manage salinity intrusion related problems. Several researchers have conducted studies related to this issue.

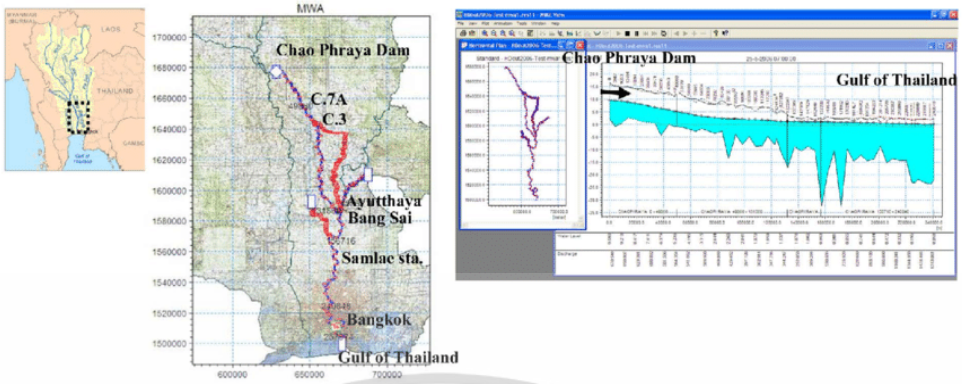

Figure 1. Study areas of the Lower Chao River and model setup [2]

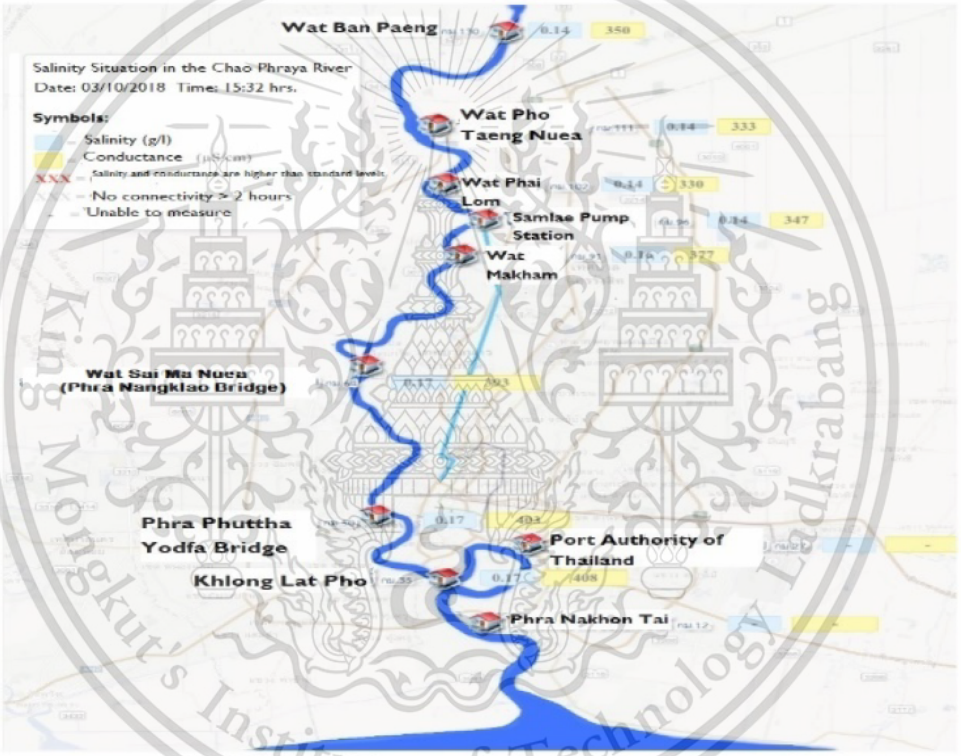

Figure 2. Real-time map of the monitoring stations focused in this study [3]

In [4], two mathematical models—Crank-Nicolson hydrodynamic model and a dispersion model with backward time central space scheme—were used to simulate pollution caused by sewage effluent in the nonuniform water flow in a stream with inconsistency in current velocity. That study demonstrates that the models were applicable to real-world cases. In [5], a better version of a finite difference scheme was used to solve advection-dispersion-reaction equation (ADRE). In that study, a hydrodynamic model and an advection-dispersion-reaction model were used to simulate pollution from sewage effluent. In [6] and [7], research has been presented on the increase of salt water.

In [8], a one-dimensional simulation of water quality

measurement in a stream was done by using a finite volume method to come up with estimated solutions for pollutant concentration equation. The solutions provide logical and rational results that can be applied to water quality measurements. In[9], an Optimal Homotopy Asymptotic Method or OHAM was used to investigate and simulate dispersion of pollutants in water.

In[10], the authors focused on salinity intrusion in the area of the Tha Chin estuary, Thailand and showed that their model was suitable for forecasting natural phenomena related to salinity intrusion. In [11], the researchers came up with a numerical model of salinity's advective transport in the coastal areas, associated with artificial diffusion using upstream differences. This model could be used with small grids of two to four kilometers in the case of tidal problems, while larger grids could be applied to non-tidal problems. In , a tidally and cross-sectionally averaged model were used with Hansen and Rattray equations to simulate the distribution of salinity as well as the vertical exchange flow along the estuary of the Hudson River. Solutions from the model were assessed for the northern San Francisco Bay and the Hudson River over forcing conditions' range.

Some researchers have used Cubic Spline interpolation technique to approximate data related to salinity intrusion and salinity value. In[13], a connection between cubic splines and a popular compact finite difference formula was detailed. The researcher claimed that the compact approach for nonuniform meshes provide some advantages while the one for uniform meshes provide an additional way that helps treating edge effects. In[14], two types of cubic spline functions—cubic spline interpolation with C^2 continuity and Piecewise Cubic Hermite Spline (PCHIP) with C^1 continuity—were used for interpolation. In[15], stream water quality modeling was done by a simple modification of MacCormack and Saulyev schemes. They were used to solve dynamic one-dimensional advection–dispersion–reaction equations (ADRE). The results showed a better prediction accuracy without major loss of efficiency in computation. In[16], the general form of teeth method was compared with a cubic spline method applied to a mathematical model of teeth of a child in order to obtain a minimum error in showing the form of general teeth while creating a better view of the nature of orthodontic wires. The results of this cubic spline method showed a symmetrical teeth's shape of curve of a normally asymmetrical curve. An example was provided in that study to show how efficient, accurate, and simple the proposed method is.

In this study, we focused on parameter optimization of a mathematical model of Chao Phraya River under the influence of tides that affected salinity values in the river. The salinity concentration generated by the model, MacCormack technique and spline interpolation were compared with real salinity concentration to see whether the model could estimate real data adequately or not.

2. One-dimensional Salinity Intrusion Measurement Model in a River with a Diversion Dam

2.1. The Governing Equation

The mathematical model describing transportation and diffusion processes is a one-dimensional advection-diffusion-reaction equation (ADRE).The advection-diffusion equation is [5,10,17 and 18]

$$\frac{\partial S}{\partial t}+U\frac{\partial S}{\partial x}=D\frac{\partial^2 S}{\partial x^2},\quad \text{for all } 0\le x\le L \text{ and } 0\le t\le T \tag{1}$$

where $S(x,t)$ is the salinity concentration (g/l); U is the water flow velocity in x-directions (m/s); D is the salinity diffusion coefficient (m^2/s); L is the length of a condimental stream; and T is the stationary time of simulation.

Letting that

$$U=u_s-ku_w, \tag{2}$$

where u_s is the salinity advection rate; u_w is the fresh water flow velocity function that is released by the diversion dam; and k is the dilution rate of salinity by fresh water, for all $0<x\le L$ and $0\le t\le T$.

Substituting Eq. (2) into Eq. (1), we get

$$\frac{\partial S}{\partial t}+(u_s-ku_w)\frac{\partial S}{\partial x}=D\frac{\partial^2 S}{\partial x^2}. \tag{3}$$

2.2. Initial and Boundary Conditions

The effects of salinity intrusion in this estuarine, which likely will become more severe in the future, are caused by ocean tides. The mathematical model was applied to analyze the salinity intrusion. The initial salinity values were different depending on the time and distance along the river.

2.2.1. The Initial Condition

The initial condition was assumed to be

$$S(x,0)=f(x),\quad \text{for all } 0\le x\le L, \tag{4}$$

where $f(x)$ is a given initial measurement of salinity concentration function along the considered river.

2.2.2. The Boundary Condition

The left boundary condition was assumed to be

$$S(0,t)=g(t),\quad \text{for all } 0<t\le T, \tag{5}$$

where $g(t)$ is a given present measurement of salinity

concentration function at the first monitoring station which is the closest to the estuary. The right boundary condition was assumed to be

$$\frac{\partial S}{\partial x}(L,t)=k_0, \quad \text{for all } 0<t\le T, \tag{6}$$

where k_0 is the rate of change of salinity concentration around the most distant monitoring station.

3. Numerical Techniques

The salinity concentration was calculated by using MacCormack Scheme, and the values at the left boundary condition and initial values were calculated by using Cubic spline interpolation, as described below.

3.1. MacCormack Scheme

We can approximate $S(x_i,t_n)$ by S_i^n, the value of the approximation of $S(x,t)$ at any point $x=i\Delta x$ and $t=n\Delta t$, where $0\le i\le n$ and $0\le n\le N$. The grid point (x_n,t_n) is defined by $x_i=i\Delta x$ for all $i=0,1,2,\ldots,M$ and $t_n=n\Delta t$ for all $n=0,1,2,\ldots,N$ in which M and N are positive integers.

3.1.1 The First Step of the MacCormack Scheme

The first step of the MacCormack scheme is to approximate S and its derivatives in equation (3) by forward time and forward space scheme (FTFS) as follows:

$$\begin{aligned} S &\cong S_i^n, \\ \frac{\partial S}{\partial t} &\cong \frac{S_i^{n+1}-S_i^n}{\Delta t} \\ \frac{\partial S}{\partial x} &\cong \frac{S_{i+1}^n-S_i^n}{\Delta x} \\ \frac{\partial^2 S}{\partial x^2} &\cong \frac{S_{i+1}^n-2S_i^n+S_{i-1}^n}{(\Delta x)^2}. \end{aligned} \tag{7}$$

Substituting (7) into (3), we get

$$\left[\frac{S_i^{n+1}-S_i^n}{\Delta t}\right]+U\left[\frac{S_{i+1}^n-S_i^n}{\Delta x}\right]=D\left[\frac{S_{i+1}^n-2S_i^n+S_{i-1}^n}{(\Delta x)^2}\right] \tag{8}$$

for $1\le i\le M$ and $0\le n\le N-1$, and simplify form (8) by

$$\left[\frac{S_i^{n+1}-S_i^n}{\Delta t}\right]=-\frac{U}{\Delta x}\left[S_{i+1}^n-S_i^n\right]=\frac{D}{(\Delta x)^2}\left(S_{i+1}^n-2S_i^n+S_{i-1}^n\right). \tag{9}$$

Define $(C_i)_1$ by LHS of (9), we have

$$(C_i)_1=-\frac{U}{\Delta x}\left(S_{i+1}^n-S_i^n\right)+\frac{D}{\Delta x^2}\left(S_{i+1}^n-2S_i^n+S_{i-1}^n\right) \tag{10}$$

and

$$(C_i)_1=-\frac{U}{\Delta x}S_{i+1}^n-\frac{U}{\Delta x}S_i^n+\frac{D}{\Delta x^2}S_{i+1}^n-\frac{2D}{\Delta x^2}S_i^n+\frac{D}{\Delta x^2}S_{i-1}^n. \tag{11}$$

Let $A_1=-\frac{U}{\Delta x}+\frac{D}{(\partial x)^2}, A_2=\frac{U}{\Delta x}-\frac{2D}{(\partial x)^2}, A_3=\frac{D}{(\partial x)^2}$.

We obtain $A_1=-\frac{U}{\Delta x}+\frac{D}{(\partial x)^2}, A_2=\frac{U}{\Delta x}-\frac{2D}{(\partial x)^2}, A_3=\frac{D}{(\partial x)^2}$, we have

$$\left(C_1\right)_i=A_1S_{i+1}^n+A_2S_i^n+A_3S_{i-1}^n. \tag{12}$$

For left boundary, where $i=1$, we obtain

$$\begin{aligned} \left(C_1\right) &= A_1S_2^n+A_2S_1^n+A_3S_0^n \\ &= A_1S_2^n+A_2S_1^n+A_3S_0. \end{aligned} \tag{13}$$

For right boundary, where $i=M$, substitute the approximate unknown value the right boundary by forward difference approximation to $\frac{\partial S}{\partial x}=0$. Let $S_M=S_{M-1}$, we have

$$\left(C_M\right)_1=A_1S_M^n+A_2S_{M+1}^n+A_3S_{M-2}^n \tag{14}$$

$$=\left(A_1+A_2\right)S_{M-1}^n+A_3S_{M-2}^n \tag{15}$$

we obtain the MacCormack predictor step formulation

$$S_i^{n+1}=S_i^n+\left(C_i\right)_1\Delta t. \tag{16}$$

3.1.2. The Second Step of the MacCormack Scheme

The second step of the MacCormack scheme is approximation equation (3) by a backward time and backward space scheme (BTBS) following by:

$$\begin{aligned} \frac{\partial S}{\partial t} &\cong \frac{S_i^{n+1}-S_i^n}{\Delta t} \\ \frac{\partial S}{\partial x} &\cong \frac{S_i^{n+1}-S_{i-1}^{n+1}}{\Delta x} \\ \frac{\partial^2 S}{\partial x^2} &\cong \frac{S_{i+1}^{n+1}-2S_i^{n+1}+S_{i-1}^{n+1}}{(\Delta x)^2}. \end{aligned} \tag{17}$$

Substituting (17) into, we get

$$\frac{S_i^{n+1}-S_i^n}{\Delta t}+U\left[\frac{S_i^{n+1}-S_{i-1}^{n+1}}{\Delta x}\right]=D\left[\frac{S_{i+1}^{n+1}-2S_i^{n+1}+S_{i-1}^{n+1}}{(\Delta x)^2}\right], \tag{18}$$

and simplify (18) by

$$\frac{S_i^{n+1}-S_i^n}{\Delta t}=-U\left[\frac{S_i^{n+1}-S_{i-1}^{n+1}}{\Delta x}\right]+D\left[\frac{S_{i+1}^{n+1}-2S_i^{n+1}+S_{i-1}^{n+1}}{(\Delta x)^2}\right]. \tag{19}$$

Define $\left(C_i\right)_2$ by LHS of (3.13), we have

$$(C_i)_2 = -\frac{U}{\Delta x}\left(S_i^{n+1} - S_{i-1}^{n+1}\right) + \frac{D}{(\Delta x)^2}\left(S_{i+1}^{n+1} - 2S_i^{n+1} + S_{i-1}^{n+1}\right) \quad (20)$$

$$= \frac{D}{(\Delta x)^2} S_{i+1}^{n+1} + \left(-\frac{U}{\Delta x} - \frac{2D}{(\Delta x)^2}\right) S_i^{n+1} + \left(\frac{U}{\Delta x} + \frac{D}{(\Delta x)^2}\right) S_{i-1}^{n+1}.$$

Let

$$B_1 = \frac{D}{(\Delta x)^2}, B_2 = -\frac{U}{\Delta x} - \frac{2D}{(\Delta x)^2}, B_3 = \frac{U}{\Delta x} + \frac{D}{(\Delta x)^2},$$

we have

$$(C_i)_2 = B_1 S_2^{n+1} + B_2 S_1^{n+1} + B_3 S_0^{n+1}. \quad (21)$$

For left boundary, where $i = 1$

$$\begin{aligned}(C_1)_2 &= B_1 S_2^{n+1} + B_2 S_1^{n+1} + B_3 S_0^{n+1} \\ &= B_1 S_2^{n+1} + B_2 S_1^{n+1} + B_3 S_0.\end{aligned} \quad (22)$$

For right boundary, where $i = M$ and approximate unknown value at right boundary by backward difference approximation to $\frac{\partial S}{\partial x} = 0$. Let $S_{M+1} = S_M$, we have

$$(C_M)_2 = \left(B_1 + B_2\right) S_M^{n+1} + B_3 S_{M-1}^{n+1}. \quad (23)$$

From first and second step for the MacCormack scheme takes following form:

$$S_i^{M+1} = S_i^n + \frac{\Delta t}{2}\left(\left(C_i\right)_1 + \left(C_i\right)_2\right). \quad (24)$$

With conditionally stable for this scheme by

$$\text{condition } \frac{D\Delta t}{(\Delta x)^2} < 0.5, \quad (25)$$

and

$$\frac{U\Delta t}{(\Delta x)} < 0.9. \quad (26)$$

3.2 Interpolation Technique for the Initial and Boundary Condition Interpolation

3.2.1. Cubic Spline Interpolation

Raw salinity concentration data were obtained by field measurement at the first monitoring station which is the closest to the Chao Phraya estuary. Function $f(x)$ and $g(t)$ were defined by using those data. In this research, cubic spline interpolation was introduced to represent the field data for initial and boundary conditions as described below.

The cubic spline interpolation method, which is a piecewise polynomial approximation, considers a unique cubic equation of each subinterval such that they have necessary conditions as first and second derivatives of a continuous cubic spline [19, 20].

Suppose $(x_0, y_0), (x_1, y_1), (x_2, y_2), \ldots, (x_n, y_n)$ are nodes. In all, there are $n+1$ pairs of nodes where $a = x_0 < x_1 < \ldots < x_n = b$. Function $S(x)$ is approximated to be between a pair of nodes. It is called a cubic spline if there exist n cubic polynomials that satisfy these conditions:

(1). $S(x)$ is a cubic polynomial on each subinterval $[x_i, x_{i+1}]$ where $i = 0, 1, \ldots, n-1$

$$S_i(x) = a_i + b_i(x - x_i) + c_i(x - x_i)^2 + d_i(x - x_i)^3, \quad (27)$$

a_i, b_i, c_i, and d_i are unknown constant coefficients of each cubic polynomial,

(2). $S_{i+1}(x_{i+1}) = S_i(x_{i+1})$ where $i = 0, 1, \ldots, n-2$, (28)

(3). $S'_{i+1}(x_{i+1}) = S'_i(x_{i+1})$ where $i = 0, 1, \ldots, n-2$, (29)

(4). $S''_{i+1}(x_{i+1}) = S''_i(x_{i+1})$ where $i = 0, 1, \ldots, n-2$, (30)

(5). One of sets of boundary conditions is satisfied according to this condition as

(i). $S''(x_0) = S''(x_n) = 0$ (natural boundary), (31)

(ii). $S'(x_0) = y'_0$ and $S'(x_n) = y'_n$ (clamped boundary). (32)

For the natural boundary conditions, there are n linear equations for coefficients $c_0, c_1, c_2, \ldots, c_n$ so we can solve the solution of c_i from a tridiagonal linear system $T\mathbf{x} = \mathbf{b}$, where T is a tridiagonal matrix of $n \times n$ as follows

$$T = \begin{bmatrix} 1 & 0 & 0 & 0 & 0 & 0 \\ h_0 & 2(h_0+h_1) & h_1 & \ddots & \ddots & 0 \\ 0 & h_1 & 2(h_1+h_2) & h_2 & \ddots & 0 \\ 0 & \ddots & \ddots & \ddots & \ddots & 0 \\ 0 & \ddots & \ddots & h_{n-2} & 2(h_{n-2}+h_{n-1}) & h_{n-1} \\ 0 & 0 & 0 & 0 & 0 & 1 \end{bmatrix}, \quad (33)$$

$$\mathrm{b} = \begin{bmatrix} \alpha_0 \\ \alpha_1 \\ \vdots \\ \alpha_{n-1} \\ \alpha_n \end{bmatrix} = \begin{bmatrix} 0 \\ \frac{3}{h_1}(a_2 - a_1) - \frac{3}{h_0}(a_1 - a_0) \\ \vdots \\ \frac{3}{h_{n-1}}(a_n - a_{n-1}) - \frac{3}{h_{n-2}}(a_{n-1} - a_{n-2}) \\ 0 \end{bmatrix}, \quad (34)$$

$$\text{and } \mathrm{x} = \begin{bmatrix} c_0 \\ c_1 \\ \ddots \\ c_n \end{bmatrix}. \quad (35)$$

Then $\mathbf{b}$ and $\mathbf{x}$ are the vectors dimension of n,

$$h_i = x_{i+1} - x_i, \quad (36)$$

$$\alpha_i = \frac{3}{h_i}(a_{i+1} - a_i) - \frac{3}{h_{i-1}}(a_i - a_{i-1}) \text{ for } i = 1, 2, \ldots, n-1.$$

(37)

a_i, b_i and d_i can be calculate by the following these equations

$$a_i = y_i \text{ where } i = 0,1,\ldots,n, \quad (38)$$

$$b_i = \frac{(a_{i+1} - a_i)}{h_i} - \frac{h_i(c_{i+1} - 2c_i)}{3} \text{ where } i = 0,1,\ldots,n-1, \quad (39)$$

$$\text{And } d_i = \frac{(c_{i+1} - c_i)}{3h_i} \text{ where } i = 0,1,\ldots,n-1. \quad (40)$$

The results of coefficients can always be written in the form of cubic function on $[x_i, x_{i+1}]$ where $i = 0,1,\ldots,n-1$ as

$$S_i(x) = a_i + b_i(x - x_i) + c_i(x - x_i)^2 + d_i(x - x_i)^3. \quad (41)$$

4. Numerical Experiment

This study is divided into two main steps. In the first step, hourly-based data collected at 8 monitoring stations along the Chao Phraya River during 05/3-10/2019 were interpolated with cubic spline to the initial condition $S(x,0)$ (g/l) and left boundary condition $S(0,t)$ (g/l), adequately approximating the values at these conditions (see Figure 3 and 4). In the second step, salinity intrusion concentrations at all monitoring stations were numerically simulated and approximated by a simple advection-diffusion equation and MacCormack Scheme. Figure 5 and 6 show the approximated salinity concentrations in a red line together with scattered points of real data from two monitoring stations, one closest to the estuary and another one more distant to the estuary.

The optimum values of u_s and u_w of our model were found by assigning 6 u_s values and 6 u_w values (see Figure 7 to 10) to the model and determining the simulated salinity concentration for each combination of these u_s and u_k values. Then, the simulated concentration was compared to real salinity concentration to find the best match. It turned out that at $D = 0.1$, $k = 0.15$, $u_w = 0.6$, $u_s = 0.1$, the simulated concentrations best matched the real concentrations at two monitoring stations. We also used these optimum parameters to run our model at different times and compared the resulting simulated salinity concentrations to the real concentrations at 4, 8, 12, 16, 20 and 24 (hrs.) at one monitoring station and found a good match between those values (See Table 1).

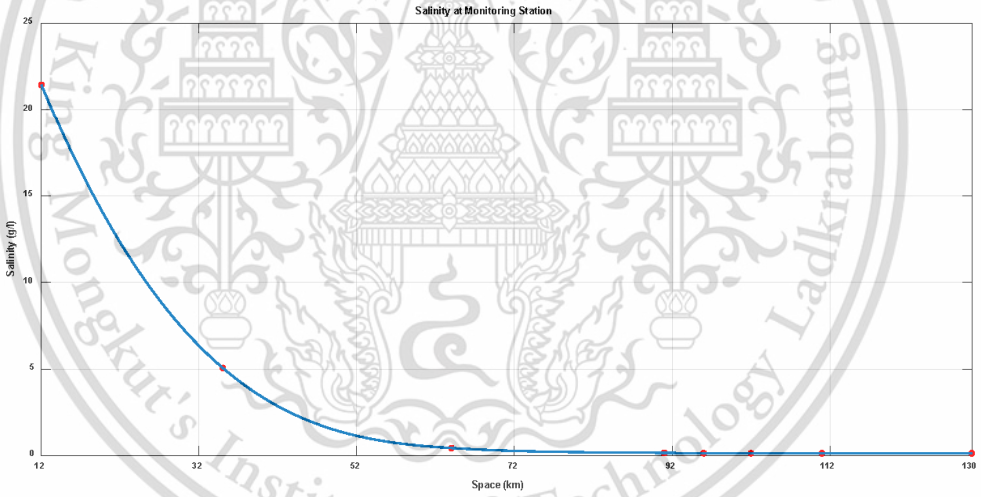

Figure 3. Cubic spline interpolated initial condition, $S(x,0)$ (g/l)

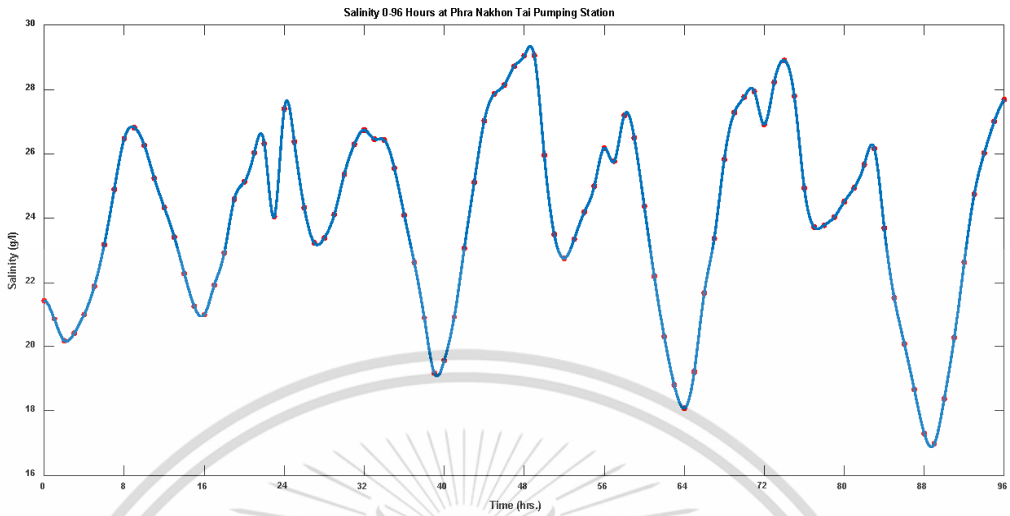

Figure 4. Cubic spline interpolated left boundary condition, $S(0,t)$ (g/l)

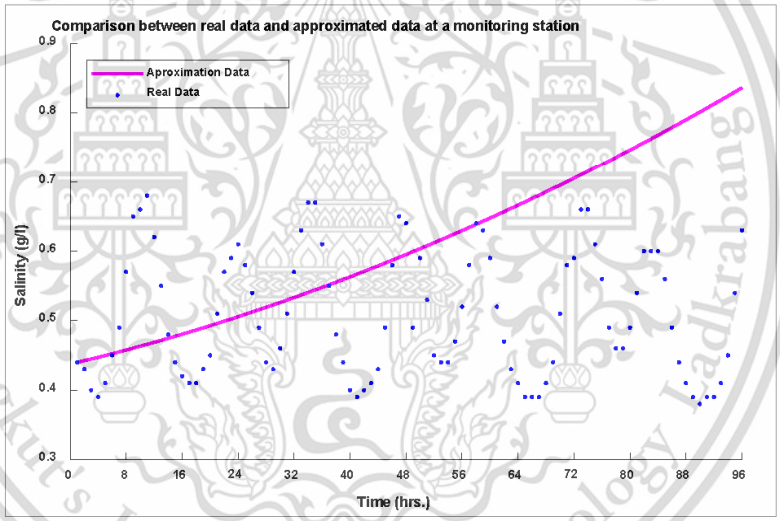

Figure 5. Comparison of salinity intrusion concentration (g/l) in 05/3-10/2019 between real data (blue -line) and approximated data (red-line) at a monitoring station, closest to the estuary

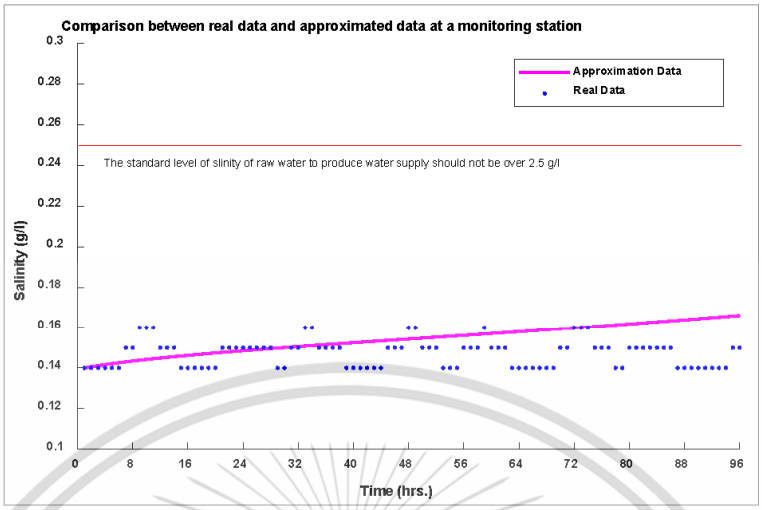

Figure 6. Comparison of salinity intrusion concentration (g/l) in 05/3-10/2019 between real data (blue-line) and approximated data (red-line) at another monitoring station, more distant to the estuary

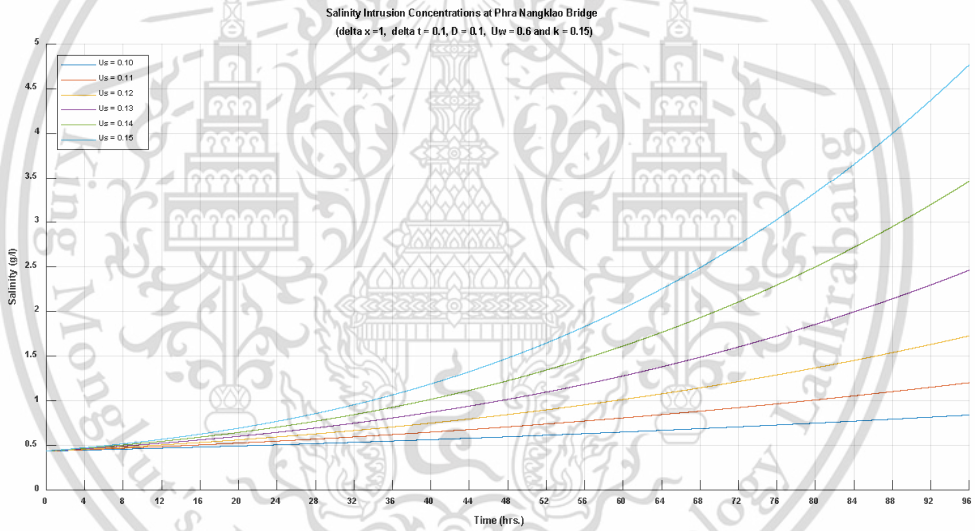

Figure 7. Comparison of salinity intrusion concentration curves for different u_s at a monitoring station, distant to the estuary

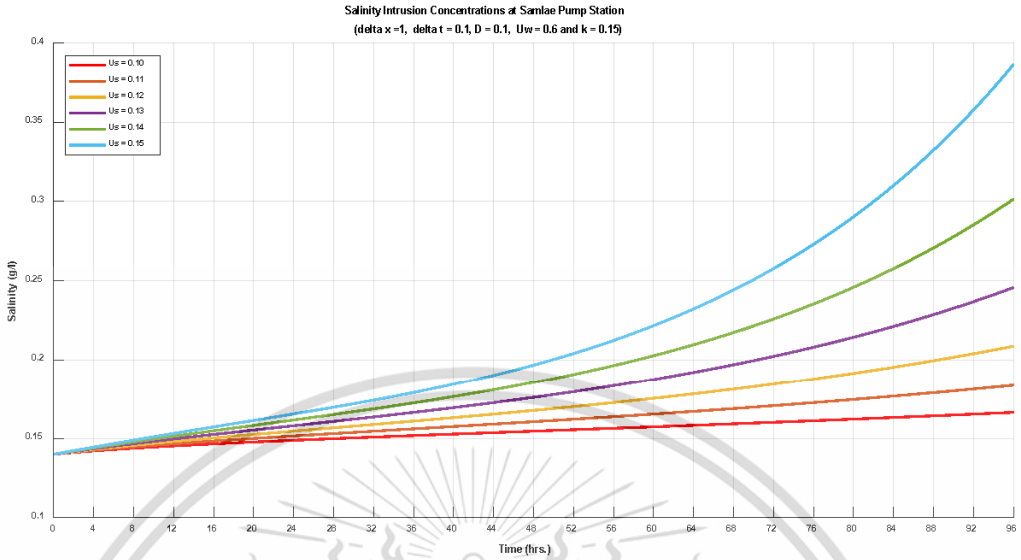

Figure 8. Comparison of salinity intrusion concentration curves for different u_s at a monitoring station, more distant to the estuary

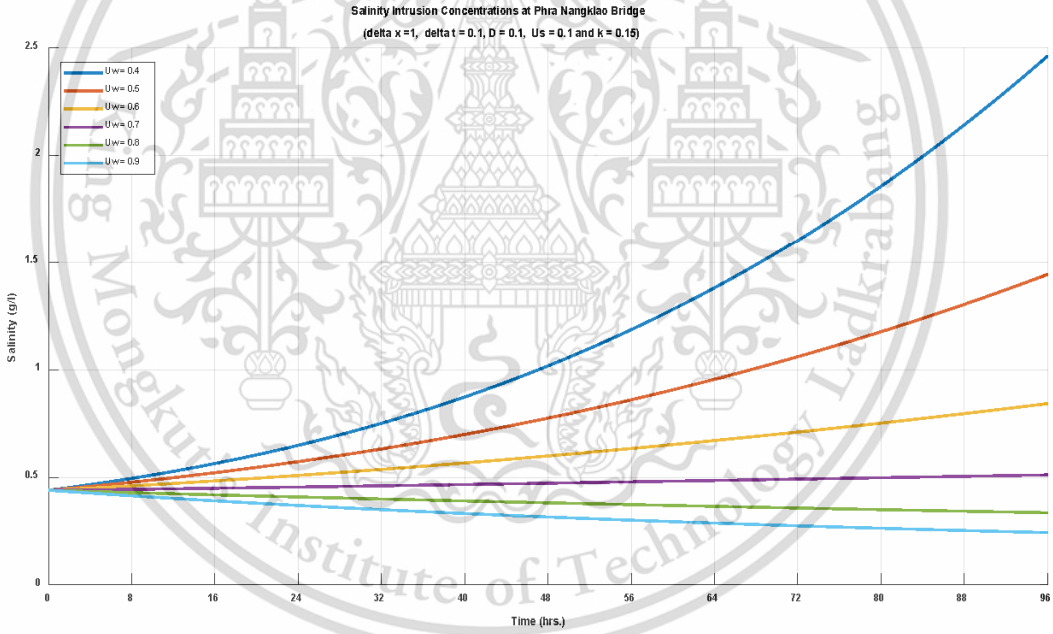

Figure 9. The comparison of the salinity intrusion concentration curves for different u_w at a monitoring station, close to the estuary

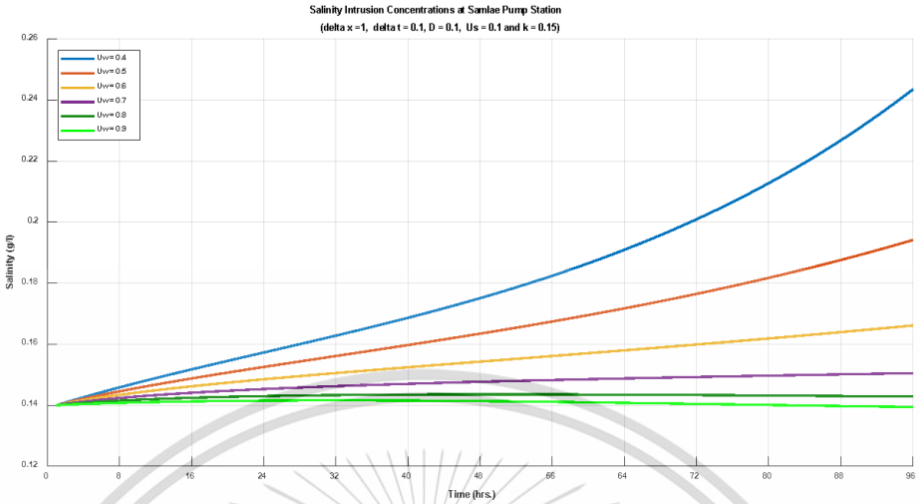

Figure 10. Comparison of salinity intrusion concentration curves for different u_w at a monitoring station, more distant to the estuary

Table 1. Comparison of real salinity intrusion concentrations (g/l) and approximated concentrations with $D = 0.1$, $k = 0.15$, $u_w = 0.6$, $u_s = 0.1$ at a monitoring station and 4, 8, 12, 16, 20 and 24 hr collection times

Date 3-May-19	**Salinity Intrusion Concentration $S(x,t)$ (g/l)**					
	4 hr	**8 hr**	**12 hr**	**16 hr**	**20 hr**	**24 hr**
Real data	0.14	0.16	0.15	0.14	0.15	0.15
Approximated data	0.1421	0.1438	0.1452	0.1465	0.1477	0.1488
Error (%)	1.5019	10.1335	3.1820	4.6474	1.5509	0.8261
Date 4-May-19	**Salinity Intrusion Concentration $S(x,t)$ (g/l)**					
	4 hr	**8 hr**	**12 hr**	**16 hr**	**20 hr**	**24 hr**
Real data	0.14	0.16	0.15	0.14	0.15	0.16
Approximated data	0.1498	0.1508	0.1517	0.1527	0.1536	0.1545
Error (%)	6.9928	5.7643	1.1563	9.0511	2.3971	3.4291
Date 5-May-19	**Salinity Intrusion Concentration $S(x,t)$ (g/l)**					
	4 hr	**8 hr**	**12 hr**	**16 hr**	**20 hr**	**24 hr**
Real data	0.14	0.15	0.15	0.14	0.14	0.16
Approximated data	0.1554	0.1563	0.1573	0.1582	0.1592	0.1601
Error (%)	11.0213	4.2329	4.8506	13.0091	13.6879	0.0810
Date 6-May-19	**Salinity Intrusion Concentration $S(x,t)$ (g/l)**					
	4 hr	**8 hr**	**12 hr**	**16 hr**	**20 hr**	**24 hr**
Real data	0.15	0.15	0.15	0.14	0.14	0.16
Approximated data	0.1611	0.1621	0.1631	0.1642	0.1653	0.1664
Error (%)	7.4098	8.0805	8.7666	17.2888	18.0613	3.9978

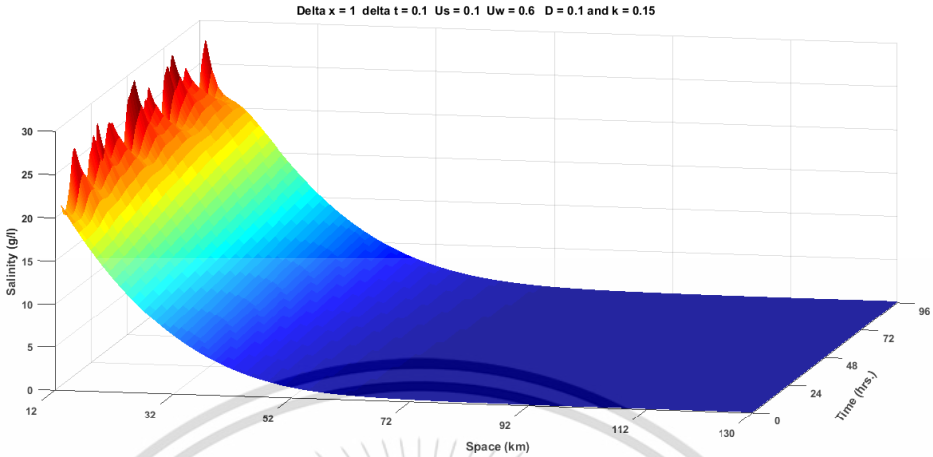

Figure 11. Approximated salinity intrusion concentrations (g/l) in 05/3-10/2019 calculated by the MacCormack Scheme with cubic spline interpolated initial and boundary conditions

5. Discussion and Conclusions

In this study, salinity intrusion concentrations along the Chao Phraya River were approximated with a one-dimensional advection-diffusion equation and compared with real concentrations automatically monitored in real-time at several monitoring stations (from which data were affected by tides at the downstream). The values of the parameters (u_s , u_w) of the equation were optimized. The resulting match between the approximated and real values was satisfactory. These optimum parameter values will be used in a future experiment that will test a new, improved model.

Conflicts of Interest

The authors declare that there are no conflicts of interest with any parties whatsoever.

Acknowledgements

This research was supported by the Center of Excellence in Mathematics, the Commission on Higher Education, Thailand. The authors greatly appreciate valuable comments from the referees from the metropolitan Waterworks Authority, Water Resources and Environment Department.

REFERENCES

[1] Department, Royal Irrigation. Summary of situation of salinity and Measures to reduce the impact. Bangkok: Bureau of Water Management and Hydrology, 2014.

[2] S. Wongsa. "Impact of Climate Change on Water Resources Management in the Lower Chao Phraty Basin,Thailand." Journal of Geoscience and Environment Protection, vol 3, pp. 53-58, 2015.

[3] Water Resources and Enviroment Department of Metropolitan Waterworks Authority, "Salinity Situation in the Chao Phraya River". 2018. Retrieved from http://rwc.mwa.co.th

[4] N. Pochai. "A numerical computation of a non-dimensional form of stream water quality model with hydrodynamic advection-dispersion-reaction equations." Nonlinear Analysis: Hybrid System, vol. 3, pp. 666-673, 2009.

[5] N. Pochai. "A numerical Treatment of Nondimensional Form of Water Quality Model in a Nonuniform Flow Stream Using Saulyev Scheme." Mathematical Problems in Engineering, vol. 2011, pp. 1-15, 2011.

[6] K. Leewatchanakul. "Salinity intrusion in the Chao Pharya river." PhD thesis, Chulalongkirn University, 1988.

[7] P. Othata, and N. Pochai. "A one – dimensionl mathematical simulation to salinity control in a river with a barrage dam using an unconditionally stable explicit finite difference method." Advances in Difference Equations, vol. 2019, pp. 1-12, 2019.

[8] N. Seesod, and N. Pochai. "A numerical Computation to a Water-Quality Measurement in a Stream Using the Finite Volume Method." International Conference on Engineering, Applied Sciences,and Technology, vol. 2013, pp. 98-100, 2013.

[9] F. Mabood, and N. Pochai. "Asymptotic Solution for a water Quality Model in a Uniform Stream." International Journal of Engineering Mathematics, vol. 2013, pp. 1-4, 2013.

[10] N. Intaboot, and W. Taesombat. "Longitudinal Salinity

Intrusion and Dispersion along the Thachin River Due to Sea Level Rise." Journal of Science and Technology, vol. 3, pp. 71-86, 2014.

[11] A. Owen, "Artificial diffusion in the numerical modelling of the advective transport of salinity." Applied Mathematical Modelling, vol. 8, pp. 116-120, 1984.

[12] K.Ralston, David, W. Rockwell Geyer, and J.A. Lerczak. "Subtidal Salinity and Velocity in the Hudson River Estuary: Observations and Modeling." American Meteorological Society, vol. 2008, pp. 753-770, 2008.

[13] R.M. Corless. "Compact finite differences and cubic splines." May 19, 2018. Online: https://www.researchgate.net/publication/325282964_Compact_Finite_Differences_and_Cubic_Splines.

[14] S. Ariffin, and A. Karim. "Cubic Spline Interpolation for Petroleum Engineering Data." Applied mathematical sciences, vol. 8, pp. 5083-5098, 2014.

[15] G. Li, and C.R. Jackson. "Simple, accurate, and efficient revisions to MacCormack and Saulyev schemes: High peclet numbers." Applied mathematics and computation, vol 186, pp. 610-622, 2007.

[16] R.R. Ahmad, N. Ghazali, A.S. Rambely, U.K.S. Din, and N. Hassan. "Application of Cubic Spline in the implementation of braces for the case of a child." Journal of mathematics and statistics, vol 8, pp. 144-149. 2012.

[17] N. Pochai. "Unconditional stable numericl techniques for a water-quality model in a non-uniform flow stream." Advances in Difference Equations, vol. 2017, pp. 1-13, 2017.

[18] M. Dehghan. "Weighted finite difference techniques for the one-dimensional advection-diffusion equation." Applied Mathematics and Computation, vol. 147, pp. 307-319, 2004.

[19] G. Shang, Z. Zaiyue, and C. Cungen. "Differentiation and numerical integral of the cubic spline interpolation." Journal of computers, vol. 6, pp. 2037-2044, 2011.

[20] L.B. Richard, and J.D. Faires. Numerical Analysis. 9th ed., Brooks/Cole, Cengage Learning, 2010.

Appendix B

“A Numerical Model for Salinity Intrusion Measurement and Control Based on MacCormack Finite Difference Method and Cubic Spline Interpolation”

IJSSST V21, No. 1, 2020; EDAS identifier 1763611,

Accepted February 13, 2020

A Numerical Model for Salinity Intrusion Measurement and Control Based on MacCormack Finite Difference Method and Cubic Spline Interpolation

Khemisara Kulmart[1] and Nopparat Pochai [1,2]

[1]Department of Mathematics, Faculty of Science King Mongkut's Institute of Technology Ladkrabang Bangkok 10520 Thailand

[2]Centre of Excellence in Mathematics CHE, Si Ayutthaya Rd. Bangkok 10400Thailand

Abstract

The purpose of this research was to develop a numerical model of one-dimensional advection-diffusion equation for estimating salinity level in Lower Chao Phraya River, Thailand. The main numerical technique was MacCormack finite-difference scheme with initial and boundary conditions approximated by cubic spline interpolation. The estimates matched satisfactorily with actual measurement data from several salinity monitoring stations along the river. The final model was first used by Thailand's Metropolitan Waterworks Authority for planning salinity control in 2018.

Keywords: salinity intrusion, MacCormack scheme, cubic spline interpolation, Chao Phraya River

1. Introduction

Freshwater is one of the most important natural resources for the livelihood of humans, animals, and plants. In Thailand, tap water produced from freshwater along Chao Phraya River is consumed by millions of people in Bangkok metropolitan. Good quality freshwater is also depended on by agricultural and manufacturing industries situated near the river. Recently, seawater intrusion from the estuary into lower Chao Phraya River has become more aggressive, creating problems with tap water production and low water quality for said industries. To counter the intrusion, freshwater needed to be released from an upriver dam. However, during dry season, the amount of freshwater held by the dam is low, and there is a need to strictly control the amount released for countering the intrusion. In planning out a good control strategy, fast and accurate salinity level readings are necessary, which may not be readily and timely supplied by various salinity monitoring stations along the river. Therefore, a numerical model that can accurately and immediately provide good salinity level estimates at key points along the river is in dire need. Our work is an attempt to solve this issue.

Chao Phraya River is the major river in the central region of Thailand starting from a confluence of four rivers at Pak Nam Pho ($14.23848^{\circ}N, 100.575364^{\circ}E$), flowing pass several provinces including Bangkok and down to the estuary ($13.58^{\circ}-15.67^{\circ}N, 100.10^{\circ}-101.00^{\circ}E$) to the Gulf of Thailand for the total distance of 300 kilometers.

Several salinity monitoring stations have been erected along the river. Samlae pumping station that acts as a salinity monitoring station and a pumping station for tap water production for Bangkok Metropolitan is 96 km upriver from the estuary (see Figure 1). The actual measurement data for our reference was taken from this station [1].

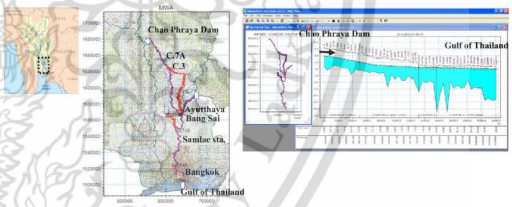

Figure1. Lower Chao Phraya River and levels of seawater intrusion along the river [2]

Recently, the use of mathematical models to calculate natural phenomena has become more popular due to in-depth findings of natural phenomena processes and advancement in computer hardware and software. Solutions of complex system of equations representing natural processes can be approximated quickly with new numerical techniques. Many researchers have used water-quality models to approximate salinity level in rivers. Intaboot and

Taesombat [3] investigated salinity intrusion in the area of the Tha Chin estuarine. They used a mathematical model called "MIKE-HD/AD" to predict that the maximum distance of salinity intrusion would reach 55 kilometers further up the river than it was in 2015 and provided a suitable freshwater flow rate to counter the intrusion of about 20-40 cubic meters per second. A higher flow rate would not help pushing salinity out any better. As another example, A. Owen [4] has reported a development of numerical modeling of salinity's advective transport in coastal areas, associated with artificial diffusion using upstream differences. This particular model can be used small grids of two to four kilometers for tidal problems, while larger grids are used for non-tidal problems. Ralston et al. [5] applied Hansen and Rattray equations to simulate the distribution of salinity and vertical exchange flow along the estuary of the Hudson River. N. Pochai [6] used an improved finite difference scheme to solve an advection-dispersion-reaction equation (ADRE) that takes into account the effect of stream's nonuniform water flow. Two mathematical models, a hydrodynamic model and an advection-dispersion-reaction model were used to simulate pollution from sewage effluent. Li and Jackson [7] reported another case of stream water quality modeling using simple modifications of MacCormack and Saulyev schemes to solve dynamic one-dimensional advection–dispersion–reaction equations (ADRE). The prediction accuracy was better than the original schemes without major loss of computational efficiency.

Several researchers have used Cubic Spline interpolation technique to approximate data related to salinity intrusion and level in rivers. R.M. Corless [8] detailed a connection between cubic splines and a popular compact finite difference formula, claiming that a compact approach with nonuniform meshes provides some advantages while the approach with uniforms meshes helps treat edge effects. Ariffin and Karim [9] used two types of cubic spline functions—cubic spline interpolation with C^2 continuity and Piecewise Cubic Hermite Spline (PCHIP) with C^1 continuity for interpolating data. Both cubic splines were numerically compared with each other as well as with linear spline and achieved good results. In a paper by Ahmad et al. [10], a mathematical model of teeth of a child was compared with cubic spline method to see which one produced a minimum error in showing the general form of normal teeth and created a better view of the nature of orthodontic wires. The cubic spline method showed a more symmetrical teeth's shape; the curves of a tooth were more symmetrical than the normally asymmetrical curves. An example was provided to show how efficient, accurate, and simple the cubic spline method actually was.

In this research, we began by developing a mathematical model using an extension of one-dimensional advection-diffusion equation to simulate seawater intrusion counteracted by flow of freshwater released from an upriver dam, with MacCormack scheme and Cubic Spline interpolation to approximate field data—salinity levels at initial and left boundary conditions.

2. One-dimensional salinity intrusion model

2.1 Governing equation

The mathematical model that we used to describe transportation and diffusion processes of salinity in a river is a one-dimensional advection-diffusion-reaction equation (ADRE) [4, 11, and 12].

$$\frac{\partial S}{\partial t}+U\frac{\partial S}{\partial x}=D\frac{\partial^2 S}{\partial x^2}, \quad \text{for all } 0\le x\le L \text{ and } 0\le t\le T, \tag{2.1}$$

where $S(x,t)$ is the salinity concentration (g/l); U is the water flow velocity in the x-direction (m/s); D is the salinity diffusion coefficient (m²/s); L is the length of lower Chao Phraya river; and T is the simulated time period.

Letting

$$U=(u_s-ku_w), \tag{2.2}$$

where u_s is the salinity flow velocity; u_w is the fresh water flow velocity released by the diversion dam; and k is the dilution rate of salinity by fresh water, for all $0<x\le L, 0\le t\le T$.

Substituting Eq. (2.2) into Eq. (2.1), we get

$$\frac{\partial S}{\partial t}+(u_s-ku_w)\frac{\partial S}{\partial x}=D\frac{\partial^2 S}{\partial x^2}. \tag{2.3}$$

2.2 Initial and boundary conditions

The salinity intrusion in Chao Phraya estuary, which is likely to become more severe in the future, are caused by high ocean tide. In calculation, initial

salinity level can be different depending on the time and distance from the estuary.

2.2.1 The initial condition

The initial condition is assumed to be

$$S(x,0)=f(x), \quad \text{for all} \quad 0\le x\le L, \tag{2.4}$$

where $f(x)$ is a given salinity level function along the river.

2.2.2 The boundary condition

The left boundary condition is assumed to be

$$S(0,t)=g(t), \quad \text{for all} \quad 0<t\le T, \tag{2.5}$$

where $g(t)$ is a given salinity level function at the first monitoring station, closest closed to the estuary. The right boundary condition is assumed to be

$$\frac{\partial S}{\partial x}(L,t)=k_0, \quad \text{for all} \quad 0<t\le T, \tag{2.6}$$

where k_0 is the rate of change of salinity level at the last monitoring station, located furthest upriver from the estuary.

3. Numerical Techniques

The solution to the set of equations in Section 2 is numerically approximated by an explicit finite difference method, MacCormack scheme for advection, below.

3.1 MacCormack Scheme for Advection

We can approximate $S(x_i,t_n)$ by S_i^n, the value of the difference approximate of $S(x,t)$ at point $x=i\Delta x$ and $t=n\Delta t$, where $0\le i\le n$ and $0\le n\le N$. The grid point (x_n,t_n) is defined by $x_i=i\Delta x$ for all $i=0,1,2,...,M$ and $t_n=n\Delta t$ for all $n=0,1,2,...,N$ in which M and N are positive integers. The first step of the MacCormack scheme is to approximate equation (2.3) by forward time and forward space scheme (FTFS) as follows,

$$\begin{aligned} S &\cong S_i^n, \\ \frac{\partial S}{\partial t} &\cong \frac{S_i^{n+1}-S_i^n}{\Delta t}, \\ \frac{\partial S}{\partial x} &\cong \frac{S_{i+1}^n-S_i^n}{\Delta x}, \\ \frac{\partial^2 S}{\partial x^2} &\cong \frac{S_{i+1}^n-2S_i^n+S_{i-1}^n}{(\Delta x)^2}. \end{aligned} \tag{3.1}$$

Substituting (3.1) into (2.3), we get

$$\left[\frac{S_i^{n+1}-S_i^n}{\Delta t}\right]+U\left[\frac{S_{i+1}^n-S_i^n}{\Delta x}\right]=D\left[\frac{S_{i+1}^n-2S_i^n+S_{i-1}^n}{(\Delta x)^2}\right] \tag{3.2}$$

for $1\le i\le M$ and $0\le n\le N-1$. Simplifying (3.2) to

$$\left[\frac{S_i^{n+1}-S_i^n}{\Delta t}\right]=-\frac{U}{\Delta x}\left[S_{i+1}^n-S_i^n\right]+\frac{D}{(\Delta x)^2}\left(S_{i+1}^n-2S_i^n+S_{i-1}^n\right). \tag{3.3}$$

Define $(C_i)_1$ by LHS of (3.3), we have

$$(C_i)_1=-\frac{U}{\Delta x}\left(S_{i+1}^n-S_i^n\right)+\frac{D}{\Delta x^2}\left(S_{i+1}^n-2S_i^n+S_{i-1}^n\right) \tag{3.4}$$

and

$$(C_i)_1=-\frac{U}{\Delta x}S_{i+1}^n-\frac{U}{\Delta x}S_i^n+\frac{D}{\Delta x^2}S_{i+1}^n-\frac{2D}{\Delta x^2}S_i^n+\frac{D}{\Delta x^2}S_{i-1}^n. \tag{3.5}$$

Let

$$A_1=-\frac{U}{\Delta x}+\frac{D}{(\partial x)^2}, A_2=\frac{U}{\Delta x}-\frac{2D}{(\partial x)^2}, A_3=\frac{D}{(\partial x)^2}.$$

We obtain

$$A_1=-\frac{U}{\Delta x}+\frac{D}{(\partial x)^2}, A_2=\frac{U}{\Delta x}-\frac{2D}{(\partial x)^2}, A_3=\frac{D}{(\partial x)^2},$$

so we have

$$(C_1)_i=A_1S_{i+1}^n+A_2S_i^n+A_3S_{i-1}^n. \tag{3.6}$$

For left boundary, where $i=1$, we obtain

$$\begin{aligned} (C_1) &= A_1S_2^n+A_2S_1^n+A_3S_0^n \\ &= A_1S_2^n+A_2S_1^n+A_3S_0. \end{aligned} \tag{3.7}$$

For right boundary, where $i=M$, substitute the approximate unknown value of the right boundary with forward difference approximation to $\frac{\partial S}{\partial x}=0.$

Let $S_M = S_{M-1}$, we have

$$\left(C_M\right)_1 = A_1 S_M^n + A_2 S_{M+1}^n + A_3 S_{M-2}^n \tag{3.8}$$

$$= \left(A_1 + A_2\right) S_{M-1}^n + A_3 S_{M-2}^n \tag{3.9}$$

we obtain a MacCormack predictor step formulation

$$S_i^{n+1} = S_i^n + \left(C_i\right)_1 \Delta t. \tag{3.10}$$

The second step of the MacCormack scheme is to approximate equation (2.3) with a backward time and backward space scheme (BTBS) as follows,

$$\begin{aligned} \frac{\partial S}{\partial t} &\cong \frac{S_i^{n+1} - S_i^n}{\Delta t}, \\ \frac{\partial S}{\partial x} &\cong \frac{S_i^{n+1} - S_{i-1}^{n+1}}{\Delta x}, \\ \frac{\partial^2 S}{\partial x^2} &\cong \frac{S_{i+1}^{n+1} - 2S_i^{n+1} + S_{i-1}^{n+1}}{(\Delta x)^2}. \end{aligned} \tag{3.11}$$

Substitute (3.11) into Eq. 2.3, we get

$$\frac{S_i^{n+1} - S_i^n}{\Delta t} + U\left[\frac{S_i^{n+1} - S_{i-1}^{n+1}}{\Delta x}\right] = D\left[\frac{S_{i+1}^{n+1} - 2S_i^{n+1} + S_{i-1}^{n+1}}{(\Delta x)^2}\right]. \tag{3.12}$$

Simplify (3.12) to

$$\frac{S_i^{n+1} - S_i^n}{\Delta t} = -U\left[\frac{S_i^{n+1} - S_{i-1}^{n+1}}{\Delta x}\right] + D\left[\frac{S_{i+1}^{n+1} - 2S_i^{n+1} + S_{i-1}^{n+1}}{(\Delta x)^2}\right]. \tag{3.13}$$

Define $\left(C_i\right)_2$ by LHS of (3.13), we have

$$(C_i)_2 = -\frac{U}{\Delta x}\left(S_i^{n+1} - S_{i-1}^{n+1}\right) + \frac{D}{(\Delta x)^2}\left(S_{i+1}^{n+1} - 2S_i^{n+1} + S_{i-1}^{n+1}\right) \tag{3.14}$$

$$= \frac{D}{(\Delta x)^2} S_{i+1}^{n+1} + \left(-\frac{U}{\Delta x} - \frac{2D}{(\Delta x)^2}\right) S_i^{n+1} + \left(\frac{U}{\Delta x} + \frac{D}{(\Delta x)^2}\right) S_{i-1}^{n+1}$$

Let

$$B_1 = \frac{D}{(\Delta x)^2}, B_2 = -\frac{U}{\Delta x} - \frac{2D}{(\Delta x)^2}, B_3 = \frac{U}{\Delta x} + \frac{D}{(\Delta x)^2},$$

we have

$$(C_i)_2 = B_1 S_2^{n+1} + B_2 S_1^{n+1} + B_3 S_0^{n+1}, \tag{3.15}$$

for left boundary, where $i=1$.

$$\begin{aligned} (C_1)_2 &= B_1 S_2^{n+1} + B_2 S_1^{n+1} + B_3 S_0^{n+1} \\ &= B_1 S_2^{n+1} + B_2 S_1^{n+1} + B_3 S_0. \end{aligned} \tag{3.16}$$

For right boundary, where $i=M$, the unknown values are approximated by backward difference approximation to $\frac{\partial S}{\partial x}=0.$ Let $S_{M+1} = S_M$, we have

$$\left(C_M\right)_2 = \left(B_1 + B_2\right) S_M^{n+1} + B_3 S_{M-1}^{n+1}. \tag{3.17}$$

From the first and second steps, the MacCormack scheme takes on following form:

$$S_i^{M+1} = S_i^n + \frac{\Delta t}{2}\left(\left(C_i\right)_1 + \left(C_i\right)_2\right). \tag{3.18}$$

The stable conditions for this scheme are the following,

condition $$\frac{D\Delta t}{(\Delta x)^2} < 0.5, \tag{3.19}$$

and $$\frac{U\Delta t}{(\Delta x)} < 0.9. \tag{3.20}$$

3.2 Interpolation technique for the initial and boundary conditions

3.2.1 Cubic spline interpolation

Salinity measurement data were collected as discrete points in time and space. To construct a continuous model based on those discrete data, some interpolation was necessary. A cubic spline interpolation method could do this interpolation job well. A cubic spline interpolation is a piecewise polynomial approximation, representing the interpolated points in a subinterval with a unique cubic equation. A necessary condition for cubic spline construction is that the first and second derivatives of a cubic spline must be continuous [13, 14].

Suppose $(x_0, y_0), (x_1, y_1), (x_2, y_2), \ldots, (x_n, y_n)$ are $n+1$ node pairs where $a = x_0 < x_1 < \ldots < x_n = b.$ Function

$S(x)$ approximating the values between each pair of nodes is called a cubic spline if there exist n cubic polynomials that satisfy these conditions.

(1) $S(x)$ is a cubic polynomial on each subinterval $[x_i, x_{i+1}]$ where $i = 0,1,...,n-1$

$$S_i(x) = a_i + b_i(x - x_i) + c_i(x - x_i)^2 + d_i(x - x_i)^3, \quad (3.21)$$

$a_i, b_i, c_i,$ and d_i are unknown constant coefficients of the cubic polynomial of each subinterval,

(2) $S_{i+1}(x_{i+1}) = S_i(x_{i+1})$ where $i = 0,1,...,n-2$, (3.22)

(3) $S'_{i+1}(x_{i+1}) = S'_i(x_{i+1})$ where $i = 0,1,...,n-2$, (3.23)

(4) $S''_{i+1}(x_{i+1}) = S''_i(x_{i+1})$ where $i = 0,1,...,n-2$, (3.24)

(5) Boundary conditions to be satisfied and interpolated by this cubic spline are the following:

(i) $S''(x_0) = S''(x_n) = 0$ (natural boundary), (3.25)

(ii) $S'(x_0) = y'_0$ and $S'(x_n) = y'_n$ (clamped boundary). (3.26)

For the natural boundary condition, there are n linear equations for coefficients $c_0, c_1, c_2, ..., c_n$ so we can solve the solution for c_i from a tridiagonal linear system $T\mathbf{x} = \mathbf{b}$, where T is a tridiagonal matrix of $n \times n$ as follows:

$$T = \begin{bmatrix} 1 & 0 & 0 & 0 & 0 & 0 \\ h_0 & 2(h_0+h_1) & h_1 & \ddots & \ddots & 0 \\ 0 & h_1 & 2(h_1+h_2)_2 & h_2 & \ddots & 0 \\ 0 & \ddots & \ddots & \ddots & \ddots & 0 \\ 0 & \ddots & \ddots & h_{n-2} & 2(h_{n-2}+h_{n-1}) & h_{n-1} \\ 0 & 0 & 0 & 0 & 0 & 1 \end{bmatrix}, \quad (3.27)$$

$$\mathbf{b} = \begin{bmatrix} \alpha_0 \\ \alpha_1 \\ \vdots \\ \alpha_{n-1} \\ \alpha_n \end{bmatrix} = \begin{bmatrix} 0 \\ \frac{3}{h_1}(a_2 - a_1) - \frac{3}{h_0}(a_1 - a_0) \\ \vdots \\ \frac{3}{h_{n-1}}(a_n - a_{n-1}) - \frac{3}{h_{n-2}}(a_{n-1} - a_{n-2}) \\ 0 \end{bmatrix}, \quad (3.28)$$

and $\mathbf{x} = \begin{bmatrix} c_0 \\ c_1 \\ \ddots \\ c_n \end{bmatrix}$. (3.29)

Then $\mathbf{b}$ and $\mathbf{x}$ are vectors of dimension n,

$$h_i = x_{i+1} - x, \quad (3.30)$$

$$\alpha_i = \frac{3}{h_i}(a_{i+1} - a_i) - \frac{3}{h_{i-1}}(a_i - a_{i-1})$$

for $i = 1,2,...,n-1$. (3.31)

a_i, b_i and d_i can be calculated by the following equations,

$$a_i = y_i \text{ where } i = 0,1,...,n, \quad (3.32)$$

$$b_i = \frac{(a_{i+1} - a_i)}{h_i} - \frac{h_i(c_{i+1} - 2c_i)}{3}$$

where $i = 0,1,...,n-1$, (3.33)

and $d_i = \frac{(c_{i+1} - c_i)}{3h_i}$ where $i = 0,1,...,n-1$. (3.34)

The cubic function on $[x_i, x_{i+1}]$, $i = 0,1,...,n-1$, with these coefficients can always be written as

$$S_i(x) = a_i + b_i(x - x_i) + c_i(x - x_i)^2 + d_i(x - x_i)^3. \quad (3.35)$$

4. Numerical Experiment

4.1 Cubic spline interpolation based on field data

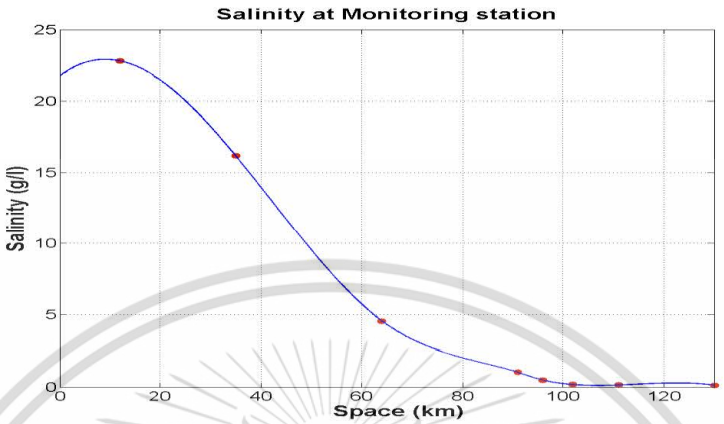

Figure2. Cubic spline interpolated initial condition $S(x,0)$ (g/l)

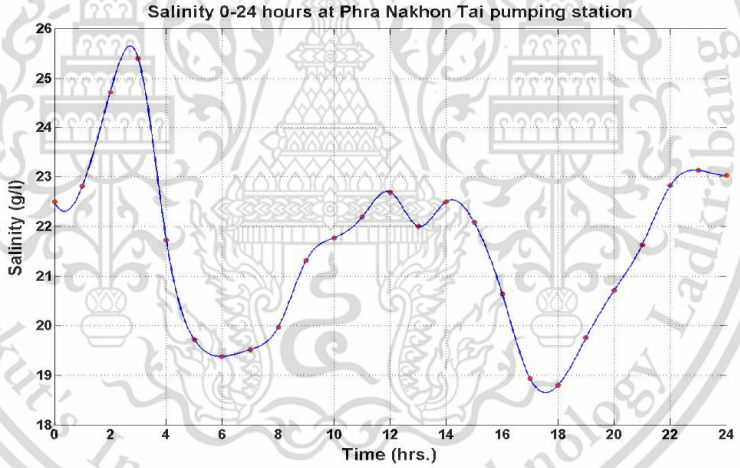

Figure3. Cubic spline interpolated left boundary condition $S(0,t)$ (g/l) (the left boundary was the sea)

4.2 Approximation of salinity intrusion by MacCormack Scheme

4.2.1 Fig. 4–9 are MacCormack generated graphs of salinity level versus distance in space, when u_s was varied from 0.13, 0.25 and 0.5 m/s and was u_w varied from 0.52, 0.72, 0.82 and 0.92 m/s, at 4, 8, 12, 16, 20 and 24 hours after the initial time point. The graphs were produced in order to find the optimum value of u_s *and* u_w for the model.

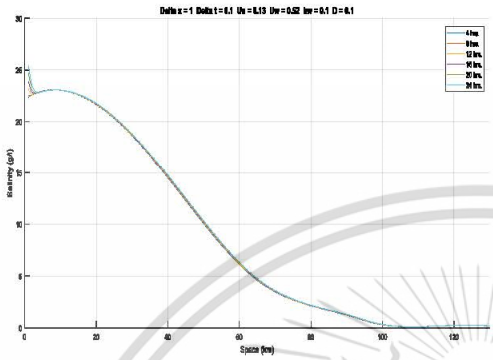

Figure 4. Approximated salinity intrusion levels (g/l) when $u_s = 0.13$ and at time 4, 8,12,16,20 and 24 hrs after the initial time point

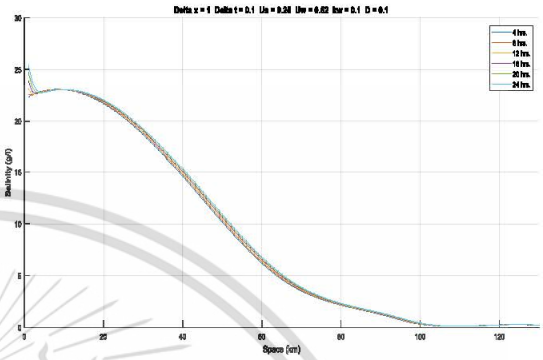

Figure 5. Approximated salinity intrusion levels (g/l) when $u_s = 0.25$ and at time 4, 8,12,16,20 and 24 hrs after the initial time point

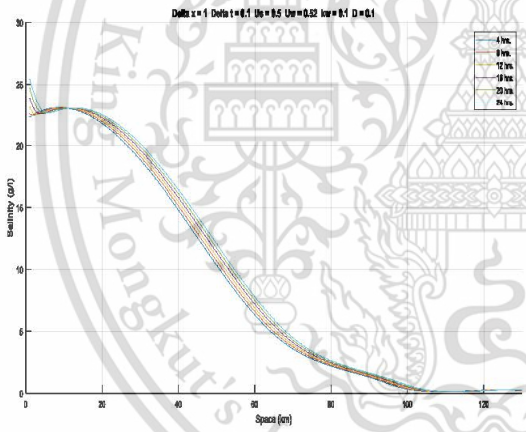

Figure 6. Approximated salinity intrusion levels (g/l) when $u_s = 0.5$ and at time 4, 8,12,16,20 and 24 hrs after the initial time point

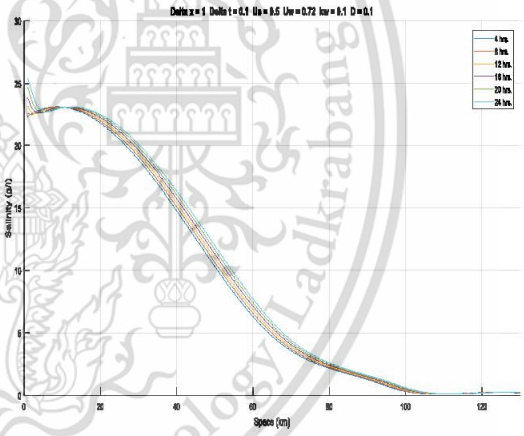

Figure 7. Approximated salinity intrusion levels (g/l) when $u_s = 0.5$ and at time 4, 8,12,16,20 and 24 hrs after the initial time point

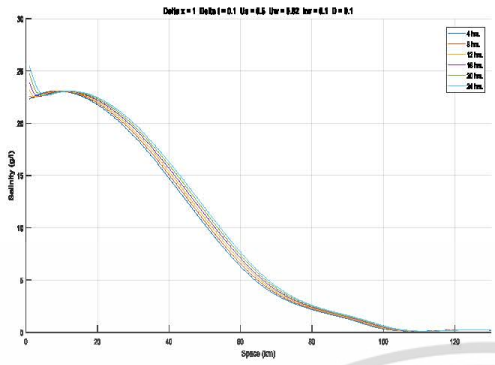

Figure 8. Approximated salinity intrusion levels (g/l) when $u_s = 0.5$ and at time 4, 8,12,16,20 and 24 hrs after the initial time point

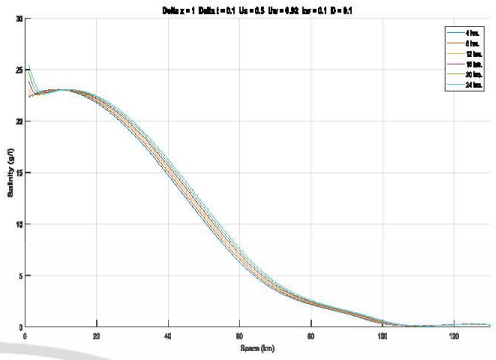

Figure 9. Approximated salinity intrusion levels (g/l) when $u_s = 0.5$ and at time 4, 8,12,16,20 and 24 hrs after the initial time point

Table 1 Approximation of the salinity intrusion concentrations (g/l) of the MacCormack Scheme solution when u_s as varied from 0.13, 0.25 and 0.5 m/s and u_w was varied from 0.52, 0.72, 0.82 and 0.92 m/s, $D = 0.1$, $k_w = 0.1$ at distance 12, 35, 64, 91, 96,102,111 and 130 (km) and at time 4 hrs.

Monitoring Station/ Distance (km)	Salinity Intrusion Concentrations at time 4 hrs. $D = 0.1$, $k_w = 0.1$						Real data Salinity (g/l) 04-01-2018
	$u_w = 0.52$, $u_s = 0.13$	$u_w = 0.52$, $u_s = 0.25$	$u_w = 0.52$, $u_s = 0.5$	$u_w = 0.72$, $u_s = 0.5$	$u_w = 0.82$, $u_s = 0.5$	$u_w = 0.92$, $u_s = 0.5$	
Phra Nakhon Tai/12	22.8212	22.8431	22.8850	22.8818	22.8802	22.8786	21.84
Khlong Lat Pho/35	16.2369	16.3253	16.5049	16.4908	16.4837	16.4766	12.60
Wat Sai Ma Nuea/64	4.5998	4.6564	4.7743	4.7649	4.7602	4.7555	5.53
Wat Makham/91	1.0339	1.0563	1.1014	1.0979	1.0961	1.0944	0.49
Samlae Pump Station/96	0.5046	0.5237	0.5642	0.5610	0.5593	0.5577	0.25
Wat Phai Lom/102	0.1749	0.1809	0.1940	0.1929	0.1924	0.1918	0.16
Wat Pho Taeng Nuea/111	0.1387	0.1362	0.1314	0.1317	0.1319	0.1321	0.15
Wat Ban Paeng Temple/130	0.1395	0.1442	0.1546	0.1537	0.1533	0.1528	0.13

Table 2 Approximation of the salinity intrusion concentrations (g/l) of the MacCormack Scheme solution when u_s as varied from 0.13, 0.25 and 0.5 m/s and u_w was varied from 0.52, 0.72, 0.82 and 0.92 m/s, $D = 0.1$, $k_w = 0.1$ at distance 12, 35, 64, 91, 96,102,111 and 130 (km) and at time 24 hrs.

Monitoring Station/ Distance (km)	Salinity Intrusion Concentrations at time 24 hrs. $D = 0.1$, $k_w = 0.1$						Real data Salinity (g/l) 04-01-2018
	$u_w = 0.52$, $u_s = 0.13$	$u_w = 0.52$, $u_s = 0.25$	$u_w = 0.52$, $u_s = 0.5$	$u_w = 0.72$, $u_s = 0.5$	$u_w = 0.82$, $u_s = 0.5$	$u_w = 0.92$, $u_s = 0.5$	
Phra Nakhon Tai/12	22.8711	22.9695	23.0632	23.0613	23.0599	23.0583	22.77
Khlong Lat Pho/35	16.5191	17.0368	18.0532	17.9751	17.9358	17.8964	13.55
Wat Sai Ma Nuea/64	4.8035	5.1683	5.9919	5.9233	5.8891	5.8550	4.37
Wat Makham/91	1.1023	1.2292	1.4699	1.4516	1.4424	1.4331	1.27
Samlae Pump Station/96	0.5781	0.7043	0.9829	0.9608	0.9497	0.9386	0.58
Wat Phai Lom/102	0.2026	0.2517	0.3996	0.3854	0.3784	0.3715	0.16
Wat Pho Taeng Nuea/111	0.1330	0.1223	0.1168	0.1163	0.1161	0.1160	0.15
Wat Ban Paeng Temple/130	0.1739	0.2010	0.2511	0.2480	0.2464	0.2447	0.13

4.3 The approximation of the salinity intrusion concentrations of a simple advection-diffusion equation numerical simulation using the MacCormack Scheme

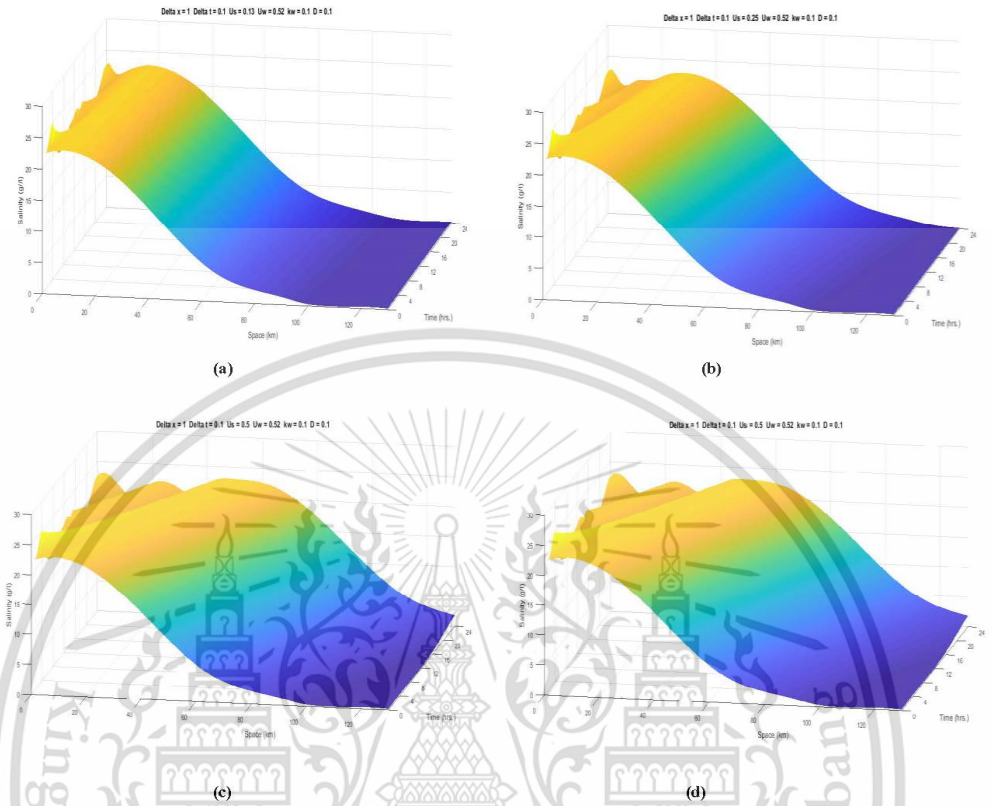

Figure10. The salinity intrusion concentrations (g/l) of the MacCormack Scheme solution with cubic spline interpolation to the initial and boundary conditions as shown in Surfaces (a), (b), (c), and (d).

5. Discussion

In this paper, the approximation of the salinity intrusion concentrations of a simple advection-diffusion equation numerical simulation using the MacCormack Scheme is shown in Figures 10. The numerical technique is tested by changing parameters (u_w, u_s), which affected the change in salinity intrusion concentrations in six different cases used in this study. We used the same points of time throughout every case, which are at 4, 8,12,16,20 and 24 hrs. respectively. In the first case (Figure 4), the parameters are when $D = 0.1$, $k_w = 0.1$, $u_w = 0.52$ and $u_s = 0.13$, In the second case (Figure 5), the parameters are when $D = 0.1$, $k_w = 0.1$, $u_w = 0.52$ and $u_s = 0.25$, In the third case (Figure 6), the parameters are when $D = 0.1$, $k_w = 0.1$, $u_w = 0.52$ and $u_s = 0.5$, In the fourth case (Figure 7), the parameters are when $D = 0.1$, $k_w = 0.1$, $u_w = 0.72$ and, $u_s = 0.5$, In the fifth case (Figure 8), the parameters are when $D = 0.1$, $k_w = 0.1$, $u_w = 0.82$ and $u_s = 0.5$, In the sixth case (Figure 9), the parameters are when $D = 0.1$, $k_w = 0.1$, $u_w = 0.92$ and $u_s = 0.5$, the salinity intrusion concentrations is show in Table 1-2.

6. Conclusion

The MacCormack Scheme with the cubic spline interpolation to the initial and boundary conditions technique is one-dimensional form of finite difference method. The numerical experiment shows that the calculated results are reasonable approximations. The interpolation technique is suitable to be used to solve the real-world problems because it is easy for computer-coding. According to the field salinity data collected at monitoring stations, the initial and boundary conditions are in the form of functions. The results are very satisfactory because we found that the salinity intrusion concentrations of each monitoring station incline towards the same trend with the actual salinity concentrations measured at each station. The computed results are verified by the numerical accuracy. In summary, the numerical model for salinity intrusion control using the MacCormack finite difference method with Cubic Spline interpolation can be applied with problems in the real-world situations. If there are more parameters, the measured data will be even more accurate. This numerical model is not only easy to analyze, but also save more time and cost to do the field work. Most importantly, the results can be used to support the water management plans in the future.

Conflicts of Interest

The authors declare that there are no conflicts of interest regarding the publication of this paper.

Acknowledgments

This research is supported by the Center of Excellence in Mathematics, the Commission on Higher Education, Thailand. Metropolitan Waterworks Authority, Water Resources and Environment Department and Authors greatly appreciate valuable comments received from referees.

Reference

[1] Department, Royal Irrigation. Summary of situation of salinity and Measures to reduce the impact. *Bangkok: Bureau of Water Management and Hydrology,* 2014.

[2] S. Wongsa. "Impact of Climate Change on Water Resources Management in the Lower Chao Phraty Basin,Thailand." *Journal of Geoscience and Environment Protection*, vol 3, pp. 53-58, 2015.

[3] N. Intaboot, and W. Taesombat. "Longitudinal Salinity Intrusion and Dispersion along the Thachin River Due to Sea Level Rise." *Journal of Science and Technology*, vol. 3, pp. 71-86, 2014.

[4] A. Owen, "Artificial diffusion in the numerical modelling of the advective transport of salinity." *Applied Mathematical Modelling*, vol. 8, pp. 116-120, 1984.

[5] K.Ralston, David, W. Rockwell Geyer, and J.A. Lerczak. "Subtidal Salinity and Velocity in the Hudson River Estuary :Observations and Modeling." *American Meteorological Society,* vol. 2008, pp. 753-770, 2008.

[6] N. Pochai. "A numerical computation of a non-dimensional form of stream water quality model with hydrodynamic advection-dispersion-reaction equations ." *Nonlinear Analysis: Hybrid System*, vol. 3, pp. 666-673, 2009.

[7] G. Li, and C.R. Jackson. "Simple, accurate, and efficient revisions to MacCormack and Saulyev schemes : High peclet numbers." *Applied mathematics and computation*, vol 186, pp. 610-622, 2007.

[8] R.M. Corless. "Compact finite differences and cubic splines." May 19, 2018. Online : https://www.researchgate.net/publication/325282964_Compact_Finite_Differences_and_Cubic_Splines.

[9] S. Ariffin, and A. Karim. "Cubic Spline Interpolation for Petroleum Engineering Data." *Applied mathematical sciences*, vol. 8, pp. 5083-5098, 2014.

[10] R.R. Ahmad, N. Ghazali, A.S. Rambely, U.K.S. Din, and N. Hassan. "Application of Cubic Spline in the implementation of braces for the case of a child." *Journal of mathematics and statistics*, vol 8, pp. 144-149. 2012.

[11] N. Pochain. "Unconditional stable numericl techniques for a water-quality model in a non-uniform flow stream." *Advances in Difference Equations*, vol. 2017, pp. 1-13, 2017.

[12] M. Dehghan. "Weighted finite difference techniques for the one-dimensional advection-diffusion equation." *Applied Mathematics and Computation,* vol. 147, pp. 307-319, 2004.

[13] G. Shang, Z. Zaiyue, and C. Cungen. "Differentiation and numerical integral of the cubic spline interpolation." *Journal of computers*, vol. 6, pp. 2037-2044, 2011.

[14] L.B. Richard, and J.D. Faires. *Numerical Analysis.* 9th ed., Brooks/Cole, Cengage Learning, 2010.

Appendix C

"Numerical Simulation of Salinity Intrusion modeled with MacCormack Finite Difference Method and Lagrange Interpolation"

Journal of Interdisciplinary Mathematics; Paper #JIM-T-1031 (1905030), Accepted March 02, 2020

Research Article

Numerical Simulation of Salinity Intrusion modeled with MacCormack Finite Difference Method and Lagrange Interpolation

Khemisara Kulmart[1] *and Nopparat Pochai*[1,2]

[1]*Department of Mathematics, Faculty of Science King Mongkut's Institute of Technology*
Ladkrabang Bangkok 10520 Thailand

[2]*Centre of Excellence in Mathematics CHE, Si Ayutthaya Rd.Department of, Faculty of Science*
Bangkok 10400 Thailand

Abstract

This study aimed to develop a one-dimensional advection-diffusion model for estimating seawater intrusion salinity level in an estuary upstream into a river. We explored two methods in our development of the model. The first method was a forward time centered space (FTCS) method, while the second method was MacCormack combined with Lagrange interpolation method. When the estimates from the two methods were compared to actual measured data, the latter method provided better results. Our one-dimensional advection-diffusion model using MacCormack combined with Lagrange interpolation provided accurate estimates with

the maximum error of 0.0036% in the range of actual measured salinity level of 0–0.25 g/l.

Keywords: salinity intrusion, finite difference method, forward time centered space (FTCS), MacCormack scheme

1. Introduction

Global development of nation states during the last couple of decades has been clearly shown in the form of their economic expansion as well as expansion of various sectors. The expansions have caused a tremendous demand of water supply, especially by agricultural and industrial sectors. Consequently, fresh water has become more and more valuable. It has been estimated that two-thirds of human population will face a huge pressure in terms of available freshwater and its quality by the year 2025 [1]. In addition, global warming causes severe freshwater shortage due to natural sea level becoming higher and seawater intrusion into estuaries and rivers becoming more severe [1]. Freshwater flowing out of and seawater flowing into an estuary (baroclinic flow) is different from that in the upstream location of the river in terms of the flow of saltwater intrusion just above the riverbed because it has a higher density than freshwater. Volume and flow direction of seawater vary with tidal changes. The quality of freshwater near an estuary is inversely proportional to sea level [2].

Ocean tide affects the flow into and out of an estuary. Seawater flowing into an estuary at high tide deposits layers of salty sediment onto the riverbed, while freshwater flowing out of an estuary at ebb tide washes away these layers. During high tide, seawater rich in salt content of its own and of those salty sediment layers intrudes upstream into the river. Recently, high tide has become increasingly higher, and the issue of saltwater intrusion has become more severe [3].

Chao Phraya River, Thailand, is one of the rivers that suffers from this issue [4]. The salinity data, used here, was from salinity monitoring stations along the lower part of the river to its estuary $(13.58^\circ - 15.67^\circ N, 100.10^\circ - 101.00^\circ E)$. Chao Phraya River is a major river in Thailand. It is a confluence of Ping, Wang, Yom and Nan rivers that merge at Pak Nam Pho, Nakhon Sawan Province, ~300 km upstream from the estuary. It flows pass several highly agricultural and industrial provinces that depend on high-quality freshwater supply.

A tidal bore advances upstream to as far as Phra Nakhon Si Ayutthaya Province $(14.23848^{\circ}N, 100.575364^{\circ}E)$, 160 km upstream from the estuary. Salinity intrudes at various points along the river and is sometimes too high for consumption, agriculture and freshwater fishery, especially around Samlae Canal, Pathum Thani Province $(14.04083056^{\circ}N, 100.555875^{\circ}E)$, which sources raw water for the Metropolitan Waterworks Authority to produce tap water for Bangkok Metropolitan Area inhabitants [4].

In 1992, the Royal Irrigation Department began to measure the salinity level along Chao Phraya River during the dry season from January to June. The monitoring points were as listed in Table 1. The alarm salinity level at these monitoring points was over 2 g/L, the standard for agricultural purposes [2]. World Health Organization set a standard level for raw water for consumer water supply as < 0.25 g/L. If it is over 0.5 g/l, it will also affect the industrial sector, such as paint manufacturer, metal producer, and medical industry. Later in 2004, there was a change in the monitoring points. Because areas in Bangkok previously used for agriculture areas had been turned into living complexes and industrial parks, but large areas in Nonthaburi, upstream from Bangkok, were still used for agricultural and farming purposes. The previous, more downstream pump station for Bangkok Metropolitan was moved upstream; therefore, the previous salinity level monitoring point had to also be moved upstream. Another reason is that putting more upstream monitoring points up would tremendously assist in the estimation of freshwater budget to be released from an upstream dam for the purpose of countering ever-increasing salinity intrusion [4].

Recently, the use of mathematical models for calculating parameters of natural phenomena has become more popular because more powerful computers became widely available and in-depth studies on natural phenomena provided more useful data. From the findings from those studies, scientists can derive more accurate equations for explaining natural phenomena based on firmer hypotheses. Solutions to those equations are solved by numerical methods, made practical by new powerful computer hardware and software. For example, solutions can be found from mathematical models for estimating salinity level and levels of other substances in a water passage [3, 7, 8]. Accurate models can be constructed if there are sufficient and valid data about the convection and diffusion rates of those

substances as well as the flow and size of the water passage. Depending on both good estimates and actual measurement data is better than depending solely on measurement data provided by water stations because sometimes water management planning cannot wait for actual measurement data to be obtained first.

Several authors have used mathematical models for various purposes. A water-quality model called "MIKE-HD/AD" was used for estimation of salinity intrusion in the area of Tha Chin estuary by N. Intaboot and W. Taesombat [3]. They also suggested that the model could be applied to estimation of parameters of other natural phenomena related to salinity intrusion. The model predicted that the maximum distance of salinity intrusion into this river would reach 55 km from the estuary, about 3 km further up along the river than the actual distance found in 2015. This accurate result demonstrated to the authority that a measure had to be adopted to control the salinity level in Tha Chin River, a measure such as increasing the freshwater flow rate down the River to push seawater intrusion further downstream. The model also suggested an optimum flow rate of about 20-40 m^3/s and that a higher flow rate would not help pushing salinity intrusion downstream any better. Another paper by the same authors [5] used two mathematical models called "MIKE11-HD/AD" developed by DHI Water Environment and Health to investigate the longitudinal salinity intrusion and dispersion in Tha Chin River caused by rising sea level. The main model was MIKE11-AD Advectic Dispersal Model and the other model was MIKE11-HD Hydrodynamic Module for forecasting dispersion and salinity intrusion along the mentioned river. It was found that the coefficient of salinity dispersion was 400 m^2/s according to the information during 2010. In [6], the researchers studied salinity intrusion in the Tha Chin River using a MIKE11-HD, Hydrodynamic Module developed by DHI Water Environment and Health. The hydrography of the river, the dispersion of salinity intrusion along the river, and the directions to solving the salinity intrusion in agricultural areas along the river were investigated. They found that the release of water at 40 m^3/s was able to push against salinity intrusion and kept the remaining the salinity level to be less than 0.75 g/l. Intaboot, N. [7] studied the salinity intrusion in the lower Tha Chin River caused by addition of shortcut canals. The additional canals were dug in order to increase the water-draining efficiency during the rainy season. The MIKE11-AD Advection-Dispersion Model computed out the coefficient of dispersion in the Tha Chin River to

be 400 m^2/s. It was also found that the addition of shortcut canals caused more salinity intrusion. Wongsa, S. [8] investigated the effects of climate change on the rise of sea level using a MIKE 11 model. The rise of sea level, in turn, affected hydraulic condition, water supply, salinity level, and agricultural areas in the lower area of Chao Phraya River. The model itself was divided into two different parts: a hydrodynamic module and an advection-dispersion model. Calibrations of both models were done by adjusting their own key coefficients. A scenario in IPCC SRES (RCP8.5) report was simulated, showing that the rise of sea level would reach 1.16 meters in 2100. The salinity level at Samlae Pumping Station would also rise to around 0.37 - 0.75 g/l, exceeding the standard salinity level. The level would also exceed the standard for used in agricultural sector. The results from that study provided a good guideline for us in terms of raw water resource management of tap water supply and water used for agricultural purposes in Chao Phraya River Basin. Owen, A. [9] came up with a numerical model of salinity advective transport in coastal areas, associated with diffusion. This particular model could be used with small grids of two to four kilometers in the case of tidal problems, while larger grids could be applied in non-tidal problems. David, K. et al. [10] used a tidally and cross-sectionally averaged model with a Hansen and Rattray equation to simulate the distribution of salinity as well as the vertical exchange flow along the estuary of Hudson River. The solutions from the model were assessed for the northern San Francisco Bay and the Hudson River. Despite huge differences in terms of bathymetry, this approach could be used to investigate other estuaries. However, an alternative approach should be used when there was inconsistency between observations of the high river discharge and the model output. Guraslan G. et al. [11] aimed to produce “numerical solutions of one-dimensional advection-diffusion equation using a sixth-order compact difference scheme in space and a four-order Runge-Kutta scheme in time”. Those particular solutions were very accurate and quite flexible in solving equation of contaminant transport. Pochai, N. [12] used two mathematical models to simulate pollution caused by sewage effluent in nonuniform water flow in a stream with inconsistent current velocity. The two models were a Crank-Nicolson system of hydrodynamic model and a backward-time central-space scheme of a dispersion model. This study clearly showed that the Crank-Nicholson hydrodynamic model could be applied in the real cases of sewage

effluent in canals connected to other reservoirs or streams. Pochai, N. [13] focused on a better version of finite difference scheme for solving the advection-dispersion-reaction equation (ADRE) that took into account the effect of nonuniform water flows. Two mathematical models: a hydrodynamic model and an advection-dispersion-reaction model, were used to simulate pollution from sewage effluent. The Crank-Nicolson system of a hydrodynamic model as well as an explicit scheme of the dispersion model were used as numerical techniques. The author revised and modified the explicit scheme for the dispersion model from forward-time central-space (FTCS) to Saulyev scheme. Both schemes were compared in terms of stability in order to show how they were applicable to the real-world problem. Pochai, N. [14] formulated two mathematical models of one-dimensional equations: a hydrodynamic model related to elevation of water and flow velocity field and a dispersion model related to pollutant concentration field. The models were used to simulate the quality of water in a nonuniform flow stream. The traditional Crank-Nicolson method was used in the first hydrodynamic model. The second model used velocity fields of water, calculated from the hydrodynamic model, as field data. The model employed a modified MacCormack method as the numerical technique. The author proposed a modified MacCormack scheme that resulted in better prediction accuracy and no major loss of computational efficiency. Pochai, N. [15] used a similar process and structure that he had used in [14] to simulate the quality of water in a nonuniform flow stream. The first model was exactly the same as that in [14], while the advection-diffusion-reaction model providing a pollutant concentration field was used as the second model. Both models were in the form of one-dimensional equation. Similarly, the traditional Crank-Nicolson numerical technique was used in the first model. The advection-diffusion-reaction model used flow velocity fields calculated from the hydrodynamic model as input. In the second model, a new fourth-order scheme and Saulyev scheme were employed. As a result, a simple alteration of both schemes helped to improve the accuracy of prediction in comparison to that of traditional schemes. Pochai, N. [16] used a finite difference method to solve a “one-dimensional steady convection-diffusion equation with variable coefficients”. The solution was used to optimize the cost of water treatment. Dehghan, M. [17] proposed several numerical methods based on two-level finite difference approximation and compared those methods in solving one-

dimensional advection-diffusion equation with constant coefficient. The methods were based on a modified version of equivalent partial differential equation approach, developed by Warming and Hyett in 1974. As a result, those new methods were found to be more precise and efficient than those of conventional techniques. The new schemes were also without numerical diffusion. Seesod, N. and Pochai, N. [18] developed a dimensional simulation of stream water quality measurement, using a finite volume method to come up with estimates for pollutant concentration. The schemes provided logical and rational results that can be applied to water quality measurement. Pochai, N. et al. [19] developed a finite element technique of solving one-dimensional steady convection-diffusion equation with constant coefficients that was used in this study to optimize costs of water treatment and used it to demonstrate that a hazardous water pollution level can be lowered down to a standard level with a minimal cost. Mabood, F. and Pochai, N. [20] used an Optimal Homotopy Asymptotic Method (OHAM) to investigate and simulate dispersion of pollutants in water. A numerical technique, a fourth-fifth order Runge-Kutta-Fehlberg, was also used to approximate the solution. The end results show that the OHAM solution and the numerical solution agreed well with each other. An example is provided in that paper to show how efficient, accurate, and simple the Runge-Kutta-Fehlberg technique actually was.

This paper is divided into two main parts as follows. The first part shows the details of a finite difference simulation of salinity intrusion into Chao Phraya River, Thailand $(13.58^{\circ}-15.67^{\circ}N, 100.10^{\circ}-101.00^{\circ}E)$. Forward-time centered-space (FTCS) and MacCormack scheme were used to numerically estimate the salinity intrusion. This study also tests between the estimation efficiencies of the FTCS and MacCormack techniques. Finally, the test results from both techniques were compared with the exact solution under simplified conditions.

In the second part, we interpolated the salinity levels of the initial and boundary conditions and confirmed that the interpolated values tracked the actual values closely.

2. One-dimensional salinity intrusion measurement model that takes into account a diversion dam

2.1 The governing equation

The mathematical model describing the transportation and diffusion processes in this study is a one-dimensional advection-diffusion-reaction equation (ADRE). The advection-diffusion equation is expressed [9, 11, 15, 17] as the following equation,

$$\frac{\partial S}{\partial t} + U\frac{\partial S}{\partial x} = D\frac{\partial^2 S}{\partial x^2}, \quad \text{for all } 0 \le x \le L \text{ and } 0 \le t \le T, \tag{2.1}$$

where $S(x,t)$ is the salinity level (g/l); U is the water flow velocity in x-directions(m/s); D is the salinity diffusion coefficient (m^2/s); L is the length of the river; and T is the time period of the simulation.

Letting

$$U = (u_s - ku_w). \tag{2.2}$$

Substituting Eq. (2.2) into Eq. (2.1), we get

$$\frac{\partial S}{\partial t} + (u_s - ku_w)\frac{\partial S}{\partial x} = D\frac{\partial^2 S}{\partial x^2}, \tag{2.3}$$

where u_s is the seawater flow velocity; u_w is the freshwater flow velocity released from the diversion dam; and k is the salinity dilution rate freshwater, for all $0 < x \le L, 0 \le t \le T$.

2.2 Initial and boundary conditions

The effects of salinity intrusion into an estuarine, which will likely become more severe in the future, are caused by ocean tides. The mathematical model was applied to analyze salinity intrusion into Chao Phraya River. The initial salinity values used in the model were different depending on the actual time and distance from the estuary that the actual salinity levels were measured.

2.2.1 The initial condition

The initial condition was assumed to be

$$S(x,0) = f(x), \quad \text{for all} \quad 0 \le x \le L, \tag{2.4}$$

where $f(x)$ is a given salinity level function along the river.

2.2.2 The boundary conditions

The left boundary condition was assumed to be

$$S(0,t) = g(t), \quad \text{for all} \quad 0 < t \le T, \tag{2.5}$$

where $g(t)$ is a given salinity level function constructed according to the actual salinity level measured at the first monitoring station. The right boundary conditions was assumed to be

$$\frac{\partial S}{\partial x}(L,t) = k_0, \quad \text{for all} \quad 0 < t \le T, \tag{2.6}$$

where k_0 is the rate of change of salinity level at the last monitoring station.

3. Numerical techniques

Salinity levels were approximated by two explicit finite difference methods. We approximated $S(x_i,t_n)$ by S_i^n, the value of the difference approximate of $S(x,t)$ at point $x = i\Delta x$ and $t = n\Delta t$, where $0 \le i \le n$ and $0 \le n \le N$. The grid point (x_i,t_n) was defined by $x_i = i\Delta x$, for all $i = 0,1,2,...,M$ and $t_n = n\Delta t$ for all $n = 0,1,2,...,N$, where M and N are positive integers.

3.1 Forward-time centered-space (FTCS) model

In view of [13], the equations of forward-time centered-space technique are the following:

$$S \cong S_i^n, \tag{3.1}$$

$$\frac{\partial S}{\partial x} \cong \frac{S_i^{n+1} - S_1^n}{\Delta t}, \tag{3.2}$$

$$\frac{\partial S}{\partial x} \cong \frac{S_{i+1}^n - S_{i-1}^n}{2\Delta x}, \tag{3.3}$$

$$\frac{\partial^2 S}{\partial x^2} \cong \frac{S_{i+1}^{n+1} - 2S_1^n + S_{i-1}^n}{(\Delta x)^2}, \tag{3.4}$$

$$u_s = u_{s_i}^n, \tag{3.5}$$

$$u_w = u_{w_i}^n. \tag{3.6}$$

Substituting these terms into Eq. (2.3), we get the following discretization:

$$\frac{S_i^{n+1} - S_i^n}{\Delta t} + (u_{s_i}^n - ku_{w_i}^n)\left(\frac{S_{i+1}^n - S_{i-1}^n}{2\Delta x}\right) = D\left(\frac{S_{i+1}^n - 2S_i^n + S_{i-1}^n}{(\Delta x)^2}\right). \tag{3.7}$$

It follows that

$$\begin{aligned} S_i^{n+1} &= \frac{\Delta tD}{(\Delta x)^2}\left(S_{i+1}^n - 2S_i^n + S_{i-1}^n\right) - \frac{(u_{s_i}^n - ku_{w_i}^n)\Delta t}{2\Delta x}\left(S_{i+1}^n - S_{i-1}^n\right) + S_i^n, \\ &= \frac{\Delta tD}{(\Delta x)^2}S_{i+1}^n - \frac{2\Delta tD}{(\Delta x)^2}S_i^n + \frac{\Delta tD}{(\Delta x)^2}S_{i-1}^n - \frac{(u_{s_i}^n - ku_{w_i}^n)\Delta t}{2\Delta x}S_{i+1}^n + \frac{(u_{s_i}^n - ku_{w_i}^n)\Delta t}{2\Delta x}S_{i-1}^n + S_i^n, \\ &= \left(\frac{\Delta tD}{(\Delta x)^2} + \frac{(u_{s_i}^n - ku_{w_i}^n)\Delta t}{2\Delta x}\right)S_{i+1}^n + \left(-\frac{2\Delta tD}{(\Delta x)^2} + 1\right)S_i^n + \left(\frac{\Delta tD}{(\Delta x)^2} - \frac{(u_{s_i}^n - ku_{w_i}^n)\Delta t}{2\Delta x}\right)S_{i+1}^n, \end{aligned} \tag{3.8}$$

where $$\lambda = \frac{D\Delta t}{(\Delta t)^2}, \tag{3.9}$$

and $$\gamma_i^n = \frac{\Delta t}{\Delta x}(u_{s_i}^n - ku_{w_i}^n), \tag{3.10}$$

$$= \left(\lambda + \frac{1}{2}\gamma_i^n\right)S_{i+1}^n + (-2\lambda + 1)S_i^n + \left(\lambda - \frac{1}{2}\gamma_i^n\right)S_{i+1}^n. \tag{3.11}$$

3.2 MacCormack Scheme for advection equation in the proposed model

We assume that the length of the river is $L=1$.We also assume that the salinity levels at the initial condition are the initial input into the first step of the MacCormack scheme. The scheme approximates Eq. (2.3) according to a forward-time and forward-space scheme (FTFS) as follows [14],

$$S \cong S_i^n, \tag{3.12}$$

$$\frac{\partial S}{\partial t} \cong \frac{S_i^{n+1} - S_i^n}{\Delta t}, \tag{3.13}$$

$$\frac{\partial S}{\partial x} \cong \frac{S_{i+1}^n - S_i^n}{\Delta x}, \tag{3.14}$$

$$\frac{\partial^2 S}{\partial x^2} \cong \frac{S_{i+1}^n - 2S_i^n + S_{i-1}^n}{(\Delta x)^2} \tag{3.15}$$

$$u_s = u_{s_i}^n, \tag{3.16}$$

$$u_w = u_{w_i}^n. \tag{3.17}$$

Substituting Eqs. (3.12) - (3.17) into Eq. (2.3), we get

$$\left(\frac{S_i^{n+1} - S_i^n}{\Delta t}\right) + (u_{s_i}^n s - k u_{w_i}^n)\left(\frac{S_{i+1}^n - S_i^n}{\Delta x}\right) = D\left(\frac{S_{i+1}^n - 2S_i^n + S_{i-1}^n}{(\Delta x)^2}\right), \tag{3.18}$$

for all $1 \le i \le M$ and $0 \le n \le N-1$. Hence, we obtain

$$\left(\frac{S_i^{n+1} - S_i^n}{\Delta t}\right) = -\frac{(u_{s_i}^n - k u_{w_i}^n)}{\Delta x}\left(S_{i+1}^n - S_i^n\right) + \frac{D}{(\Delta x)^2}\left(S_{i+1}^n - 2S_i^n + S_{i-1}^n\right). \tag{3.19}$$

Let $(C_i)_1 = \left(\frac{S_i^{n+1} - S_i^n}{\Delta t}\right)$. Then, Eq. (3.19) becomes

$$(C_i)_1 = -\frac{(u_{s_i}^n - k u_{w_i}^n)}{\Delta x}\left(S_{i+1}^n - S_i^n\right) + \frac{D}{\Delta x^2}\left(S_{i+1}^n - 2S_i^n + S_{i-1}^n\right), \tag{3.20}$$

$$= -\frac{(u_{s_i}^n - ku_{k_i}^n)}{\Delta x} S_{i+1}^n - \frac{(u_{s_i}^n - ku_{k_i}^n)}{\Delta x} S_i^n + \frac{D}{\Delta x^2} S_{i+1}^n - \frac{2D}{\Delta x^2} S_i^n + \frac{D}{\Delta x^2} S_{i-1}^n. \quad (3.21)$$

$$= A_1 S_{i+1}^n + A_2 S_i^n + A_3 S_{i-1}^n, \quad (3.22)$$

where $A_1 = -\frac{(u_{s_i}^n - ku_{w_i}^n)}{\Delta x} + \frac{D}{(\Delta x)^2}, A_2 = \frac{(u_{s_i}^n - ku_{w_i}^n)}{\Delta x} - \frac{2D}{(\Delta x)^2}$ and $A_3 = \frac{D}{(\Delta x)^2}$.

On the left boundary condition, where $i = 1,$ we obtain

$$\left(C_{_1}\right)_1 = A_1 S_2^n + A_2 S_1^n + A_3 S_0^n = A_1 S_2^n + A_2 S_1^n + A_3 S_0. \quad (3.23)$$

For the right boundary condition, where $i = M$, we substitute the approximated unknown value on the right boundary condition by using a forward difference approximation, and we have

$$S_M = S_{M-1}. \quad (3.24)$$

$$\left(C_M\right)_1 = A_1 S_M^n + A_2 S_{M-1}^n + A_3 S_{M-2}^n, = \left(A_1 + A_2\right) S_{M-1}^n + A_3 S_{M-2}^n. \quad (3.25)$$

We obtain the MacCormack predictor step formulation,

$$S_i^{n+1} = S_i^n + \left(C_i\right)_1 \Delta t. \quad (3.26)$$

The second step of MacCormack scheme is the approximation of Eq. (2.3) with a backward time and backward space scheme (BTBS).

$$\frac{\partial S}{\partial t} \cong \frac{S_i^{n+1} - S_i^n}{\Delta t}, \quad (3.27)$$

$$\frac{\partial S}{\partial x} \cong \frac{S_i^{n+1} - S_{i-1}^{n+1}}{\Delta x}, \quad (3.28)$$

$$\frac{\partial^2 S}{\partial x^2} \cong \frac{S_{i+1}^{n+1} - 2S_i^{n+1} + S_{i-1}^{n+1}}{(\Delta x)^2}. \quad (3.29)$$

Substituting Eqs. (3.27) - (3.29) into Eq. (2.3), we get

$$\frac{S_i^{n+1}-S_i^n}{\Delta t}+(u_{s_i}^n-ku_{w_i}^n)\left(\frac{S_i^{n+1}-S_{i-1}^{n+1}}{\Delta x}\right)=D\left(\frac{S_{i+1}^{n+1}-2S_i^{n+1}+S_{i-1}^{n+1}}{(\Delta x)^2}\right). \tag{3.30}$$

Then

$$\frac{S_i^{n+1}-S_i^n}{\Delta t}=-(u_{s_i}^n-ku_{w_i}^n)\left(\frac{S_i^{n+1}-S_{i-1}^{n+1}}{\Delta x}\right)+D\left(\frac{S_{i+1}^{n+1}-2S_i^{n+1}+S_{i-1}^{n+1}}{(\Delta x)^2}\right). \tag{3.31}$$

Let $(C_i)_2=\dfrac{S_i^{n+1}-S_i^n}{\Delta t}$. Then Eq. (3.31) becomes

$$(C_i)_2=-\frac{(u_{s_i}^n-ku_{w_i}^n)}{\Delta x}\left(S_i^{n+1}-S_{i-1}^{n+1}\right)+\frac{D}{(\Delta x)^2}\left(S_{i+1}^{n+1}-2S_i^{n+1}+S_{i-1}^{n+1}\right), \tag{3.32}$$

$$=\frac{D}{(\Delta x)^2}S_{i+1}^{n+1}+\left(-\frac{(u_{s_i}^n-ku_{w_i}^n)}{\Delta x}-\frac{2D}{(\Delta x)^2}\right)S_i^{n+1}+\left(\frac{(u_{s_i}^n-ku_{w_i}^n)}{\Delta x}+\frac{D}{(\Delta x)^2}\right)S_{i-1}^{n+1},$$

$$(C_i)_2=B_1S_2^{n+1}+B_2S_1^{n+1}+B_3S_0^{n+1}, \tag{3.33}$$

Where $B_1=\dfrac{D}{(\Delta x)^2}, B_2=-\dfrac{(u_{s_i}^n-ku_{w_i}^n)}{\Delta x}-\dfrac{2D}{(\Delta x)^2}$ and $B_3=\dfrac{(u_{s_i}^n-ku_{w_i}^n)}{\Delta x}+\dfrac{D}{(\Delta x)^2}$.

For the left boundary condition, where $i=1$, we obtain

$$(C_1)_2=B_1S_2^{n+1}+B_2S_1^{n+1}+B_3S_0^{n+1}=B_1S_2^{n+1}+B_2S_1^{n+1}+B_3S_0. \tag{3.34}$$

For the right boundary condition, where $i=M$, we substitute the approximated unknown value on the right boundary condition with a backward difference approximation, we have

$$S_{M+1}=S_M. \tag{3.35}$$

$$(C_M)_2=\left(B_1+B_2\right)S_M^{n+1}+B_3S_{M-1}^{n+1}. \tag{3.36}$$

From the stability condition, the MacCormack scheme takes on the following form,

$$S_i^{M+1} = S_i^n + \frac{\Delta t}{2}\left(\left(C_i\right)_1 + \left(C_i\right)_2\right), \tag{3.37}$$

where the stable condition for the scheme is

$$\frac{D\Delta t}{(\Delta x)^2} < 0.5, \tag{3.38}$$

and

$$(u_s - ku_w)\frac{\Delta t}{(\Delta x)} < 0.9. \tag{3.39}$$

3.3 Iterative method for interpolation of the initial and boundary conditions

Lagrange interpolating polynomials

The problem of determining a polynomial of degree one that passes through distinct points (x_0, y_0) and (x_1, y_1) is the same as determining an approximation of a function f for which $f(x_0) = y_0$ and $f(x_1) = y_1$ by means of a first-degree polynomial interpolation. The approximated value agrees with the value of f at a given point [21].

Define the functions

$$L_0 = \frac{x - x_0}{x_0}, \tag{3.40}$$

and

$$L_1(x) = \frac{x - x_0}{x_1 - x_0}. \tag{3.41}$$

The linear Lagrange interpolating polynomials through (x_0, y_0) and (x_1, y_1) is

$$P(x) = L_0(x)f(x_0) + L_1(x)f(x_1), \tag{3.42}$$

and

$$\frac{x-x_1}{x_1-x_2}\, f(x_0) \;+\; \frac{x-x_0}{x_1-x_0}\, f(x_1). \tag{3.43}$$

Note that

$$L_0(\mathrm{x}_0)=1\,,\;\; L_0(\mathrm{x}_1)=0,\qquad L_1(\mathrm{x}_0)=0 \;\text{ and }\; L_1(x_1)=1.$$

These imply that

$$P(x_0)=1\cdot f(x_0)+0\cdot f(x_1)=f(x_0)=y_0$$

And

$$P(x_1)=0\cdot f(x_0)+1\cdot f(x_1)=f(x_1)=y_1.$$

Therefore, P is a unique polynomial of degree at most one that passes through (x_0,y_0) and (x_1,y_1).

Theorem 3.31 If $x_0,x_1,...,x_n$ are $n+1$ distinct points and f is a function whose values are given at these points, then a unique polynomial $P(x)$ of degree at most n exists with

$$f(x_k)=P(x_k),\quad \text{for each}\quad k=0,1,...,n,$$

and the polynomial is given by

$$P(x)=f(x_0)L_{n,0}(x)+...+f(x_n)L_{n,n}(x)=\sum_{k=0}^{n} f(x_k)L_{n,k}(x), \tag{3.44}$$

where,

$$L_{n,k}=\frac{(x-x_0)(x-x_1)...(x-x_{k-1})(x-x_{k+1})...(x-x_n)}{(x_k-x_0)(x_k-x_1)...(x_k-x_{k-1})(x_k-x_{k+1})...(x_k-x_n)}, \tag{3.45}$$

$$= \prod_{\substack{i=0 \\ i \neq k}}^{n} \frac{(x - x_i)}{(x_k - x_i)}, \tag{3.46}$$

for each $k = 0,1,...,n.$

4. Numerical accuracy experiment

Since the exact solution is known for simplified initial and boundary conditions, it was used to test the two numerical methods for solving the advection-diffusion equation.

4.1 Performance testing of numerical FTCS and MacCormack Scheme using exact solution as the baseline

Let the length of the river be $L = 1$. Assuming that the physical parameter are $u_s = 0.10,\quad u_w = 0.50, k = 0.10$ and $D = 0.001$ as well as assuming that the initial and boundary conditions are constants, the exact solution to the problem is [11,15]

$$S(x,t) = \frac{1}{2} erfc\left(\frac{x - (u_s - ku_w)t}{\sqrt{4Dt}}\right) + \frac{1}{2} e^{\frac{(u_s - ku_w)x}{D}} erfc\left(\frac{x + (u_s - ku_w)t}{\sqrt{4Dt}}\right). \tag{4.1}$$

As the FTCS technique Eq. (3.11) and the MacCormack finite difference technique Eq. (3.37) were employed, the approximated solutions were obtained and illustrated in Figure 1-2. The maximum errors of both techniques are compared in Table 1.

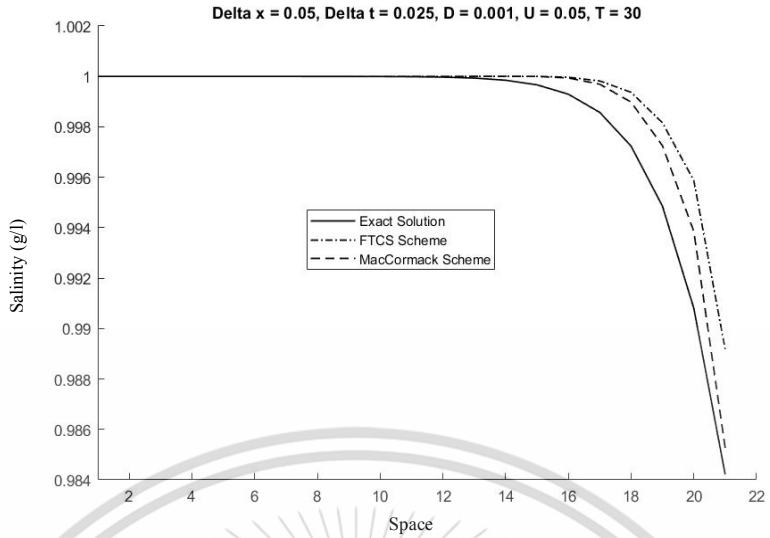

Figure 1 Performance comparison between FTCS and the MacCormack Scheme $(T = 30)$ with the exact solution as the baseline (variation along the space dimension).

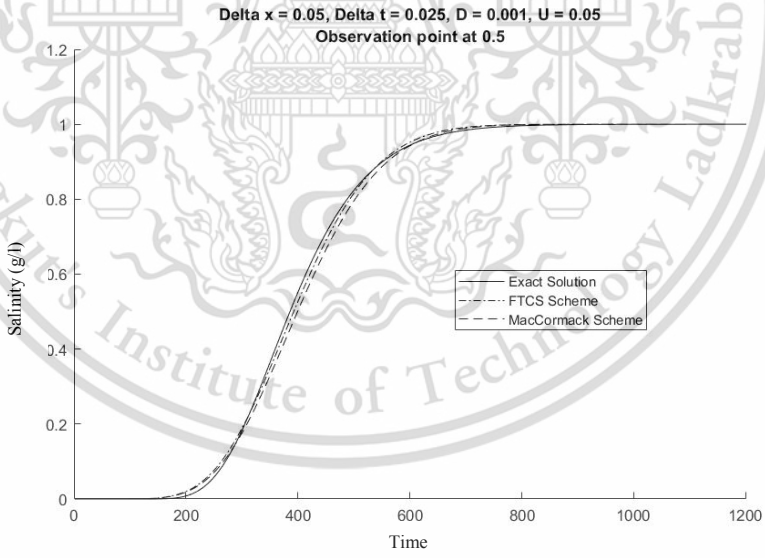

Figure 2 Performance comparison between FTCS and the MacCormack Scheme ($\boldsymbol{T = 30}$ and $\boldsymbol{x = 0.5}$) with the exact solution as the baseline (variation along the time dimension).

Table 1 Maximum errors produced by FTCS and MacCormack Scheme ($T = 30$).

			Maximum Error $T = 30$	
U	Δx	Δt	FTCS $(\times 10^{-3})$	MacCormack $(\times 10^{-3})$
		0.025	4.9603	1.0560
0.05	0.05	0.0125	4.3918	2.5147
		0.0025	3.9305	3.5663
	Δx	Δy	FTCS $(\times 10^{-4})$	MacCormack $(\times 10^{-4})$
		0.025	4.2020	4.4842
0.06	0.05	0.0125	4.2101	4.3272
		0.0025	4.2039	4.2236
	Δx	Δy	FTCS $(\times 10^{-6})$	MacCormack $(\times 10^{-6})$
		0.025	3.3521	2.5421
0.07	0.05	0.0125	3.1199	2.7862
		0.0025	2.8867	2.8267
	Δx	Δy	FTCS $(\times 10^{-8})$	MacCormack $(\times 10^{-8})$
		0.025	11.992	8.9140
0.08	0.05	0.0125	7.7429	0.23177
		0.0025	4.2872	3.0090
	Δx	Δy	FTCS $(\times 10^{-3})$	MacCormack $(\times 10^{-3})$
	0.05		3.9305	3.5662
0.05	0.025	0.0025	3.0798	2.2728
	0.0125		3.3893	1.0846

4.2 Performance testing of MacCormack Scheme with interpolated left boundary using exact solution as the baseline

4.2.1 Assuming that the flow velocity and diffusion coefficients are $u_s = 0.10$, $u_w = 0.90$, $k = 0.10$ and $D = 1$ in this experiment, and let the length of the river be $L = 1$, the exact solution of this problem has already been solved and shown in [17].

The exact solution is

$$S(x,t) = \frac{0.025}{\sqrt{0.000625 + 0.02t}} \exp\left[-\frac{(x + 0.5 - t)^2}{(0.00125 + 0.04t)} \right]. \tag{4.2}$$

The approximated solution of Eq. (3.37) by MacCormack finite difference technique and the exact solution are shown in Figure 3.

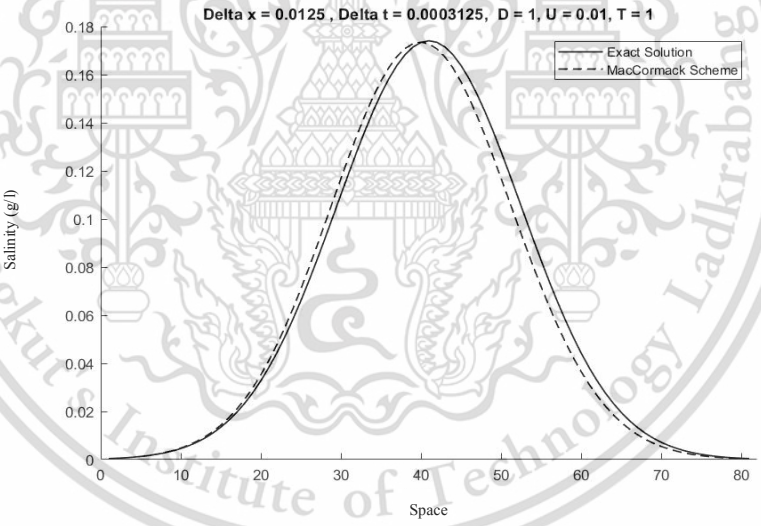

Figure 3 Comparison of the exact solution and the approximated solution by MacCormack Scheme $(T = 30)$.

4.2.2 Assume that the flow velocity and diffusion coefficients are $u_s = 1.1$, $u_w = 1.0$, $k = 0.10$, and $D = 0.01$. Let the length of the river be $L = 1$. As MacCormack finite difference technique Eq. (3.37) and Lagrange interpolation technique Eq. (3.44) were employed, we obtained approximated solutions. The numerical solution when the Lagrange interpolation was employed were compared to the theoretical solution

of Eq. (4.2), as shown in Figure 4. The absolute errors of the technique are shown in Table 2.

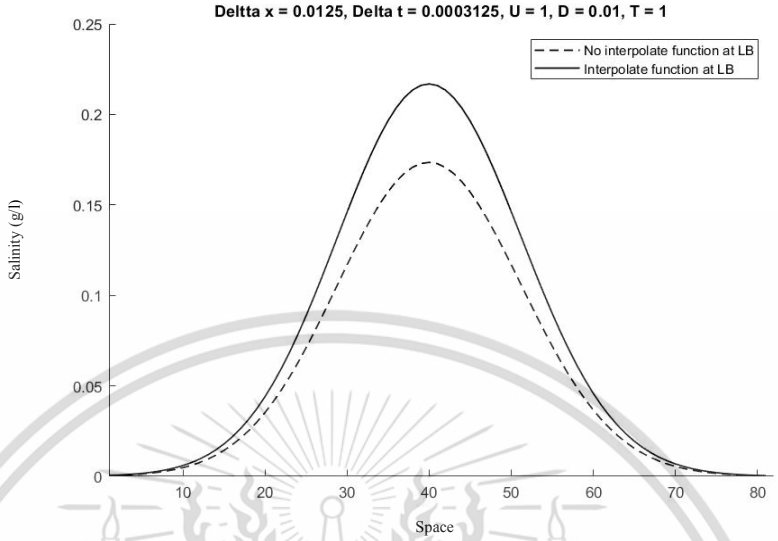

Figure 4 Solutions with interpolated LB and with no interpolation.

Table 2 Absolute errors at $\Delta x = 0.0125, \Delta t = 0.0003125, U = 1, D = 0.01, T = 1$ when LB was interpolated.

Space	Interpolated values of the LB	Given	Absolute Error
0.1	0.00373196	0.004657925	0.000925965
0.2	0.020993865	0.026210873	0.005217008
0.3	0.070919809	0.088575277	0.017655468
0.4	0.143042256	0.178725066	0.03568281
0.5	0.172768923	0.215963928	0.043195005
0.6	0.126011625	0.157593105	0.03158148
0.7	0.056151619	0.070261077	0.014109459
0.8	0.015495382	0.019399664	0.003904282
0.9	0.002686808	0.003365737	0.000678929

5. Numerical simulation

5.1 Simulation with different values of parameters u_s, u_w, k and D

Simulation 1: We considered a segment of a river with 160 km. of length. The salinity flow velocities were $u_s = 0.5, 0.7, 0.9$ m/s. The salinity diffusion coefficient was 0.1 m^2/s. The flow velocity of fresh water released by the diversion dam was 0.5 m/s. The percentage ability of freshwater to dilute salinity was 30%. All assumed physical parameters are listed in Table 3.

Table 3 Set values of physical parameters in the simulation.

$L(km)$	u_s	u_w	D	k	$T(hrs)$
160	0.5	0.5	0.1	0.30	222.23
160	0.7	0.5	0.1	0.30	158.73
160	0.9	0.5	0.1	0.30	123.46

The values of approximated salinity intrusion or $S(x,0)$ (g/l) by MacCormack finite difference technique are shown in Figure 5 and Table 4.

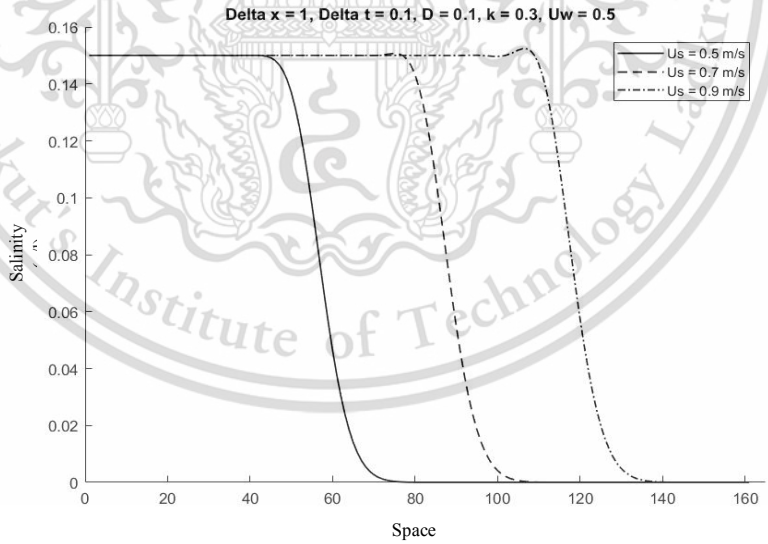

Figure 5 Curves of salinity level at the initial condition, $S(x,0)=0$, and boundary conditions, $S(0,t)=0.15 \quad S(160,t)=0.$

Table 4 Analytically-computed and numerically approximated salinity intrusion levels $S(x,0)$ (g/l) (when $u_s = 0.5, 0.7, 0.9$).

Distance from the estuary (km.)	Salinity (g/l)		
	u_s = 0.5 m/s	u_s = 0.7 m/s	u_s = 0.9 m/s
20	0.1500	0.1500	0.1500
40	0.1500	0.1500	0.1500
60	0.0379	0.1500	0.1500
80	1.6753×10^{-5}	0.1385	0.1500
100	1.9767×10^{-11}	0.0029	0.1497
120	2.2452×10^{-19}	1.6686×10^{-7}	0.0480
140	5.6023×10^{-29}	9.7113×10^{-14}	6.4519×10^{-5}
160	5.1481×10^{-40}	1.2894×10^{-21}	6.8165×10^{-10}

Simulation 2: We later changed the initial and boundary conditions to be $S(x,0) = f(x)$ and $S(160,t) = 0$. The peak salinity levels were compared between $u_s = 0.5, 0.7, 0.9$ m/s, shown in Figure 6.

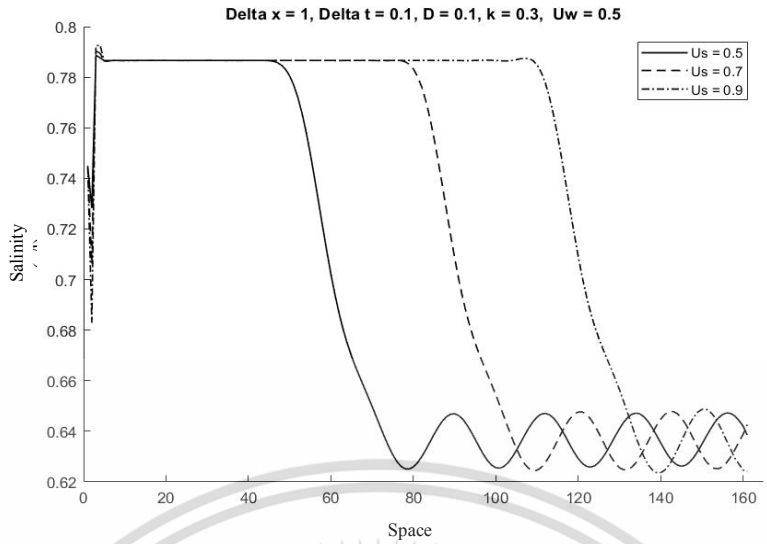

Figure 6 Curves of salinity level at the initial condition of $S(x,0)=f(x)$ **and boundary conditions of** $S(0,t)=g(t).$ **and** $S(160,t)=0.$

Simulation 3: We later changed to interpolated initial and boundary conditions, where the right boundary condition was set to $S(160,t)=0.$ The peak salinity levels were compared between $u_s = 0.5, 0.7, 0.9$ m/s. The curves of salinity level (g/l) are shown in Figure 7.

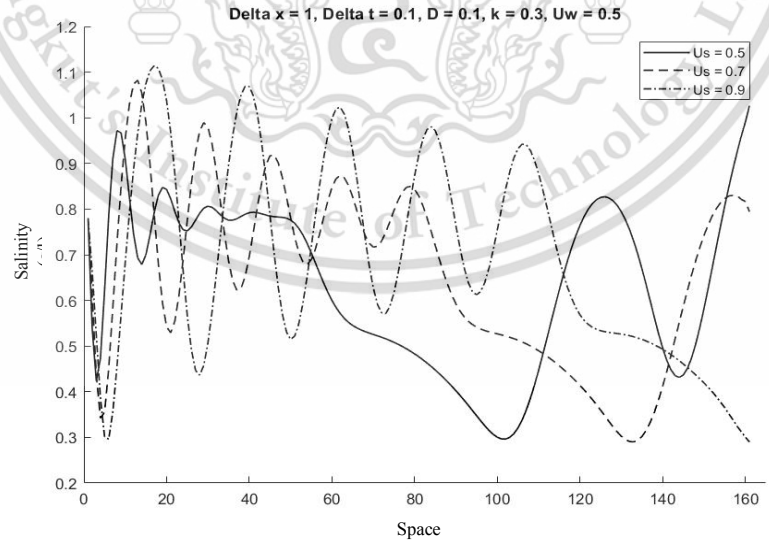

Figure 7 Curves of salinity level with interpolated initial and boundary conditions, where the right boundary condition was $S(160,t)=0.$

Simulation 4: We considered a segment of river 160 km. long. The salinity intrusion had a flow velocity of $u_s = 0.9$ m/s. The salinity diffusion coefficient was $D = 0.1, 0.3, 0.5$ m^2/s. Freshwater was released by the diversion dam at a flow velocity of 0.5 m/s. The percentage salinity dilution ability of freshwater was 30%. All assumed physical parameters are listed in Table 5.

Table 5 Set values of physical parameters in the simulation.

$L(km)$	u_s	u_w	D	k	$T(hrs)$
160	0.9	0.5	0.1	0.30	123.46

The values of approximated salinity intrusion or $S(x,0)$ (g/l) by MacCormack finite difference technique are shown in Figure 8.

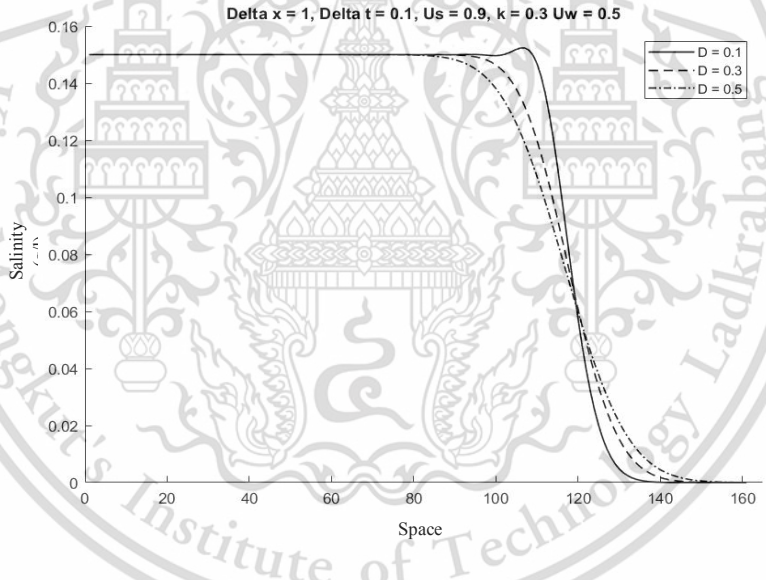

Figure 8 Analytically-computed and numerically approximated salinity intrusion levels, when the initial condition was $S(x,0)$ (g/l) and $D = 0.1, 0.3$ and 0.5 m/s.

Simulation 5: We considered a segment of a river 160 km. long. The salinity intrusion had a flow velocity of $u_s = 0.9$ m/s. The salinity diffusion coefficient was $D = 0.1$ m^2/s. The flow velocity of freshwater released by the diversion dam was 0.5 m/s. The percentage salinity dilution ability of freshwater was either 30, 50, or 70%. All assumed physical parameters are listed in Table 6.

Table 6 All assumed physical parameters in the simulation

$L(km)$	u_s	u_w	D	k	$T(hrs)$
160	0.9	0.5	0.1	0.30	123.46

The values of approximated salinity intrusion or $S(x,0)$ (g/l) by MacCormack finite difference technique are shown in Figure 9.

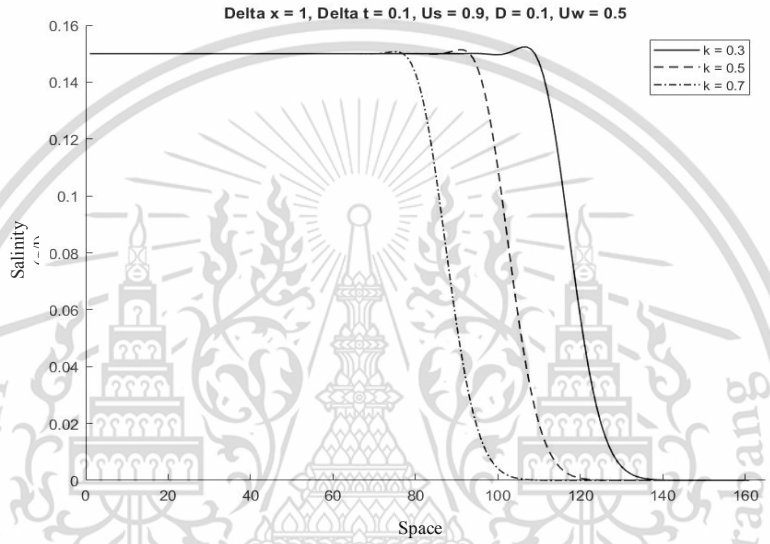

Figure 9 Analytically-computed and numerically approximated salinity intrusion levels, where the initial condition was $S(x,0)$ (g/l), $k = 0.3, 0.5$ and 0.7.

Simulation 6: We considered a segment of a river 160 km. long. The salinity intrusion had a flow velocity of $u_s = 0.9$ m/s. The salinity diffusion coefficient was $D = 0.1\,\text{m}^2/\text{s}$. The flow velocities of freshwater released by the diversion dam were 0.5, 0.7, and 0.9 m/s. The percentage salinity dilution ability of freshwater was 30%. All assumed physical parameters are listed in Table 7.

Table 7 All assumed physical parameters in the simulation

$L(km)$	u_s	u_w	D	k	$T(hrs)$
160	0.9	0.5	0.1	0.30	123.46

The curves of approximated salinity intrusion $S(x,0)$ (g/l) by MacCormack finite difference technique are shown in Figure 10.

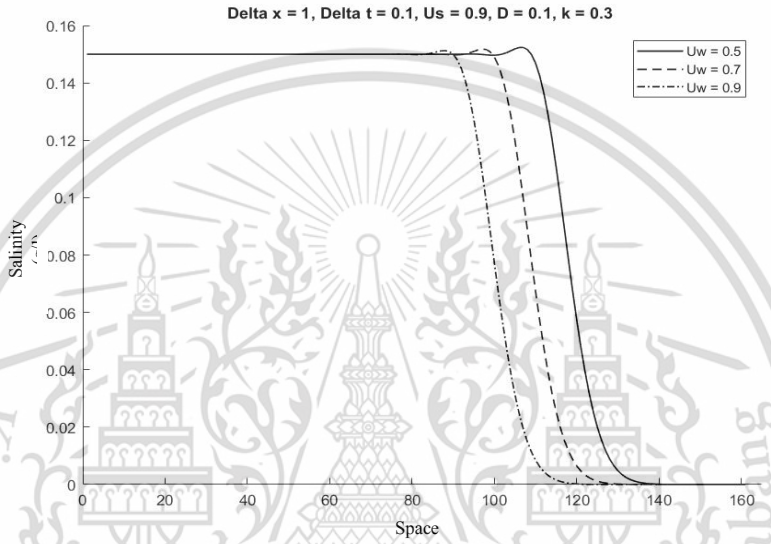

Figure 10 Analytically-computed and numerically approximated salinity intrusion levels with the initial condition of $S(x,0)$ (g/l), $u_s = 0.9$; $u_w = 0.5, 0.7$ and 0.9 m/s.

Simulation 7: We considered a segment of a river 160 km. long. The salinity intrusion had a flow velocity of $u_s = 0.9$ m/s. The salinity diffusion coefficient was $D = 0.1\,\text{m}^2/\text{s}$. The flow velocities of freshwater released by the diversion dam were 0.5, 0.7, and 0.9 m/s. The percentage salinity dilution ability of freshwater was 30%. All assumed physical parameters are listed in Table 8.

Table 8 All assumed physical parameters in the simulation.

$L(km)$	u_s	u_w	D	k	$T(hrs)$
160	0.5	0.5	0.1	0.30	222.23

The curves of approximated salinity intrusion at the initial condition of $S(x,0)$ (g/l) by MacCormack finite difference technique are shown in Figure 11.

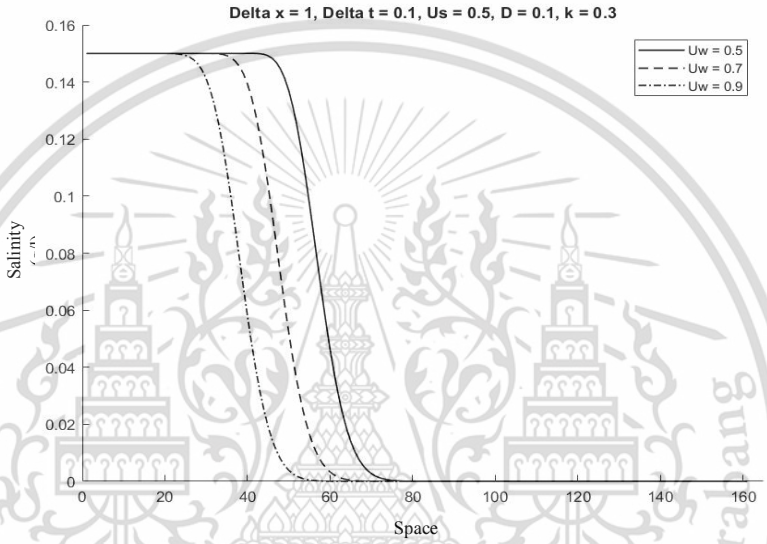

Figure 11 Analytically-computed and numerically approximated salinity intrusion levels with the initial condition of $S(x,0)$ (g/l) and $u_s = 0.5$; $u_w = 0.5, 0.7$ and 0.9 m/s.

All of these results were obtained from using MacCormack technique (3.37) to numerically approximate the solution of the advection-diffusion equation (2.3). The values of salinity intrusion $S(x,0)$ (g/l) depended on the parameter values u_s, u_w, k and D. If the value of u_s is high, salinity will intrude to a longer distance upstream from the estuary. In the future, this kind of situation will happen more frequently. It should be noted that u_w affected u_s, which is logical and stems from the laws of nature and natural phenomena.

5.2 Numerical approximation of salinity intrusion by MacCormack Scheme.

Figure (a)-(d) show the surfaces of salinity intrusion plotted against space (distance) and time.

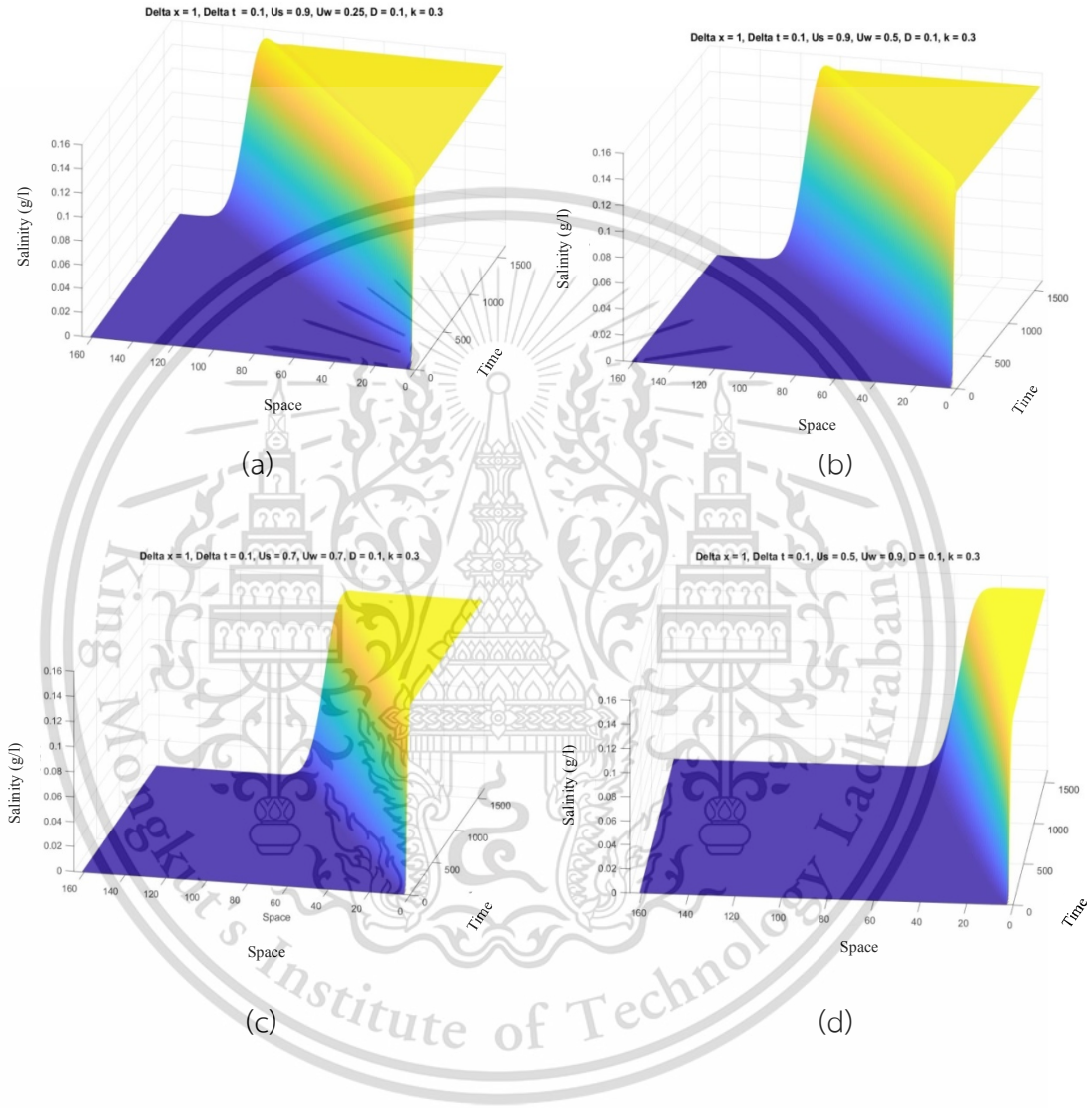

Figure (a)-(d) numerically approximated salinity intrusion $S(x,0)$ (g/l) with different values of u_s and u_w m/s, at delta $x=1$, delta $t=0.1$, $D=0.1,$ and $k=0.3.$

6. Discussion and Conclusion

The results from the numerical simulation of one-dimensional advection-diffusion equation of salinity intrusion model show that the numerical techniques, MacCormack scheme and interpolation function was truly able to approximate

salinity intrusion along the river. Salinity intrusion, u_s, is high during the dry season of every year. This is because the amount of freshwater in the river released from the upstream dam is small. Fluctuation of salinity level is caused by ocean tides at the estuary. Salinity intrusion into the river will be worsened in the future because of global warming. When freshwater is released from the dam's door, it decreases the salinity level in the river to an acceptable level. This study shows that the chosen equations, methods, and parameters can model well the situation where salinity intrusion is countered by released freshwater. From the efficiency test, it was found that the simulation models and parameters were sufficiently reliable for the staff of the Metropolitan Waterworks Authority to plan their raw water supply pumping strategy and for the staff of the Royal Irrigation Department to plan their freshwater release strategy to counter the intrusion. To conclude, the one-dimensional advection-diffusion Eq. (2.3) and the MacCormack Scheme numerical technique and Lagrange interpolation technique are sufficiently accurate and reliable for estimating intruding salinity level in Chao Phraya River for water management of the near future.

Conflicts of Interest

The authors declare that there are no conflicts of interest to any parties whatsoever, regarding the publication of this paper.

Acknowledgments

This research was supported by the Center of Excellence in Mathematics, the Commission on Higher Education, Thailand. We would like to thank the Metropolitan Waterworks Authority, Water Resources and Environment Department and the Royal Irrigation Department for providing us with essential data and to thank Mr. Pratana Kangsadal, a KMITL proofreader, for revising the English in this paper.

Reference

[1] C. Chinnarasri,K. Phothiwijit,and S. Apipattanavis . "A Study of Flow Characteristics in the Lower Chao Phraya River using Acoustic Doppler Velocity Technology ." *KMUTT Research and Development Journal*, vol 40, pp. 217-235, 2017.

[2] National Research Council of Thailand. *National research policy and strategy.* Bangkok: *National Research Council of Thailand*, 2012-2016.

[3] N. Intaboot, and W. Taesombat. "Longitudinal Salinity Intrusion and Dispersion along the Thachin River Due to Sea Level Rise." *Journal of Science and Technology*, vol. 3, pp. 71-86, 2014.

[4] Department, Royal lrrigation. Summary of situation of salinity and Measures to reduce the impact. *Bangkok: Bureau of Water Management and Hydrology,* 2014.

[5] N. Intaboot, and W. Taesombat. "A study on salinity intrusion and control measuer in the Thachin River. " *Research and Development Journal*, vol. 25, pp. 45-57, 2014.

[6] K. Atiharuthaisook, and J. Kanasut. "Salinity intrusion Analysis in Thachin River." *Thaicid National Symposium*, vol. 2017, pp. 137-154, 2017.

[7] N. Intaboot. " The salinity intrusion effected form addition shortcut canal in the lower Thachin River. " *Kasem Bundit Engineering Journal*, vol. 6, pp. 76-90, 2016.

[8] S. Wongsa. "Impact of Climate Change on Water Resources Management in the Lower Chao Phraty Basin,Thailand." *Journal of Geoscience and Environment Protection*, vol 3, pp. 53-58, 2015.

[9] A. Owen, "Artificial diffusion in the numerical modelling of the advective transport of salinity." *Applied Mathematical Modelling*, vol. 8, pp. 116-120, 1984.

[10] K.Ralston, David, W. Rockwell Geyer, and J.A. Lerczak. "Subtidal Salinity and Velocity in the Hudson River Estuary :Observations and Modeling." *American Meteorological Society,* vol. 2008, pp. 753-770, 2008.

[11] G. Gurarslan, H. Karahan, D. Alkaya et al., "Numerical Solution of Advection-Diffusion Equation Using a Sixth-Order Compact Finite Difference Method." *Mathematical Problems in Engineering*, vol. 2013, pp. 1-7, 2013.

[12] N. Pochai. "A numerical computation of a non-dimensional form of stream water quality model with hydrodynamic advection-dispersion-reaction equations ." *Nonlinear Analysis: Hybrid System*, vol. 3, pp. 666-673, 2009.

[13] N. Pochai. "A numerical Treatment of Nondimensional Form of Water Quality Model in a Nonuniform Flow Stream Using Saulyev Scheme." *Mathematical Problems in Engineering*, vol. 2011, pp. 1-15, 2011.

[14] N. Pochai. "Numerical Treatment of a Modified MacCormack Scheme in a Nondimensional Form of the Water Quality Models in a Nonuniform Flow Stream." *Journal of Applied Mathematics* , vol. 2014, pp. 1-8, 2014.

[15] N. Pochain. "Unconditional stable numericl techniques for a water-quality model in a non-uniform flow stream." *Advances in Difference Equations*, vol. 2017, pp. 1-13, 2017.

[16] N. Pochai, and R. Deepana. "An Optimal Control of Water Pollution in a Stream Using a Finite Difference Method." *World Academy of Science*, vol. 80, pp. 1186-1188, 2011.

[17] M. Dehghan. "Weighted finite difference techniques for the one-dimensional advection-diffusion equation." *Applied Mathematics and Computation,* vol. 147, pp. 307-319, 2004.

[18] N. Seesod, and N. Pochai. "A numerical Computation to a Water-Quality Measurement in a Stream Using the Finite Volume Method." *International Conference on Engineering,Applied Sciences,and Technology,* vol. 2013, pp. 98-100, 2013.

[19] N. Pochai, S. Tangmanee, L.J. Crane, and J.J.H. Miller. "A Mathematical Model of Water Pollution Control Using the Finite Element Method." *PAMM.Proc.Appl.Math.Mech,* vol. 6, pp. 755-756, 2006.

[20] F. Mabood, and N. Pochai. "Asymptotic Solution for a water Quality Model in a Uniform Stream." *International Journal of Engineering Mathematics*, vol. 2013, pp. 1-4, 2013.

[21] R.L., Burden, and J.D. Faires. *Numerical Analysis.* Boston,Mass,USA: Brook and Cole, 2011.

Appendix D

Concentrations automatically monitored in real-time at several monitoring stations (from which data were affected by tides at the estuary) in 02/03/2017

Table I Report of water-quality measurements at Wat Ban Paeng station

-	วันที่	เวลา	กรด-ด่าง pH	ความเค็ม Salinity (g/l)	ความขุ่น Turbidity (NTU)	ความนำไฟฟ้า Conductivity (µS/cm)	สารละลาย TDS(mg/l)	คลอโรฟิลล์ Chlorophyll (µg/l)	ออกซิเจนในน้ำ DO(mg/l)	อุณหภูมิ Temp (°C)	ความลึกหัววัดDepth (Meters)	ความนำไฟฟ้า 25 °CConductivity 25 °C(µS/cm)	ระดับน้ำ Water Level (ม.รทก)
1	2/3/2560	0:00	7.76	0.13	14.1	306	183	48.63	5.07	29.59	-	283	-
2	2/3/2560	1:00	7.76	0.13	7,503.47	305	182	49.8	5.02	29.48	-	282	-
3	2/3/2560	2:00	7.76	0.13	6,706.85	305	182	49.08	5.01	29.43	-	282	-
4	2/3/2560	3:00	-	-	-	-	-	-	-	-	-	-	-
5	2/3/2560	4:00	7.75	0.13	3,759.28	303	181	50.52	5.02	29.33	-	280	-
6	2/3/2560	5:00	7.75	0.13	4,354.90	301	181	50.26	5.01	29.21	-	278	-
7	2/3/2560	6:00	7.75	0.13	5,050.57	299	180	51.2	4.96	29.19	-	276	-
8	2/3/2560	7:00	7.76	0.13	2,924.39	298	179	51.44	5.11	29.16	-	275	-
9	2/3/2560	8:00	7.79	0.13	9,257.58	298	179	51.16	5.37	29.31	-	275	-
10	2/3/2560	9:00	-	-	-	-	-	-	-	-	-	-	-
11	2/3/2560	10:00	7.8	0.13	14,685.50	299	179	51.74	5.1	29.51	-	276	-
12	2/3/2560	11:00	7.8	0.13	12,397.00	299	179	53.01	5.19	29.62	-	276	-
13	2/3/2560	12:00	7.79	0.13	14.62	300	179	53.06	5.17	29.71	-	277	-
14	2/3/2560	13:00	7.8	0.13	16.86	301	179	52.95	5.35	29.85	-	278	-
15	2/3/2560	14:00	7.81	0.13	22.29	305	180	52.67	5.67	30.32	-	277	-
16	2/3/2560	15:00	7.79	0.13	22.09	304	180	52.68	5.47	30.08	-	276	-
17	2/3/2560	16:00	7.77	0.13	24.29	303	180	53.01	5.26	29.89	-	280	-
18	2/3/2560	17:00	7.76	0.13	23.3	303	180	53.47	5.08	29.79	-	280	-
19	2/3/2560	18:00	7.75	0.13	22.12	303	180	53.98	5.04	29.77	-	280	-
20	2/3/2560	19:00	7.73	0.13	23.76	303	180	53.89	4.92	29.7	-	280	-
21	2/3/2560	20:00	-	-	-	-	-	-	-	-	-	-	-
22	2/3/2560	21:00	-	-	-	-	-	-	-	-	-	-	-
23	2/3/2560	22:00	7.77	0.13	16.55	303	181	53.02	5.12	29.66	-	280	-
24	2/3/2560	23:00	7.79	0.13	15.18	302	180	53.28	5.31	29.66	-	279	-
สูงสุด			7.81	0.13	14685.5	306	183	53.98	5.67	30.32	-	283	-
ต่ำสุด			7.73	0.13	14.1	298	179	48.63	4.92	29.16	-	275	-
ค่าเฉลี่ย			7.77	0.13	3,342.74	302	180.2	51.94	5.16	29.61	-	278.5	-

Table II Report of water-quality measurements at Wat Pho Taeng Nuea station

-	วันที่	เวลา	กรด-ด่าง pH	ความเค็ม Salinity (g/l)	ความขุ่น Turbidity (NTU)	ความนำไฟฟ้า Conductivity (µS/cm)	สารละลาย TDS(mg/l)	คลอโรฟิลล์ Chlorophyll (µg/l)	ออกซิเจนในน้ำ DO(mg/l)	อุณหภูมิ Temp (°C)	ความลึกหัววัดDepth (Meters)	ความนำไฟฟ้า 25 °CConductivity 25 °C(µS/cm)	ระดับน้ำ Water Level (ม.รทก)
1	2/3/2560	0:00	7.17	0.14	-	317	190	1.1	4.76	29.03	1.97	293	-
2	2/3/2560	1:00	7.18	0.14	-	317	190	0.6	4.86	28.99	1.78	299	-
3	2/3/2560	2:00	7.17	0.14	-	317	190	1.1	4.92	28.99	1.62	299	-
4	2/3/2560	3:00	7.2	0.14	-	316	190	1.5	4.9	28.97	1.48	298	-
5	2/3/2560	4:00	7.17	0.14	-	316	190	0.9	4.86	28.95	1.35	298	-
6	2/3/2560	5:00	7.18	0.14	-	315	190	1.1	4.85	28.92	1.23	297	-
7	2/3/2560	6:00	7.17	0.14	-	315	190	0.9	4.82	28.91	1.17	297	-
8	2/3/2560	7:00	7.17	0.14	-	313	190	0.6	4.76	28.9	1.39	295	-
9	2/3/2560	8:00	7.19	0.14	-	315	190	1.3	4.91	28.89	1.69	297	-
10	2/3/2560	9:00	7.19	0.14	-	316	190	1.3	4.95	28.94	1.88	298	-
11	2/3/2560	10:00	7.2	0.14	-	317	190	1.2	4.99	29.01	2.02	293	-
12	2/3/2560	11:00	7.21	0.14	-	317	190	1.1	4.95	29.09	2.12	293	-
13	2/3/2560	12:00	7.19	0.14	-	317	190	0.5	4.75	29.09	2.14	293	-
14	2/3/2560	13:00	7.19	0.14	-	318	190	0.9	4.83	29.14	2.05	294	-
15	2/3/2560	14:00	7.21	0.14	-	317	190	1	4.97	29.2	1.85	293	-
16	2/3/2560	15:00	7.19	0.14	-	318	190	0.9	4.96	29.18	1.67	294	-
17	2/3/2560	16:00	7.2	0.14	-	317	190	0.8	5.01	29.24	1.53	293	-
18	2/3/2560	17:00	7.25	0.14	-	318	190	1.1	5.34	29.34	1.42	294	-
19	2/3/2560	18:00	7.23	0.14	-	317	190	1.2	5.21	29.21	1.34	293	-
20	2/3/2560	19:00	7.23	0.14	-	318	190	0.7	4.89	29.17	1.4	294	-
21	2/3/2560	20:00	7.2	0.14	-	316	190	1.1	4.95	29.09	1.66	292	-
22	2/3/2560	21:00	7.2	0.14	-	316	190	0.5	4.97	29.03	1.86	292	-
23	2/3/2560	22:00	7.22	0.14	-	316	190	1	5	29.05	1.99	292	-
24	2/3/2560	23:00	7.21	0.14	-	316	190	0.8	4.96	29.03	2.08	292	-
สูงสุด			7.25	0.14	16.4	318	190	1.5	5.34	29.34	2.14	299	-
ต่ำสุด			7.17	0.14	10.8	313	190	0.5	4.75	28.89	1.17	292	-
ค่าเฉลี่ย			7.2	0.14	12.53	316.46	190	0.97	4.93	29.06	1.7	294.71	-

Table III Report of water-quality measurements at Wat Phai Lom station

-	วันที่	เวลา	กรด-ด่าง pH	ความเค็ม Salinity (g/l)	ความขุ่น Turbidity (NTU)	ความนำไฟฟ้า Conductivity (µS/cm)	สารละลาย TDS(mg/l)	คลอโรฟิลล์ Chlorophyll (µg/l)	ออกซิเจนในน้ำ DO(mg/l)	อุณหภูมิ Temp (°C)	ความลึกหัววัดDepth (Meters)	ความนำไฟฟ้า 25 °CConductivity 25 °C(µS/cm)	ระดับน้ำ Water Level (ม.รทก)
1	2/3/2560	0:00	-	-	-	-	-	-	-	-	-	-	-
2	2/3/2560	1:00	-	-	-	-	-	-	-	-	-	-	-
3	2/3/2560	2:00	-	-	-	-	-	-	-	-	-	-	-
4	2/3/2560	3:00	-	-	-	-	-	-	-	-	-	-	-
5	2/3/2560	4:00	-	-	-	-	-	-	-	-	-	-	-
6	2/3/2560	5:00	-	-	-	-	-	-	-	-	-	-	-
7	2/3/2560	6:00	-	-	-	-	-	-	-	-	-	-	-
8	2/3/2560	7:00	-	-	-	-	-	-	-	-	-	-	-
9	2/3/2560	8:00	-	-	-	-	-	-	-	-	-	-	-
10	2/3/2560	9:00	-	-	-	-	-	-	-	-	-	-	-
11	2/3/2560	10:00	-	-	-	-	-	-	-	-	-	-	-
12	2/3/2560	11:00	7.54	0.15	25.3	345	210	-	5.19	28.98	1.24	325	-
13	2/3/2560	12:00	7.53	0.17	19.7	381	230	-	5.01	29.02	1.22	352	-
14	2/3/2560	13:00	7.56	0.15	21.8	354	210	-	5.25	29.17	1.09	327	-
15	2/3/2560	14:00	7.55	0.16	20.5	366	220	-	5.18	29.17	0.89	338	-
16	2/3/2560	15:00	7.57	0.15	21.2	350	210	-	5.34	29.32	0.73	324	-
17	2/3/2560	16:00	7.56	0.15	22.6	351	210	-	5.28	29.22	0.58	325	-
18	2/3/2560	17:00	7.57	0.15	20.9	342	210	-	5.35	29.24	0.48	316	-
19	2/3/2560	18:00	7.54	0.15	15.9	339	200	-	5.23	29.2	0.42	313	-
20	2/3/2560	19:00	7.54	0.15	22	335	200	-	5.24	28.99	0.6	316	-
21	2/3/2560	20:00	7.54	0.15	22.4	333	200	-	5.24	28.82	0.83	314	-
22	2/3/2560	21:00	7.52	0.15	34.9	351	210	-	5.08	28.81	1	331	-
23	2/3/2560	22:00	7.54	0.16	21.5	366	220	-	5.13	28.92	1.11	345	-
24	2/3/2560	23:00	7.54	0.16	19.5	364	220	-	5.11	28.84	1.19	343	-
สูงสุด			7.57	0.17	34.9	381	230	-	5.35	29.32	1.24	352	-
ต่ำสุด			7.52	0.15	15.9	333	200	-	5.01	28.81	0.42	313	-
ค่าเฉลี่ย			7.55	0.15	22.17	352.08	211.54	-	5.2	29.05	0.88	328.38	-

Table IV Report of water-quality measurements at Sam Lae station

-	วันที่	เวลา	กรด-ด่าง pH	ความเค็ม Salinity (g/l)	ความขุ่น Turbidity (NTU)	ความนำไฟฟ้า Conductivity (µS/cm)	สารละลาย TDS(mg/l)	คลอโรฟิลล์ Chlorophyll (µg/l)	ออกซิเจนในน้ำ DO(mg/l)	อุณหภูมิ Temp (°C)	ความลึกหัววัดDepth (Meters)	ความนำไฟฟ้า 25 °CConductivity 25 °C(µS/cm)	ระดับน้ำ Water Level (ม.รทก)
1	2/3/2560	0:00	7.39	0.51	4.3	1129	680	2.5	3.52	29.17	2.1	1045	-
2	2/3/2560	1:00	7.42	0.41	7.3	910	550	3.2	3.99	29.11	1.94	842	-
3	2/3/2560	2:00	7.45	0.31	12.3	700	420	2.6	4.28	29.11	1.77	648	-
4	2/3/2560	3:00	7.47	0.27	9.1	609	370	2.4	4.49	29.09	1.63	563	-
5	2/3/2560	4:00	7.52	0.19	9.6	432	260	2	4.91	29.04	1.5	400	-
6	2/3/2560	5:00	7.52	0.17	10.5	396	240	2.3	5.01	29.02	1.4	366	-
7	2/3/2560	6:00	7.53	0.16	12.7	371	220	1.8	5.09	28.98	1.49	350	-
8	2/3/2560	7:00	-	-	-	-	-	-	-	-	-	-	-
9	2/3/2560	8:00	7.53	0.17	14.4	398	240	1.4	5.01	28.97	2.03	375	-
10	2/3/2560	9:00	7.51	0.2	14.4	456	280	2.5	4.83	29.01	2.2	422	-
11	2/3/2560	10:00	7.47	0.27	18	602	360	2.8	4.48	29.06	2.33	557	-
12	2/3/2560	11:00	7.44	0.34	13.8	754	450	3.5	4.18	29.09	2.4	698	-
13	2/3/2560	12:00	7.4	0.49	14.9	1079	650	3.4	3.73	29.13	2.36	999	-
14	2/3/2560	13:00	7.39	0.55	15.6	1210	730	3.8	3.62	29.15	2.2	1120	-
15	2/3/2560	14:00	7.43	0.44	8.4	973	580	3.3	4.05	29.31	2.01	900	-
16	2/3/2560	15:00	7.47	0.32	10.4	730	440	2.7	4.52	29.37	1.85	675	-
17	2/3/2560	16:00	7.51	0.27	10.2	616	370	2.5	4.81	29.44	1.7	570	-
18	2/3/2560	17:00	7.52	0.21	12.7	488	290	2.4	4.91	29.21	1.59	451	-
19	2/3/2560	18:00	7.54	0.18	10.4	411	250	1.9	5.1	29.18	1.57	380	-
20	2/3/2560	19:00	7.55	0.17	12.7	381	230	2.3	5.09	29.15	1.81	352	-
21	2/3/2560	20:00	7.53	0.19	11.6	433	260	1.9	5.03	29.15	2.02	400	-
22	2/3/2560	21:00	7.5	0.25	19.6	559	340	2.3	4.19	29.19	2.17	517	-
23	2/3/2560	22:00	7.48	0.28	13.9	642	390	3.4	4.51	29.19	2.28	594	-
24	2/3/2560	23:00	7.44	0.35	17.8	773	470	3.3	3.41	29.18	2.34	715	-
สูงสุด			7.55	0.55	19.6	1210	730	3.8	5.1	29.44	2.4	1120	-
ต่ำสุด			7.39	0.16	4.3	371	220	1.4	3.41	28.97	1.4	350	-
ค่าเฉลี่ย			7.48	0.29	12.37	654.43	394.35	2.62	4.47	29.14	1.94	606.04	-

Table V Report of water-quality measurements at Wat Makham station

-	วันที่	เวลา	กรด-ด่าง pH	ความเค็ม Salinity (g/l)	ความขุ่น Turbidity (NTU)	ความนำไฟฟ้า Conductivity (µS/cm)	สารละลาย TDS(mg/l)	คลอโรฟิลล์ Chlorophyll (µg/l)	ออกซิเจนในน้ำ DO(mg/l)	อุณหภูมิ Temp (°C)	ความลึกหัววัดDepth (Meters)	ความนำไฟฟ้า 25 °CConductivity 25 °C(µS/cm)	ระดับน้ำ Water Level (ม.รทก)
1	2/3/2560	0:00	7.38	1.11	18.4	2356	1420	-	1.79	29.26	2.7	2181	-
2	2/3/2560	1:00	7.38	1.05	15.9	2251	1350	-	1.92	29.23	2.55	2084	-
3	2/3/2560	2:00	7.39	0.89	15.2	1919	1150	-	2.03	29.18	2.4	1776	-
4	2/3/2560	3:00	7.41	0.69	18.4	1509	910	-	2.36	29.14	2.26	1397	-
5	2/3/2560	4:00	7.45	0.46	19.3	1016	610	-	2.93	29.09	2.14	940	-
6	2/3/2560	5:00	7.46	0.35	20.5	770	460	-	3.18	29.07	2.05	712	-
7	2/3/2560	6:00	7.47	0.3	21.8	667	400	-	3.38	29.04	2.23	617	-
8	2/3/2560	7:00	7.47	0.27	23.1	599	360	-	3.36	29.02	2.58	554	-
9	2/3/2560	8:00	7.46	0.28	27	633	380	-	3.46	29.03	2.75	586	-
10	2/3/2560	9:00	7.44	0.33	26.4	734	440	-	3.06	29.04	2.92	679	-
11	2/3/2560	10:00	7.41	0.57	26.8	1244	750	-	2.37	29.08	3.04	1151	-
12	2/3/2560	11:00	7.38	0.83	39.2	1785	1070	-	2.04	29.13	3.08	1652	-
13	2/3/2560	12:00	7.38	1.02	42.8	2182	1310	-	1.95	29.17	3	2020	-
14	2/3/2560	13:00	7.37	1.12	46.7	2377	1430	-	1.99	29.18	2.81	2200	-
15	2/3/2560	14:00	7.4	1.04	56.1	2226	1340	-	2.25	29.33	2.62	2061	-
16	2/3/2560	15:00	7.41	0.94	42.8	2026	1210	-	2.36	29.37	2.48	1875	-
17	2/3/2560	16:00	7.43	0.73	46.9	1594	960	-	2.63	29.33	2.34	1475	-
18	2/3/2560	17:00	7.45	0.56	53.3	1232	740	-	2.95	29.25	2.25	1140	-
19	2/3/2560	18:00	7.47	0.38	45.8	837	500	-	3.4	29.21	2.27	775	-
20	2/3/2560	19:00	7.44	0.3	43.7	665	400	-	3.41	29.22	2.56	615	-
21	2/3/2560	20:00	7.45	0.29	55.9	658	400	-	3.16	29.19	2.75	609	-
22	2/3/2560	21:00	7.44	0.43	45.7	948	570	-	2.87	29.2	2.87	877	-
23	2/3/2560	22:00	7.4	0.65	45.8	1420	850	-	2.45	29.21	2.98	1314	-
24	2/3/2560	23:00	7.38	0.85	49.9	1825	1100	-	2.23	29.22	3.02	1689	-
สูงสุด			7.47	1.12	56.1	2377	1430	14.5	3.46	29.37	3.08	2200	-
ต่ำสุด			7.37	0.27	15.2	599	360	4.6	1.79	29.02	2.05	554	-
ค่าเฉลี่ย			7.42	0.64	35.31	1,394.71	837.92	8.13	2.65	29.17	2.61	1,290.79	-

Table VI Report of water-quality measurements at Wat Sai Ma Nuea station

-	วันที่	เวลา	กรด-ด่าง pH	ความเค็ม Salinity (g/l)	ความขุ่น Turbidity (NTU)	ความนำไฟฟ้า Conductivity (µS/cm)	สารละลาย TDS(mg/l)	คลอโรฟิลล์ Chlorophyll (µg/l)	ออกซิเจนในน้ำ DO(mg/l)	อุณหภูมิ Temp (°C)	ความลึกหัววัดDepth (Meters)	ความนำไฟฟ้า 25 °CConductivity 25 °C(µS/cm)	ระดับน้ำ Water Level (ม.รทก)
1	2/3/2560	0:00	7.4	4.3	38.24	8443	5090	26.61	1.34	29.09	-	7817	-
2	2/3/2560	1:00	7.41	4.03	44.92	7942	4787	22.33	1.28	29.1	-	7353	-
3	2/3/2560	2:00	7.43	3.39	16.07	6759	4070	18.22	1.25	29.15	-	6258	-
4	2/3/2560	3:00	7.45	3	12.69	6037	3633	21.43	1.23	29.2	-	5589	-
5	2/3/2560	4:00	7.45	2.85	26.69	5749	3458	19.81	1.25	29.2	-	5323	-
6	2/3/2560	5:00	7.46	2.7	12.12	5467	3289	19.09	1.26	29.2	-	5062	-
7	2/3/2560	6:00	7.46	2.65	14.14	5376	3238	24.24	1.29	29.15	-	4977	-
8	2/3/2560	7:00	7.45	2.7	32.8	5473	3296	22.06	1.19	29.15	-	5067	-
9	2/3/2560	8:00	7.43	2.93	24.09	5905	3556	25.23	0.9	29.15	-	5467	-
10	2/3/2560	9:00	7.4	3.39	37.44	6748	4067	29.82	0.74	29.11	-	6248	-
11	2/3/2560	10:00	7.37	4.02	30.39	7925	4780	40.17	0.69	29.08	-	7337	-
12	2/3/2560	11:00	7.45	4.57	12.21	8911	5382	26.93	0.66	29	-	8250	-
13	2/3/2560	12:00	7.38	4.56	25.02	8927	5367	32.59	1.44	29.24	-	8265	-
14	2/3/2560	13:00	7.49	4.35	37.98	8584	5142	29.92	3.09	29.46	-	7948	-
15	2/3/2560	14:00	7.51	4.13	15.74	8177	4899	27.92	3.08	29.45	-	7571	-
16	2/3/2560	15:00	7.55	3.64	16.03	7270	4352	38.47	3.37	29.49	-	6731	-
17	2/3/2560	16:00	7.51	3.14	15.8	6321	3787	23.21	2.3	29.4	-	5852	-
18	2/3/2560	17:00	7.51	2.94	20.97	5934	3560	23.22	2.12	29.36	-	5494	-
19	2/3/2560	18:00	7.5	2.87	21.2	5798	3480	21.75	2.08	29.33	-	5368	-
20	2/3/2560	19:00	7.49	2.93	17.2	5906	3548	21.93	1.97	29.29	-	5468	-
21	2/3/2560	20:00	7.45	3.2	34.49	6433	3865	25.68	1.48	29.3	-	5956	-
22	2/3/2560	21:00	7.43	3.64	68.35	7246	4358	40.89	1.54	29.24	-	6709	-
23	2/3/2560	22:00	7.41	4.18	42.9	8238	4955	46.48	1.42	29.22	-	7627	-
24	2/3/2560	23:00	7.37	4.57	42.33	8938	5379	30.99	1.17	29.2	-	8275	-
สูงสุด			7.55	4.57	68.35	8938	5382	46.48	3.37	29.49	-	8275	-
ต่ำสุด			7.37	2.65	12.12	5376	3238	18.22	0.66	29	-	4977	-
ค่าเฉลี่ย			7.45	3.53	27.49	7,021.13	4,222.42	27.46	1.59	29.23	-	6,500.50	-

Table VII Report of water-quality measurements at Khlong Lat Pho station

-	วันที่	เวลา	กรด-ด่าง pH	ความเค็ม Salinity (g/l)	ความขุ่น Turbidity (NTU)	ความนำไฟฟ้า Conductivity (µS/cm)	สารละลาย TDS(mg/l)	คลอโรฟิลล์ Chlorophyll (µg/l)	ออกซิเจนในน้ำ DO(mg/l)	อุณหภูมิ Temp (°C)	ความลึกหัววัดDepth (Meters)	ความนำไฟฟ้า 25 °CConductivity 25 °C(µS/cm)	ระดับน้ำ Water Level (ม.รทก)
1	2/3/2560	0:00	-	15.41	-	27292	16510	-	-	28.88	0.57	25747	-
2	2/3/2560	1:00	-	14.49	-	25781	15610	-	-	28.85	0.56	24321	-
3	2/3/2560	2:00	-	13.95	-	24891	15080	-	-	28.82	0.54	23482	-
4	2/3/2560	3:00	-	13.18	-	23604	14310	-	-	28.76	0.54	22267	-
5	2/3/2560	4:00	-	12.14	-	21873	13270	-	-	28.72	0.56	20634	-
6	2/3/2560	5:00	-	11.95	-	21553	13090	-	-	28.68	0.6	20333	-
7	2/3/2560	6:00	-	12.91	-	23161	14050	-	-	28.76	0.63	21850	-
8	2/3/2560	7:00	-	13.76	-	24559	14890	-	-	28.78	0.65	23168	-
9	2/3/2560	8:00	-	14.64	-	26011	15760	-	-	28.81	0.66	24538	-
10	2/3/2560	9:00	-	15.41	-	27262	16510	-	-	28.83	0.66	25718	-
11	2/3/2560	10:00	-	16.28	-	28662	17360	-	-	28.84	0.64	27039	-
12	2/3/2560	11:00	-	16.44	-	28956	17520	-	-	28.89	0.62	27316	-
13	2/3/2560	12:00	-	16.18	-	28594	17260	-	-	29.01	0.6	26475	-
14	2/3/2560	13:00	-	15.4	-	27330	16510	-	-	28.99	0.58	25783	-
15	2/3/2560	14:00	-	14.68	-	26271	15810	-	-	29.2	0.57	24325	-
16	2/3/2560	15:00	-	13.93	-	24945	15060	-	-	29.01	0.56	23097	-
17	2/3/2560	16:00	-	13.48	-	24198	14610	-	-	29	0.57	22405	-
18	2/3/2560	17:00	-	12.95	-	23283	14080	-	-	28.91	0.59	21965	-
19	2/3/2560	18:00	-	13.45	-	24132	14590	-	-	28.94	0.62	22766	-
20	2/3/2560	19:00	-	14.06	-	25113	15180	-	-	28.93	0.64	23691	-
21	2/3/2560	20:00	-	14.82	-	26373	15930	-	-	28.98	0.65	24880	-
22	2/3/2560	21:00	-	15.67	-	27755	16770	-	-	28.98	0.65	26183	-
23	2/3/2560	22:00	-	16.28	-	28746	17360	-	-	29	0.63	26616	-
24	2/3/2560	23:00	-	16.22	-	28640	17300	-	-	28.98	0.61	27018	-
สูงสุด			-	16.44	-	28956	17520	-	-	29.2	0.66	27316	-
ต่ำสุด			-	11.95	-	21553	13090	-	-	28.68	0.54	20333	-
ค่าเฉลี่ย			-	14.49	-	25,791.04	15,600.83	-	-	28.9	0.6	24,234.04	-

Table VIII Report of water-quality measurements at Phra Nakhon Tai station

-	วันที่	เวลา	กรด-ด่าง pH	ความเค็ม Salinity (g/l)	ความขุ่น Turbidity (NTU)	ความนำไฟฟ้า Conductivity (µS/cm)	สารละลาย TDS(mg/l)	คลอโรฟิลล์ Chlorophyll (µg/l)	ออกซิเจนในน้ำ DO(mg/l)	อุณหภูมิ Temp (°C)	ความลึกหัววัดDepth (Meters)	ความนำไฟฟ้า 25 °CConductivity 25 °C(µS/cm)	ระดับน้ำ Water Level (ม.รทก)
1	2/3/2560	0:00	-	-	-	-	-	-	-	-	-	-	-
2	2/3/2560	1:00	-	-	-	-	-	-	-	-	-	-	-
3	2/3/2560	2:00	-	22.08	-	37902	22895	-	-	28.98	-	35756	-0.75
4	2/3/2560	3:00	-	20.64	-	35696	21536	-	-	29.05	-	33051	-0.75
5	2/3/2560	4:00	-	18.93	-	33019	19917	-	-	29.06	-	30573	0.16
6	2/3/2560	5:00	-	18.8	-	32783	19789	-	-	29.02	-	30354	0.72
7	2/3/2560	6:00	-	19.76	-	34351	20706	-	-	29.1	-	31806	1.1
8	2/3/2560	7:00	-	20.71	-	35853	21605	-	-	29.12	-	33197	1.39
9	2/3/2560	8:00	-	21.63	-	37352	22472	-	-	29.21	-	34585	1.48
10	2/3/2560	9:00	-	22.82	-	39332	23595	-	-	29.37	-	36418	1.34
11	2/3/2560	10:00	-	23.13	-	39802	23881	-	-	29.37	-	36853	0.98
12	2/3/2560	11:00	-	23.03	-	39685	23787	-	-	29.42	-	36745	0.57
13	2/3/2560	12:00	-	22.81	-	39338	23584	-	-	29.41	-	36424	0.15
14	2/3/2560	13:00	-	24.72	-	41797	25339	-	-	28.78	-	39431	-0.12
15	2/3/2560	14:00	-	25.4	-	42691	25963	-	-	28.6	-	40274	-0.26
16	2/3/2560	15:00	-	21.72	-	37737	22564	-	-	29.56	-	34941	-0.19
17	2/3/2560	16:00	-	19.72	-	34483	20674	-	-	29.41	-	31928	0.19
18	2/3/2560	17:00	-	19.38	-	34011	20353	-	-	29.51	-	31491	0.64
19	2/3/2560	18:00	-	19.52	-	34100	20480	-	-	29.31	-	31574	1.04
20	2/3/2560	19:00	-	19.97	-	34846	20908	-	-	29.36	-	32264	1.22
21	2/3/2560	20:00	-	21.31	-	36951	22175	-	-	29.35	-	34213	1.28
22	2/3/2560	21:00	-	21.77	-	37634	22608	-	-	29.29	-	34846	1.16
23	2/3/2560	22:00	-	22.19	-	38333	23002	-	-	29.36	-	35493	0.79
24	2/3/2560	23:00	-	22.69	-	39112	23470	-	-	29.36	-	36214	0.38
สูงสุด			8.05	25.4	89.09	42691	25963	-	5.72	29.56	-	40274	1.48
ต่ำสุด			7.36	18.8	12.25	32783	19789	-	1.04	28.6	-	30354	-0.75
ค่าเฉลี่ย			7.53	21.49	46.89	37,127.64	22,331.95	-	2.4	29.23	-	34,474.14	0.57

Author biography

Name	Miss Khemisara Kulmart
Date of Birth	6 August 1975
Address	83/702,704 Ramkhamhaeng road, Ratpattana, Sapansoong, Bangkok 10240
Education	(2010) B.S. Mathematics, Ramkhamhaeng University (2013) Master of Education, Ramkhamhaeng University
Occupation	Educator
Academic Publication	K. Kulmart and N. Pochai. 2019. "Simulation of Salinity Intrusion in Chao Phraya River by a Developed Mathematical Model and MacCormack scheme with Cubic Spline Interpolation"386-397, Universal Journal of Mechanical Engineering. K. Kulmart and athers. 2019. "Factors Affecting the Outcomes of the Royal Strategy of Understanding, Approaching, and Developing" of People in Local Communities Overseen by the Office of Private Education, Ra-ngae District, Narathiwat Province, Thailand, Thesis, Ministry of Education. K. Kulmart and athers. 2017. "Early Childhood Education Pram C.E. 2017" Ministry of Education. K. Kulmart and athers. 2016. "Bachelor of Science Program in Applied Statistics" Ramkhamhaeng University

K. Kulmart and athers.
2014-2015. “Achievement Examination Report Basic Education Course C.E. 2008” Ministry of Education.

K. Kulmart and athers.
2014. “Educational television programs Mathematics Course and Mathematics daily life” Educational Technology Center, Ministry of Education.

K. Kulmart and athers.
2013. “Internal quality assurance guidelines District Non-Formal and Informal Education Center/ county” Ministry of Education.